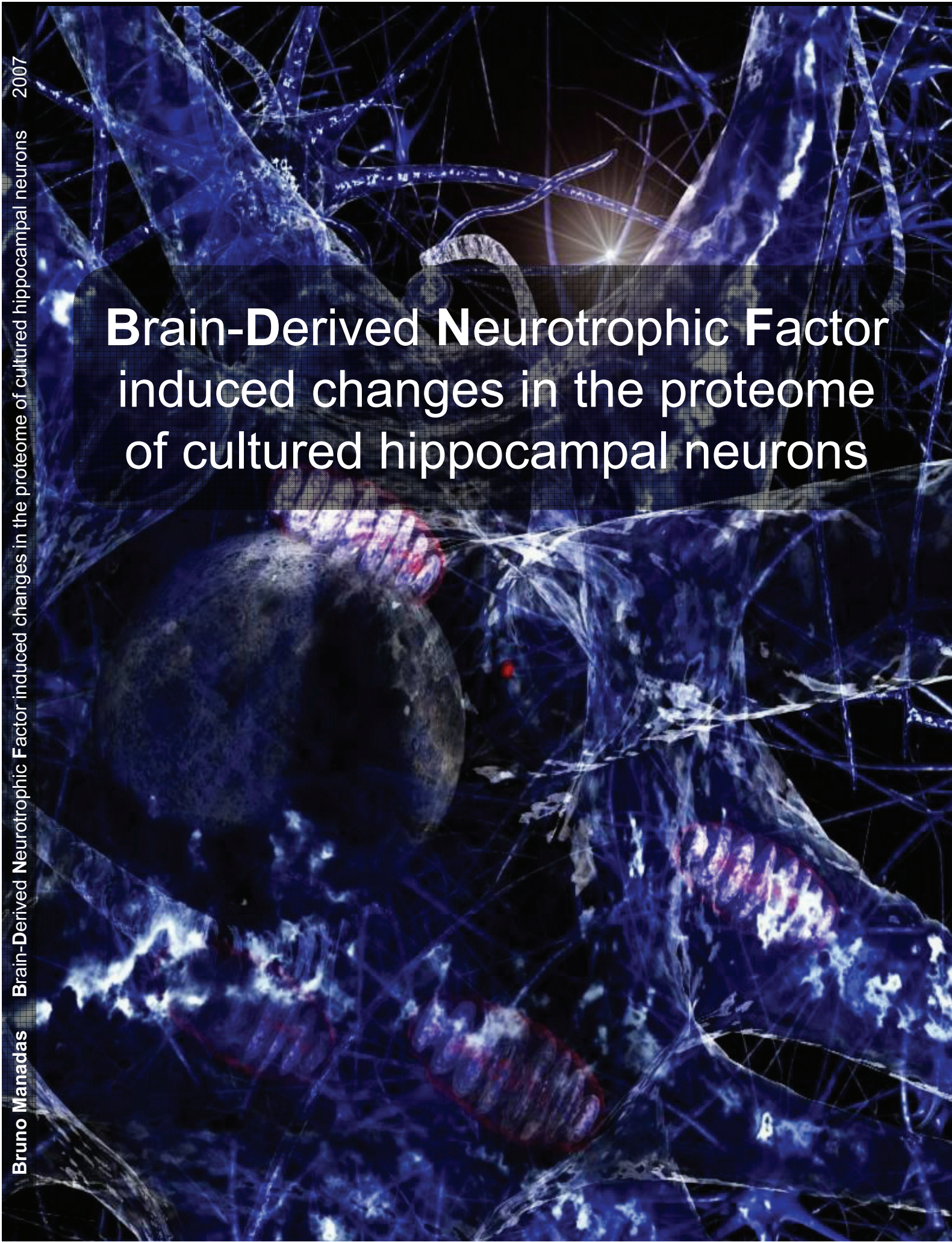

Brain-Derived Neurotrophic Factor induced changes in the proteome of cultured hippocampal neurons

Bruno Manadas

Brain-Derived Neurotrophic Factor induced changes in the proteome of cultured hippocampal neurons 2007

Brain-Derived Neurotrophic Factor induced changes in the proteome of cultured hippocampal neurons

Alterações no proteoma de neurónios de hipocampo em cultura induzidas pelo BDNF

Bruno José Fernandes Oliveira Manadas

Dissertação apresentada à Faculdade de Ciências e Tecnologia da Universidade de Coimbra para prestação de provas de Doutoramento em Biologia, na especialidade de Biologia Celular.

Dissertion presented to Faculdade de Ciências e Tecnologia da Universidade de Coimbra in partial fulfillment of the requirements for a Doctoral degree in Biology (Cell Biology).

Universidade de Coimbra
2007

Este trabalho foi realizado no Centro de Neurociências e Biologia Celular, Universidade de Coimbra, sob a supervisão do Professor Doutor Carlos Jorge Alves Bandeira Duarte e no Institute of Biotechnology, Foundation for Biomedical Research of the Academy of Athens, sob orientação do Doutor Michael Fountoulakis. A sua realização foi suportada pela bolsa SFRH/BD/6194/2001 da Fundação para a Ciência e Tecnologia, Lisboa, Portugal.

This work was performed at the Center for Neuroscience and Cell Biology, University of Coimbra, under the supervision of Professor Doctor Carlos Jorge Alves Bandeira Duarte and at the Institute of Biotechnology, Foundation for Biomedical Research of the Academy of Athens, under the supervision of Doctor Michael Fountoulakis. Its execution was supported by grant SFRH/BD/6194/2001 from Fundação para a Ciência e Tecnologia, Lisbon, Portugal.

Ciência.Inovação 2010

Financiamento no âmbito do III Quadro Comunitário de Apoio, comparticipado pelo Fundo Social Europeu e por fundos nacionais do MCES

Agradecimentos
Acknowledgment

Gostaria de começar por agradecer ao Professor Doutor Carlos Duarte por me aceitar no seu laboratório ainda como estagiário. Por me ter confiado um projecto de doutoramento, dando-me asas para voar e céu para descobrir, fazendo depender de mim a força para as bater e o caminho a seguir. Mais do que um supervisor, foste para mim um tutor e o responsável pelo que hoje tenho de bom enquanto cientista e enquanto pessoa.

O meu muito obrigado aos mais próximos: Pai, Mãe, Manito e Nilza, psicólogos ocasionais ou diários que me ouviram e ajudaram nesta travessia zelando pelo meu bem-estar físico e mental, incentivando-me e suscitando em mim a força de vontade que me faz querer mais e melhor.

A todos os elementos do laboratório de biologia celular: Professor Doutor Arsélio, Dra. Emília, Dra. Caetana, Armando, Paulo, Francisco, Armanda, Graça,....., obrigado pelo vosso apoio fundamental naquela fase importante do projecto, o início!

Aos elementos do laboratório de biotecnologia, Professor Doutor Euclides, Doutor Carlos Faro, Ana Luísa, Isaura, Castanheira, pelos vossos ensinamentos e pela simplicidade e subtileza com que os transmitiram.

To my Greek friends Dr. Michael Fountoulakis, Spiros, Panos and Panos, Aggeliki, Elena, Ploumisti, Kostas, and Sofia, special thanks for the way you accepted me, your friendship, and the knowledge you gave me and allowed to share. Ευχαριστω.

Ao Professor Doutor Manuel Santos, Professor Doutor Francisco Amado, Professor Doutor Pedro Domingues e Raquel por me terem iniciado e acompanhado na proteómica, com as vossas críticas construtivas, apoio e transmissão de conhecimentos.

E como não poderia deixar de ser, aos cajonianos!!!!! Elisabete, Edgar, Sandra, Guida, Carlos, João, Andrea, Joana e Rita, pelo vosso companheirismo, não esquecendo Ramiro, Ricardo, Diogo, Paulo e Mário, amigos e companheiros de longas noites no laboratório...

Aos outros colegas e amigos da colheita de 96: Catarina, Girão, Coelho, Bruno e Joana, por estarem à distância de um clique, de uma tecla...

Finalmente, a todos aqueles que ao longo destes anos conheci e que contribuíram para a minha formação científica e pessoal com bons comportamentos, posturas, ideias e personalidades, mas também aqueles que conseguiram demonstrar maus exemplos em todas estas áreas e muitas outras, tornando-se pontos de referência de modelos a evitar. Afinal de contas, sem eles poderia ser eu a cometer esses erros.

Table of contents

Abbreviations

2D-LC	**T**wo-**D**imensional **L**iquid **C**hromatography
2D-SDS-PAGE	**T**wo-**D**imensional **S**odium **D**odecyl**s**ulphate **P**oly**a**crylamide **G**el **E**lectrophoresis
ACN	**Ac**eto**n**itrile
AD	**A**lzheimer's **D**isease
Arc	**A**ctivity-**r**egulated **c**ytoskeletal
BBB	**B**lood-**B**rain **B**arrier
BD	**B**ipolar **D**isorder
BDNF	**B**rain-**D**erived **N**eurotrophic **F**actor
BIND	**B**iomolecular **I**nteraction **N**etwork **D**atabase
BrdU	**Br**omo**d**eoxy**u**ridine
BSA	**B**ovine **S**erum **A**lbumin
Btk	**B**ruton's **t**yrosine **k**inase
CAD	**C**ollisionally **A**ctivated **D**issociation
cAMP	**c**yclic **A**denosine **M**ono**p**hosphate
CaMKII	**Ca**lcium/cal**m**odulin-dependent protein **k**inase II
CHAPS	3-[(3-**Ch**olamidopropyl)dimethyl**a**mmonio]-1-**p**ropane**s**ulfonate
CID	**C**ollision **I**nduced **D**issociation
CNS	**C**entral **N**ervous **S**ystem
CP1	**C**arboxy**p**eptidase **1**
CPE	**C**arboxy**p**eptidase **E**
CR	**C**ysteine-**R**epeat domains
CRE	**C**alcium **R**esponse **E**lement
CREB	**CRE B**inding protein
CSF	**C**erebro**s**pinal **F**luid
DAG	**Di**a**g**lycerol
DD	**D**eath **D**omain
DG	**D**entate **G**yrus
DIV	**D**ay **I**n **V**itro
DMEM	**D**ulbecco's **M**odified **E**agle's **M**edium
DR	**D**ietary **R**estriction
DTE	**Di**thio**e**rytol
DTT	**Di**thio**t**reitol
E18	**E**mbryonic day **18**
EBI	**E**uropean **B**ioinformatics **I**nstitute
EGF	**E**pidermal **G**rowth **F**actor
eIF	**e**ukaryote **I**nitiation **F**actor
ER	**E**ndoplasmic **R**eticulum
ERK	**E**xtracellular signal-**r**egulated protein **k**inase
ESI-Qq-TOF	**E**lectro**s**pray **I**onization **Q**uadrupole **T**ime-**O**f-**F**light
FA	**F**ormic **A**cid
FDR	**F**alse **D**iscovery **R**ate
Gab1	**G**rb2-**a**ssociated **b**inder **1**
GABA	**G**amma-**a**mino**b**utyric **a**cid
GDP	**G**uanine **Di**phosphate
GEF	**G**uanine-nucleotide **E**xchange **F**actors
GeLC	**Ge**l-**e**lectrophoresis and **L**iquid **C**hromatography
GeneNote	**Gene No**rmal **T**issue **E**xpression

GFP	**G**reen **F**luorescence **P**rotein
GO	**G**ene **O**ntology
Grb2	**Gr**owth factor receptor-**b**ound protein 2
GRP-1	**G**eneral **R**eceptor for **P**hosphoinositides-1
GTP	**G**uanosine **T**ri**p**hosphate
HAD	**H**IV-1 **A**ssociated **D**ementia
HBPP	**H**uman **B**rain **P**roteome **P**roject
HED	**H**ydroxi**e**thyl**d**isulfate
HFS	**H**igh-**F**requency **S**timulation
HIV-1	**H**uman **I**mmunodeficiency **V**irus type **1**
HPLC	**H**igh **P**erformance **L**iquid **C**hromatography
htt	**h**unt**t**ingt**i**n
HUPO	**Hu**man **P**roteome **O**rganization
ICAT	**I**sotope-**C**oded **A**ffinity **T**ags
ICPL	**I**sotope **C**oded **P**rotein **L**abelling
IEF	**I**so**e**lectric **F**ocusing
IMAC	**I**mmobilized **M**etal **A**ffinity **C**hromatography
IPG	**I**mmobilized **p**H **G**radient
iTRAQ	isotope **T**ags for **R**elative and **A**bsolute **Q**uantitation
JBD	**J**uvenile **B**ipolar **D**isorder
JNK	**J**un **N**-terminal **K**inase
KSR	**K**inase **S**uppressor of **R**as
LC	**L**iquid **C**hromatography
LRR	**L**eucine **R**ich **R**epeats
LTD	**L**ong-**T**erm **D**epression
LTP	**L**ong-**T**erm **P**otentiation
MALDI-TOF-TOF	**M**atrix-**A**ssisted **L**aser **D**esorption/**I**onization tandem **T**ime-**O**f-**F**light
MAPK	**M**itogen-**A**ctivated **P**rotein **K**inase
Mash1	**M**ammalian **A**chaete-**S**chute **H**omolog **1**
MCAO	**M**iddle **C**erebral **A**rtery **O**cclusion
MEK1	**M**APK and **E**RK **K**inase-**1**
MMP	**M**atrix **M**etallo**p**roteinases
MP1	**M**EK **P**artner **1**
MS	**M**ass **S**pectrometry
MS/MS	tandem **M**ass **S**pectrometry
mTOR	**m**ammalian **T**arget **O**f **R**apamycin
mhtt	**m**utant **h**unt**t**ingt**i**n
MudPIT	**Mu**lti**d**imensional **P**rotein **I**dentification **T**echnology
NCBI	**N**ational **C**enter for **B**iotechnology **I**nformation
NeuN	**Neu**ronal **N**uclei
NGF	**N**erve **G**rowth **F**actor
NMDA	**N**-**M**ethyl-**D**-**A**spartic acid
NRSE	**N**uclear **R**estrictive **S**ilencer **E**lement
NRSF	**N**euron **R**estrictive **S**ilencer **F**actor
NT-3	**N**euro**t**rophin **3**
NT-4/5	**N**euro**t**rophin **4/5**
$p75^{NTR}$	p75 **N**euro**t**rophin **R**eceptors
pBC	**p**re**B**otzinger **C**omplex
PC1	**P**rotein **C**onvertase-**1**
PCR	**P**olimerase **C**hain **R**eaction

PD	**P**arkinson's **D**isease
PDK-1	**P**hosphoinositide-**D**ependent Protein **K**inase **1**
PH	**P**lesckstrin **H**omology
PI3-K	**P**hosphatidyl**i**nositol **3-K**inase
PKA	**P**rotein **K**inase **A**
PKB	**P**rotein **K**inase **B**
PKC	**P**rotein **K**inase **C**
PLC-γ	**P**hospho**L**ipase **C-γ**
PMF	**P**eptide **M**ass **F**ingerprint
PMSF	**P**henyl**m**ethyl **S**ulfonyl **F**luoride
PP2A	**P**rotein **P**hosphatase **2A**
PSD-95	**P**ost-**S**ynaptic **D**ensity protein **95**
PSI	**P**rotein **S**tandards **I**nitiative
PTB	**P**hospho**t**yrosine **B**inding domain
PTM	**P**ost **T**ranslational **M**odification
QqTOF	**Q**uadrupole **T**ime-**O**f-**F**light
RNG105	**RN**A **G**ranule protein **105**
RPLC	**R**everse **P**hase **L**iquid **C**hromatography
RSK	**R**ibosomal **S**6 **K**inase
S126	Ultracentrifugation **S**ediment at **126**,000×g_{av}
SCX	**S**trong **C**ation E**x**change
SDS	**S**odium **D**odecyl**s**ulphate
Shc	**S**rc **h**omology 2 domain-containing transforming protein **C**
SILAC	**S**table **I**sotope **L**abeling by **A**mino acids incorporation in **C**ell culture
SOS	**s**on **o**f **S**evenless
TCA	**T**ri**c**hloro**a**cetic Acid
TFA	**T**ri**f**luoro**a**cetic Adic
TNF	**T**umour **N**ecrosis **F**actor
TOF	**T**ime-**O**f-**F**light
tPA	**T**issue **P**lasminogen **A**ctivator
Trk	**T**ropomyosin-**r**elated **K**inase

Abstract

The hippocampus plays an important role in learning and memory formation, and the cellular and molecular mechanisms involved have been elucidated to some extent. This brain region is particularly vulnerable and is highly affected in stroke episodes. Brain trauma, Alzheimer's disease and Huntington's disease are also known to affect the hippocampus.

Brain-derived neurotrophic factor (BDNF) belongs to the neurotrophin family of proteins and is known to activate the high-affinity TrkB receptor and the pan-neurotrophin low-affinity receptor $p75^{NTR}$. BDNF and its cognate receptor, TrkB, are widely expressed in the brain, including the hippocampus, where they play important roles in development, synaptogenesis, regulation of synaptic transmission, and in synaptic plasticity. Furthermore, BDNF plays a neuroprotective role in stroke episodes. In this work we performed a comprehensive study of the effect of BDNF in the proteome of cultured hippocampal neurons, which will contribute to elucidate some of the biological effects of the neurotrophin.

The proteome of a mammalian organism exceeds hundreds of thousands of different proteins. The hippocampal proteome is still being mapped, with several studies being conducted aiming at mapping the complement of the genome in this brain region. However, a comprehensive proteomic analysis of the mammalian proteome using conventional broad range two-dimensional gel electrophoresis has been limited by the resolving power of the technique. In order to increase the number of proteins of the hippocampal proteome resolved by 2D-SDS-PAGE, narrow range immobilized pH gradient gels were used in isoelectric focusing together with sample fractionation by ultracentrifugation. Two-dimensional gel electrophoresis is particularly sensitive to contaminants including salts, lipids, nucleic acids, and other non-soluble content (e.g. membrane and membrane-associated proteins). The majority of these interfering components can be removed from protein samples through ultracentrifugation and TCA precipitation followed by acetone washing. However, the protein pellet obtained after TCA precipitation is difficult to solubilize using two-dimensional gel electrophoresis compatible buffers, which results in loss of sample and decrease in the reproducibility of the technique. In order to overcome these two drawbacks, sample (rat brain hippocampus and cultured hippocampal neurons) sonication was introduced to increase sample recovery and improve the reproducibility of two-dimensional gel electrophoresis. This resulted in a better and faster software analysis, with an increase in the number of spots automatically matched across the gel image.

BDNF exerts long-term actions on hippocampal neurons through the modulation of protein synthesis mechanisms. However, the changes in the proteome induced by BDNF have only been monitored in a neuroblastoma cell line. Therefore, this work focused on the proteomic changes induced by the neurotrophin in cultured hippocampal neurons upon exposure to BDNF for 12h. In order to evaluate the differential gene expression induced by BDNF, the neurotrophic stimulation was performed in the presence of radiolabelled amino acids, which allows monitoring the expression levels of newly synthesized proteins. The proteomic changes induced by BDNF in cultured hippocampal neurons were mainly analysed using two-dimensional gel electrophoresis of the soluble fraction and the pellet resulting from the ultracentrifugation at 126,000×g_{av} (S126), taking advantage of the increased reproducibility achieved. The differential gene expression analysis was performed using gel images of narrow pH ranges (4.5-5.5, 5.0-6.0, 5.5-6.7 and 6.0-9.0) in order to increase the number of detected spots. Proteins from both fractions resolved in all pH ranges were identified using MALDI-TOF mass spectrometry. Once differential expression levels were correlated with protein identification, selected gene products were clustered according to their ontologies. Gene ontologies provide detailed information of gene products based on their molecular function, biological processes and cellular components. Clustering gene products associated with differential expression induced by a specific stimulus allows the functional interpretation of obtained data. Therefore, this approach was used for the evaluation of changes in protein expression induced by BDNF (upregulation and downregulation), retrieving several regulated ontologies, including “carbohydrate metabolism”, “protein metabolism” (“protein biosynthesis” and “translation”) and “nucleobase, nucleoside, nucleotide and nucleic acid metabolism” (particularly “RNA processing”). Besides these clusters, several gene products belonging to other ontologies showed changes in expression in response to BDNF stimulation.

The S126 fraction represents a protein fraction containing mainly membrane proteins, membrane-associated proteins, and other gene products insoluble in two-dimensional gel electrophoresis buffers. Therefore, another high-throughput proteomic approach, two-dimensional liquid chromatography coupled with tandem mass spectrometry, was used to increase the proteome coverage of cultured hippocampal neurons and to further investigate the differential gene expression induced by BDNF. This technique resolves peptides and identifies gene products based on the fragmentation pattern of resolved peptides, in contrast with the gel-based approach which resolves proteins. The quantification analysis was performed using the peptide isotope labelling conferred by iTRAQ. The analysis of the identified proteins showed that the gel-based and liquid-based approaches are

complementary techniques for the coverage of the proteome of a given species, with several proteins being identified by only one of the methods.

In conclusion, the work presented in this thesis provided improved methodologies for resolving complex protein mixtures on two-dimensional gel electrophoresis and two-dimensional liquid chromatography, and their identification by mass spectrometry. Several gene products regulated by BDNF were clustered according to their ontologies and the results are expected to contribute as starting points for further analysis of the physiological effects of the neurotrophin, particularly its role in the mechanisms of neuroprotection and brain repair. The diversity of proteins which expression is affected by BDNF may also explain the multiplicity of effects of this neurotrophin in the nervous system.

Resumo

O hipocampo desempenha um papel importante nos processos de aprendizagem e formação de memória, e os mecanismos celulares e moleculares envolvidos neste processo foram ainda apenas parcialmente esclarecidos. Esta região do cérebro é particularmente vulnerável sendo severamente afectada em episódios de trombose cerebral. Nas doenças de Alzheimer e de Huntington, assim como os traumatismos cerebrais, afectam também o hipocampo, ainda que de uma forma menos acentuada.

O BDNF (*Brain-Derived Neurotrophic Factor*) pertence à família das neurotrofinas, activando receptores de elevada afinidade, do tipo TrkB, e receptores de baixa afinidade, do tipo $p75^{NTR}$. O BDNF e o seu receptor, TrkB, são expressos abundantemente no cérebro, incluindo no hipocampo, onde desempenham funções importantes no desenvolvimento, sinaptogénese, regulação da transmissão sináptica e na plasticidade sináptica. O BDNF também possui um papel neuroprotector em episódios de trombose cerebral. Neste trabalho efectuou-se um estudo exaustivo dos efeitos do BDNF no proteoma dos neurónios do hipocampo em cultura, com o objectivo de melhor compreender alguns dos efeitos biológicos das neurotrofinas.

O proteoma de um mamífero ultrapassa as centenas de milhar de proteínas diferentes. O proteoma do hipocampo ainda não foi concluído, havendo vários estudos a decorrer no sentido de "mapear" o complemento do genoma desta região do cérebro. Uma análise proteómica exaustiva desta região cerebral não poderá ser efectuada por electroforese bi-dimensional na sua forma convencional com a utilização de géis para focagem isoeléctrica de gama mais alargada, dado que esta abordagem não possui poder de resolução suficiente. Para aumentar a capacidade de resolução de proteínas através de 2D-SDS-PAGE neste trabalho foram usados géis com gradiente de pH de apenas uma unidade para a focagem isoeléctrica em combinação com fraccionamento por ultracentrifugação. A electroforese bi-dimensional é particularmente sensível à presença de contaminantes como sais, lípidos, ácidos nucleicos e outras substâncias não solúveis (p.e. proteínas membranares e proteínas associadas à membrana). A maioria das substâncias que interferem com a técnica pode ser removida das amostras proteicas utilizando ultracentrifugação seguida de precipitação por TCA e lavagem com acetona. No entanto, o precipitado proteico que se obtém deste processo é de difícil solubilização quando se utiliza um tampão compatível com a electroforese bi-dimensional, resultando na perda de amostra

e diminuição da reprodutibilidade associada à técnica. Para ultrapassar estas desvantagens técnicas, introduziu-se um passo de sonicação da amostra na presença de tampão de solubilização de modo a aumentar a solubilização e melhorar a reprodutibilidade dos géis obtidos. Este processo resultou num melhoramento na qualidade e na velocidade da análise das imagens obtidas a partir dos géis utilizando software apropriado, com um aumento no número de manchas correlacionadas de forma automática em todo o gel.

O BDNF exerce acções lentas e duradouras nos neurónios de hipocampo através da modulação dos mecanismos de síntese proteica. Porém, as alterações no proteoma induzidas pelo BDNF apenas foram ainda monitorizadas numa linha celular com origem num neuroblastoma. Neste trabalho foram investigadas as alterações do proteoma induzidas pela neurotrofina em neurónios de hipocampo em cultura, expostos ao BDNF durante 12h. De modo a avaliar a expressão genética diferencial induzida pelo BDNF, o estímulo neurotrófico foi realizado na presença de aminoácidos marcados com enxofre radioactivo. As alteração proteómicas induzidas pelo BDNF em neurónios de hipocampo em cultura foram analisadas recorrendo principalmente à electroforese bidimensional da fracção solúvel e do sedimento obtido após ultracentrifugação a 126,000×g_{me} (S126), tirando partido do aumento da reprodutibilidade adquirido. A análise da expressão diferencial foi realizada em géis com uma gama de pH estreita (4.5-5.5, 5.0-6.0, 5.5-6.7, 6.0-9.0) de modo a aumentar o número de spots a serem detectados. As proteínas das duas fracções, resolvidas em todas as gamas de pH apresentadas, foram identificadas utilizando espectrometria de massa (MALDI-TOF). Uma vez correlacionados os níveis de expressão diferencial com a identificação das proteínas, os produtos dos genes apresentando alterações de expressão foram agrupados de acordo com as suas ontologias. As ontologias dos genes permitem caracterizar os produtos dos genes com base na sua função molecular, processo biológico ou componente celular do qual fazem parte. O agrupamento dos produtos de genes cuja abundância é afectada em resposta a um determinado estímulo contribui para a interpretação funcional dos dados obtidos. Assim, esta abordagem foi utilizada para avaliar as alterações induzidas pelo BDNF na expressão de proteínas (aumento e diminuição da expressão) em neurónios do hipocampo em cultura tendo retribuído várias ontologias que são reguladas pelo BDNF: “metabolismo dos hidratos de carbono”, “metabolismo proteico” (“biosíntese de proteínas” e “tradução”) e “metabolismo das bases nucleicas, nucleósidos, nucleótidos e ácidos nucleicos” (particularmente “processamento de RNA”). Para além destas ontologias, outras proteínas pertencentes a outras ontologias mostraram ser reguladas em resposta ao estímulo com BDNF em neurónios do hipocampo em cultura.

A fracção S126 contém principalmente proteínas membranares, proteínas associadas à membrana e outras proteínas insolúveis nos tampões utilizados na electroforese bi-dimensional. Por isso, foi utilizada outra abordagem para análise em larga escala do proteoma contido nesta fracção, a cromatografia bidimensional acoplada a espectrometria de massa com fragmentação, de forma a aumentar a cobertura do proteoma dos neurónios de hippocampo em cultura e permitir a investigação da expressão diferencial dos genes induzida pelo BDNF. Esta técnica permite o fraccionamento de péptidos e identifica os produtos da expressão dos genes com base no padrão de fragmentação dos péptidos separados por cromatografia, ao contrário da abordagem com base em separação em gel, que permite a separação de proteínas. A análise quantitativa foi realizada utilizando a marcação isotópica dos péptidos conferida pelo iTRAQ. A análise das proteínas identificadas levou-nos a concluir que as abordagens líquida e em gel são técnicas complementares para a cobertura do proteoma de uma dada espécie, tendo-se observado a identificação de várias proteínas por apenas um dos métodos.

No seu conjunto, o trabalho apresentado nesta tese permitiu melhorar as metodologias utilizadas na análise do proteoma do hipocampo, utilizando electroforese bi-dimensional e cromatografia bi-dimensional, com a identificação de proteínas por espectrometria de massa. Foi possível agrupar vários produtos de genes regulados pelo BDNF de acordo com as suas ontologias, e os resultados obtidos poderão constituir pontos de partida para uma análise dos efeitos fisiológicos da neurotrofina, em particular do seu papel nos mecanismos de neuroprotecção e reparação cerebral. A diversidade de proteínas que revelaram alterações na sua expressão induzidas pelo BDNF poderá explicar a multiplicidade dos efeitos desta neurotrofina no sistema nervoso.

Chapter 1

Introduction

1.1 - Proteomics

The term proteomics was first used in September 1994 by Marc Wilkins, a student at Australia's Macquarie University, at a scientific conference in Italy. While struggling to find the right word that could replace the repeated sentence in his PhD thesis "all proteins expressed by a genome, cell or tissue", he settled on proteome, after discarding 'proteinome' and 'protome', 'the one that seemed to work best and roll off the tongue nicely (Huber, L. A., 2003).

Proteome projects are a direct consequence of the various ongoing and/or already concluded genome projects and most of the search algorithms currently used rely on these large databases for protein identification. In contrast with the **genome** projects, which are based on a static collection of genes of a given species, the proteome projects are not based on a concrete entity, but rather on a dynamic collection of proteins that differ from individual to individual, from cell to cell, and in different life stages. Although there is 'the human genome' as a species-specific set of genes, it is highly unlikely that there will be a single collection of proteins that can be defined as 'the human proteome', because, for instance, there will be many proteomes that are characteristic of specific cell types, developmental stages and disease conditions. Therefore, proteomics represents, at least in part, the next step in understanding how genes are related to biological functions and disease states. Another major aim of proteomics is the identification of new targets for disease intervention and treatment, given the fact that most drug targets are proteins (Huber, L. A., 2003). Proteomic projects intend to perform the systematic analysis of gene function at the protein level, which has direct implications in the understanding of most of the reactions necessary for cell function (Andersen, J. S. and Mann, M., 2000).

The launching of the Human Genome Project provided researches with new and better equipment, as a result of competition between manufacturers. The same is true for proteomics, with **mass spectrometry** and separation/fractionation techniques entering an exponential developmental stage due to competition and market takeover by several companies. For most protein based approaches to gene function, mass spectrometry is the method of choice, allowing the identification of proteins with a very high sensitivity and medium to high throughput. Mass spectrometry instrumentation continues to improve and novel instrumental concepts are also being put into use (Andersen, J. S. and Mann, M., 2000).

The mapping of the **human genome**, one of the major scientific challenges of the past

century, was also one of the biggest hopes for overcoming disease and ageing. It is now evident that genetic information alone is not sufficient for the understanding of cellular processes, with the protein complement of the genome being more complex, because it is not known which messenger RNA (mRNA) and/or alternative splicing form(s) will be translated, and which post-translational modifications will be present in the protein. Consequently, little advances have been made so far in the diagnosis and therapy of most neurodegenerative disorders and ageing processes. The most promising approach, therefore, is to analyse the whole proteome of a cell or tissue, at a distinct stage or status, hopefully leading to the identification of disease-related biomarkers that can be used in diagnosis and drug targeting (Meyer, H. E. et al., 2003).

Although the total number of coding genes in humans appears to be about 25,000 (±5,000), the complexity of the human proteome can, nevertheless, be overwhelming (Righetti, P. G. et al., 2005). An illuminating example on such a vast complexity is the identification of more than 300 distinct types of amino acid modifications in prokaryotic and eukaryotic proteins, each being specific to one or more amino acids, according to the RESID database (release 41) (Garavelli, J. S., 2004). One or more distinct types of modifications can occur in a protein, and in various combinations, extending the structural diversity of a gene product (Boeckmann, B. et al., 2005), with cysteine being the amino acid which undergoes the most possible kinds of alterations. Assuming that there are just 500 true “plasma proteins”, each present in 20 variously glycosylated forms and in five different sizes, one would end up with 50,000 molecular forms. Moreover, considering that the human proteome contains about 25,000 gene products, each having on average 10 splice variants and cleavage products, this would yield a further 250,000 protein forms. Finally, single proteins, such as antibodies, might contain more than 1,000,000 different epitope sequences, which add complexity to the serum content. Therefore, considering the diversity of protein modifications, it is thought that a mammalian proteome may contain more then 10 million different proteins. An additional difficulty in the study of the proteome comes from the fact that there is a large difference in the abundance of the various proteins, which in the serum show a dynamic range of more than 10 orders of magnitude (Huber, L. A., 2003; Boeckmann, B. et al., 2005; Righetti, P. G. et al., 2005).

Given the large number of proteins that comprise the proteome of mammalian species, the dynamic ranges, the differences in tissue proteome, etc, an organization was formed, the **Human Proteome Organization** (HUPO), to promote research and large-scale analysis of the human proteome. By consolidating national proteome organizations into an international

body, HUPO coordinates international initiatives, biological resources, protocols, standards and data for studying the human proteome (Merrick, B. A., 2003). HUPO coordinates several different projects through various departments, with two of them having major relevance for the purpose of this review. The protein standards initiative (**PSI**), and the Human Brain Proteome Project (**HBPP**). The first project was initiated due to the complexity and difficulty to process the proteomics data with the available tools, which do not allow easy interchange of data among different hardware, software and operating systems or application platforms. Currently, not all proteomic data are definitive since identification of a single peptide is not enough to determine the identity of the protein or protein isoform from which it is derived. There is also the problem of analysis and interpretation of enormous volumes of proteomic data coming from different software and equipment, particularly for gel-free approaches. This hurdles marathon resulted in the need of informatics standards for data representation in proteomics to facilitate data comparison, exchange and verification (Ravichandran, V. and Sriram, R. D., 2005). The HBPP intends to define and decipher the normal brain proteome, including polymorphisms and modifications, and to identify brain-derived proteins present in body fluids. It also intends to identify, validate, and functionally characterise disease-related proteins, by techniques and methods available within the participating groups. Brain derived proteins are analysed in the CSF and plasma in order to search for early-onset markers or pharmacological targets in Alzheimer's disease (AD), Down's syndrome, Parkinson's disease (PD), and ageing. The participants of this project created several committees and made decisions about basic strategies such as standardisation guidelines for specimen handling, methods, and data formats, taking into account the international standardisation programmes of the Brain-Net Europe and the HUPO standardisation initiatives (Meyer, H. E. et al., 2003).

Although PCR allows signal amplification in nucleotide studies, a technical capability lacking in protein studies, the analysis of relative **mRNA** expression cannot provide detailed information on all changes in protein content of cell systems (Unwin, R. D. et al., 2006). Furthermore, DNA microarrays have limited utility for the analysis of biological fluids, and for uncovering assayable biomarkers directly in body fluids. Also, changes may occur at the protein level that do not correlate with the original DNA, or even changes at the mRNA level (Hanash, S., 2003). The lack of correlation between changes in mRNA and in protein levels are due to differences in the rates of translation, posttranslational modification, subcellular localization and degradation, underlining the need for proteomic relative quantification techniques (Unwin, R. D. et al., 2006). Proteomic approaches are providing essential data for **clinical practice**, leading to a growing interest in the development of **microarrays** or

biochips for the systematic analysis of thousands of proteins (Hanash, S., 2003). Protein array approaches are now available, to quantify the changes in defined protein targets, selected in a subjective manner.

Proteomics studies facilitate the identification of proteins in a non-hypothesis-driven manner and can be taken forward by several different methodologies (Unwin, R. D. et al., 2006). The clinical proteomics approaches may find important direct bedside applications in the future, with physicians and pathologist using different proteomic analysis at many points of disease management. Several critical elements of patient care and management will be directly targeted: (i) early detection of the disease using proteomic patterns of body fluid samples, (ii) diagnosis based on proteomic signatures as a complement to histopathology, (iii) individualized selection of therapeutic combinations that best target the patient's entire disease-specific protein network, (iv) real-time assessment of therapeutic efficacy and toxicity, and (v) rational redirection of therapy based on changes in the diseased protein network associated with drug resistance (Petricoin, E. F. and Liotta, L. A., 2003). This creates numerous opportunities as well as challenges to meet the needs for high sensitivity and high throughput required for disease-related investigations (Hanash, S., 2003).

All these opportunities created a huge interest in proteomics by the **pharmaceutical industry**, evidenced by implementation of proteomics programmes by most major pharmaceutical companies. However, this interest is accompanied by a cautious attitude, from the prior heavy investment in genomics, with some uncertainty surrounding the adequacy and scalability of proteomics to meet the needs of the pharmaceutical industry. Proteomics approaches can be used not only for the identification of new targets but also to facilitate the identification of drug action mechanisms and to measure toxicity levels, both in the preclinical and clinical phases (Hanash, S., 2003).

1.1.1 - Proteomics in practice

Despite the rapid development of methodologies used in proteomics, there are still considerable limitations (Huber, L. A., 2003). The two major approaches used for protein separation before protein identification, two-dimensional electrophoresis and liquid chromatography, require proper solubilization of proteins and peptides from raw samples. The two other major limitations, the need of removing interfering substances and the proteome dynamic range, can be circumvented, at least to some extent, by sample fractionation and protein enrichment. Several different chemical mixtures and sample

processing steps have been introduced in order to improve the quality of the results obtained in proteomic studies (see below).

A chief difficulty in defining and quantifying a proteome is **sample complexity** (Unwin, R. D. et al., 2006). Besides the number of different proteins, there is an enormous diversity in protein concentrations in most proteomes, with a 10^6 difference in protein abundance in *E. coli* and 10^9 in man. Considering that most mass spectrometers have a dynamic range of 10^4, it is clear that low abundance proteins have to be enriched. When liquid chromatography is used, the coelution of peptides with low and high expression makes difficult the analysis of low abundant peptides since their ionization is suppressed and their spectra masked by high abundance species. This problem is often circumvented by removing high abundant proteins from the sample, and this step is followed by multidimensional separations to reduce the number of proteins that are coeluted (Julka, S. and Regnier, F., 2004). Alternatively, subcellular fractionation is used, providing (i) access to the proteome of intracellular organelles and multiprotein complexes, with a reduction in sample complexity, and (ii) enrichment in low abundance proteins and signalling complexes. Analyzing subcellular fractions and organelles also allows tracking proteins that shuttle between different compartments (Stasyk, T. and Huber, L. A., 2004; Righetti, P. G. et al., 2005). Fractionating organelles, coupling sonication with ultracentrifugation to isolate membrane proteins, or isolating a protein set with a specific property (e.g. tyrosine phosphorylated proteins), are only some of the approaches that have been available for several years, but only now had a great impact on state-of-the-art proteomics, providing increased penetration in the proteome of the organelles (Barnidge, D. R. et al., 2005; Unwin, R. D. et al., 2006).

In recent years subproteomes have been extensively studied by the increasing usage of complex and multistep proteomic methods. Many of these studies assume that there are minimal or no loss of proteins during the proteomic procedures, although several steps involve **sample loss**. This leads to the need of increasing the initial sample size, whenever multiple cleaning, purification, and fractionation steps are considered (Zhou, S. et al., 2005).

1.1.2 - Gel electrophoresis

Two-dimensional gel electrophoresis (2D-SDS-PAGE) allows the separation of proteins according to their isoelectric point by isoelectric focusing, in the first dimension, and according to their molecular weight, by sodium dodecyl sulphate polyacrylamide gel electrophoresis, in the second dimension. Although the initial resolution was estimated in

5000 proteins per gel (O'Farrell, P. H., 1975), under normal and reproducible conditions less then 2000 proteins can actually be resolved in a 2D gel. In order to increase the total number of protein spots detected in a 2D gel, while decreasing spot overlapping, three major approaches can be used: increase the gel size, exploit narrower pH gradients over the same separation distance, or both (Campostrini, N. et al., 2005). The use of narrow pH gradients, also named "zoom" gels [*i.e.*, a series of narrow-range immobilized pH gradient (IPG) gels covering usually only 1 pH unit (Hanash, S. M. et al., 1991)], has become available due to industrialization of IPG gels, and increased the reproducibility and protein resolution, allowing to build "cybergels" (Oguri, T. et al., 2002). These comprise overlapping "zoom" gels, and sometimes overlapping gels with different acrylamide concentrations, with distinct molecular weigh resolution capabilities. In a particular case, the number of spots identified in a pH 3-10 range was increased from 853 spots to 6677 spots by using a 70×67cm cybergel (Campostrini, N. et al., 2005).

2D-SDS-PAGE has several **advantages** and **disadvantages** over other separation techniques. It allows the separation of several hundreds to thousands of proteins and protein isoforms in a single gel (Baker, M. A. et al., 2005), and is compatible with several different visualization techniques (fluorescence, Coomassie and silver staining, radiolabelling and western-blot, among others), allowing the simultaneous quantification of hundreds to thousands of spots and proteins (Unwin, R. D. et al., 2006). The protein visualization method is chosen taking into consideration several issues: intended result (staining for all proteins, or radiolabelling, for visualization for newly synthesized proteins), dynamic range and sensitivity (silver staining is sensitive but has a reduced linear dynamic range when compared to fluorescence staining), availability of visualization instruments (fluorescence methods require expensive equipment for image acquisition) and cost (radiolabelling and fluorescent methods are usually more expensive then silver and Coomassie staining). Another advantage of 2-DE over alternative gel-free peptide-based approaches comes from the fact that protein modifications can induce changes in both mass and pI, with different isoforms and posttranslationally modified protein species being resolved (Unwin, R. D. et al., 2006), quantified and identified from a single gel.

One of the major disadvantages of 2D-gels is the poor performance of membrane proteins, which comprise the largest category of proteins that remains under-identified (Pedersen, S. K. et al., 2003; Unwin, R. D. et al., 2006). Most of them are insoluble in the protein solvents normally used in sample preparation for 2D-electrophoresis, and represent in some cases 30% of the total proteome, as is the case of yeasts (Pedersen, S. K. et al., 2003). In order to

overcome these limitations, several detergents have been tested for their efficacy in the solubilization of membrane proteins and compatibility with 1D and 2D electrophoresis, and it was concluded that a combination of detergents is preferable, but this step usually requires optimization for 2D-PAGE (Churchward, M. A. et al., 2005).

Despite the wide dynamic range of the protein staining methods, the most abundant proteins detected in 2D-gels may be present at >10,000 copies per cell and may obscure proteins expressed at a low level (10-1,000 copies per cell). Prefractionation (Unwin, R. D. et al., 2006) and "zoom" gels increase resolution and protein loading (Westbrook, J. A. et al., 2001), allowing to overcome these difficulties. The detection and quantification of low abundant proteins present in the vicinity of poorly resolved protein smears or streaks may also be made difficult due to poor focusing at pH>7. The smears and streaks can result mainly from protein intra- and/or inter-molecular disulfide bridges (-S-S-) following the oxidation of the cysteinyl thiol groups (-SH). This occurs primarily due to the depletion of the reducing agent, such as dithiotreitol (DTT) or its isomer dithioerythritol (DTE), in the basic pH range, due to migration towards the anode during the IEF. In an environment lacking a reducing agent, the cysteinyl thiol groups tend to crosslink again, leading to the restoration of the disulfide bridges (Pennington, K. et al., 2004; Bai, F. et al., 2005). Different strategies have been used to overcome this issue: decreasing the protein sample concentration, anodic cup-loading, shortening IEF duration, addition of a DTT wick to replenish DTT at the cathode, or using an alternative reducing agent such as hydroxyethyldisulphide (HED) (Pennington, K. et al., 2004; Bai, F. et al., 2005). An alternative approach consisted in preparing samples in a way to prevent the regeneration of the crosslinks between cysteinyl thiols, inducing a permanent modification of the free thiol groups through alkylation (Herbert, B. et al., 2001; Bai, F. et al., 2005). Unfortunately, both compounds tested for this purpose, iodoacetamide and acrylamide, changed the gel patterns or generated extra artifatual spots in 2-DE maps. Iodoacetamide also reacts with methionine, lysine and histidine, and the lack of specificity to the cysteinyl thiol groups in the alkylation reaction leads to the formation of multiple alkylating products with various pIs and/or molecular weights, further increasing mass spectra complexity (Bai, F. et al., 2005). Other compounds have been tested, but the drawbacks associated did not overcome the benefits (Herbert, B., 1999; Bai, F. et al., 2005).

Once most of the limitations have been overcome, 2D-SDS-PAGE is performed successfully, and gel images are acquired, image analysis is then performed using the several software packages available in the market, which make use of different approaches and distinct algorithms. Their main function is to perform spot detection, quantification, normalization,

matching, and data analysis across several gel images. Relevant quantitative information is combined in latter steps together with protein identification, usually by mass spectrometry.

In summary, two-dimensional gel electrophoresis has met several important improvements in the last 10 years. The understanding of its drawbacks allowed researchers and industry to overcome the limitations by introducing new equipment, different chemical mixtures, automation, large scale production of IPG strips, etc. Although many drawbacks have been overcome, new challenges are posed every year. Comprehensive gel analysis with differential expression can be performed, and the relevant spots identified in the latter steps, without the need of hundreds of thousand euros of investment in a mass spectrometer for data acquisition. On the other hand, liquid-based approaches, such as liquid chromatography, are not used alone and require the use of a mass spectrometer for data acquisition and subsequent analysis.

1.1.3 - Liquid chromatography

Two major approaches are presently used for large scale protein profiling and quantification, the gel-based and liquid-based approaches. In the latter case, liquid chromatography is the method of choice, with the capability of combining different separation techniques, and using two (2D-LC, two-dimensional liquid chromatography) or even more fractionation steps (MudPIT, multidimensional protein identification technology). Liquid chromatography techniques (usually associated with proteomic studies) allow sample fractionation based on the principle that the analyte interacts with a column and is subsequently eluted with increasing concentration of a mobile phase (as in the case of strong cation exchange and reverse phase). Different analytes with distinct affinities to the columns will elute at different concentrations of the mobile phase, and hence having different retention times (Aebersold, R. and Mann, M., 2003). Combining two or more types of chromatographic separation (e.g. size exclusion with reverse phase) enables further fractionation of complex mixtures, thereby increasing both the number of peptides identified and coverage of the proteome (Washburn, M. P. et al., 2001; Wang, H. and Hanash, S., 2005). Liquid chromatography has been mainly used to fractionate complex peptide mixtures prior to identification by mass spectrometry (Wang, H. and Hanash, S., 2005; Unwin, R. D. et al., 2006). Although liquid chromatography was initially used after direct incubation of complex samples with trypsin, several different approaches are presently used in combination, e.g.: (i) two peptide separations, usually

combining strong cation exchange with reverse phase; (ii) reverse phase separation of intact proteins followed by reverse phase separation of tryptic peptides; (iii) combination of gel-based and liquid based approaches (GeLC). Besides these "classic" fractionation strategies, the use of affinity columns and immunocapture are becoming more common, including biotin protein tagging and resin purification, and IMAC phosphopeptide enrichment (Wang, H. and Hanash, S., 2005).

The major advantage of peptide fractionation by liquid chromatography, when compared to 2D-SDS-PAGE of proteins, comes from the fact that peptides are more stable then proteins. This technique is usually coupled with mass spectrometry, allowing the direct identification, and in some cases quantification, of proteins from complex mixtures, resulting in time saving.

1.1.4 - Mass spectrometry

Mass spectrometry is a technique based on instruments that combine ionization techniques, a mass analyser and a detector, in order to determine the mass of a given analyte. For the purpose of this review, only MALDI-TOF-TOF and ESI-Qq-TOF will be discussed.

The identification of protein spots harvested from 2D gels is usually carried out by **MALDI-TOF** and MALDI-TOF-TOF, due to their high throughput and cost per spot analysed. Gel spots from 2D gels are usually digested, for instance with trypsin, and after peptide extraction the proteins are identified by ionization of the peptides followed by determination of their molecular weight. Peptides are ionized by energy transfer from a laser into a matrix (Matrix Assisted Laser Desorption Ionization - MALDI), and their molecular weight is estimated by the time required to travel over a defined path (Time Of Flight - TOF) when subjected to an intense electric field. This time is closely related to the molecular weight, and can be determined through the equation $\mathbf{m/z=(2eU/L^2)t^2}$ [**m**, mass of the ion; **z**, charge of the ion (mainly +1 for peptides ionized by MALDI); **e**, elementary charge; **U**, acceleration voltage; **L**, length of flight tube; **t**, time of flight]. For each given experimental condition using MALDI-TOF, all variables but two are known, t, measured by the instrument, and **m**, determined after measuring the time of flight of the peptide. In the following step, the molecular weight of the peptides, determined by the mass spectrometer, is subjected to database search algorithms, comparing possible *in silico* digestions of known genome sequences with obtained spectra from a given spot digest (Peptide Mass Fingerprint - PMF) (Cottrell, J. S., 1994). Addition of information regarding peptide fragmentation, whenever provided by the equipment, as is the case of TOF-TOF instruments, further increases identification scoring.

Besides peptide analysis, MALDI-MS has become a valuable tool to address a broad range of questions in many areas of biomedical research requiring full proteome analysis. In 1999, MALDI-MS imaging was introduced for protein analysis from intact biological tissues. MALDI tissue profiling allows rapid detection of over a thousand peptides and proteins from a variety of tissues, with its application having a special interest in disease processes, mainly when combined with histological staining prior to MALDI analysis, tissue protein profiling and imaging, and data analysis. The amount of information obtained from tissue protein profiling and imaging is considerably large, but does not replace existing molecular biological techniques. Rather, these tools together provide a comprehensive understanding and support new discoveries in biology and medicine (Caldwell, R. L. and Caprioli, R. M., 2005). Besides this increase in MS applications, there has also been a considerable upgrade in instrument sensitivity and speed, accompanied with better sample preparation and purification procedures, allowing deeper digging into the proteome (Unwin, R. D. et al., 2006).

Electrospray ionization (ESI) is normally employed when mass spectrometry is used in combination with liquid chromatography, although LC-MALDI has become a common practice. For electrospray ionization, peptides are usually eluted from the chromatography column in an acidic mobile phase, resulting mainly in positively charged peptides. Once in the electrospray needle, and in the presence of a high voltage, solvents nebulize along with the peptides. These charged droplets lose water when passing through a nitrogen curtain, leading to an increase in repulsion between positively charged peptides, and resulting in single peptide ions, ready for MS and MS/MS analysis (Fig. 1.1). Fragmentation spectra provide more information about a given peptide, allowing search algorithms to identify the protein in the database, even if the peptide is present in a complex mixture. Liquid chromatography is usually coupled to tandem mass spectrometers able to induce peptide fragmentation, such as ion-traps, triple quadrupoles or hybrid systems [e.g. ion-trap/triple quadrupoles or quadrupole/time-of-flight (**Q-TOF**) instruments]. The Q-TOF instruments combine the superior mass selection of a quadrupole, with the collision-induced dissociation (CID) or peptide fragmentation, in addition to the accuracy, resolution and rapid full scan capabilities of TOF technology (Steen, H. et al., 2001).

Although MS provides sensitive detection and identification of proteins and peptides, it is not directly **quantitative**, with two peptides from the same protein possibly generating different intensity signals, because differences in amino acid composition and sequence will affect the ionization efficiency. Differences in sample composition, in addition to the age, condition (e.g.

degradation due to solvents) and even the position of the electrospray needle can affect the ionization efficiency, changing the peptide signal, and this represents some of the causes of quantification related problems (Unwin, R. D. et al., 2006). In order to attain high throughput quantification by mass spectrometry in large proteomic studies, several methods have been developed, with chemically identical but isotopically distinct tags being used to modify different peptide populations. This allows samples from different experimental conditions, each containing a distinct label, to be pooled and analyzed by liquid chromatography, with identical peptides eluting at the same time (coeluting) and ionizing with the same efficiency. A relative or absolute quantification of the peptides is obtained by comparing their signal intensities with a defined isotope-induced mass difference (Andersen, J. S. and Mann, M., 2000; Unwin, R. D. et al., 2006). Several methods are currently being used for this purpose: iTRAQ (Isotope Tags for Relative and Absolute Quantitation), SILAC (Stable Isotope Labelling with Amino acids In Cell culture), ICAT (Isotope Coded Affinity Tag), ICPL (Isotope Coded Protein Labelling), ^{18}O labelling, among others (Blagoev, B. et al., 2003; Unwin, R. D. et al., 2006). Briefly, besides the label itself, these methods are mainly different in the labelling step, with SILAC performing the labelling by the time proteins are synthesized inside the cells. ICAT and ICPL label proteins prior to analysis, ^{18}O labels peptides when proteins are proteolyticaly digested, and iTRAQ labels peptides. All methods, but iTRAQ, allow quantification in the MS spectra, while iTRAQ only allows quantification in the fragmentation

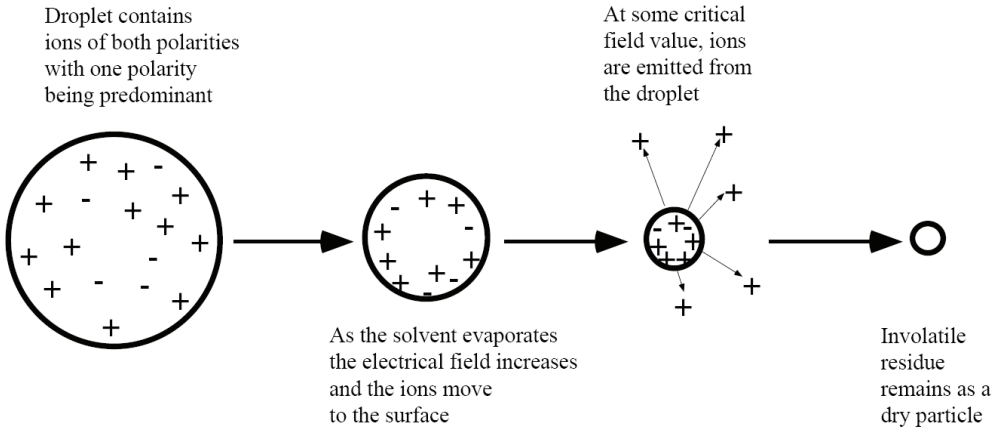

Figure 1.1 – Ion evaporation during electrospray ionization. Each charged droplet contains solvent and both positive and negative ions, with ions of one polarity being predominant (due to the acidic medium). A simple view of the droplet as a conducting medium suggests that excess charges reside at the droplet surface. As the solvent evaporates, the electrical field at the surface of the droplet increases due to the decreased radius of the droplet. At a given point, a critical field is reached at which ions are emitted from the surface. Eventually, all the solvent will evaporate from the droplet, leaving a dry particle consisting of the non-volatile components of the sample solution (Biosystems, A., 2004).

(MS/MS) spectra. This method allows quantification of up to four different samples simultaneously, by incorporating four isobaric tags that label the N terminus of every peptide (along with free amines in lysine side chains). These isobaric tags, with approximately 145Da, contain a reporter group (114, 115, 116 or 117Da), a balance group (31, 30, 29 or 28Da) and a peptide reactive group. Although equal peptides contain different tags, they behave similarly in the chromatography column and in the mass spectrometer. Once inside the mass spectrometer, identical peptides from different samples are fragmented, yielding a fragmentation spectra used for protein ID. Besides this data, each peptide also produces a fragment from its reporter group (114, 115, 116 or 117Da). Quantification becomes possible by the use of software that compares the peak intensity of reporter group ions in the fragmentation spectra. The relative abundance of these reporter ions provides relative quantification or absolute quantification if one of the ions is properly quantified before analysis. This labelling method offers several advantages: first, all peptides (in theory) are labelled, allowing multiple peptides from the same protein to be quantified and increasing confidence in protein quantification; second, because the tags are isobaric, the signal from up to four samples is summed in MS mode, providing an increase in sensitivity; and third, because peptides are isobaric, the MS spectra complexity is not multiplied by the number of different tags used, as is the case of the other methods (Unwin, R. D. et al., 2006).

1.1.5 - Bioinformatics

Large scale analysis of proteome changes requires the use of software, in order to align, group, and transform data to understand its biological significance. Besides software packages used to control equipment, proteomics data have to be processed, changed according to standards, subjected to database comparison, and evaluated, so that a protein can be identified and, in some cases, quantified. When this process is concluded, there is still the need of data interpretation, ranging from biomarker discovery to interpretation of biological pathways. This is accomplished by using some of the analysis tools available, but this is not yet standardized, as is the case of protein identification by using different databases as UniProtKB/Swiss-Prot or NCBI. Although a given protein is the result of a gene being translated, it will receive different (but similar) names, depending on the database used, and distinct accession numbers, depending on the final protein translated (full length protein, precursor, truncated,…). Accession numbers and gene names are very useful at this stage because they also allow gathering information from multiple databases. The original

concept of one gene-one protein is now obsolete, and Swiss-Prot annotates cellular mechanisms leading to an amino acid sequence different from the one expected by standard translation of the nucleotide sequence. Various native proteins, including structural proteins, hormones, neuropeptides and secreted enzymes, are cleaved to achieve their mature form, hence receiving a different accession number (Boeckmann, B. et al., 2005).

The publication of large proteomic datasets, as the ones coming from LC-MS/MS experiments of complex samples, poses new and significant challenges for authors, reviewers, and readers, as universally accepted and widely available computational tools for validation of the published results are not yet available (Carr, S. et al., 2004). There is the need of **data validation** in order to identify possible false positives. Incorrect matches result mainly from the use of low-quality MS and/or peptide MS/MS data to search the databases. However, even high-quality data can produce invalid identifications if, for example, a given peptide sequence is not in the database being searched. Many different **algorithms** are carefully used for peptide and protein assignment (*e.g.* MSTag, Mascot, SEQUEST, SpectrumMill, Sonar, etc.), and each has unique rules for scoring, to move the most probable peptide assignment to the top of the "hit" list. In addition, new filtering criteria are being developed that, when layered onto the results from the above algorithms, help to eliminate a certain additional percentage of false positives (Carr, S. et al., 2004). Finally, a new database independent scoring method (S-score) was designed, that is based on the maximum length of the peptide sequence tag provided by MS/MS data (Savitski, M. M. et al., 2005). Besides these, other proteomic related algorithms are under development, as is the case of 2D-gel analysis software, including spot detection and matching (Kaczmarek, K. et al., 2004).

Two of the largest **databases** used for protein identification are the **NCBI** and the **UniProtKB/Swiss-Prot** databases. The first database has more entries, since some of them are redundant and there is no correlation between a given protein entry and other databases, as occurs with the UniProtKB/Swiss-Prot database. In the latter database, once a protein is identified, it retrieves an accession number, which can easily be used across other European databases to obtain additional information, such as retrieving gene ontology information from EBI (European Bioinformatics Institute), and information from several databases using Bioinformatics **Harvester** (http://harvester.embl.de). Even though UniProtKB/Swiss-Prot entries generally correspond to a gene rather than a protein, it stores information regarding protein variety and functional diversity (Boeckmann, B. et al., 2005).

Harvester is an interesting "bioinformatic meta search engine for genes and protein-associated information". It works for human, mouse and rat proteins, crosslinking 16 popular

bioinformatic resources and allowing cross-searches (Liebel, U. et al., 2005). Another project, the Biomolecular Interaction Network Database (**BIND**) (http://bind.ca), archives information regarding biomolecular interaction, reactions, complexes formed and pathway information. The aim of this project is to curate the details about molecular interactions that arise from published experimental research and to provide this information, as well as tools to enable data analysis, freely to researchers worldwide. BIND has developed methods for visualization by amplification of the annotations of genes and proteins, thereby facilitating the study of molecular interaction networks (Bader, G. D. et al., 2003; Alfarano, C. et al., 2005). Another database, **GeneNote** (**Gene No**rmal **T**issue **E**xpression), collects the results of the hybridization intensity of two replicates processed and analyzed to yield the complete transcriptome for twelve human tissues. This information was gathered using the Affymetrix GeneChip HG-U95 set, which includes 62,839 probe-sets, and it was produced to portrait complete gene expression profiles in healthy human tissues (Shmueli, O. et al., 2003).

The **functional interpretation** of the results obtained in studies leading to the identification and quantification of the proteome in a large scale represents a time consuming and challenging task, with the most interesting proteins being usually presented in long lists with no biological meaning (Busold, C. H. et al., 2005). Combining protein expression levels with information regarding their molecular function, cellular component and biological processes in which they are involved, results in protein grouping according to their probable biological meaning (Andersen, J. S. et al., 2005). This grouping is made possible by using information from the **Gene Ontology** (GO) project (http://www.geneontology.org/), which provides structured and controlled vocabularies and classifications covering several domains of molecular and cellular biology, and are freely available for community use in the annotation of genes, gene products and sequences. This project is a collaborative effort to address two aspects of information integration: to provide consistent descriptors for gene products retrieved from different databases and to standardize classifications for sequences and sequence features (Gene Ontology Consortium, 2004). The GO project has three major goals: (i) to develop a set of controlled, structured vocabularies - known as ontologies - to describe key domains of molecular biology, including gene product attributes and biological sequences; (ii) to apply GO terms in the annotation of sequences, genes or gene products in biological databases; and (iii) to provide a centralized public resource allowing universal access to the ontologies, annotation data sets and software tools developed for use with GO data. Ontologies provide conceptualizations of domains of knowledge, and facilitate both the communication between researchers and the use of domain knowledge by computers for

multiple purposes. The three main categories are (i) *Molecular Function*, which describes activities, such as catalytic or binding activities, at the molecular level (e.g. “receptor signalling protein activity”), (ii) *Biological Process*, which describes biological goals accomplished by one or more ordered assemblies of molecular functions (e.g. “cell death”), (iii) *Cellular Component*, which describes locations, at the levels of subcellular structures and macromolecular complexes (e.g. “nuclear inner membrane”). Every annotation is related to a source, which may be a literature reference, another database or a computational analysis. Furthermore, the annotation indicates the type of evidence the cited source provides to support the association between the gene product and the GO term (Gene Ontology Consortium, 2004). **GoMiner** is a software package that organizes lists of genes of interest (e.g. under- and overexpressed genes) for biological interpretation in the context of the gene ontology, providing quantitative and statistical data (Zeeberg, B. R. et al., 2003). Therefore, GOMiner allows the processing of data in a large scale, combining gene ontology and differential gene expression.

1.2 - Neurotrophins and neurotrophins receptors

Neurotrophins are a family of highly conserved proteins that play important roles in the regulation of axonal and dendritic growth and guidance, synaptic structure and connections, short- and long-term changes in synaptic activity, and in neuronal survival and neuroprotection (Poo, M. M., 2001; Huang, E. J. and Reichardt, L. F., 2003; Lu, B. et al., 2005). Furthermore, neurotrophins contribute to glial cell development and survival (Althaus, H. H. and Richter-Landsberg, C., 2000; Syroid, D. E. et al., 2000; Chan, J. R. et al., 2004; Husson, I. et al., 2005; Yamauchi, J. et al., 2005). This group of low-molecular weight proteins includes nerve growth factor (NGF), brain-derived neurotrophic factor (BDNF) and neurotrophins-3 and -4/5 (NT-3 and NT-4/5). The cellular effects of neurotrophins are mediated by activation of two classes of receptors: the Trk (tropomyosin-related kinase) family, which includes the TrkA, TrkB and TrkC receptors, endowed with tyrosine kinase activity, and the p75 neurotrophin receptor ($p75^{NTR}$), a member of the tumour necrosis factor (TNF) receptor family (Chao, M. V., 2003; Huang, E. J. and Reichardt, L. F., 2003; Barker, P. A., 2004; Teng, K. K. and Hempstead, B. L., 2004). The diversity of the Trk receptors is further enhanced by the existence of TrkB and TrkC receptors lacking the tyrosine kinase domain or containing inserts in the intracellular domain that affect the signalling properties of the receptors (Huang, E. J. and Reichardt, L. F., 2003). NGF binds to TrkA receptors, BDNF and NT-4/5 to TrkB receptors, and NT-3 to TrkC (which may also target TrkB receptors). In contrast with the specificity displayed by the Trk family of receptors, the $p75^{NTR}$ binds both the mature form of the neurotrophins and their uncleaved (precursor) forms (proneurotrophins) (Lee, R. et al., 2001). The Trk receptors and the $p75^{NTR}$ may be expressed by the same cell, where they coordinate and modulate the neuronal response to neurotrophins. While the former receptors tend to mediate signals leading to cell survival and growth, the $p75^{NTR}$ may provide a trophic effect or cause cell death (Friedman, W. J. and Greene, L. A., 1999).

1.2.1 - BDNF

Brain-derived neurotrophic factor (BDNF) is one of the most extensively studied neurotrophins, playing important roles in neurogenesis, development of the nervous system, regulation of synaptic transmission, learning and memory formation and in several disorders of the nervous system (Binder, D. K. and Scharfman, H. E., 2004). BDNF is the most

abundant neurotrophin in the brain (Tardito, D. et al., 2006) with its mRNA being widely distributed in the CNS (Binder, D. K. et al., 2001), not only in neurons but also in glial cells. In the mouse hippocampus, BDNF mRNA and its protein are expressed from embryonic stage until adulthood. A stepwise increase in BDNF protein levels is observed in the mouse hippocampus from embryonic stage to postnatal day 7 (P7), and the protein levels are maintained throughout the adult lifetime (Ivanova, T. and Beyer, C., 2001).

The BDNF **gene** is located on the reverse strand of chromosome 11p13 and encodes a precursor peptide (pro-BDNF) that is proteolytically cleaved to form the mature protein (Craddock, N. et al., 2005). The structure of the rat BDNF gene is relatively complex, with four 5' noncoding exons linked to separate promoters and one 3' exon encoding the entire open reading frame of the biologically active protein (Timmusk, T. et al., 1995; Mellstrom, B. et al., 2004). The relative importance of the various regulatory regions of the BDNF gene on its expression in vivo was investigated using transgenic mice with six different promoter constructs of the BDNF gene fused to the chloramphenicol acetyl transferase reporter gene. Expression analysis revealed that regulation of BDNF expression is differentially controlled by the various regions in vivo (Figure 1.2), with specific regions of the central and peripheral nervous system regulating differently the expression of the heterologous genes (Timmusk, T. et al., 1995). BDNF gene expression can be regulated by several **promoters**, with promoters I and III or IV playing a key role in the response to neuronal activation in the brain. The influx of Ca^{2+} through voltage-sensitive calcium channels upregulates preferentially $BDNF_{III}$ transcripts in cultured cerebrocortical neurons. Ca^{2+} entry through synaptic NMDA receptors or throught L-type Ca^{2+} channels also regulates BDNF gene expression in cortical neurons (Mellstrom, B. et al., 2004), through CREB (CRE Binding protein) phosphorylation (Mellstrom, B. et al., 2004; Hajszan, T. and MacLusky, N., 2006). In contrast, the influx of Ca^{2+} through extrasynaptic NMDA receptors opposes the increase in CREB phosphorylation induced by activation of synaptic NMDA receptors (Fig. 1.2) (Mellstrom, B. et al., 2004). The expression of the BDNF gene in the hippocampus is also regulated by oestrogen, which induces striking changes in BDNF synthesis with every ovarian cycle (Hajszan, T. and MacLusky, N., 2006).

The BDNF gene shows a common polymorphism, leading to a substitution of a valine (Val) to methionine (Met) at position 66 in the prodomain ($BDNF_{Met}$) (Chen, Z. Y. et al., 2004). Heterozygous humans for the polymorphism show increased susceptibility to neurological disorders, including Alzheimer's disease (AD), Parkinson's disease (PD), bipolar disorder (BD), depression, eating disorder, obsessive compulsive disorder (Hall, D. et al., 2003), and

juvenile bipolar disorder (JBD) (Althoff, R. R. et al., 2005). Furthermore, heterozygous humans for this polymorphism suffer from memory impairment, resulting from a reduction in activity-dependent secretion of $BDNF_{Met}$. This polymorphism represents the first correlation between a change in BDNF and clinical dysfunction. Further studies concluded that BDNF polymorphism affects the trafficking of the neurotrophin in neuronal cells. Thus, when expressed together in the same cell, $BDNF_{Met}$ dimerises with $BDNF_{Val}$ changing its trafficking and decreasing its sorting to the regulated secretory pathway (Chen, Z. Y. et al., 2004).

BDNF is a 27kDa basic protein of noncovalently linked 13.5kDa subunits (Rosenthal, A. et al., 1991). The most common **structure** of BDNF (Fig. 1.3 A-B) comprises eight β-strands that contribute to four antiparallel pairs of twisted β-strands, locked by a cystine knot formed by three disulfide bonds. BDNF shares a high sequence and structure homology with the other neurotrophins, NT3, NT4 and NGF (Fig. 1.3 C) (Robinson, R. C. et al., 1999).

Specific stimuli that raise the $[Ca^{2+}]_i$ induce the transcription of the BDNF mRNA, which upon **translation** gives rise to the **precursor** form of the neurotrophin (pro-neurotrophin) (Fig. 1.4A). Pro-neurotrophins are cleaved to their **mature** form by intracellular (Fig. 1.4C) or extracellular proteases (Fig. 1.4D). Some of these intracellular proteases belong to the subtilisin/kexin-like convertase family of proteases, and include furin, PACE4, PC1 and PC5 (Seidah, N. G. et al., 1996). Extracellular proteases involved in proneurotrophin cleavage include plasmin (Lee, R. et al., 2001; Pang, P. T. et al., 2004), formed from plasminogen by

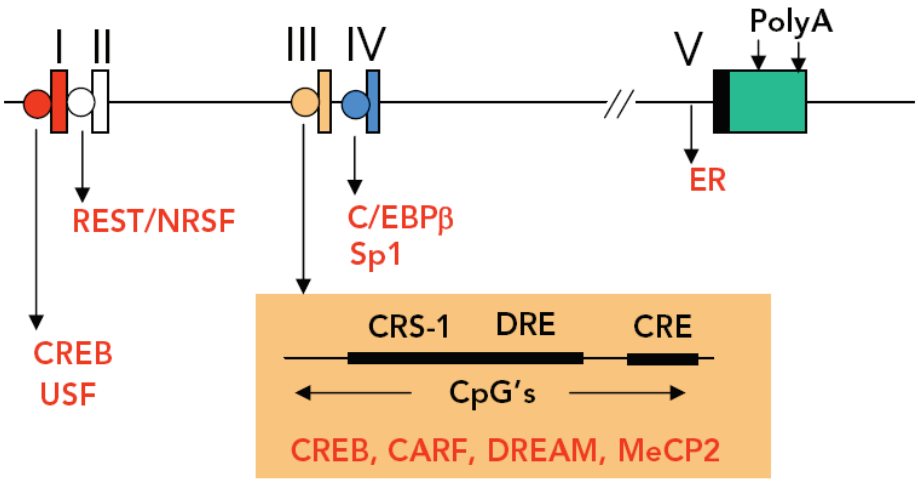

Figure 1.2 – BDNF gene structure. BDNF gene comprises five exons (boxes) and four regulatory regions (circles). The coding region (black area) is located in the 5' end of exon V, preceding two alternative polyadenylation sites (arrows). Transcription factors (red text) operate at each promoter regulating gene expression. Putative regulatory sites located in the 5′ flanking regions of exon III control its expression: calcium responsive sequence (CRS-1), cAMP responsive element (CRE), downstream regulatory element (DRE), and CpG islands (Mellstrom, B. et al., 2004).

the action of tissue plasminogen activator (tPA) (Lu, B. et al., 2005), and metalloproteinases (Lee, R. et al., 2001).

BDNF is sorted into the regulated pathway, while other neurotrophins are mainly sorted into the constitutive pathway (Brigadski, T. et al., 2005; Vaynman, S. and Gomez-Pinilla, F., 2005). This differential sorting has been attributed to the selective binding of pro-BDNF to sortilin in the trans-Golgi network, allowing the proper folding and interaction of pro-BDNF with carboxypeptidase E (CPE) (Fig. 1.4B). This process allows the sorting of pro-BDNF into the regulated secretory pathway (Chen, Z. Y. et al., 2005; Lou, H. et al., 2005) and interestingly, co-expression of BDNF with NT-3 deviates NT-3 from the constitutive secretory pathway to the regulated secretory pathway (Farhadi, H. F. et al., 2000). BDNF-containing vesicles are transported either to dendritic spines or to varicosities, in axons, by anterograde transport (Fawcett, J. P. et al., 1997; Kohara, K. et al., 2001; Adachi, N. et al., 2005). In the majority of BDNF expressing neurons the neurotrophin shows a distal dendritic targeting, and is stored within secretory granules; these vesicles exist in distinct prerelease states, differing in the intragranular pH, and this heterogeneity is responsible for the differential release of BDNF (Brigadski, T. et al., 2005).

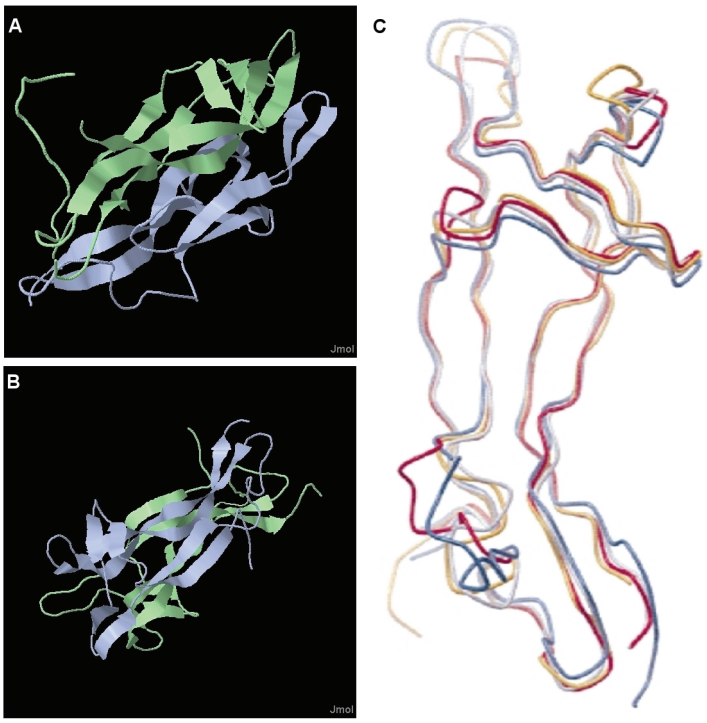

Figure 1.3 – BDNF/NT-3 heterodimer. (A-B) Different views showing the main structure of the heterodimer, and its main secondary conformations (β-strands) (Robinson, R. C. et al., 1999). (C) Neurotrophin structure homology showing mouse NGF (light blue), and human BDNF (red), NT3 (yellow) and NT4 (dark blue), in the same orientation (Robinson, R. C. et al., 1999).

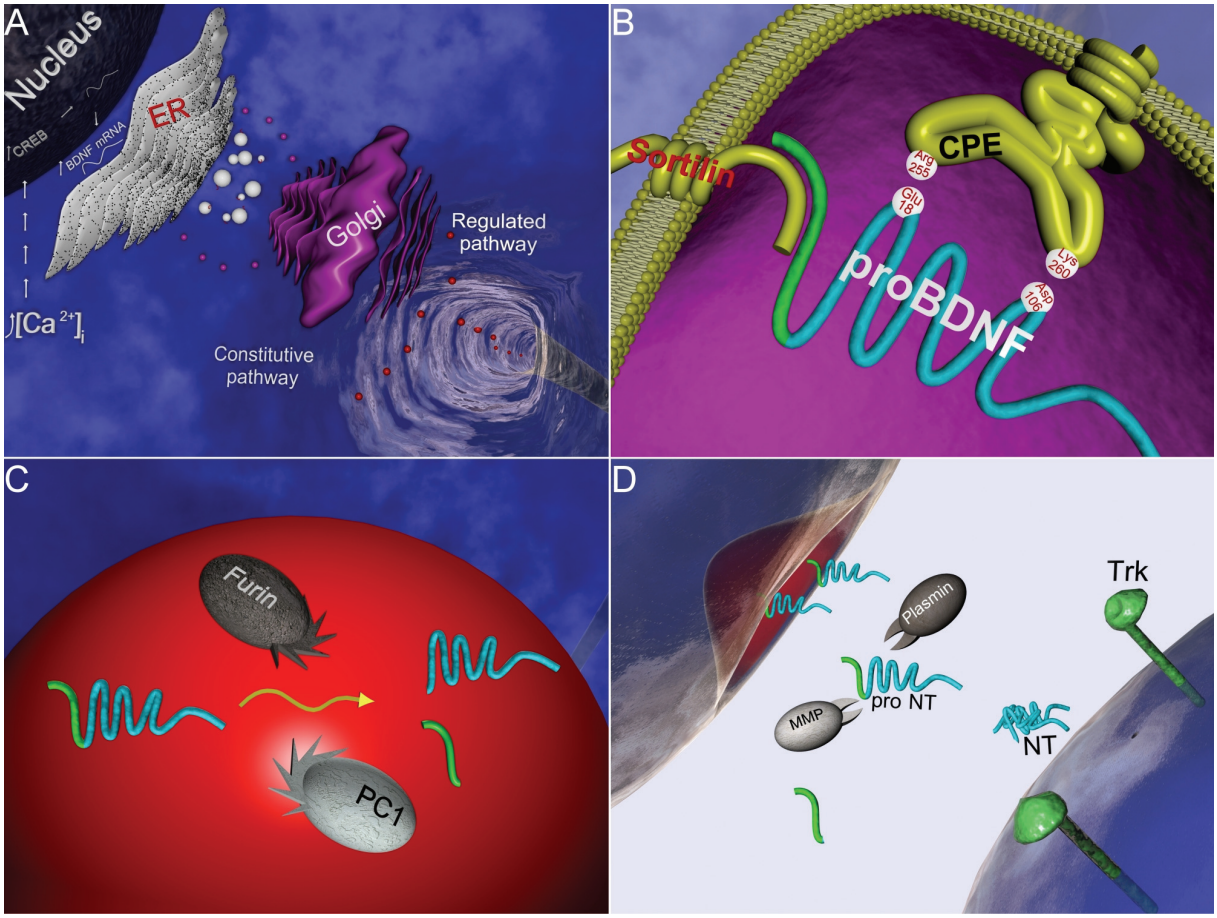

Figure 1.4 – BDNF trafficking: from the gene to the regulated secretion. (**A**) BDNF expression can be upregulated following cell stimulation and $[Ca^{2+}]_i$ increase. mRNA for BDNF is then translated in the rough endoplasmic reticulum (ER). BDNF containing vesicles are translocated from the ER to the *cis*-Golgi complex. (**B**) In the *trans*-Golgi membrane complex, pro-BDNF interacts with sortilin through its pro-domain. This binding allows the proper conformation change that results in the interaction of the BDNF acidic residues glutamate-18 and aspartic acid-106 with the basic residues arginine-255 and lysine-260 of carboxipeptidase E (CPE). CPE allows the recruitment of pro-BDNF to the regulatory secretory pathway. (**C, D**) Neurotrophins can be processed to their mature form through the action of furin or PC1, but BDNF is mainly cleaved by the extracellular protease plasmin (Pang, P. T. et al., 2004); metalloproteinases (MMP) are also able to cleave pro-BDNF (Lee, R. et al., 2001). Once released to the synaptic cleft, mature BDNF homodimers bind to their cognate receptor TrkB (See also Movie 1).

1.2.2 - Neurotrophin Receptors

Neurotrophins bind to tropomyosin-related kinase (Trk) receptors, with the receptor cognate of BDNF (**TrkB**) having its mRNA located throughout the brain (Binder, D. K. et al., 2001), including glial cells (Ivanova, T. and Beyer, C., 2001). The receptor is expressed abundantly all over the CNS with the hippocampus being particularly enriched in TrkB and BDNF gene products (Vaynman, S. and Gomez-Pinilla, F., 2005). Immunostaining of spinal cord sections against full length TrkB ($TrkB^{FL}$) and NeuN, a neuron specific marker, demonstrated for the first time that numerous $TrkB^{FL}$-positive cells of various sizes coexpressed NeuN (Skup, M. et al., 2002), indicating that $TrkB^{FL}$ is located in neuronal cells. TrkB receptors share a high degree of homology with the other tyrosine kinase receptors, with three leucine rich 24-residue motifs flanked by two cysteine clusters (Fig. 1.5). Two immunoglobulin-like domains precede the single transmembrane domain and the tyrosine kinase intracellular domain. The cytoplasmic portion of the receptor contains several tyrosines that can be phosphorylated, regulating tyrosine kinase domain activity. Binding of BDNF to TrkB receptors leads to their transphosphorylation on tyrosine residues, followed by recruitment and phosphorylation of adaptor/signalling proteins, which initiate different signalling cascades (Huang, E. J. and Reichardt, L. F., 2003).

The human $TrkB^{FL}$ has 822 amino acids and 91,999 Da (Gasteiger, E. et al., 2003), whereas the **truncated TrkB** (tTrkB) has a similar structure but lacks the cytoplasmic tyrosine kinase domain (Alderson, R. F. et al., 2000; Huang, E. J. and Reichardt, L. F., 2003). Different isoforms of tTrkB are produced by alternative splicing (T1 and T2 in rat; T1 and T-shc in humans) (Nagappan, G. and Lu, B., 2005). The T1 isoform contains 477 amino acids, 53,051Da, while the T-shc isoform contains 537 amino acids, corresponding to 59,166Da (Gasteiger, E. et al., 2003). T1 is mainly expressed in the brain and can form heterodimers with $TrkB^{FL}$, acting as a dominant negative and inhibiting BDNF signalling. Therefore, T1 isoforms control the synaptic signalling mechanisms induced by BDNF (Nagappan, G. and Lu, B., 2005). Compared to the remaining life stages of the rat, in the prenatal state there is an increase in the levels of tTrkB all over the brain, particularly in the hippocampus, with TrkB levels remaining almost unchanged. Embryonic rat hippocampal glial cells maintained in vitro also express tTrkB mRNA, while microglial cells are not endowed with this transcript. In astrocytes, $TrkB^{FL}$ mRNA was not detected, but tTrkB mRNA was identified by in situ hybridization, in the adult nervous system, in cells lining the third ventricle, cells of the choroids plexus, and in Schwann cell of the sciatic nerve (Alderson, R. F. et al., 2000).

Although high levels of TrkB mRNA have been observed in rat brain cultures devoided of neuronal cells, most TrkB transcripts present in these cells code for the truncated form, explaining in part why northern blot analysis of $TrkB^{FL}$ was unable to detect the transcript in these cultures (Condorelli, D. F. et al., 1994).

The complex formed by the neurotrophin BDNF bound to the tTrkB receptors is endocytosed and accumulated in the intracellular pool of rat hippocampal astrocytes and Schwann cells (Alderson, R. F. et al., 2000). These trapped neurotrophins were stable for more than 48h and could be released back to the incubation medium in a time and temperature dependent manner. This revealed a different mechanism for the regulation of intracellular and extracellular concentrations of neurotrophins (Biffo, S. et al., 1995; Alderson, R. F. et al., 2000). tTrkB seems to also play a role in the availability and diffusion of BDNF, capturing the neurotrophin that diffuses out of the synaptic cleft and concentrating BDNF to sites of release, probably explaining its high levels during development (Biffo, S. et al., 1995; Bramham, C. R. and Messaoudi, E., 2005). BDNF can also be internalized through $TrkB^{FL}$, in hippocampal neurons, and released upon high-frequency stimulation (HFS) (Santi, S. et al., 2006).

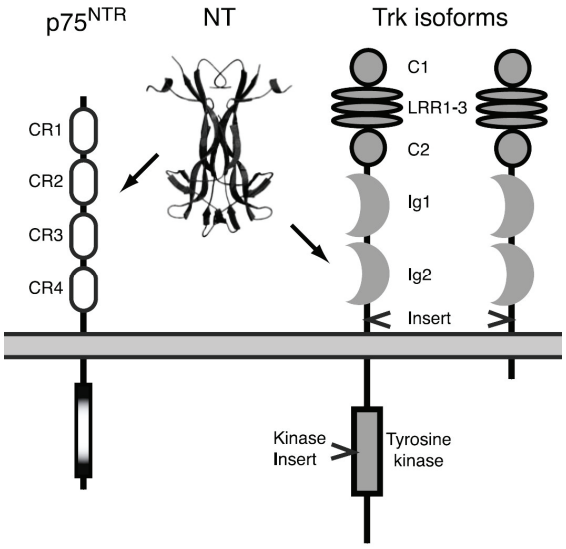

Figure 1.5 – Neurotrophin receptors. Trk receptors contain several distinct extracellular domains: cysteine clusters (C), leucine-rich repeats (LRR) and immunoglobulin-like domains (Ig). The Insert domain refers to the alternative splice region responsible for the ligand-binding specificity. Trk receptors possess a single transmembrane domain and a single cytoplasmic tyrosine kinase domain. Ig2 is the major ligand-binding interface in TrkB receptors. The truncated form of the receptor, lacking its intracellular kinase domain, is represented on the right. $p75^{NTR}$ structure is also represented on the left. The extracellular domain of this receptor contains four cysteine-repeat domains (CR), with CR2 and CR3 implicated in neurotrophin-binding. $p75^{NTR}$ also contains a single transmembrane domain and a single intracellular domain, called “death domain” (DD), similar to the DD of the tumour necrosis factor (TNF) receptors (Huang, E. J. and Reichardt, L. F., 2003).

$TrkB^{FL}$ expression is regulated by calcium entry through L-type voltage-gated Ca^{2+} channels, leading to activation of Ca^{2+}-response elements (CREs) in promoter 1 and 2 (P1 and P2), in an NMDA receptor independent manner. The regulation of TrkB expression by Ca^{2+} was confirmed in neurons transiently transfected with TrkB promoter–luciferase constructs, and the results showed that Ca^{2+} activates P2 but inhibits the upstream P1 (Kingsbury, T. J. et al., 2003).

Neuronal activity also promotes the translocation of TrkB mRNA into dendrites, both in vitro and in vivo. In resting cultured hippocampal neurons, labelled TrkB mRNA covered ~30% of total dendritic length, but the dendritic labelling was increased to ~70% following mild depolarization (10mM KCl for 3h). Trafficking of TrkB mRNA into dendrites suggests local translation of a transmembrane protein in these terminals, disregarding the idea of membrane-associated proteins being synthesized only in the cell body (Nagappan, G. and Lu, B., 2005).

TrkB protein synthesis and the surface expression of the receptors are also regulated by neuronal activity (Fig. 1.6A). Thus, depolarization with a high KCl concentration increased the levels of TrkB on the surface of retinal ganglion cells and spinal neurons (Nagappan, G. and Lu, B., 2005), and similar results were obtained in retinal ganglion cells stimulated with glutamate receptor agonists (NMDA, kainate and quisqualate) and cAMP (Meyer-Franke, A. et al., 1998). Field tetanic stimulation also increased both biotinylated TrkB and surface bound labelled BDNF, indicating that electrical stimulation facilitates the translocation of TrkB from the intracellular pool to the cell surface, particularly in dendrites, thereby facilitating receptor activation by BDNF. The activity-induced translocation of TrkB receptors to the membrane is a rapid event (~30min), dependent on calcium influx and activation of Ca^{2+}/calmodulin-dependent kinase II (CaMKII), but does not require protein synthesis (Du, J. et al., 2000). Inhibition of the excitatory synaptic transmission abrogates the effect of electric stimulation on TrkB surface expression, suggesting that insertion of TrkB is facilitated at synapses with active synaptic transmission. The role of synaptic activity in TrkB activation was also shown in studies where electrical stimulation increased TrkB phosphorylation in the presence of saturating concentration of BDNF (Haapasalo, A. et al., 2002; Du, J. et al., 2003; Nagappan, G. and Lu, B., 2005). The effects of synaptic activity may be due, at least in part, to the release of BDNF, which regulates the TrkB expression (Haapasalo, A. et al., 2002; Nagappan, G. and Lu, B., 2005). Accordingly, exposure of hippocampal neurons to BDNF rapidly increased TrkB surface levels (<15s), but longer stimuli (3h) decreased surface TrkB protein levels through proteasome-mediated degradation (Haapasalo, A. et al., 2002).

When released into the synaptic cleft BDNF induces a lateral movement of TrkB from non-raft extrasynaptic sites into synaptic lipid rafts - cholesterol and sphingolipid-rich microdomains (Fig. 1.6B). Lipid rafts compartmentalize signalling molecules on the plasma membrane, allowing BDNF activated TrkB receptors to interact with proteins only located in the rafts (Nagappan, G. and Lu, B., 2005). Taken together, the available evidences indicate that neuronal activity modulates TrkB transcription, translation and endocytosis.

In addition to the effects on BDNF expression and release, neuronal activity also increases the intracellular **cAMP** concentration (Meyer-Franke, A. et al., 1998). cAMP was proposed to act as a 'gate' that enables BDNF to achieve its synaptic effects, and the evidences for this assumption are the following: 1) BDNF-TrkB signalling was enhanced in active neurons or synapses with elevated $[cAMP]_i$, 2) cAMP facilitated the translocation of TrkB into the postsynaptic density of hippocampal neurons and; 3) TrkB and the postsynaptic density protein 95 (PSD-95) physically interact and colocalize in the dendritic spines after treatment (15min) with activators of the cAMP–PKA pathway. The cAMP signalling pathway might selectively recruit TrkB into synapses containing PSD-95 and facilitate the association with a complex containing PSD-95 (Fig. 1.6C) (Nagappan, G. and Lu, B., 2005). This signalling mechanism also regulates neurotrophin and TrkB expression in cultured astroglial cells, which may be relevant during normal neuronal activity or after injury (Condorelli, D. F. et al., 1994).

1.2.3 - Signalling pathways

The early events in intracellular signalling induced by BDNF are similar to those of NGF. The BDNF dimers induce TrkB dimerisation and trigger transphosphorylation of tyrosine residues in their intracellular domain, in a dose-dependent manner (Yuen, E. C. and Mobley, W. C., 1999). This process leads to activation of one or more of the following three major signalling pathways: mitogen-activated protein kinase (MAPK), also termed extracellular signal-regulated protein kinase (ERK), phosphatidylinositol 3-kinase (PI3-K) and phospholipase C-gamma (PLC-γ) [Manadas, B. J. et al., 2007 (in press)] (described in more detail ahead). Other proteins have been identified as either binding to the activated TrkB receptor, or being present in some of the pathways translating the signal initiated by the receptors (Easton, J. B. et al., 2006).

TrkB activation is reversible (with a half-life of 1–2h) and spatially restricted, taking place only at active synapses (Nagappan, G. and Lu, B., 2005), as described above. The majority of the

signalling induced by growth factors terminates with their receptor **endocytosis** (Sorkin, A. and Waters, C. M., 1993). The activity of TrkB receptors constitutes an exception to this general rule, since endocytosis is still an important step in neurotrophin signalling. The complex formed by BDNF and TrkB is internalized either through clathrin-mediated endocytosis, through clathrin-independent endocytosis, or pincher-mediated macropinocytosis with membrane ruffles. The complex formed by the receptor and the neurotrophin is then driven to the "signalling endosome", a specialized vesicular compartment (Nagappan, G. and Lu, B., 2005). Receptor internalization has been observed in BDNF$^{-/-}$ hippocampal neurons subjected to electric stimulation, in the presence of exogenous BDNF. Following calcium entry through NDMA receptors and voltage-gated

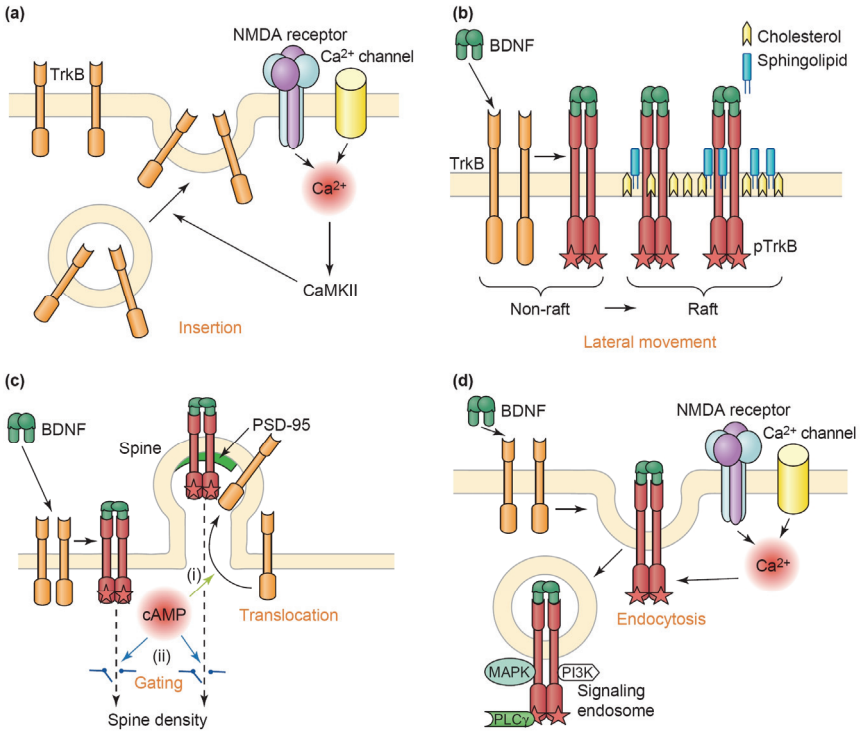

Figure 1.6. Regulation of TrkB trafficking by neuronal and/or synaptic activity. (a) Insertion of TrkB into the plasma membrane by an activity-dependent and BDNF-independent mechanism. Calcium influx through NMDA receptors leads to activation of calcium-calmodulin dependent protein kinase II (CaMKII) resulting in the fusion of TrkB containing vesicles with the plasma membrane. (b) BDNF-induced recruitment of TrkB into lipid rafts. BDNF binding to TrkB receptors induces their activation and lateral movement from non-raft to raft regions of plasma membrane. (c) cAMP-induced translocation of TrkB into the postsynaptic density and gating of TrkB signalling by cAMP. The increase in $[cAMP]_i$ can contribute to synaptic modulation in two ways: (i) inducing translocation of TrkB into dendritic spines or (ii) gating TrkB signal from either inside or outside synapses. (d) Activity-dependent endocytosis of the BDNF–TrkB complex. Local synaptic activity can enhance calcium entry through NMDA receptors and voltage-gated calcium channels facilitating endocytosis of BDNF activated TrkB receptors, which form the signalling endosome and initiates different pathways (e.g.ERK, PI3-K and PLCγ pathways) (Nagappan, G. and Lu, B., 2005).

calcium channels, TrkB kinase activity increased and induced receptor internalization. Inhibition of the tyrosine kinase activity prevents receptor internalization, suggesting a critical role for the receptor kinase activity in the activity-dependent receptor endocytosis. Therefore, TrkB kinase activity and internalization is modulated not only by neurotrophin binding but also by neuronal activity and calcium entry (Du, J. et al., 2003). A higher response to BDNF in active synapses can be achieved by facilitation of the endocytosis of neurotrophin bound TrkB receptors. (Figure 1.6b) (Nagappan, G. and Lu, B., 2005). The TrkB kinase activity is maintained in the internalized receptors, keeping their signalling activity.

1.2.3.1 - Ras-ERK pathway

Although most studies concerning the activation of this signalling pathway have been made in TrkA-expressing PC12 cells stimulated with NGF, evidences point to a similar mechanism for TrkB receptors. After the initial steps of TrkB activation, Shc binds to one of the phosphorylated tyrosines in the receptor, through a phosphotyrosine binding (PTB) domain. **Shc** is itself phosphorylated, allowing the interaction with Grb2 through a SH2 domain. This interaction brings the complex Grb2-SOS closer to the plasma membrane. SOS has a GEF (Guanine-nucleotide Exchange Factors) activity, activating the low molecular weight G-protein Ras, which is anchored to the membrane (Roy, S. et al., 2005). Thus, SOS activates Ras by exchanging its bound GDP with the more abundant GTP [Manadas, B. J. et al., 2007 (in press)]. **Ras** is an important mediator in signalling pathways regulating cell growth in all eukaryotic cells, and plays important roles in neuroprotection, tumour development (mutant), and synaptic plasticity, among others (Vojtek, A. B. and Der, C. J., 1998; Reichardt, L. F., 2006). Ras is the bottleneck of several signalling pathways (e.g. calcium influx, NMDA stimulation, cAMP and neurotrophin signalling) and an initiator of others (ERK pathway, PI3-K pathway) from a variety of stimuli (Iida, N. et al., 2001). Ras-GTP and protein phosphatase 2A (**PP2A**) are responsible for the initial steps of **Raf** activation, with Ras-GTP playing a role in the recruitment of Raf to the membrane vicinity. PP2A contributes to Raf activation by dephosphorylating amino acid residues important for the interaction of the kinase with the 14-3-3 protein. Once activated by multiple phosphorylations, Raf can phosphorylate **MEK1** present in the MEK1-ERK1-MP1 complex. MEK1 phosphorylates **ERK1** releasing the latter kinase from the complex, and allowing phospho-ERK1 dimerisation. This active ERK1 dimer phosphorylates **RSK**, and both active kinases may be translocated to the nucleus, where other proteins are regulated, including transcription factors (Movie 2, Figure 1.7) [Manadas,

B. J. et al., 2007 (in press)]. Alternative mechanisms have also been proposed involving new players, such as **KSR** and β-Arrestin (Anderson, D. H., 2006).
The kinase ERK5 is also activated by BDNF stimulation, through phosphorylation by MEK5. ERK5 is a mediator in a signalling cascade distinct from the Ras/ERK pathway, and has different targets. Furthermore, activation of ERK5 by neurotrophins is not affected by cAMP or neuronal activity (Cavanaugh, J. E. et al., 2001).

1.2.3.2 - PI3-K/Akt

Similarly to the Ras/ERK pathway, the **PI3-K/Akt** pathway requires the initial binding of Shc to the receptor and its phosphorylation, followed by recruitment of the **Grb2-SOS** complex. This pathway diverges from the Ras/ERK pathway at the point where **GAB1** binds to the Grb2, which may be important for Gab1 phosphorylation on tyrosine [Manadas, B. J. et al., 2007 (in press)], followed by interaction of the adaptor protein with the p85 subunit of PI3-K (Chan, T. O. et al., 1999). Once bound to GAB1, p85 no longer inhibits the p110 subunit, allowing it to phosphorylate the phosphatidylinositol 4,5-bisphosphate (PtdIns(4,5)P_2) into phosphatidylinositol 3,4,5-trisphosphate (PtdIns(3,4,5)P_3). PI3-K belongs to a family of enzymes that phosphorylate the D3 hydroxyl group of phosphoinositides producing also PtdIns3P, PtdIns(3,4)P_2, and PtdIns(3,5)P_2. These lipids are recognized by proteins containing a Pleckstrin homology (PH) domain, a 100-120 amino acid motif that was first recognized in pleckstrin, the major phosphorylation substrate for PKC in platelets. These domains comprise seven antiparallel β-sheets forming a hydrophobic pocket that is capped by a carboxy-terminal amphipathic helix. They are mainly lipid-binding modules, although they are also involved in mediating protein-protein interactions. PH domains are present in several proteins, including Akt (also termed protein kinase B - PKB), PDK-1 (phosphoinositide-dependent protein kinase 1), GRP-1 (general receptor for phosphoinositides), Btk (Bruton's tyrosine kinase), and PIP3BP (phosphatidylinositol 3,4,5-trisphosphate-binding protein) which bind specifically PtdIns(3,4)P_2 and/or PtdIns(3,4,5)P_3 (Chan, T. O. et al., 1999).
PI3-K can be activated in a **Ras**-dependent or independent-manner, and has been described as a key regulator of many cellular processes, including apoptosis, cellular proliferation, vesicular trafficking, cytoskeletal structure and cellular morphology, glucose utilization, protein biosynthesis, and lipid metabolism (Chan, T. O. et al., 1999). The roles played by PI3-K are cell-type and stimulus dependent, and included the regulation of G1 progression

during the cell cycle, control of cell survival, and control of invasion and metastasis. Other known targets of PI3-K, like the small GTPases Rho, Rac and cdc42, play important roles in the modulation of the actin cytoskeleton (e.g. formation of membrane ruffles/lamellipodia, filopodia and actin stress fibers and actin contractility). In the late 80s, viral studies showed that PI3-K has a role in the oncogenic transformation of eukaryotic cells, being involved in several aspects of tumours' pathogenesis, including cell-cycle progression, adhesion, motility, metastasis, cell survival and angiogenesis (Roymans, D. and Slegers, H., 2001).

The increase in plasma membrane PtdIns(3,4,5)P_3 leads to **Akt** recruitment to its vicinity and

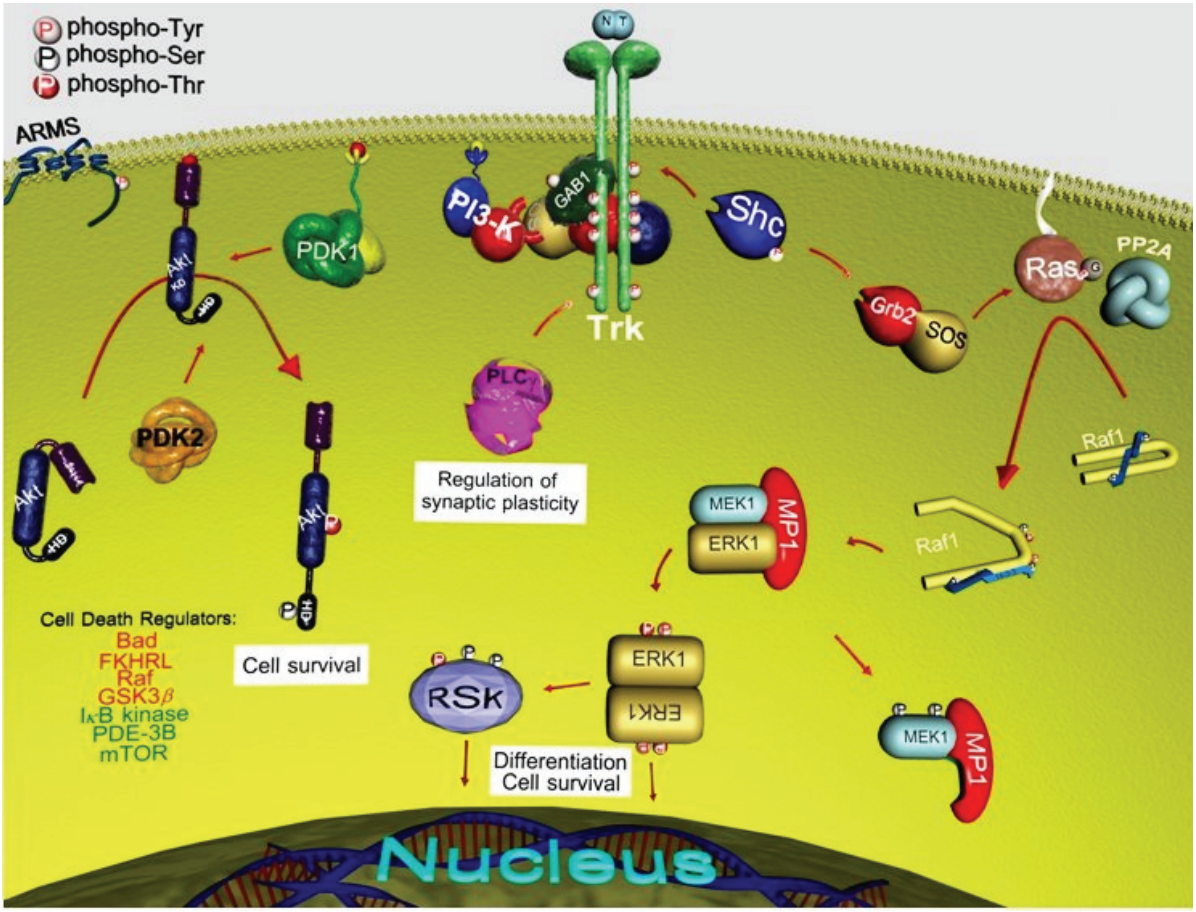

Figure 1.7 - Intracellular signalling mechanisms activated by Trk neurotrophin receptors. Neurotrophin binding to Trk receptors induces transphosphorylation of intracellular tyrosine residues of the receptor, which constitute binding sites for adaptor proteins, such as Shc, and signalling enzymes (PLCγ). Phosphorylation of Shc leads to the activation of PI3-K and ERK (see text for further details), whereas PLCγ is activated directly by tyrosine phosphorylation. The latter signalling pathway is involved in the regulation of synaptic transmission. The PI3-K pathway plays a major role in neurotrophin-induced cell survival, and these effects are mediated through the regulation of the activity of various enzymes by Akt phosphorylation [phosphorylation may increase (green) or decrease (red) enzyme activity]. Activity of the Ras/ERK pathway accounts for the effects of neurotrophins on cell differentiation and also contributes to cell survival under conditions of neuronal injury or toxicity [Manadas, B. J. et al., 2007 (in press)].

phosphorylation of the kinase by PDK2 at a serine residue (Ser^{473}) localized in the hydrophobic domain. The kinase domain is then exposed to PDK1, which phosphorylates Akt at Thr^{308}. The activity of Akt is also regulated by phosphorylation of additional sites (Tyr^{315} and Tyr^{326}) (Chen, R. et al., 2001), and the active kinase regulates several proteins, many of them involved in the control of cell survival (Fig. 1.7 and Movie 3) [Manadas, B. J. et al., 2007 (in press)]. Akt was initially identified as an oncogene, isolated from acute transforming retrovirus (Akt-8) (Chan, T. O. et al., 1999). It encodes a serine-threonine protein kinase, composed of a carboxy-terminal kinase domain very similar to that of PKC and PKA, and an amino terminal PH domain (Bellacosa, A. et al., 1991). Stimulation of the NMDA receptors also activates Akt, but the kinetics is slower than that observed for BDNF-induced Akt activation. Interestingly, the NMDA-induced Akt activation was partially blocked by the TrkB inhibitor K252a in cerebellar granule neurons, indicating that the neurotrophin receptors are required for full activation of the kinase upon activation of the glutamate receptors (Zhu, D. et al., 2002). Neurotrophins play a role in neuroprotection by activating proteins that are also actively present in some tumours. Therefore, the survival mechanisms induced by neurotrophins also depend on the precise equilibrium between the effect of tumour associated proteins and the control of cellular proliferation (Nakagawara, A. et al., 1994).

1.2.3.3 - PLCγ

The third effector system activated following TrkB receptor stimulation is **PLCγ**, which binds directly to the phosphorylated TrkB receptor through an SH2 domain. PLCγ becomes activated through tyrosine phosphorylation, and hydrolyses PtdIns $(4,5)P_2$ to generate inositol-1,4,5-trisphosphate [$Ins(1,4,5)P_3$] and diacylglycerol (DAG) [Manadas, B. J. et al., 2007 (in press)]. $Ins(1,4,5)P_3$ releases Ca^{2+} stored in intracellular compartments, such as the endoplasmic reticulum, raising the $[Ca^{2+}]_i$. The change in the concentration of this relevant second messenger leads to a differential activation/inhibition of Ca^{2+}-dependent effector systems, including CaMKII as well as protein kinase C (PKC). On the other hand, DAG stimulates DAG-regulated PKC isoforms. PLCγ plays an important role in BDNF-induced synaptic plasticity modulation (Fig. 1.7) (Minichiello, L. et al., 2002).

1.2.3.4 - p75^{NTR}

The p75^{NTR} is activated by pro-neurotrophins, including pro-BDNF and pro-NGF (Lee, R. et al., 2001; Volosin, M. et al., 2006) (Fig. 1.5), leading to **apoptotic** cell death in basal forebrain neurons in culture. The intracellular pathways activated upon binding of pro-neurotrophins to p75^{NTR} receptors are different from those activated upon stimulation of Trk receptors, and include phosphorylation of JNK and cleavage of caspase-6 and -3. In those cells expressing simultaneously p75^{NTR} and Trk receptors, the stimulation of Akt and ERK signalling pathways by the Trk receptors prevent the induction of apoptosis by pro-neurotrophins (Volosin, M. et al., 2006).

The proapoptotic pathways activated by p75^{NTR} include the Jun N-terminal kinase (JNK) signalling cascade, increase in sphingolipid turnover and interaction of the receptor with several protein adaptors that directly promote cell cycle arrest and apoptosis (Nykjaer, A. et al., 2005; Schor, N. F., 2005). G proteins like Rac (a known activator of JNK) and RhoA are also involved (Harrington, A. W. et al., 2004). The cytosolic proteins that interact with p75^{NTR} present in a certain cell determine, to some extent, the type of response observed. The effect p75^{NTR} on sphingolipid turnover is antagonized by active Trk receptors, which prevent the action of the former receptors on cell survival and differentiation induced by neurotrophins (Dobrowsky, R. T. et al., 1995). The ceramide produced by the activated sphingomyelinase has been shown to promote apoptosis and mitogenic responses, depending on the experimental settings, through the control of various signalling pathways, including ERK, PI3-K and atypical PKC isoforms (Muller, G. et al., 1998; Zhou, H. et al., 1998). The Trk receptors suppress the activation of acidic sphingomyelinase by p75^{NTR} through association of PI3-K with acidic sphingomyelinase in caveoli-related domains (Dobrowsky, R. T. et al., 1995; Bilderback, T. R. et al., 2001).

The p75^{NTR} may also be activated by mature neurotrophins, including BDNF, as shown in PC12 cells (MacPhee, I. J. and Barker, P. A., 1997) and in cultured hippocampal neurons at DIV5 (Brann, A. B. et al., 2002). In the latter model, where p75^{NTR} are higly expressed (Brann, A. B. et al., 2002), the activation of the receptor by BDNF promotes cell death (Troy, C. M. et al., 2002). In contrast, activation of p75^{NTR} was shown to promote the survival of neocortical subplate neurons through stimulation of sphingolipid signalling pathways, possibly with TrkB acting as a coreceptor for p75^{NTR} (DeFreitas, M. F. et al., 2001).

1.2.4 - Effects of BDNF signalling

The activation of neurotrophin receptors and of downstream signalling events induces changes in the conformation, activity, and location of several proteins, which ultimately end in the development/initiation of a major cellular response or even phenotype changes. The activation of Trk receptors by BDNF induces rapid changes in signalling activity, including activation of PI3-K, Ras, Akt, MEK and/or ERK (see above), followed by long-term alterations, resulting from changes in protein expression. Thus, BDNF may have rapid effects in synaptic transmission, mediated by activation of protein kinases, followed by delayed and more sustained responses, including effects on neurite outgrowth and synaptogenesis, which have been associated with learning and memory. The manifold effects of BDNF on neuronal modifications is partially mediated by **genomic** and/or proteomic changes (Ring, R. H. et al., 2006), with two of the targets identified and involved in this issue comprising the eukaryote initiation factor (eIF) 4E and its binding protein (eIF4E-binding protein-1). The activation of eIF4E-binding protein-1 is mediated through phosphorylation by the mammalian target of rapamycin (mTOR). These evidences, among others, link BDNF signalling and initiation of translation in neurons (Takei, N. et al., 2001). Transcription is also modulated downstream of the activation of Trk receptors, with several transcription factors involved, including CREB (phosphorylated by an ERK-dependent mechanism) (Ying, S. W. et al., 2002), FKHRL1 (via Trk receptors and PI3-K/Akt kinase in neuronal and non-neuronal cells) (Zheng, W. H. et al., 2002), the mammalian achaete-schute homolog 1 (Mash1) and the helix-loop-helix protein mATH-1 (atonal homolog 1), also known as Math1. This transcription factor was shown to facilitate differentiation of cultured neuronal stem cells into neurons (Ito, H. et al., 2003).

Dendrites have been shown to possess all the components necessary for **translation**, including ribosomes (Steward, O. and Levy, W. B., 1982), mRNAs (Job, C. and Eberwine, J., 2001) and translation factors (Gardiol, A. et al., 1999; Inamura, N. et al., 2003), and protein synthesis has been observed in dendrites (Steward, O. and Schuman, E. M., 2001). It has been hypothesized that neural activity enhances local protein synthesis in dendrites, which in turn induces or maintains **long-term synaptic plasticity** (Takei, N. et al., 2004; Shiina, N. et al., 2005; Schratt, G. M. et al., 2006). Accordingly, rapamycin and protein synthesis inhibitors (cyclohexamide or anisomycin) have been shown to affect synaptic plasticity, and LTP is also affected in mice deficient in BDNF (Korte, M. et al., 1995). Inhibition of synaptic plasticity by rapamycin implicates mTOR as a mediator of synaptic plasticity induced by BDNF, by regulating local translation in neuronal dendrites (Takei, N. et al., 2004). Recently, BDNF was

shown to regulate protein synthesis by releasing a translational repressor from RNA granules in dendrites of hippocampal neurons. RNA granules contain mRNA and several proteins, including RNG105 (RNA granule protein 105), which keeps these structures arrested in their basal conditions. BDNF releases the RNG105 translational repressor, allowing mRNAs to be translated (Shiina, N. et al., 2005; Schratt, G. M. et al., 2006).

BDNF and its cognate receptor TrkB have been associated with **neurogenesis**, the birth of new neuronal cells. Thus, TrkB activation plays an important role in the regulation of the basal level of neurogenesis in dentate gyrus of adult mice, and enhances neurogenesis under conditions of dietary restriction (DR), by promoting survival of newly generated neurons. BDNF is also a key regulator in the signalling pathways leading to proliferation of stem cells in vivo, as determined with bromodeoxyuridine (BrdU). The newly generated neurons in the hippocampal dendate gyrus already contain BDNF (Lee, J. et al., 2002).

During **development**, it is estimated that half of the neurons die during pre- and post-natal development in certain regions of the nervous system (Copani, A. et al., 1995). In order to survive, neurons compete for limiting amounts of neurotrophins released by peripheral targets (Levi-Montalcini, R., 1987; Oppenheim, R. W., 1991), with neurotrophins playing a major role in neuronal survival and development, in both peripheral and central nervous systems (Korsching, S., 1993; Davies, A. M., 1994; Snider, W. D., 1994). Neurons also struggle to establish pathways of communication between different organs, tissues or cells, so they can become functional, as is the case of respiratory control, where BDNF is required for the development of specific subsets of primary sensory and brainstem neurons, and the preBotzinger complex (pBC - a critical site for respiratory rhythm generation and control during the development of normal breathing after birth). The importance of BDNF in the development of the respiratory system was also confirmed when mutations in pathways dependent on this neurotrophin resulted in human developmental disorders of breathing (Katz, D. M., 2005).

BDNF **knockout** mice represent an interesting model to study the physiological roles of BDNF. $BDNF^{+/-}$ mice showed hyperphagia, obesity, elevated strial dopamine levels, loss of mechanosensitivity, loss of neurons of the peripheral nervous system and an impairment in LTP. This last phenotype indicates that the availability of BDNF is important for synaptic plasticity leading to LTP (Chao, M. V., 2003). In other studies, a close correlation was found between BDNF, glucose control, **insulin** levels, and body weight. BDNF knockout mice were hypoglycaemic, and obese. Interestingly, exogenous administration of BDNF in diabetic rodents resulted in a reduction of body weight, normalization of glucose levels and increase

in insulin sensitivity (Vaynman, S. and Gomez-Pinilla, F., 2005).

BDNF/TrkB plays a pivotal role in **neuroprotection** against several types of toxic injury to neurons, such as excitotoxicity and serum withdrawal, in the peripheral and central nervous systems (e.g. Korsching, S., 1993; Davies, A. M., 1994; Snider, W. D., 1994). Neuroprotection by TrkB receptors was also observed following activation of adenosine A_{2A} receptors. The neurotrophic effects of adenosine are mainly mediated through activation of a population of intracellular Trk receptors associated with Golgi membranes, and this may be exploited in the development of new agents for the treatment of neurodegenerative diseases (Lee, F. S. and Chao, M. V., 2001; Rajagopal, R. et al., 2004). BDNF reduces the infarct volume following focal cerebral ischemia, primarily in the cortex, when administered intracerebroventricularly. It also protects neurons against glutamate-induced toxicity and the subsequently increase in intracellular calcium concentration (Popp, E. and Bottiger, B. W., 2006). Some of the neuroprotective mechanisms induced by BDNF depend on the ERK pathway, and may involve (1) posttranslational modifications (inactivation of components of the death machinery or activation of components of the survival machinery), and (2) increase in the transcription of pro-survival genes (Bonni, A. et al., 1999). BDNF protected cerebrocortical neurons from camptothecin through activation of ERK, while PI3-K played a major role in neuroprotection under conditions of serum deprivation, suggesting that different signalling pathways mediate neuroprotection from different stimuli and may be cell-type specific (Hetman, M. et al., 1999). Despite numerous in vitro studies showing neuroprotective effects of BDNF (e.g. Almeida, R. D. et al., 2005), subcutaneous or intravenous application of BDNF results in limited effect in the brain because of the poor penetration of BDNF across the blood-brain barrier (BBB), and because the peptide has a plasma half-life of less than 10 minutes. A combined conjugate, designated BDNF-PEG^{2000}-biotin/OX26-SA, showed an improved plasma pharmacokinetics and BBB permeability when compared to unconjugated BDNF. This BDNF chimeric peptide showed neuroprotective effects in rats subjected to transient forebrain ischemia, permanent focal ischemia, or transient focal ischemia, with an effective time window of 1-2h after the insult. Rats subjected to permanent middle cerebral artery occlusion (MCAO), and treated with the BDNF chimeric peptide via intravenous injection immediately after the lesion, showed a dose-dependent neuroprotection, with a reduction of the infarct volume of up to 65% (Wu, D., 2005).

Some patients infected with human immunodeficiency virus type 1 (**HIV-1**) develop HIV-1 associated dementia (HAD), a disorder characterized by motor and cognitive dysfunction. In vitro and in vivo experiments showed that viral envelope glycoprotein 120 (gp120) toxicity

could be reduced by BDNF in cortical neurons and cerebellar granule cells (Nosheny, R. L. et al., 2005).

Besides these beneficial actions of BDNF/TrkB, the TrkB receptors also play an unwanted role in tumour growth, contributing to the aggressive behaviour of a substantial percentage of human tumours (Desmet, C. J. and Peeper, D. S., 2006).

1.2.5 - Synaptic plasticity, Memory, Learning and Exercise

BDNF gene expression may be controlled at the transcription level, by multiple promoters, and by changing mRNA stability, and the neurotrophin protein levels may be regulated at the translation level. Furthermore, the subcellular distribution of BDNF is also subjected to regulation, thereby fulfilling the different functions of the neurotrophin. The expression of BDNF mRNA is enhanced when the non-NMDA-type glutamate receptor is activated and suppressed when $GABA_A$ receptor is activated (Lu, B., 2003).

Activity-dependent modification of synapses, or **synaptic plasticity**, is a powerful mechanism resulting in the formation of neuronal circuits during development, and controls cognitive functions and complex behaviours in the adult (Nagappan, G. and Lu, B., 2005). This experience-dependent change in synaptic strength (Bliss, T. V. and Collingridge, G. L., 1993) is input-specific or synapse-specific, occurring only at synapses that experience changes in their activity, as is the case in LTP (Nagappan, G. and Lu, B., 2005), with BDNF emerging as a key regulator of synaptic transmission and plasticity (Bramham, C. R. and Messaoudi, E., 2005). The local and synapse-specific modulation by neurotrophins, together with the preference for active neurons/synapses, suggests that neurotrophins must preferentially regulate active synapses with little or no effect on nearby, less active, synapses. Although the selection process is not fully understood, several hypotheses have been raised. First, the transcription of BDNF can be regulated by neuronal activity, as this phenomenon has been repeatedly observed in the many different populations of neurons in the CNS, with activity-dependent dendritic targeting of BDNF mRNA and its local translation. BDNF has been shown to induce dendritic targeting of BDNF mRNA, and although the mechanisms are not fully understood it was proposed that the BDNF mRNA is transported to dendritic spines in a non-selective manner before being trapped by synapses that undergo high-frequency stimulation. This implies that the secretion of BDNF should not only be regulated, but also be local and controlled by specific patterns of neuronal activity. BDNF is found in large dense-core vesicles of sensory neurons and in brain synaptosomes, and the

BDNF–GFP (green fluorescence protein) fusion protein is packaged into secretory vesicles that are transported to somatodendritic compartments and, to some extent, to axons. The BDNF-GFP fusion protein is secreted postsynaptically upon high-frequency presynaptic stimulation, and the release is dependent on activation of postsynaptic glutamate receptors. Second, activity-dependent secretion of BDNF can occur locally at the site of active synapses, and mechanisms are available to limit its diffusion. In favour of this hypothesis is the fact that BDNF is a sticky molecule with limited diffusion capacity, and truncated TrkB molecules are highly expressed in the cell surface of mature CNS neurons, limiting BDNF diffusion. Third, active neurons/synapses may respond better to BDNF compared to inactive ones (Lu, B., 2003), with BDNF acting together with glutamate at some excitatory synapses (Bramham, C. R. and Messaoudi, E., 2005). This may be due to an activity-dependent control of the number of TrkB receptors on the cell surface, and also to the increased availability of the remaining proteins required for signalling (Lu, B., 2003). Mild depolarization and sustained neuronal firing also upregulates TrkB mRNA in dendrites of cultured hippocampal neurons, with increased local dendritic translation of TrkB mRNA and local insertion of the receptor (Lu, B., 2003; Nagappan, G. and Lu, B., 2005). Finally, neuronal activity can also facilitate the internalization of the BDNF-receptor complex, which is a key signalling event mediating many of the BDNF functions (Lu, B., 2003).

The regulation of synaptic strength through dendritic protein synthesis depends on the accessibility of the message for translation, the positioning of the translational apparatus, and the biochemical regulation of translation factors, with BDNF essentially involved in all of these steps. There are two main hypotheses to explain the BDNF induced synaptic plasticity: the **synaptic tagging** and the **synaptic consolidation** hypothesis. According to the first model, BDNF upregulates translation activity and/or induces the synthesis of mRNA and its tagging to the synaptic terminal. The synaptic consolidation hypothesis proposes that the effect of BDNF is mediated through TrkB-dependent phosphorylation of eIF4E, and the enhanced translational states tag the synapse. The latter mechanism may serve to facilitate translation and capture of mRNA released from local storage granules as well as new mRNA coming into the dendrites (Bramham, C. R. and Messaoudi, E., 2005). At the protein level, using synaptoneurosomes and KCl depolarization, it was shown that BDNF increases the synthesis of a particular set of proteins without affecting the overall protein synthesis. One of these proteins is Arc (activity-regulated cytoskeletal), which expression is inhibited by TrkB and NMDA receptor inhibitors. Interestingly, inhibition of Arc synthesis blocks long-term potentiation (LTP) stabilization and results in spatial learning deficits (Yin, Y. et al., 2002).

Changes in the synaptic strength are important in information storage during the process of learning and **memory** formation (Morris, R. G., 2003; Whitlock, J. R. et al., 2006). The increase in synaptic activity induced by HFS raises the intracellular calcium concentration in postsynaptic dendritic spines, mainly due to Ca^{2+} influx through the NMDA receptor channels, affecting TrkB signalling (see above). The early events leading to long-term synaptic potentiation and possibly to memory formation are triggered by the $[Ca^{2+}]_i$ increase, and require covalent modification of existing proteins, in addition to protein trafficking at synapses. The development of late LTP, like long-term memory, depends on *de novo* transcription and protein synthesis (Bramham, C. R. and Messaoudi, E., 2005). Experiments performed in organotypic cultures of hippocampal slices showed that long-term administration of BDNF increased the number of docked synaptic vesicles, but did not affect the reserve pool at CA1 excitatory synapses. The neurotrophin also upregulates several synaptic vesicle proteins, including synaptophysin, synaptobrevin, and synaptotagmin, but no effect of BDNF was found on the presynaptic membrane proteins syntaxin and SNAP-25 in hippocampal neurons (Tartaglia, N. et al., 2001). BDNF also increased the phosphorylation state of synapsin I in cerebrocortical synaptosomes. Synapsins keep small synaptic vesicles attached to the actin cytoskeleton in a phosphorylation-dependent manner, regulating the amount of vesicles available for release, including the glutamate containing synaptic vesicles. Accordingly, BDNF increased the depolarization-evoked glutamate release and induced the phosphorylation of synapsin I in isolated cerebrocortical synaptosomes, and the neurotrophin had no effect on glutamate release in nerve terminals isolated from synapsin $I^{-/-}$, synapsin $II^{-/-}$, and synapsin $I^{-/-}$ and $II^{-/-}$ mice (Jovanovic, J. N. et al., 2000). Inhibition of synapsin I (with antibodies against the protein) disrupted the synaptic vesicle reserve pool and decreased neurotransmitter release (Hilfiker, S. et al., 1999), suggesting a role for synapsins I and II in LTP.

The effect of BDNF on synaptic plasticity may also occur post-synaptically, and may be due to modulation of NMDA receptors. Accordingly, BDNF restored the activity of NMDA receptors previously decreased by cAMP in hippocampal neurons (Sun, J. et al., 2001). These effects may be modulated by the non-receptor tyrosine kinase Fyn, which phosphorylates the NMDA receptors, particularly the NR2B subunit. Accordingly, Fyn coimmunoprecipitated with TrkB and NR2B in the hippocampus, particularly in well-trained rats. Phosphorylation of NMDA receptors by Fyn also plays an important role in spatial memory formation in a radial arm maze (Mizuno, M. et al., 2003).

Taken together, the available evidences suggest that BDNF plays a major role in three

mechanisms associated with LTP: permissive (increases vesicle docking), acute instructive (modulation of calcium influx), and late instructive (Arc-dependent consolidation) (Bramham, C. R. and Messaoudi, E., 2005). In addition to the effects in LTP, BDNF was also shown to contribute to long-term depression (LTD), certain forms of short-term synaptic plasticity, as well as homeostatic regulation of intrinsic neuronal excitability (Bramham, C. R. and Messaoudi, E., 2005; Vaynman, S. and Gomez-Pinilla, F., 2005).

Blocking BDNF signalling in the hippocampus impairs spatial learning and **memory** in rats subjected to water maze training, and reduces LTP. A key role for BDNF in LTP is further suggested by the results showing the highest BDNF expression in the animals with the highest memory recalls, and CREB also had the highest expression levels in the same group of animals. Other studies, using alternative hippocampal-dependent learning paradigms, have also shown increases in hippocampal BDNF mRNA levels in response to contextual fear conditioning. It was also found that animals which learned the fastest, and had the best recall, also had the highest levels of BDNF in their hippocampi, suggesting that hippocampal BDNF levels are related to learning efficiency. During aging, the decrease in BDNF signalling in the brain, specially in hippocampal pyramidal and dentate granule cells, as shown in studies conducted in monkeys (Vaynman, S. and Gomez-Pinilla, F., 2005), is closely related to a decrease in learning and memory.

LTP is part of a learning and memory process resulting in activity-driven neuronal and synaptic plasticity (Morris, R. G., 2003; Whitlock, J. R. et al., 2006). Numerous studies have shown that BDNF plays a key role in both the early- and late phase LTP (E-LTP and L-LTP) in the hippocampus. Furthermore, BDNF was shown to potentiate “preferentially” or “selectively” active synapses, when applied with weak presynaptic stimulation. The TrkB receptor is also significantly increased by LTP-induced tetanic stimulation, with almost no effect on other Trk receptors (Nagappan, G. and Lu, B., 2005). The role of BDNF on LTP was also demonstrated when deletion of the BDNF gene ($BDNF^{+/-}$ and $BDNF^{-/-}$ mice) selectively impaired LTP in the hippocampus (Korte, M. et al., 1995) and deletion of one copy of the BDNF gene ($BDNF^{+/-}$ mice) impaired LTP on the layer IV–III pathway in the cortex, although there was no change in ocular dominance plasticity (Bartoletti, A. et al., 2002).

Exercise has also been shown to up-regulate BDNF mRNA and protein levels in the hippocampus, cerebral cortex, cerebellum (Vaynman, S. and Gomez-Pinilla, F., 2005), and in the spinal cord (Skup, M. et al., 2002; Vaynman, S. and Gomez-Pinilla, F., 2005). Furthermore, it was shown that BDNF mRNA levels are increased in the hippocampi of rats that have undergone 3 or 6 days of Morris water maze training, with growing evidence for the

association between BDNF and plasticity in the effects of exercise in the brain, especially in the hippocampus, an area vital for supporting learning and memory processes (Kesslak, J. P. et al., 1998). This led to the use of motor training in the healing plan of transplanted tissue in stroke and Parkinsonian models, to enhance the survival and integration of cell grafts into the existing circuitry.

1.2.6 - Disorders associated with neurotrophins

Deregulation of BDNF protein levels, either downregulation or upregulation, has been associated with a large number of disorders. Some of the major disorders are briefly mentioned in this section. Although in some cases there is a close relationship between the disease phenotype and a deregulation in BDNF or TrkB receptors, in other cases it remains to be determined whether the changes observed represent a cause or a consequence of the disorder.

BDNF is upregulated in areas implicated in epileptogenesis, such as hippocampus and entorhinal cortex. **Epilepsy** is a disorder of the brain characterized by the periodic and unpredictable occurrence of seizures. The increased neuronal activity in epileptic seizures upregulates both BDNF and TrkB mRNA and protein levels and this is expected to further potentiate neuronal excitability. The hippocampus and closely related structures are particularly important in the pro-epileptogenic effect of BDNF. It has been shown that inhibitors of BDNF signalling mechanisms decrease the development of the epileptic state in vivo (Binder, D. K. et al., 2001), further suggesting that the neurotrophin plays an important role in this disorder.

Huntington's disease (HD) is a neurodegenerative disorder dominantly inherited, resulting from a genetic defect consisting in a CAG repeat expansion in the huntingtin (htt) gene. This genetic modification results in a mutant protein with a polyglutamine expansion and abnormal conformation, resulting in toxic activity of the mutant and loss of function of normal huntingtin (Zuccato, C. et al., 2005). The disorder is characterized by neuronal degeneration in the striatum and cerebral cortex, and leads to chorea (abnormal involuntary movements), dementia and death 15 to 20 years after the onset (Reiner, A. et al., 1988). htt keeps the neuron restrictive silencer factor (NRSF) in the cytoplasm, away from its target (nuclear restrictive silencer element - NRSE), a consensus sequence found in genes such as the

BDNF gene (Borrell-Pages, M. et al., 2006), thereby increasing BDNF gene transcription (del Toro, D. et al., 2006).

Mutant huntingtin (mhtt) regulates BDNF at different levels (i) reduces BDNF expression by not restricting NRSF movements (Zuccato, C. et al., 2005), (ii) impairs post-Golgi trafficking of $BDNF_{Val}$ containing vesicles that follow the regulated secretory pathway, without affecting $BDNF_{Met}$ containing vesicles, (iii) impairs the transport of BDNF-containing vesicles along the microtubules, promoted by htt, and (iv) consequently reduces KCl-evoked release of BDNF, affecting the pro-survival action of BDNF on striatal neurons. Reports also show that HD patients heterozygous for the BDNF polymorphism (containing $BDNF_{Val}$ and $BDNF_{Met}$) have a later age of onset of the disease when compared with homozygous $BDNF_{Val}$ patients (del Toro, D. et al., 2006). TrkB levels were also reduced in transgenic exon-1 and full-length knock-in HD mice, and continuous expression of mhtt was required for TrkB downregulation (Gines, S. et al., 2006), although it is not clear whether this effect is directly mediated by mhtt or by reduced levels of BDNF. Interestingly, a candidate drug for HD, cysteamine, increased BDNF levels in the brain, and induced neuroprotection in HD mouse models (Borrell-Pages, M. et al., 2006). Neuronal stem cells transplanted into a rat model of PD revealed BDNF expression and secretion, with the protective effects observed from grafted cells possibly being mediated by BDNF (Ryu, J. K. et al., 2004).

Alzheimer's disease (AD) is a chronic neurodegenerative disorder, which progression is associated with neuronal degeneration and progressive development of dementia. Pathologically, the disease is characterized by the formation of senile plaques and neurofibrillary tangles, loss of synaptic contacts, degeneration of cholinergic neurons of the forebrain with consequent reduction in acetylcholine, and progressive but inexorable clinically observed cognitive deterioration. The origin of the disease is still in debate, with many factors, including neurotrophic factors, being suggested as playing a major role in its origin and/or development (Fumagalli, F. et al., 2006a). Post mortem analysis of AD brains, revealed a decrease in BDNF and TrkB receptor in the hippocampus (Vaynman, S. and Gomez-Pinilla, F., 2005; Fumagalli, F. et al., 2006a), but it is still not known if this phenomenon is either the cause or a consequence of the disease. Deficits of BDNF synthesis might be involved in the deterioration of cellular homeostasis that leads to AD, as observed when AD patients were compared to age matched controls for three human BDNF mRNA transcripts. In terms of disease treatment, it is interesting to notice that drugs clinically used to fight AD and therapeutic interventions (including physiotherapy) mimic some of the

effects of BDNF modulation in brain regions involved in the pathophysiology of the disease. Besides the induction of survival and differentiation of basal forebrain cholinergic neurons, BDNF also stimulates the release of acetylcholine, the neurotransmitter defective in AD patients (Fumagalli, F. et al., 2006a).

Parkinson disease (PD) is a progressive degenerative disorder characterized by selective loss of nigral dopaminergic neurons, resulting in a pronounced depletion of striatal dopamine, and leading to motor dysfunctions. The disease development is accompanied by a decline in the cognitive processes, suggesting that other brain regions are affected besides the nigrostriatal network. BDNF has been pointed as having a major role in the etiology of the disease based on several evidences. Dopamine transporter knockout mice showed a marked decrease in BDNF expression in the frontal cortex, creating threatening situations to other structures, such as the striatum, where BDNF is anterogradely transported. In PD patients nigrostriatal dopaminergic neurons showed a decrease in BDNF and TrkB levels, suggesting a critical role of the neurotrophin in the well being of the neurons during senescence (Fernandez-Espejo, E., 2004; Fumagalli, F. et al., 2006b).

Another neurological disorder that has been associated with BDNF is **depression**. The neurotrophin is pointed as being involved not only in the pathophysiology of affective disorders (Hajszan, T. and MacLusky, N., 2006) but also in the mechanisms of action of antidepressant drugs (Tardito, D. et al., 2006). The continuous study of the mechanisms associated with the activity of antidepressant drugs indicate that they work, at least in part, through their effects not only on BDNF synthesis and neurogenesis in the hippocampus, but also by enhancing the expression of BDNF and TrkB receptor in the hippocampus of both intact and stressed laboratory animals (Hajszan, T. and MacLusky, N., 2006). Several antidepressant drugs (e.g.: TCP, sertraline, DMI, and mianserin) significantly increased BDNF mRNA in the hippocampus, and all but mianserin increased TrkB mRNA. BDNF also increases the serotonergic activity within the brain, when injected in the hippocampal dentate gyrus (DG) and in the midbrain, producing an antidepressant effect (Tardito, D. et al., 2006). It also appears that BDNF expression is sufficient for antidepressant efficacy (Hajszan, T. and MacLusky, N., 2006).

Patients with allergic **asthma** have shown increased blood and bronchoalveolar fluid BDNF levels. This increase was also observed after allergen stimulation. When comparing T cells

isolated either from the inflamed lungs or from the spleen, the former had higher levels of BDNF gene products while the latter had no detectable BDNF, suggesting that either different populations behave in a different way or that T cells were pre-activated in the lungs, where local inflammation occurs. Although BDNF is widely expressed in visceral epithelial cells of virtually all organs, in the case of asthma it has an increased expression in airway epithelia, contributing to neuronal hyperresponsiveness. During inflammatory diseases, BDNF elicits angiogenesis and survival of endothelial cells, playing an important role in blood vessel formation. During allergic inflammation, cells of the monocyte/macrophage lineage were identified as strong producers of NGF and BDNF in humans and other mammalian species, showing a strong upregulation of neurotrophin expression. The inflammatory cytokines IL-6 and TNF-α, released during monocyte/macrophage activation, also increase BDNF secretion (Nockher, W. A. and Renz, H., 2006).

Besides these disorders, BDNF has been pointed as playing important roles in many other diseases, including multiple sclerosis (Stadelmann, C. et al., 2002), Rett syndrome (Sun, Y. E. and Wu, H., 2006), bipolar disorder (Nakata, K. et al., 2003; Hayden, E. P. and Nurnberger, J. I., Jr., 2006), schizophrenia (Prathikanti, S. and Weinberger, D. R., 2005), and mood disorders (Prathikanti, S. and Weinberger, D. R., 2005; Tardito, D. et al., 2006). The list of disorders discussed in this section was selected in order to provide examples concerning the mechanisms that can regulate BDNF/TrkB expression or illustrate pathologies where interfering with BDNF signalling may contribute to a successful therapy.

1.3 - Objectives of the study

BDNF plays important roles in neurogenesis, development of the nervous system, regulation of synaptic transmission, and in several disorders of the nervous system, as previously mentioned. In the hippocampus BDNF has been shown to contribute to synaptogenesis (Ring, R. H. et al., 2006), development (Binder, D. K. et al., 2001), synaptic plasticity (Du, J. et al., 2000), particularly to long-term potentiation of synaptic transmission, learning and memory formation (Levine, E. S. et al., 1995; Kesslak, J. P. et al., 1998; Mizuno, M. et al., 2003; Binder, D. K. and Scharfman, H. E., 2004; Whitlock, J. R. et al., 2006), and to neuroprotection under ischemia (Kokaia, Z. et al., 1996). The effects of BDNF are, at least in part, mediated by the induction of protein synthesis, through activation of transcription and/or by regulation of the translation machinery (Tartaglia, N. et al., 2001; Minichiello, L. et al., 2002; Ying, S. W. et al., 2002).

The aim of this thesis was to provide a comprehensive description of the BDNF-induced changes in the proteome of cultured hippocampal neurons, which will contribute to the understanding of the physiological roles of this neurotrophin. Furthermore, a systematic study of the effect of BDNF on the proteome may contribute to elucidate some of the roles of this neurotrophin in diseases of the nervous system, and allow predicting some of the beneficts that may arise from its use under disease conditions.

Proteomics based approaches using two-dimensional gel electrophoresis and MALDI-TOF mass spectrometry have been successfully employed in the characterization of the protein content of simple organisms (mainly bacteria). Most of the proteome of these organisms can be resolved in one broad range (pH 3-10) 2D-gel. However, the complexity of mammalian organisms makes difficult the use of this technique, since only highly expressed proteins can be resolved in one single gel (without specific enrichment of the sample). The limit of 1200-1500 spots resolved in one gel is an obstacle for the complete examination of the proteome of a given organism. The technique also presents some limitations due to difficulties in solubilization and reproducibility of the results obtained for membrane proteins, membrane associated proteins, and other proteins with a stable and/or strong 3D structure that is not disrupted using 2D-SDS-PAGE compatible reagents. Therefore, in order to benefict the most from the use of proteomics to characterize the effect of BDNF in the proteome of hippocampal neurons, several technical improvements in solubilization of proteins and resolving power of 2D-gels were performed, including fractionation, sonication and use of “zoom” IPG strips (Chapter 3).

The technical improvements achieved in the first part of the work were then used in a comprehensive study of the BDNF-induced changes in the proteome of cultured hippocampal neurons. Since BDNF regulates transcription and translation, this study was focused on the newly synthesized proteins (Chapter 4), which provides a better indication of the physiological response to the neurotrophin than the analysis of the changes in the gene expression at the mRNA level. After protein identification and quantification, the accession numbers and the gene names of the proteins were used to gather information from different databases for each protein, allowing off-line data analysis and integration (for instance, metabolic and signalling pathways affected). Furthermore, proteins which expression levels achieved our established requirements for further analysis were clustered according to their ontologies, in order to perform a functional analysis.

Given the difficulties in analyzing membrane proteins using gel-based approaches, a complementary study was performed using a liquid-based proteomic approach (Chapter 4.2.6) to characterize a fraction containing mainly membrane proteins from cultured hippocampal neurons. This approach, 2D-LC-MS/MS, allows the identification and quantification of the total protein content in one step, and overcomes the low solubility of membrane proteins by handling peptides instead of proteins.

Chapter 2

Materials and methods

2.1 - Preparation of protein samples from rat hippocampus

Adult Wistar rats were sacrificed and the hippocampi were removed. The hippocampi were then sonicated (Chan, L. L. et al., 2002; Chemale, G. et al., 2003) in 50mM Tris-HCl pH 7.3, 1mM DTT, chymostatin (1μg/mL), leupeptin (1μg/mL), antipain (1μg/mL), pepstatin A (1μg/mL), and 0.1mM PMSF (Sigma), and the resulting suspension was divided into two equal samples. In each case soluble proteins were isolated in the supernatant resulting from ultracentrifugation at 126,000×g_{av} (Chan, L. L. et al., 2002), for 1 hour at 4ºC. Proteins in the pellets (S126) were resuspended in 10% (w/v) TCA (Merk) whereas soluble proteins were precipitated by adding 100% (w/v) TCA, to a final concentration of 10% (w/v) (Chan, L. L. et al., 2002; Chemale, G. et al., 2003; Nandakumar, M. P. et al., 2003). TCA-precipitated fractions were frozen and thawed, in order to improve precipitation, and centrifuged at 14,000×g_{max}, for 15min at 4ºC (Nandakumar, M. P. et al., 2003). Pellets were washed with ice-cold acetone, maintained at 4ºC, vortexed during 1min every 20min, for 1h, and centrifuged at 14,000×g_{max}, for 15min at 4ºC (Chan, L. L. et al., 2002; Chemale, G. et al., 2003; Nandakumar, M. P. et al., 2003). Proteins were solubilized for 2 hours in 2D-sample buffer [6M urea (Amersham Biosciences), 1.5M thiourea (Sigma), 3% CHAPS (Amersham Biosciences USB Chemicals), and 60mM DTT (Amersham Biosciences USB Chemicals)], and sonicated (except for non-sonicated samples). Non-sonicated samples were vortexed for 2min after disruption of the pellet with a pipette tip. Protein quantification was performed using the 2D-Quant kit (Amersham Biosciences). IPG Buffer (1.5%, pH 4.5–5.5, pH 5.0-6.0, pH 5.5–6.7 or pH 6-9) was added to the samples prior to IEF (Amersham Biosciences).

2.2 - Hippocampal cultures

E18 hippocampal neurons were cultured as previously described (Almeida, R. D. et al., 2005). Briefly, pregnant female rats were sacrificed by cervical displacement and the E18-E19 Wistar rat embryos were removed (Fig. 2.1A). Embryos were decapitated (Fig. 2.1B) and their brains (Fig. 2.1C) placed under the dissection microscope for further dissection. The hemispheres were separated (Fig. 2.1D) and the hippocampi were dissected after removing the meninges (Fig. 2.1E). The hippocampi were then treated with trypsin (0.5mg/mL, 15min, 37ºC), in Ca^{2+} and Mg^{2+}-free Hank's balanced salt solution (HBSS: 137mM NaCl, 5.36mM KCl, 0.44mM KH_2PO_4, 0.34mM $Na_2HPO_4.2H_2O$, 4.16mM $NaHCO_3$,

5mM glucose, supplemented with 0.001% phenol red, 1mM sodium pyruvate and 10mM HEPES, pH 7.4). Trypsin activity was stopped by washing the hippocampi in HBSS supplemented with 10% (v/v) FCS, and the cells were then mechanically dissociated in Neurobasal medium. Hippocampal cultures (Fig. 2.1F) were maintained in serum-free Neurobasal medium (Gibco), supplemented with B27 supplement (Gibco), glutamate (25μM), glutamine (0.5mM) and gentamicin (0.12mg/mL). The cells were kept at 37ºC in an humidified incubator of 5% CO_2/95% air, for 7 days (Fig. 2.1G), the time required for maturation of hippocampal neurons. The glial content of hippocampal cultures maintained in Neurobasal medium, supplemented with B27 supplement, was estimated to be about 5% of the total cell population (Brewer, G. J. et al., 1993). Cells were cultured at a population density of 90,000 cells/cm^2, in 6-well microplates (MW6), or 65,000 cells/cm^2, in 12-well microplates (MW12).

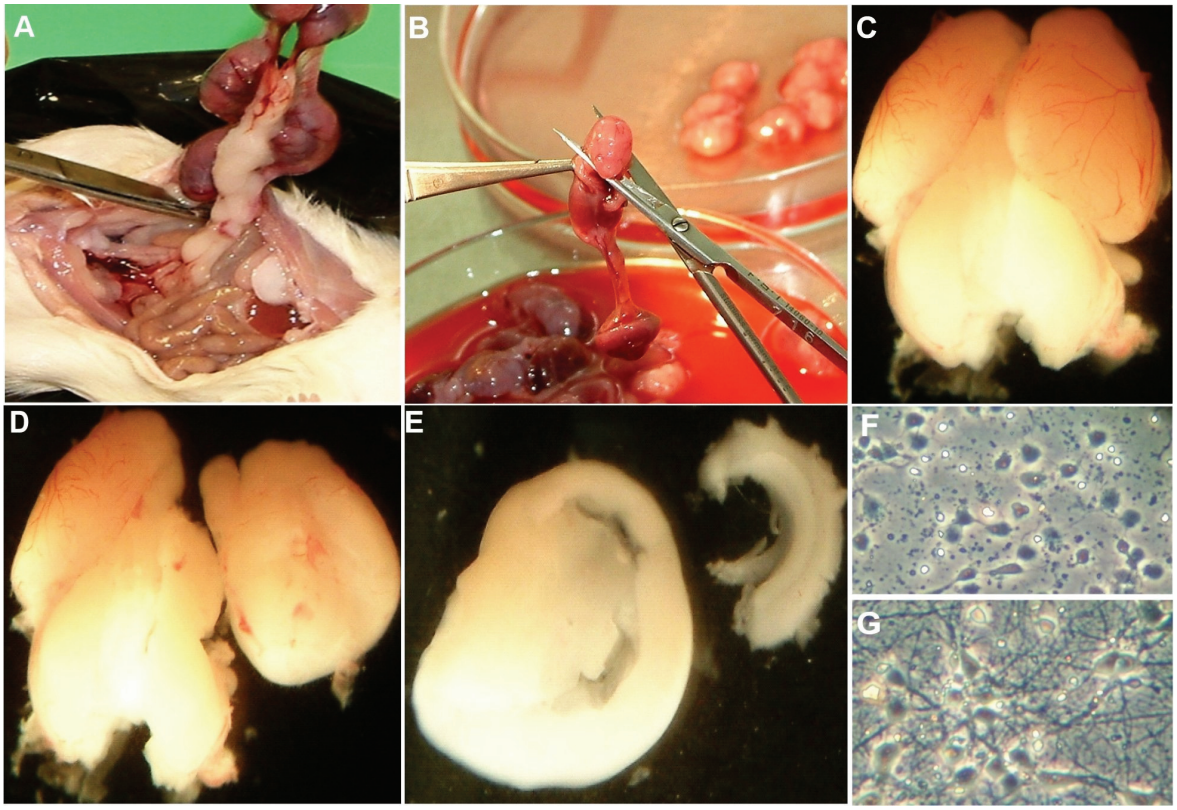

Figure 2.1 – Cultured hippocampal neurons preparation. See text for details.

2.3 - Radiolabelling experiments

2.3.1 - Amino acid incorporation into proteins

Hippocampal neurons cultured for 7 days (DIV7) in MW12 (65,000 cell/cm^2) were starved from methionine and cysteine, for 30min, by replacing the culture medium with methionine- and cysteine-free Dulbecco's modified Eagle's medium (DMEM - Sigma). The incubation medium was then replaced by DMEM with [^{35}S]cysteine and [^{35}S]methionine (Redivue Pro-mix, 7.5μCi/mL, Amersham Biosciences), with or without BDNF (100ng/mL). After the indicated incubation period, cells were washed with 1mL of Na^+ medium (140mM NaCl, 5mM KCl, 1mM $CaCl_2$, 1mM $MgCl_2$, 5.5mM glucose, 20mM HEPES and 1mM NaH_2PO_4, pH 7.4), and 0.5mL of 0.5mg/mL BSA together with 0.5mL of 20% (w/v) TCA was then added to each well. Due to the low amount of protein present in each well, BSA was added in order to improve protein precipitation. Cells were scrapped and the suspension was centrifuged, at 14,000×*g*, for 15min at 4ºC, and the resulting pellet was collected to a vial and resuspendend in 1mL of 10% (w/v) TCA. This suspension was centrifuged as before and the pellet was solubilized in 1M NaOH. The radioactivity was measured using a Packard 2,000 scintillation counter and the Universol scintillation cocktail (ICN, USA) (Huh, K. H. and Wenthold, R. J., 1999; Takei, N. et al., 2001). For each experimental set, two wells of MW12 plates (65,000 cells/cm^2) were used for each time point. Each experiment was performed in duplicates and the results are the average ± SEM of 3 different experiments performed in independent preparations.

2.3.2 - 2D gels

After 7 days in culture, cells were starved from methionine and cysteine for 30min in methionine- and cysteine-free DMEM, and ^{35}S-radiolabeled amino acids (Redivue Pro-mix, 7.5μCi/mL) were then added, in DMEM, with or without BDNF (100ng/mL). After 12h of incubation the cells were washed with PBS (137mM NaCl, 2.7mM KCl, 1.8mM KH_2PO_4, 10mM $Na_2HPO_4.2H_2O$, pH 7.4), scrapped, and sonicated in 50mM Tris-HCl pH 7.3, 1mM DTT, chymostatin (1μg/mL), leupeptin (1μg/mL), antipain (1μg/ mL), pepstatin A (1μg/mL), and 0.1mM PMSF. Soluble proteins were separated from the remaining protein fraction as described in Section 2.1.

2.4 - Sonication procedure

Sonication was performed as previously described (Chan, L. L. et al., 2002) with slight modifications. Briefly, samples were kept on ice and sonicated, using a 3mm stepped microtip (#630-0422) with a Vibra Cell system (Sonics & Materials), in six cycles of 10s, each consisting of 5s sonication followed by a 5s break (to keep the samples at low temperature). Each sonication was performed with increasing amplitude, starting from zero, and the amplitude was maintained below 40. Special care was taken to avoid foaming.

2.5 - 2D-SDS-PAGE

Two hundred and fifty micrograms of protein were actively rehydrated for 12h at 50V. IEF was performed according to the manufacturer instructions, with slight modifications: 500V [500V.h step and hold (SH)], 1,000V (1,000V.h SH), 10,000V (15,000V.h with linear increase), and final focusing at 10,000V during 14h (SH), using a Protean IEF cell (BioRad). For the pH 6-9 range, strips were rehydrated overnight (12-16h) in 2D buffer [with 15% (v/v) 2-propanol, 5% (v/v) glycerol and 1.2% (v/v) DeStreak – Amersham Biosciences] and 250μg of protein were applied by cup loading in the anode end of the IPG strip (Pennington, K. et al., 2004). Strips were then equilibrated to SDS [50mM Tris-HCl pH 8.8, 30% (v/v) glycerol, 2% (w/v) SDS, and trace amount of bromophenol blue] for 20min, in the presence of 10mg/mL DTT, followed by another 20min step in the presence of 25mg/mL iodoacetamide. The second dimension was performed in a Protean Plus Dodeca Cell (BioRad), at 3W/gel for 30min, followed by 200V for 5h30m, using 10% (w/v) acrylamide gels, except where otherwise stated. All steps were performed at 20ºC.

2.6 - Protein spot visualization and image adquisition

2.6.1 - Silver staining

Gels were silver stained as previously described (O'Connell, K. L. and Stults, J. T., 1997), dried, digitalized (using an office scanner), and analyzed using PDQuest™ (Bio-Rad). The staining protocol included (500mL in all steps): 30min in 25% (v/v) methanol and 5% (v/v) acetic acid, 10min in 50% (v/v) ethanol, 10min in 30% (v/v) ethanol, 1min in 0.2g/L sodium thiosulfate, two times 5min in water, and 20min in 2.0g/L silver nitrate (Sigma) followed by

development in 0.7mL/L formaldehyde (37%) (Sigma), 30g/L sodium carbonate anhydrous (Fluka), and 10mg/L sodium thiosulfate (Sigma). Once the desired staining was achieved, development was stopped by addition of 50g/L Tris-Base (Calbiochem) in 2.5% (v/v) acetic acid for 1min. Gels were maintained in water with sodium azide until further processing.

2.6.2 - Radiolabelling

Gels from radiolabelled samples were dried and placed in contact with a phosphor screen (Amersham Biosciences) for a period of 7-10 days, and the images were subsequently acquired with a laser scanner (Storm™ - Amersham Biosciences).

2.6.3 - Ruthenium staining

Gel staining with ruthenium was performed as described (Rabilloud, T. et al., 2001; Lamanda, A. et al., 2004). The gels were fixed overnight in 30% (v/v) ethanol and 10% (v/v) acetic acid, and were then rinsed 4×30min in 20% (v/v) ethanol, in order to remove acetic acid which strongly quenches the fluorescence of the chelate. The gels were then stained for 6h in 20% (v/v) ethanol containing 200nM ruthenium chelate (see protocol of preparation in the footnote). Finally, the gels were reequilibrated in water (2×10min) prior to colloidal Coomassie staining.

2.6.4 - Colloidal Coomassie staining

Colloidal Coomassie staining was performed as previously described (Candiano, G. et al., 2004), with slight modifications. Gels were allowed to stain overnight. Whenever necessary, more Coomassie powder was added or the staining solution was replaced. Once the desired staining was achieved, gels were washed with water and maintained in water with sodium

---

The **ruthenium solution** was prepared as previously described (Rabilloud, T. et al., 2001): 0.2g of potassium pentachloro aquo ruthenate ($K_2Cl_5Ru.H_2O$) (26.9% Ru) (Alfa Aesar) were dissolved in 20mL boiling water and kept under reflux, resulting in the formation of a deep red-brown solution. Three molar equivalents of bathophenanthroline disulfonate (disodium salt, Sigma), i.e. 0.9g of the anhydrous compound, were then added and the refluxing continued for 20min. The solution turned to a deep greenish brown. Meanwhile, a 500mM sodium ascorbate solution (Sigma) was prepared (10–15mL). Five mL of this solution were then added to the refluxing mixture and refluxing was continued for another 20min. The solution turned rapidly to a deep orange-brown. After cooling, the pH was adjusted to 7 with sodium hydroxide and the volume was adjusted to 26mL with water.

azide until further analysis (see protocol of preparation in the footnote).

2.7 - Gel analysis

Spot intensity in silver-stained gels and autoradiography images was normalized to the total intensity in valid spots, using PDQuest. This normalization procedure is useful when comparing different gels, wherever possible sources of sample variation cannot be predicted and there is no major difference in total spot number. For autoradiography images of sonication experiments (section 3.2.2), the results were normalized to the total intensity in the gel image. This normalization is recommended when there are significant differences between images. Decisions concerning the normalization procedure were taken based on the recommendations of the PDQuest software manual.

2.8 - Protein identification

For protein ID 500μg of protein were applied to IPG gels for in-gel rehydration, followed by 500μg by cup-loading. IEF and second dimension were performed as described in Section 2.5. Gels were double stained, first with Ruthenium II bathophenanthroline disulfonate (Rabilloud, T. et al., 2001) and then with home-made colloidal Coomassie (Candiano, G. et al., 2004). Spots were picked with the Bruker Spot Picker system, using a spot cutter with 1.5mm diameter. Spots were destained [50mM ammonium bicarbonate, 30% (v/v) ACN], washed with water, dehydrated using a speedvac, and incubated overnight with 3μL trypsin [Roche, proteomics grade (10mg/mL in 10mM ammonium bicarbonate)]. Peptides were then extracted using 10mL of 50% (v/v) ACN and 0.1% (v/v) TFA. Peptide containing solutions were applied on a 384 steel MALDI target (Bruker) followed by 1μL matrix containing standards [50% (v/v) ACN, 0.1% (v/v) TFA, 0.3% (w/v) cyano-4-hydroxycinnamic acid, 10pmol/mL bradykinin fragment 1–8 (*m/z* 904.4861) and 40pmol/mL adrenocorticotropic

---

Colloidal coomassie staining solution: to prepare 1L of the staining solution, 117mL of 85% solution phosphoric acid was added to 200mL of water [final concentration 10% (v/v)], 100g ammonium sulfate powder mixed with the previous solution (final concentration 10%) and water was added to a final volume of 800mL. Once the ammonium sulfate was solubilized, 200mL of methanol were added just previous to the staining procedure. This staining solution was placed on top of each gel (500mL/per gel) and up to 0.2% (1g) (w/v) of Coomassie Brilliant Blue G (Alfa Aesar) was added to the solution with a filter to prevent clotting of the dye and allow development of colloidal particles.

hormone fragment 18–39 (*m/z* 2465.1983)]. MALDI Ultraflex (Bruker Daltonics) was used for spectra acquisition, with the software controller Bruker Daltonics FlexControl (Version 2.2) The instrument, operating in Reflector Mode, was calibrated using 400 laser shots accumulated from external standards. Spectra were acquired using a laser power range of 45–65% and a detection range of *m/z* 900–3500. A total of 8×50-laser shots were accumulated for each spot. The accumulation of spectra was performed after automatic spectra evaluation, and all spectra analyzed had a resolution higher than 6500 in the range *m/z* 1200–2700. For spectra processing the Bruker Daltonics FlexAnalysis (Version 2.2) was used, with SNAP algorithm for detection, Centroid algorithm for editing, and Savitzky Golay algorithm for smoothing. The S/N ratio in the spectra analyzed was at least 2.5, and a quality factor threshold of 50 was selected. Background peak removal was performed based on the contaminant peak list provided by Bruker Daltonics, containing tryptic autodigest peaks and common keratin fragment peaks. A local MASCOT Server (Version 2.0) was used for protein identification. Several identification cycles were performed and the most stringent parameters used were the following: Swiss-Prot/TrEMBL databases, *Rattus norvegicus*, trypsin with zero missed cleavages, carbamidomethylation and methionine oxidation as fixed and variable modifications, respectively, and 25ppm error tolerance. Identified proteins had at least four peptides below 10ppm. GO annotations were automatically acquired and manually processed from EBI (http://www.ebi.ac.uk/EGO).

2.9 - iTRAQ and 2D-LC-MS/MS

2.9.1 - iTRAQ labelling

The samples were kept in 10% (w/v) TCA and centrifuged immediately before analysis. They were then solubilized and boiled in 2% (w/v) SDS solution, 100mM DTE, 0.7% (w/v) Tris/HCl pH 7.3. After protein quantification, SDS was removed by using 5,000 cut-off filters (Millipore). For each sample, 100µg of protein content were diluted in 3 volumes of 25mM HEPES, and the samples were centrifuged at 4ºC. Once the sample volume was reduced to 50-100µl, it was diluted with 3 volumes of 25mM HEPES and centrifuged, and this washing step was repeated once. The resulting solution was taken to a clean tube and the filter was washed with 3 steps of increasing ACN concentration [30, 50 and 70% (v/v)]. The samples were pulled, subjected to speedvac until dryness, and were then treated according to the iTRAQ manufacturer's instructions. Once digested with trypsin and labelled with the iTRAQ

reagents, samples were combined and peptides were fractionated and identified by off-line 2D-LC-MS/MS.

2.9.2 - Strong cation exchange (SCX) High Performance Liquid Chromatography (HPLC)

Samples were diluted 4 times in mobile phase [25% (v/v) ACN in 10mM KH_2PO_4, pH 3], filtered using 0.22μm PVDF filters (Millex-GV 13mm) and applied to a PolySULFOETHYL A™ column 200×4.6mm, 5μm, 1000Å (The Nest Group). Peptides were eluted using 25% (v/v) ACN in 10mM KH_2PO_4, pH 3, and 1M KCl, with a gradient from 0 to 75%, in 30 minutes, with a flow of 1mL/min (Dionex), and then from 75% to 100%, in 5 minutes. One minute (1mL) fractions were collected into separate tubes.

2.9.3 - Trap-RP

Samples were subjected to speedvac until complete dryness and resuspended in mobile phase for reverse phase liquid chromatography (RPLC) [mobile phase A: 2% ACN (v/v), 0.1% (v/v) FA]. After filtration, as for SCX, samples were applied to a cartridge C18 Trap column in order to remove salts. Peptides were eluted using a step to 100% mobile phase B [98% (v/v) ACN, 0.1% (v/v) FA] with a 1mL/min flow. The peaks containing the peptides were collected, filtered and subject to speedvac before being used in LC-MS/MS.

2.9.4 - LC-MS/MS

Peptides were eluted into the MS system with a binary gradient (300nL/min) (model 1100, Agilent) from 100% mobile phase A [2% (v/v) ACN, 0.5% (v/v) FA] to 70% mobile phase B [98% (v/v) ACN, 0.5% (v/v) FA], over 110min, followed by 70–100% mobile phase B in 20min, and finally, held at mobile phase B for an additional 10min. The QSTAR XL [quadrupole time-of-flight (QqTOF) tandem mass spectrometer] was operated in an information-dependent acquisition (IDA) mode. Proteins were identified using the Interrogator algorithm (Applied Biosystems) and the Rat fasta file from UniProtKB/Swiss-Prot database.

2.10 - Data analysis

The following software packages were used for data analysis, handling and visualization: GraphPad Prism, PDQuest, Excel, VBA, Image Quant, Melanie, ProteinScape, Biotools, Analyst, Protein Pilot, GOminer, PowerPoint, and GIMP.

Chapter 3

Optimization of 2D-SDS-PAGE

Data presented in this chapter was partially published in:
Manadas, B.J., Vougas, K., Fountoulakis, M., and Duarte, C.B. 2006. Sample sonication after trichloroacetic acid precipitation increases protein recovery from cultured hippocampal neurons, and improves resolution and reproducibility in two-dimensional gel electrophoresis. *Electrophoresis* 27:1825-1831.

3.1 - Introduction

The mammalian proteome comprises several million different proteins (Wooley, J. C., 2002). Their resolution in 2D-SDS-PAGE is a great effort requiring fractionation (Fountoulakis, M., 2004) and building of cybergels from “zoom” IEF gels (Oguri, T. et al., 2002). Although no attempt has been made to resolve the proteome of cultured hippocampal neurons, 469 individual proteins were identified in the adult hippocampus using 2D-gels (Pollak, D. D. et al., 2006). The use of various approaches also allowed to characterize, to some extent, the protein content of the hippocampal plasma membranes: 345 proteins were identified using 1D-SDS-PAGE and ESI-Q-TOF, 452 proteins were found using LC-ESI-ion trap MS/MS of tryptic digest, and 335 proteins with biotin purification of membrane proteins followed by 1D-SDS-PAGE and ESI-Q-TOF MS/MS of gel bands (Chen, P. et al., 2006). Among the hippocampal plasma membrane proteins identified a significant fraction was detected using only one of the approaches. These findings clearly show that there is no optimum approach for a large scale proteomic analysis and profiling, and show the need of multiple approaches in order to cover as many proteins as possible (Chen, P. et al., 2006).

Although an improved protein spot resolution is achieved with “zoom” gels, a higher degree of reproducibility is also required (Challapalli, K. K. et al., 2004) in order to allow a quick matching of the gels by the algorithms available (Church, S., 2004), and to speed up the analysis. Protein samples to be analyzed by 2-DE should be free from salts and other compounds that interfere mainly with IEF, such as nucleic acids and lipids (Nandakumar, M. P. et al., 2003). This may be achieved by various means, including TCA precipitation followed by acetone washing, which was identified as one of the best protocols (Jiang, L. et al., 2004). The main problem associated with TCA precipitation is the solubilization of the pellet. A chemical approach was previously used to solubilize TCA-precipitated proteins (Nandakumar, M. P. et al., 2003). In SDS-PAGE, proteins are solubilized using a combination of chemical (SDS and DTT) and physical (sample heating) methods. However, samples used in 2D-SDS-PAGE cannot be heated in order to avoid protein modifications induced by urea. The aim of this task was to design experimental conditions in order to (i) increase the number of resolved spots in 2D-gels (section 3.2.1), and (ii) increase the resolution and reproducibility between gels prepared from hippocampal samples (section 3.2.2).

3.2 – Results and discussion

3.2.1 – "Zoom" gels and extract fractionation increase the number of visualized spots

The first approach used to resolve the proteome of cultured hippocampal neurons consisted in the application of cell extracts to commonly used IPG strips pH 3-10. Fig. 3.1 shows the overall protein content (silver staining; top panel) and newly synthesized proteins (radiolabelled; bottom panel), resolved with these strips. Clearly, this pH range does not allow the visualization of more than 1000-1300 spots, barely scratching the proteome of hippocampal neurons. In order to dig deeper inside the proteome, we tested "zoom" gels using IPG strips with one resolving pH unit (pH 5.5-6.7, Fig. 3.2B). Comparing with the

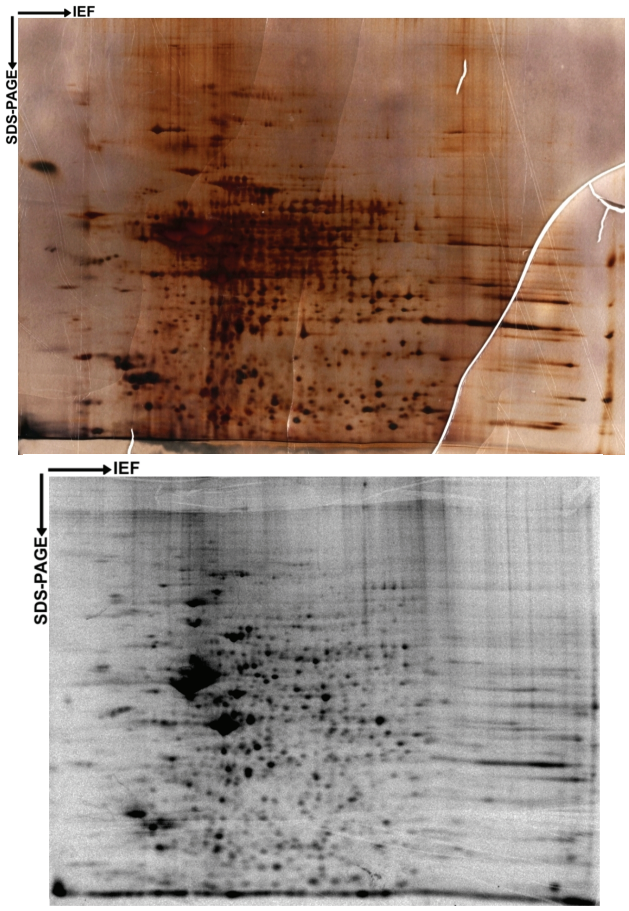

Figure 3.1 – 2D-PAGE of cultured hippocampal neurons. Images represent silver (top panel) and radiolabelled (bottom panel) gels obtained from DIV7 hippocampal neurons. For radiolabelling experiments, cells were cultured in the presence of [^{35}S]-cysteine and [^{35}S]-methionine for 12h. In both cases 250μg of protein were loaded into IEF strips pH 3-10, and the second dimension was performed in 10% acrylamide gels.

corresponding range in a pH 3-10 strip (Fig. 3.2A), more spots could be resolved when the pH 5.5-6.7 IPG strip was used (376 spots detected in Fig. 3.2A and 1396 spots detected in Fig. 3.2B), although high values of electric current during IEF indicated the presence of contaminants (salt, nucleic acids, and/or lipids). In order to clean the samples, two approaches were used: (i) **ultracentrifugation**, to separate soluble from membrane fractions, and (ii) TCA **precipitation** followed by acetone washing, to remove salts and lipids. Fractionation of the extracts before 2D-PAGE was performed by ultracentrifugation, giving rise to a soluble fraction (supernatant; Fig. 3.2C), which is clean and easy to use, and a pellet containing membrane proteins, membrane associated proteins and high dense core proteins (S126 fraction; Fig. 3.2D). Besides reducing sample complexity, fractionation also increases the relative abundance of low abundant proteins, allowing their visualization and thereby increasing the total amount of spots quantified and identified. Fractionation reduced

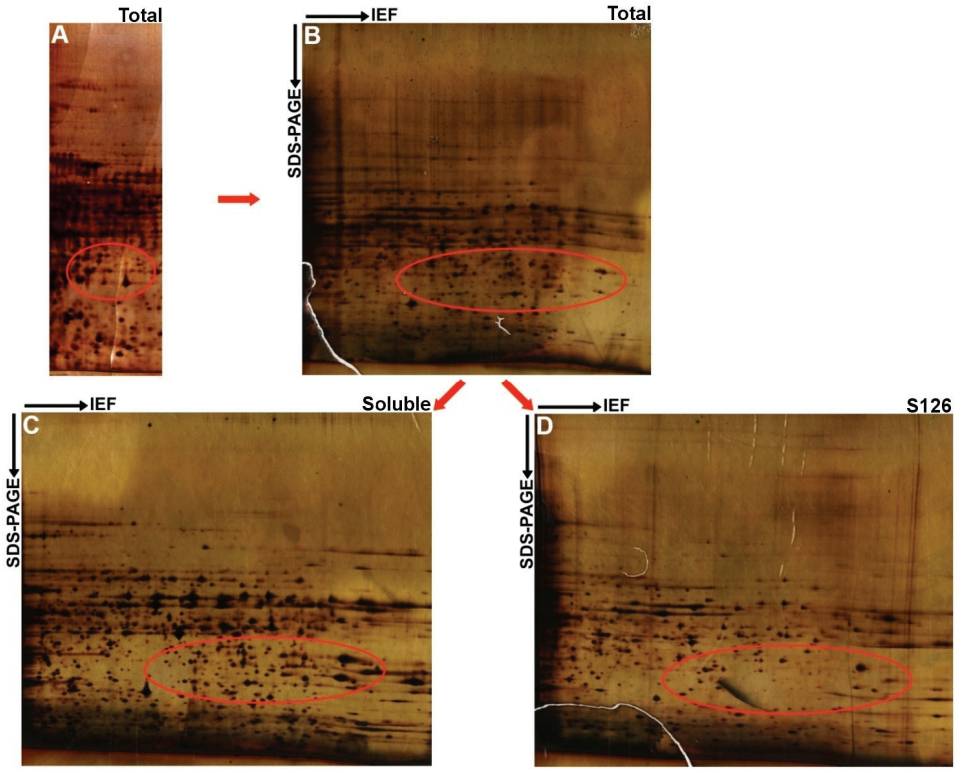

Figure 3.2 – Increase in spot number and resolution by sample fractionation and using "zoom" gels. Images represent 2D gels from DIV7 cultured rat hippocampal neurons using total extracts in broad range IPG strips pH 3-10 (A) and narrow range IPG strips pH 5.5-6.7 (B). In the former case only the range corresponding to approximately pH 5.5-6.7 is shown. Total extracts were fractionated in soluble fraction (C) and S126 pellet (D) and applied in narrow range IPG strips pH 5.5-6.7. Red circles highlight major differences between images. Second dimension was performed in 10% acrylamide (A) or using a linear gradient 8%-12% acrylamide (B-D). The spots were detected using PDQuest™.

gel complexity, and the total number of spots detected increased (Fig. 3.2C with 1212 spots; Fig. 3.2D with 805 spots) when compared with the number of spots found in the non-fractionated sample (Fig. 3.2B with 1396 spots).

High molecular weight proteins have some difficulty in migrating, not only inside a gel matrix but also passing from a relatively large matrix (as is the case of IPG gel, which is made of 4% acrylamide) to a smaller gel matrix (which is the case of second dimension gel, made of 10% acrylamide). This problem led us to test the usage of gradient gels in the second dimension, aiming at facilitating the entry of large protein into the gel and improving the resolving power to higher molecular weigh proteins. Proteins were either resolved by using a 10% acrylamide gel (Fig. 3.2A) or gradient gels ranging from 8% (top of the gel and near to the strip) to 12% acrylamide (bottom of the gel, Fig. 3.2B-D). This process was expected to increase the entry of high molecular weight proteins into the gel, allowing the visualization of more spots. However, the results show that there was no significant increase in the number of spots corresponding to high molecular weight proteins. Furthermore, there was a decrease in spot resolution in the range 50-150kDa, with the upper part of the gel being depleted of spots. Therefore, all other experiments were performed using 10% acrylamide gels in the second dimension.

3.2.2 - Increase in resolution and reproducibility by sample sonication

2D-gels have proven to be the best way to resolve thousands of proteins in a single gel (Gorg, A. et al., 2000; Wooley, J. C., 2002). The technique has been improved over the last decades allowing a broad range comparison of different proteomes in different experimental conditions (Gorg, A. et al., 2000; Molloy, M. P., 2000; Oguri, T. et al., 2002; Wooley, J. C., 2002). Isoelectric focusing is very sensitive to the non-protein content of the samples and requires a clean solution with as little contaminants as possible (Celis, J. E. and Gromov, P., 1999; Gorg, A. et al., 2000; Molloy, M. P., 2000; Nandakumar, M. P. et al., 2003). The increasing number of steps used to prepare these clean samples has resulted in a decrease in protein recovery from consecutive steps. This is the case of TCA precipitation, where solubilization of the pellet represents a critical step. Centrifugation after sample solubilization is a common procedure to remove insoluble material (Gorg, A. et al., 2000; Chemale, G. et al., 2003; Nandakumar, M. P. et al., 2003). However, in our experiments we noticed a significant variability in the size of the pellets resulting from the solubilization of proteins precipitated with TCA, even in samples prepared from the same amount of original tissue.

This led us to question the solubilization and reproducibility capacity of the buffers generally used in this type of protocol, consisting in 6-8M urea, 1-2M thiourea, 2-4% (v/v) CHAPS, 50-100mM DTT and 0.5-2% (v/v) IPG buffer (Herbert, B., 1999; Santoni, V. et al., 1999; Gorg, A. et al., 2000; Molloy, M. P., 2000; Zhou, S. et al., 2005). Protein solubilization in SDS-PAGE is increased by heating the samples in the presence of SDS. However, in 2D-PAGE the samples have to be kept at a temperature below 30ºC, in order to avoid protein modifications (Gerstner, A. et al., 2000; Henningsen, R. et al., 2002). Therefore, in this case, increased solubilization of the samples has been achieved by extending the incubation period at room temperature and by vortexing (Nandakumar, M. P. et al., 2003).

In order to improve protein recovery and to decrease the amount of proteins trapped in the insoluble fraction after TCA precipitation, we have tested the effect of sonication after elution of proteins in sample buffer. After precipitation with TCA, the protein pellets obtained from

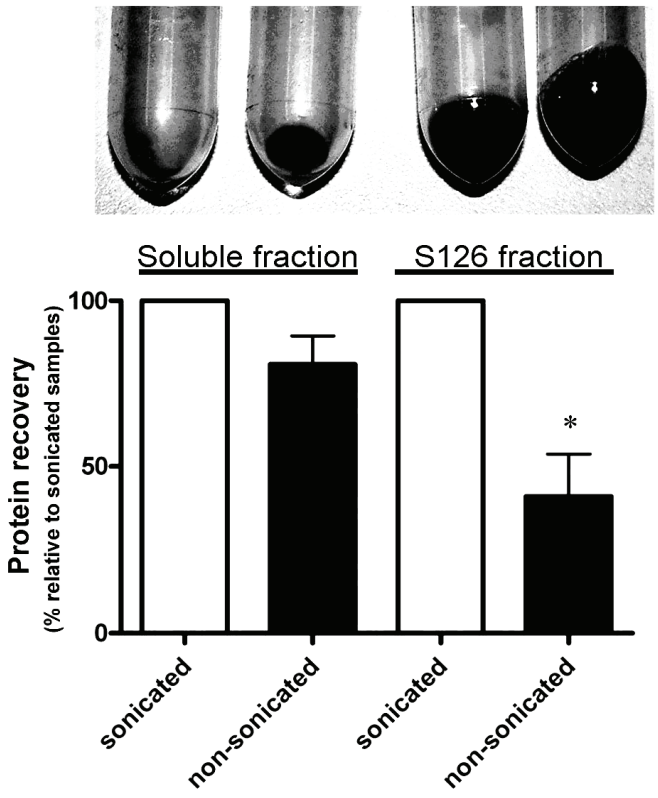

Figure 3.3 - Increase in protein recovery by sonication. Proteins from adult rat hippocampi were separated in soluble and S126 protein fractions by ultracentrifugation. Proteins were solubilized in 2D sample buffer and either sonicated or vortexed for 2min. (Top) Pellets obtained after centrifugation to remove non-soluble material. (Bottom) Protein recovery after quantification using the Amersham's 2D Quant Kit. Samples (n = 4) were analyzed using two-tailed Student's t-test with 99% confidence with P<0.05 (*) (GraphPad Prism, San Diego, CA).

the hippocampal soluble or S126 (ultracentrifugation pellet) fractions were sonicated or not in sample buffer. Sonication decreased the size of the pellets comprising insoluble material (Fig. 3.3), particularly in the S126 fraction. Quantification of the total protein content in sonicated and non-sonicated S126 fractions showed that this physical treatment increases total protein recovery by 140%, starting with the same amount of sample. Although sonication was not so important to increase protein recovery in the soluble fraction it also reduced protein trapping in the pellet and increased the reproducibility of the gels (data not shown).

The effect of sonication on 2D-PAGE was investigated in experiments where the same amount of protein, from sonicated and non-sonicated hippocampal S126 fractions, was subjected to IEF and SDS-PAGE (Fig. 3.4). Although the pattern of both gels was similar, gels from sonicated samples showed several new spots and a different focusing pattern of some spots (e.g. zoomed area in Fig. 3.4). PDQuest™ analysis of the gels (Table I) showed not only an increase in the number of spots in gels obtained from sonicated samples but also an increase in the relative intensity of several spots present in both gels. The increased diversity of spots detected in sonicated samples was associated with a decrease in relative

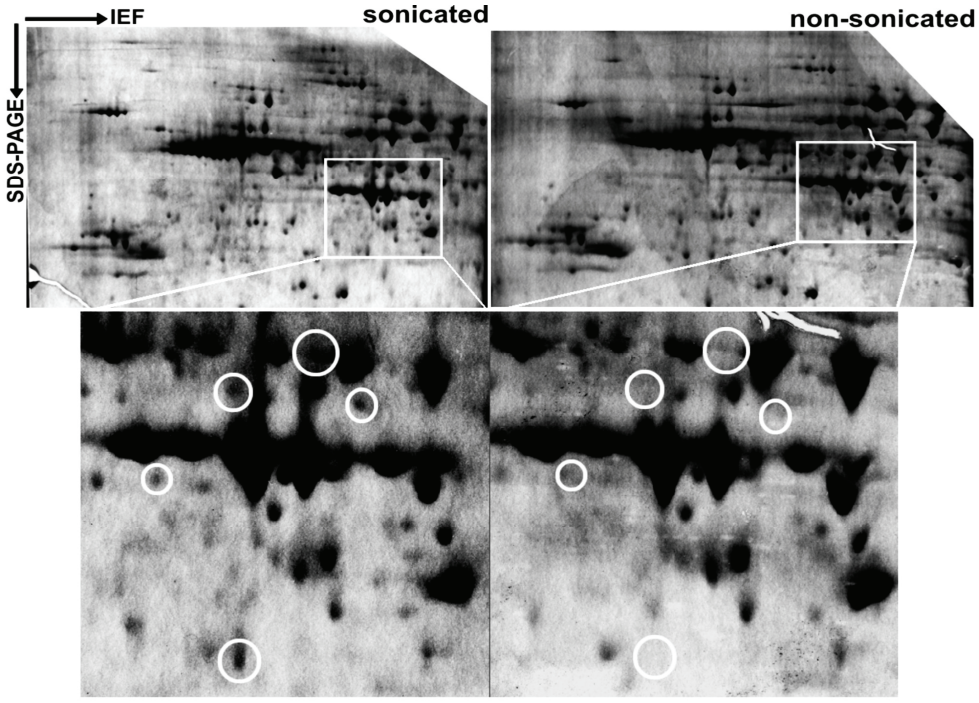

Figure 3.4 - Sonication increases protein solubility and spot resolution. 2-DE of sonicated and non-sonicated S126 fractions prepared from the rat hippocampus. IEF was performed in 24cm pH 4.5–5.5 strips (Amersham Biosciences) and the second dimension was performed in 10% SDS-PAGE. Circles represent new spots in sonicated samples.

intensity of some abundant proteins, remaining the total amount of protein constant in the two conditions. The magnitude of several spots was increased by more than three fold, clearly showing an increase in the solubility of these proteins when samples are sonicated.

In order to determine the effect of sonication in the reproducibility of the gels we used extracts prepared from cultured hippocampal neurons incubated with ^{35}S-radiolabelled amino acids for 12h. Protein spots separated by 2D-SDS-PAGE were detected by autoradiography, which has a much higher sensitivity than colorimetric or fluorescent methods of protein staining (McCarthy, J. et al., 2003). Radiolabelling experiments allow the visualization of low abundant protein spots and use of low amounts of protein, thereby decreasing spot streaking. Three replicate gels from non-sonicated and sonicated S126 fractions radiolabelled with ^{35}S-amino acids (Fig. 3.5), were analysed with PDQuest™. After spot detection, gels were automatically matched without manual editing, and the matching ratio was calculated (Table II). The results show that when gels prepared from non-sonicated samples were used as master the matching ratio with the other gels prepared from non-sonicated samples varied between 24 and 36%. Similar matching ratios were calculated in comparison to the gels from sonicated samples (22-28%). In contrast, much higher matching ratios were obtained (61-73%) when gels from sonicated samples were compared with each other. Interestingly, comparison of these gels with those prepared using non-sonicated samples still gave matching ratios between 28 and 43%. The boxed areas in Fig. 3.5 clearly show a higher reproducibility in the spots found in gels from sonicated samples than in those from non-sonicated samples. Taken together, the results show that sonication increases reproducibility between gels, thereby decreasing time spent in manual editing.

Table I. 2D gel analysis of the membrane fraction from sonicated and nonsonicated samples. Gels from Fig. 3.4 were analyzed using PDQuest.

	Sonicated sample	Nonsonicated sample
Total number of spots	173	156
New spots	20	3
Number of spots whose intensity increased when compared with the other condition	104	49
Number of spots whose intensity increased at least three times when compared with the other condition	14	4

Some spots which intensity changed by more than 75% in the gels prepared from sonicated and non-sonicated samples were identified (numbered spots in Fig. 3.5 and Table III; see also Fig. 3.6). The new spots identified in sonicated samples (Fig. 3.5; see also Fig. 3.6) migrated as predicted based on the molecular mass of the protein, indicating that protein degradation does not account for the differences observed. However, some of the new spots represent low abundant proteins that could not be identified or even seen with the double staining method used.

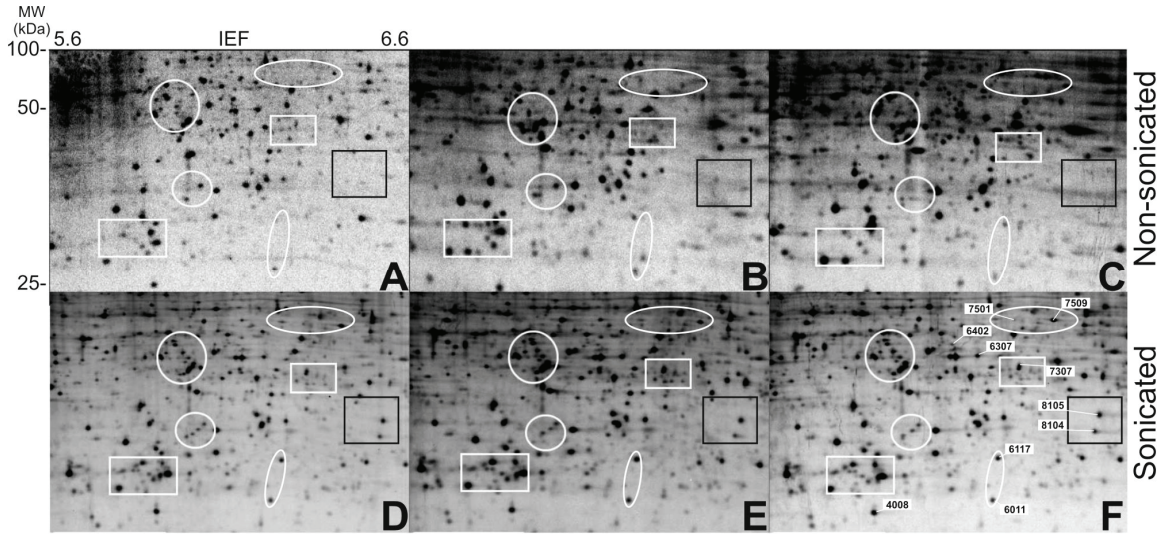

Figure 3.5 - Sonication increases reproducibility and matching ratio. 2-DE of sonicated and non-sonicated S126 fractions prepared from rat cultured hippocampal neurons, labelled with [^{35}S]-amino acids. IEF was performed in 24cm pH 5.5–6.7 IPG strips (Amersham Biosciences) and the second dimension was performed in 10% SDS-PAGE. Three replicate "zoom" gels (pH 5.6–6.6; MW<100kDa) are shown for each condition. Top panel: non-sonicated fraction; bottom panel: sonicated samples. Comparison between different gels is shown in Tab. II and protein ID in Tab. III.

Table II. Matching ratios between gels prepared from non-sonicated and sonicated samples. Gels analyzed (A–F) are those shown in Fig. 3.5. Each row presents an analysis set (PDQuest) with the score 100 corresponding to the gel used as master. (A-C, non-sonicated; D-E, sonicated)

%	A	B	C	D	E	F
A	**100**	31	24	24	26	25
B	31	**100**	27	22	24	24
C	27	36	**100**	28	26	28
D	30	29	28	**100**	61	62
E	43	39	40	70	**100**	73
F	36	40	36	68	68	**100**

Table III. Identification of spots highlighted in Fig. 3.5 by MALDI-TOF

Spot number	Accession number	Protein name	Fold change[a)]	Sequence coverage (%)	Matched peptides	MW	MASCOT score	GO process	GO function	Component
7509	Q91WQ3	Tyrosyl-tRNA synthetase	2.18	29	13	58.9	94.5	tRNA aminoacylation for protein translation	Ligase activity, nucleotide binding, RNA binding, tRNA binding	Cytoplasm[b)]
8105	P60892	Phosphoribosyl pyrophosphate synthetase I	33.9	31.5	9	34.7	90.40	Nucleoside metabolism	Kinase activity, lipoate-protein ligase B activity, metal ion binding	n.a.
8104	Q9CVB6	Actin-related protein 2/3 complex, subunit 2	18.04	48.2	8	22.2	79.10	Regulation of actin filament polymerization	Focal adhesion, Arp2/3 protein complex, cytoskeleton	Cytoplasm[b)]
7501	Q66HF8	Aldehyde dehydrogenase 1 family, member B1	1.73	22.2	8	57.6	57.60	Metabolism	Oxidoreductase activity	Cytoplasm[b)]
7307	Q7TNT7	Sept3 protein	7.56	28.5	8	38.7	61.90	Cell cycle	GTP binding	Cytoplasm[b)]
4008	P97576	GrpE protein homolog 1	2.02	24	4	24.3	53.80	Protein folding	Adenyl-nucleotide exchange factor activity, chaperone binding	Mitochondrion[c)]
6011	Q9QZ88	Vesicle protein sorting 29	4.45	36.8	7	20.5	59.7	Protein transport	Hydrolase activity	Cytoplasm and membrane associated[b)]
6117	Q9Z2L0	Voltage-dependent anion-selective channel protein 1 (VDAC-1)	4.48	40.8	7	30.6	69.10	Mitochondrial calcium ion transport	Voltage-gated ion-selective channel activity	Mitochondrial outer membrane[c)]
6307	Q8BFR5	Elongation factor TU	0.53	25	19	49.5	64.00	Protein biosynthesis, translational elongation	Nucleotide binding, translation elongation factor activity	Mitochondrion, extracellular space[c)]
6402	P50442	Transamidinase	0.35	34.5	14	48.2	94.5	Creatine biosynthesis	Glycine amidinotransferase activity	Mitochondrion[c)]

a) Fold change relative to nonsonicated samples.
b) According to database description.
c) GO component from EBI.
n.a. – not available.

Results

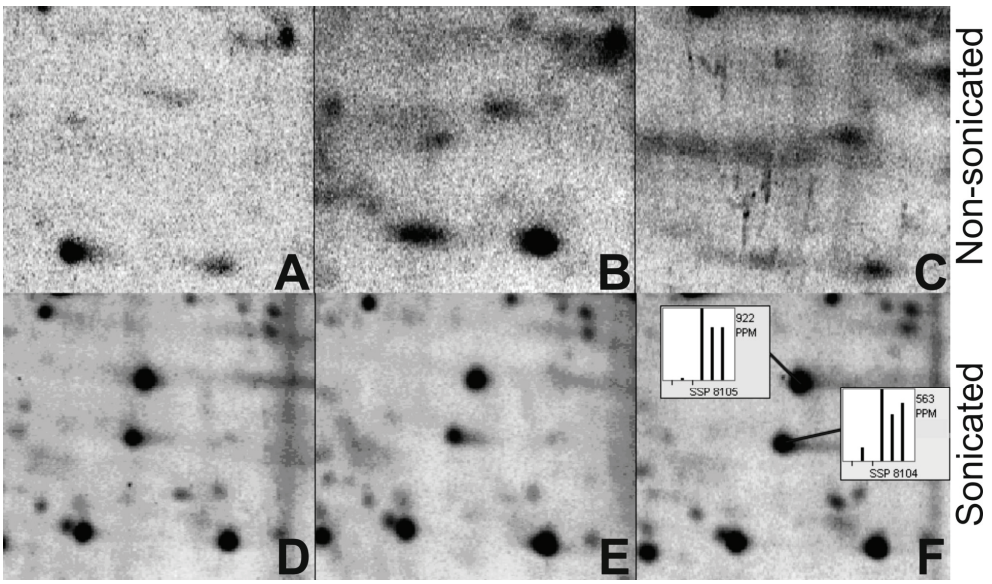

Figure 3.6 - Increase in protein solubility and reproducibility with sonication. PDQuest analysis of the spots contained within the box limited in black in Fig. 3.5. Bars represent relative intensity of the spots indicated in the replicate gels (A–C, three bars on the left; D–F, three bars on the right).

3.3 – Conclusion

In **conclusion**, the results obtained in this part of the work show an increase in the number of spots being resolved using sample fractionation and "zoom" gels. It is also shown an increase in resolved spots and in protein recovery from TCA precipitated proteins, using sonication as a physical approach for protein solubilization. These, in combination with the increase in reproducibility from different gels in different runs, allow better and faster software analysis. Sample sonication increases the rate of matching, decreases the variability of relative spot intensity between replicate gels, increases the confidence of statistically applied tests, and decreases time spent in software manual editing (Manadas, B. J. et al., 2006).

Chapter 4

BDNF-induced changes in the proteome of hippocampal neurons

4.1 – Introduction

The hippocampus plays an important role in memory formation and storage. These processes are thought to require long-term changes in the synaptic activity and de novo protein synthesis. BDNF is a key mediator of activity-induced long-term changes in synaptic strength in the hippocampus, through modulation of gene transcription and translation (Steward, O. and Schuman, E. M., 2001; Takei, N. et al., 2004; Santi, S. et al., 2006; Schratt, G. M. et al., 2006). Therefore, the characterization of the changes in the proteome of hippocampal neurons induced by BDNF will contribute to understand the mechanisms whereby the neurotrophin contributes to synaptic plasticity.

The hippocampus is also severely affected in stroke and after global forebrain ischemia (Kokaia, Z. et al., 1996; Larsson, E. et al., 1999). Addition of BDNF to cultured neurons had a protective effect against excitotoxicity induced by glutamate (Almeida, R. D. et al., 2005), and endogenous BDNF was markedly increased in rats subjected to global forebrain ischemia (Kokaia, Z. et al., 1996), protecting hippocampal neurons from cell death mechanisms (Larsson, E. et al., 1999). Under the excitotoxic conditions, the neuroprotection by BDNF is conferred in a protein synthesis dependent manner, with protein synthesis inhibitors abrogating the protective effect induced by BDNF (Almeida, R. D. et al., 2005). Furthermore, BDNF has been intimately related to Alzheimer, Parkinson, and mainly Huntington's disease mechanisms, thereby increasing the interest in the identification of target genes also responsible for the neuroprotection mechanisms.

The objective of this study was to characterize the BDNF-induced changes in the proteome of cultured hippocampal neurons. This proteomic study was performed using mainly two-dimensional gel electrophoresis of extracts prepared from cultured hippocampal neurons stimulated or not with BDNF. Since the use of standard 2D-gels resulteds in a limited coverage of the hippocampal proteome, sample fractionation was performed and "zoom" gels were used to increase the number of spots in quantification and identification analysis. In order to monitor only newly synthesized proteins, the stimulation was performed in the presence of radiolabelled amino acids, and the BDNF induced changes in the proteome were quantified from autoradiogram gel images using appropriate software. After spot identification, the characterization of the proteins was performed based on information retrieved from different databases, and a selected group of proteins was used for clustering analysis, based on Gene Ontology. In order to further increase the coverage of the cultured hippocampal neurons proteome and the differential protein expression induced by BDNF, the fraction enriched in membrane proteins was analysed using a liquid-based approach.

4.2 – Results

4.2.1 - Radiolabelling of proteins in cultured hippocampal neurons

Radiolabelling of proteins offers several advantages in studies aiming at the identification of stimuli-induced changes in the proteome: (i) possibility of monitoring exclusively newly synthesized proteins, thereby decreasing gel complexity and increasing gel analysis speed; radiolabelling not only facilitated analysis in the first automated steps, but also on manual verification and analysis, (ii) high sensitivity, (iii) large dynamic range, particularly when compared to staining methods as Coomassie, colloidal Coomassie, and silver staining, and (iv) low cost, when compared with commercially available fluorescent staining. Therefore, preliminary studies were performed to characterize the time-course of [^{35}S]-cysteine and [^{35}S]-methionine uptake by cultured hippocampal neurons (Fig. 4.1). Neurons were starved from the sulphur containing amino acids, methionine and cysteine, for 30 minutes, by replacing the standard culture medium with methionine- and cysteine-free DMEM. This incubation period allowed the incorporation of the remaining cold methionine and cysteine into proteins. The cells were then incubated in the presence of [^{35}S]-methionine and [^{35}S]-cysteine for different periods of time, and amino acid uptake was monitored. The results

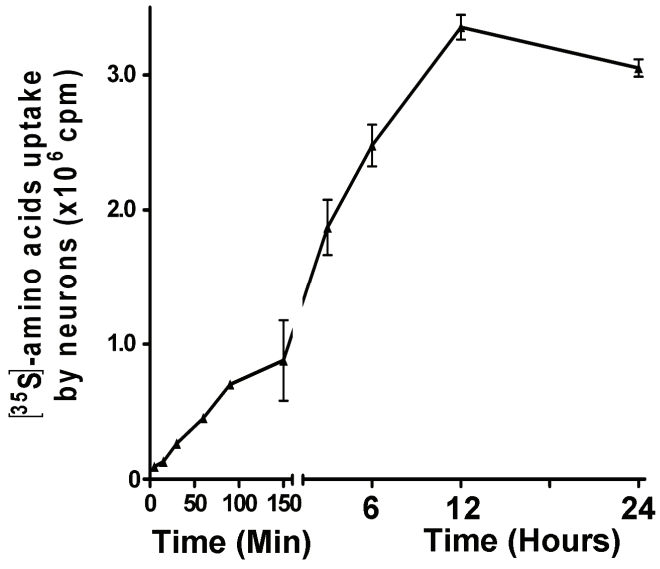

Figure 4.1 – [^{35}S]-amino acid uptake by hippocampal neurons. After DIV7, cells were starved from methionine and cysteine, for 30min, and were then incubated with [^{35}S]-cysteine and [^{35}S]-methionine for the indicated time periods. Uptake of radiolabelled amino acids was then measured after washing the cells with sodium medium. The results are the average±SEM of 3 experiments, preformed from independent preparations.

show a time-dependent accumulation of [^{35}S]-amino acids, with maximal uptake observed at 12h.

The incorporation of radiolabelled amino acids into **newly synthesized proteins** was determined after different incubation periods followed by protein precipitation with TCA and radioactivity counting (Fig. 4.2A). Due to the low amount of protein content present in the cells used in each experiment, BSA was added, in order to improve protein precipitation. The results show a time-dependent increase in radiolabelled amino acid incorporation into newly synthesized proteins, with a maximum at 24h (for the time points monitored). This indicates that neurons incorporate radiolabelled amino acids into newly synthesised proteins, and the process reaches a steady state after 24h. Longer incubation periods are expected to cause amino acids and sulphur metabolism, and are probably not appropriate for protein labelling. In order to confirm that the observed radiolabelling of proteins was due to translation activity,

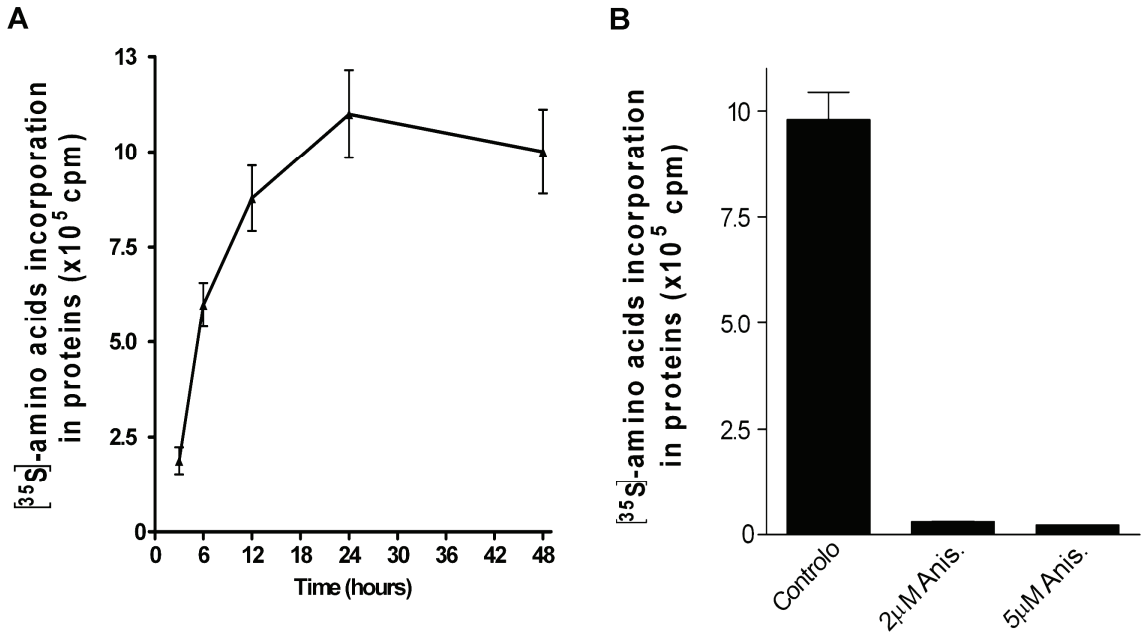

Figure 4.2 – Incorporation of radiolabelled amino acids into proteins. (**A**) Radiolabelled amino acids are incorporated into newly synthesized proteins. After radiolabelling with [^{35}S]-cysteine and [^{35}S]-methionine the cells were washed and the proteins precipitated with 10% (v/v) TCA and 0.5% (w/v) BSA. The samples were centrifuged and the precipitated proteins were washed before measuring the radiolabelled amino acids incorporated into proteins. (**B**) Anisomycin prevents [^{35}S]-amino acid incorporation into proteins in cultured hippocampal neurons. Cells were starved of methionine and cysteine, for 30min, and anisomycin was then added or not (control), at the concentrations indicated, 15min after the beginning of the starvation period. The cells were then incubated with [^{35}S]-cysteine and [^{35}S]-methionine for 6h. Incorporation of radiolabelled amino acids into newly synthesized proteins was then measured. The results are means±SEM of 3 (A) and 2 (B) experiments, performed in independent preparations.

we tested the effect of the protein synthesis inhibitor anisomycin. In the presence of anisomycin only trace amounts of radiolabelled proteins were detected (Fig. 5.2B). The amount of radioactivity detected under these conditions may be due to contamination of the samples with radiolabelled amino acids present in the culture medium.

4.2.2 - Incorporation of radiolabelled amino acids in the presence of BDNF

In order to determine whether BDNF affects the overall protein synthesis in cultured hippocampal neurons, the accumulation of [^{35}S]-cysteine and [^{35}S]-methionine in newly synthesized proteins was determined in the absence and in the presence of BDNF, using different incubation periods with the neurotrophin (Fig. 4.3).

BDNF did not change significantly total protein synthesis in cultured hippocampal neurons, for the time points evaluated. These results suggested that BDNF does not have an overall effect in total protein synthesis in cultured hippocampal neurons, but may instead control the synthesis of specific proteins.

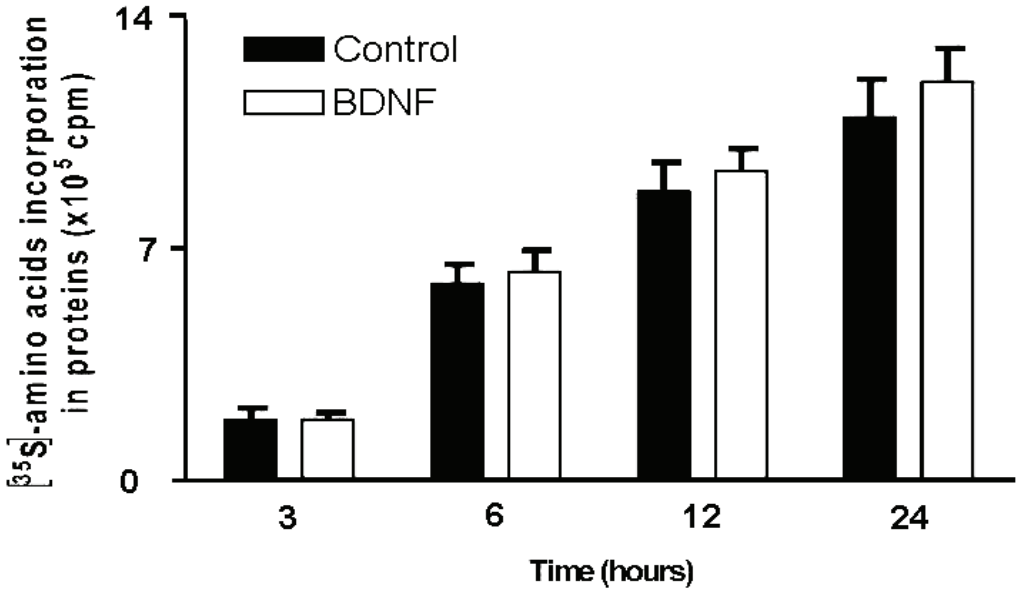

Figure 4.3 –Total protein synthesis in hippocampal neurons is not significantly changed with BDNF. Cells were treated as indicated in the caption of Fig. 4.2A. Briefly, cells were starved from methionine and cysteine for 30min, and [^{35}S]-radiolabelled amino acids were then added, with or without BDNF (100ng/mL), for the indicated periods of time. Cells were then lysed and proteins precipitated using 10% TCA and 0.5% BSA. Results show radiolabelled amino acid incorporation into newly synthesized proteins and are means of three experiments performed in independent preparations. Statistical analysis was performed using the Student's *t*-test (GraphPad Prism, San

4.2.3 - Proteomic changes induced by BDNF – Gel based approach

In order to determine the changes in the proteome of cultured hippocampal neurons induced by BDNF, 2D-PAGE was performed using extracts prepared from cells incubated with radiolabelled [^{35}S]-methionine and [^{35}S]-cysteine for 12h, in the presence or in the absence of BDNF. In order to increase the number of spots detected, the samples were fractionated in two, the soluble fraction and the pellet resulting from the ultracentrifugation at 126,000×g_{av} (S126 fraction). The proteins were resolved in the first dimension using IPG strips of the following pH ranges: 4.5-5.5, 5.0-6.0, 5.5-6.7 and 6.0-9.0. Representative gels obtained using the soluble fraction and the S126 fraction are shown in Fig. 4.4 and Fig. 4.5, respectively. All gels shown in both figures, as well as in all other figures on this section, are oriented with the anode (acidic) to the left and catode (basic) to the right, and the second dimension was performed in 10% acrylamide.

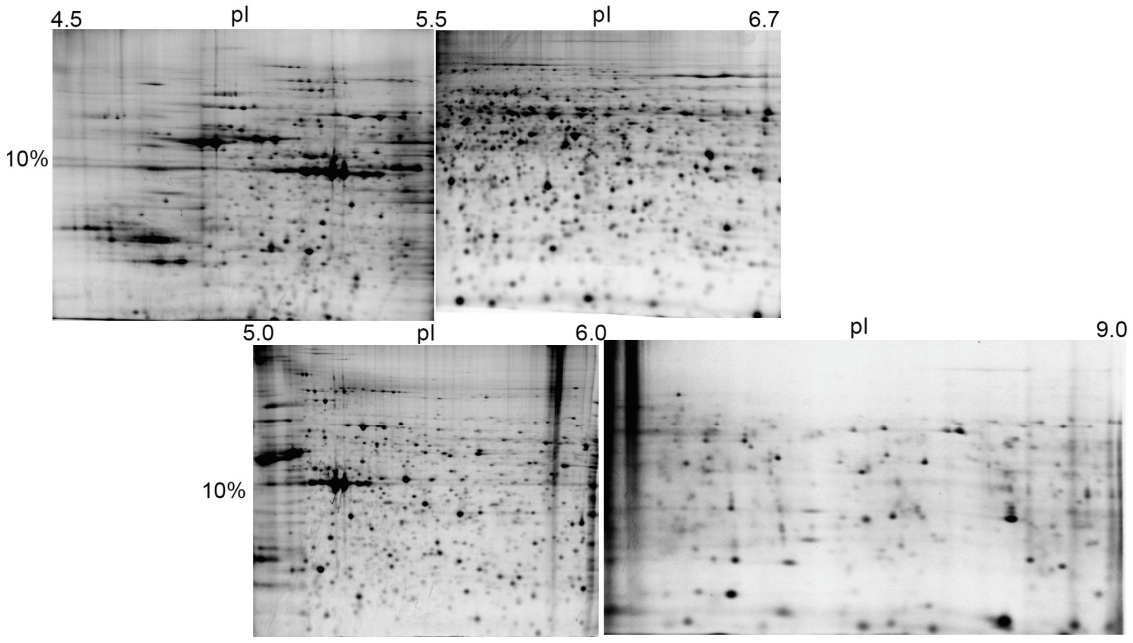

Figure 4.4 - Two dimensional gel electrophoresis of soluble proteins. Radiolabelled amino acids were incorporated into newly synthesized proteins for 12h, as indicated in the caption of Fig. 4.3. Samples were then processed as indicated in the caption of Fig. 3.5 (sonicated). Proteins were focused using IPG strips pH 4.5-5.5, 5.0-6.0, 5.5-6.7 and 6.0-9.0. After running the second dimension, the gels were dried and placed in contact with a phosphor screen. Images were acquired using a STORM laser scanner.

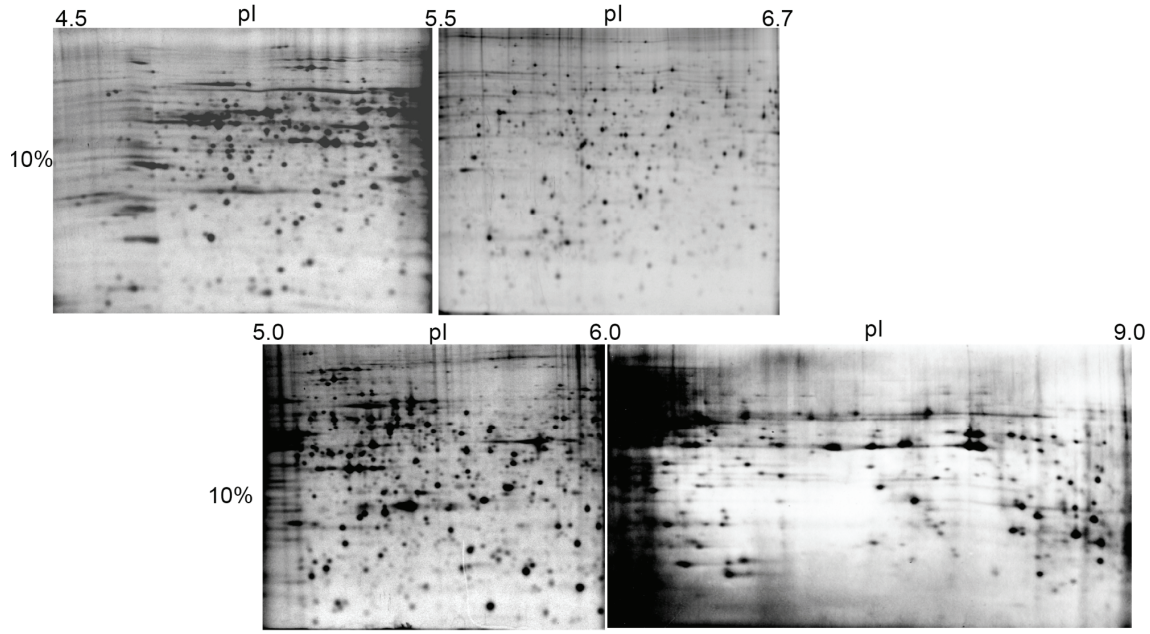

Figure 4.5 - Two dimensional gel electrophoresis of the S126 fraction. Radiolabelled amino acids were incorporated into newly synthesized proteins for 12h, as indicated in the caption of Fig. 4.3. Samples were then processed as indicated in the caption of Fig. 3.5 (sonicated). Proteins were focused using IPG strips pH 4.5-5.5, 5.0-6.0, 5.5-6.7 and 6.0-9.0. After running the second dimension, the gels were dried and placed in contact with a phosphor screen. Images were acquired using a STORM laser scanner.

4.2.3.1 – *General workflow*

The methodology used in the analysis of each gel is illustrated in this section, using as an example the experiments with the soluble fraction applied to IPG strips with a pH range of 5.5-6.7. The same approach was used for the other pH ranges as well as for the S126 fraction, using control extracts and samples prepared from hippocampal neurons incubated with BDNF (100ng/mL) for 12h. The work included the analysis of radiolabelled gels, their mapping, matching between radiolabelled and stained gels, differential expression analysis, correlation between protein ID acquired from mapping with differential expression, gathering gene information from different databases, and cluster and functional analysis (Section 4.2.5). Figure 4.6 shows a representative gel prepared from a soluble fraction containing radiolabelled proteins focused using IPG strips pH 5.5-6.7 and 10% acrylamide in the second dimension. The image was acquired with a laser scanner from an exposed phosphor screen. Analysis of the gel with PDQuest shows more than 700 spots which have been matched with at least other five gels. Six different experiments were performed for control and BDNF stimulated cells and the most reproducible set of images was chosen for software analysis. The criteria for gel images inclusion or exclusion on the analysis set consisted in the

elimination of gels which general pattern was markedly different from the mean distribution pattern of protein spots across the gel image. Gel images were imported to PDQuest™, and the spots were detected and then matched throughout the entire matchset (Fig. 4.7). After automated matching, according to the parameters choosen, manual spot detection and matching was performed in order to confirm or to correct results from software automated functions. Each spot was considered a valid spot if it was present in more then 50% of the gels from a given condition (control or BDNF). In terms of matching, spots not automatically matched by the software were considered as being the same spot if surrounding spots presented the same distortion pattern. The same approach was applied for validating

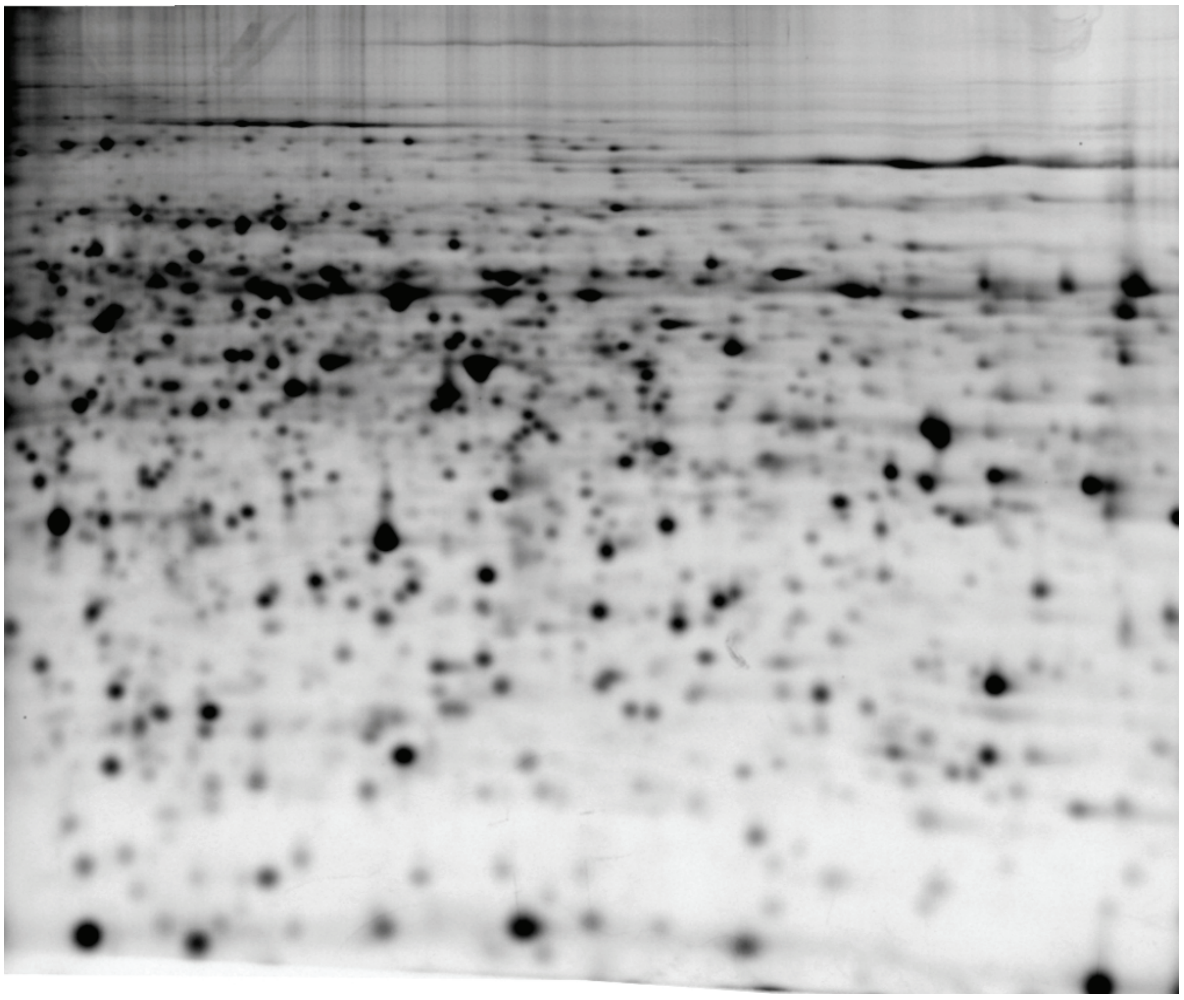

Figure 4.6 - Two dimensional gel electrophoresis of proteins from a soluble fraction isolated from cultured hippocampal neurons. Radiolabelled amino acids were incorporated into newly synthesized proteins for 12h and samples were processed as indicated in the caption of Fig. 4.4. Proteins were focused using IPG strips pH 5.5-6.7. After the second dimension, gels were dried and placed in contact with a phosphor screen. Images were acquired using a STORM laser scanner.

automated matching. After matching, gel images were normalized using the "total intensity in valid spots" algorithm. This is used when there are no major differences across gel images and when a significant change in the majority of the spots is not expected (according to the software manual). After this step, replicate groups were created in PDQuest, and statistical and quantitative analysis was performed, as well as Boolean analysis, which consisted in the combination of the statistical and quantitative analysis previously performed. Due to the variability observed in the results from different batches of experiments, data analysis may be facilitated with the use of statistical methods that allow paring data sets. Since this is not available in the PDQuest software, the normalized data were exported to Excel in order to expand the possibilities of data analysis.

The analysis consisted in the following aspects (Table IV): (1) calculating, for each given spot, the ratio between the spot intensity determined in extracts prepared from BDNF stimulated cells and control cells, in each independent experiment, and then retrieve the mean value of the ratios, (2) perform statistical analysis using the unpaired Student's *t* test to determine the statistical significance of the difference between the calculated means (unpaired analysis), and between the results from the same batch of experiments (normalized to the control), (3) indicate ratios outside of the range 1/1.5 to 1×1.5, (4) select and combine results of the previous calculations (1 through 3; e.g. spots showing statistically

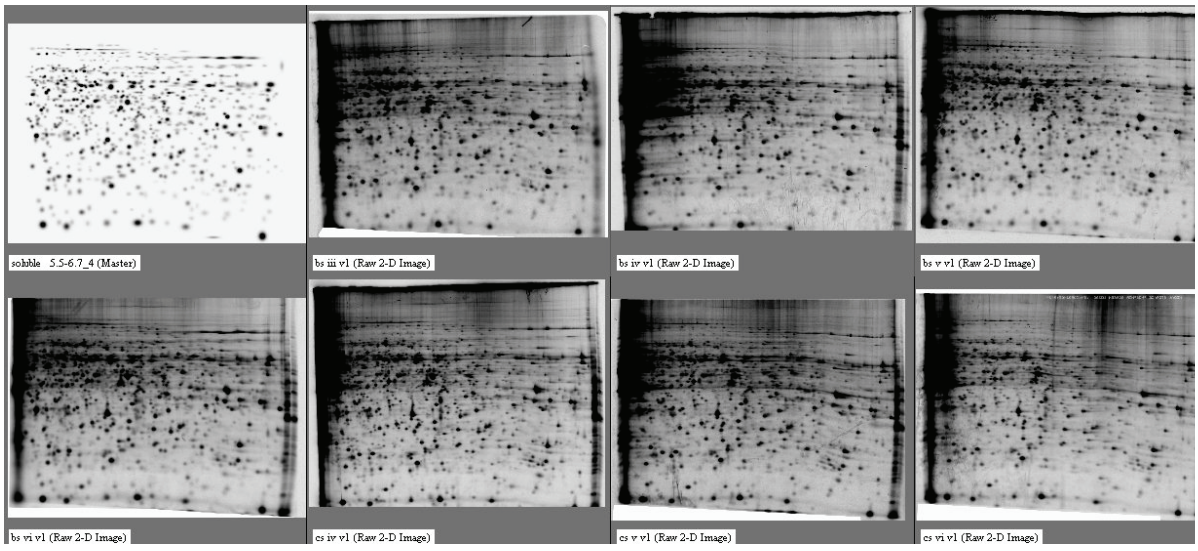

Figure 4.7 – Software analysis of gel images. Gels prepared using extracts of control or BDNF-stimulated hippocampal neurons were scanned by autoradiography, and the best gel images were chosen for differential expression analysis. The gels were prepared as indicated in the caption of Fig. 4.6. Image shows master gel image (top left corner), followed by 4 gels of BDNF stimulated cells (bs) and 3 gels of control condition (cs).

significant differences, retrieved from step 2, and outside the range, defined in step 3). The selection of the ratios outside the range 1/1.5 to 1×1.5 is distinct from the most common range presented in the literature, which is a "decrease to half or an increase to more than twice" (?/2 to ?×2) from one condition to the other. However, given the fact that the objective of this study was to identify newly synthesized proteins, and considering that the response to BDNF regulates amplification pathways, it was decided to shorten the range from a factor of 2 to a factor of 1.5 (?/1.5 to ?×1.5). Because a cluster analysis was performed as the last step, we also took into consideration spots that showed a consistent but not statistically significant changes in abundance following stimulation with BDNF, within the range 1/1.5 to1×1.5.

Legend of Table IV

Results obtained from PDQuest (Fig. 4.7) were exported to Excel which is more versatile for calculations and interpretation of the results. Rows in Table IV contain information from a specific spot indicated in the first column (SSP – single spot number). Columns **B-E** indicate the results of spot quantification by the PDQuest software in the soluble fraction isolated from BDNF stimulated hippocampal neurons, in five experiments performed in independent prepartions (BSiii; BSiv; BSv; BSvi). Columns **F-H** indicate values given by the PDQuest software for the indicated spot in control conditions in five different independent experiments (CSiv; CSv; CSvi). Columns **K-M** show ratios (BDNF/Control – normalization to control) for each experiment. Column **N** indicates the number of validated ratios obtained. Column **O** shows the calculated ratios' mean. Column **P** indicates whether an obtained ratio mean is outside the range (1/1.5-1×1.5), and if the mean is above (UP) or below (DOWN) this range. Column **Q** calls the users attention to values outside the range and with at least 3 ratios calculated. Column **S** shows the results of the unpaired Student's *t* test analysis for raw values, indicating whether the comparison between the two experimental conditions (control vs. BDNF treated cells) shows statistically significant differences. Column **T** calls the user attention to p values below 0.05, for Student's *t* test applied to raw values. Column **U** shows the results of the unpaired Student's *t* test analysis of data normalized to the control (ratios), indicating whether there are statistically significant differences between the two experimental conditions (control vs. BDNF treated cells). Column **V** calls the user attention for p values below 0.05, when the statistical analysis is performed using the unpaired Student's *t* test and data normalized to the control. Column **AL** calls the user attention for ratio values consistent in all batches, either increasing or decreasing ("trend"), even when the results obtained do not reach statistical significance.

Table IV – Differential expression analysis (extract). Table shows data obtained from the soluble fraction resolved using IPG strip pH 5.5-6.7

A	B	C	D	E	F	G	H	K	L	M	N	O	P	Q	R	S	T	U	V	AL
SSP	bs iii	bs iv	bs v	bs vi	cs iv	cs v	cs vi	bs4/cs4	bs5/cs5	bs6/cs6	N	ratios mean	1/1.5 to 1x1.5 range	N>3 and UP or DOWN		t test of Raw data	is p<0.05?	t test of ratios	is p<0.05?	Trend
2003	3160.4	3437.8	5434.4	8036.7	6072.1	6810.7	7623.9	0.57	0.80	1.05	3	0.81				0.210		0.303		
2004	1724	1095.6	3420.9	1769.9	1785.2	4242.5	2572	0.61	0.81	0.69	3	0.70				0.384		0.034	Yes	DOWN
2005	5121.8	4331.7	4389.3	5098.8	5059.8	5470.7	5861.4	0.86	0.80	0.87	3	0.84				0.074		0.017	Yes	DOWN
2006	1461.6	918.4	1428.6	1608.9	1971.4	2083.3	2032.7	0.47	0.69	0.79	3	0.65	DOWN	SEE		0.018	Yes	0.067		DOWN
2007	3642.1	2060.4	2139.9	2531.9	3052.7	2848.9	2968.8	0.67	0.75	0.85	3	0.76				0.394		0.043	Yes	DOWN
2008	215	394.3	1500.9	1787.5	1841	2186.3	507.1	0.21	0.69	3.52	3	1.48				0.451		0.691		
2009	8217.3	2394.4	1015.4	1016.9	2502	2562.3	2174.3	0.96	0.40	0.47	3	0.61	DOWN	SEE		0.693		0.155		DOWN
2010	850	413.5	470.2	645.4	972.8	1387	328.7	0.43	0.34	1.96	3	0.91				0.435		0.879		
2101	675.7	540.1	404.8	610.7	858	565.1		0.63	0.72		2	0.67				0.473		0.084		
2102	907.8	285.6	295.5	532	578	399.4	708	0.49	0.74	0.75	3	0.66				0.755		0.056		DOWN
2103	430.2	531.1	531.4	582	737.1	614.2	827.2	0.72	0.87	0.70	3	0.76				0.057		0.044	Yes	DOWN
2104	308.1	140	134.5	283.6	373.7	505.7	365.3	0.37	0.27	0.78	3	0.47	DOWN	SEE		0.029	Yes	0.077		DOWN
2105	848.2	735.6	331.5	588.4	848.1	557.3	554	0.87	0.59	1.06	3	0.84				0.862		0.362		
2106	291.8	318.1	503.1	622.3	1265.7	1004	904.2	0.25	0.50	0.69	3	0.48	DOWN	SEE		0.010	Yes	0.054		DOWN
2201	2410.8	1485.1	819.6	972.4	1267.9	1572.5	957.7	1.17	0.52	1.02	3	0.90				0.716		0.668		
2202	1090.7	1875.8	1213.3	1011.6	1363.7	1192	1527.4	1.38	1.02	0.66	3	1.02				0.787		0.936		
2203			612	720.2	1092.7	715.5	799.4		0.86	0.90	2	0.88				0.216		0.118		
2204	2385.2	3312	3088.2	3182.5	1871.4	3346	2176	1.77	0.92	1.46	3	1.39				0.368		0.260		
2205	3657.6	2993.6	3818.8	3655.6	3121.1	3936.7	3668.7	0.96	0.97	1.00	3	0.98				0.891		0.154		DOWN
2206	3050.9	2233.8	1349	1718.6	3108.7	1873.7	2300.3	0.72	0.72	0.75	3	0.73				0.541		0.001	Yes	DOWN
2207	1624.2	2673.9	1609.2	1464.9	1747.8	1910.6	1833.6	1.53	0.84	0.80	3	1.06				0.968		0.832		
2208	2665.9	2078.3	2244.2	2208.2	2437.5	2513.5	2559.3	0.85	0.89	0.86	3	0.87				0.208		0.008	Yes	DOWN
2209	977.1	696.3	681.2	704	862.5	895.9	1256.8	0.81	0.76	0.56	3	0.71				0.188		0.062		DOWN

After data analsys with Excel, the spots of interest were gathered and imported to PDQuest, in order to depict them on the gel (Fig. 4.8). These included statistically different spots, spots which intensity changed by a magnitude outside the range of interest, and spots which intensity changed in a consistent manner but did not show a statistically significant variation ("trend").

After the differential expression analysis, the next step consisted in the identification of the proteins present in the spots of interest. The strategy used involved the analysis of all (or the majority) protein spots since different protein isoforms can be found in distinct spots after separation in 2D-gels. From the functional point of view it is relevant to determine whether BDNF selectively affects certain isoforms of a given protein. Therefore, it was decided to perform a full mapping of working gels, followed by the combination of these results with data from protein expression levels (Fig. 4.8).

Full mapping of the protein spots in 2D-gels was performed under conditions similar to those

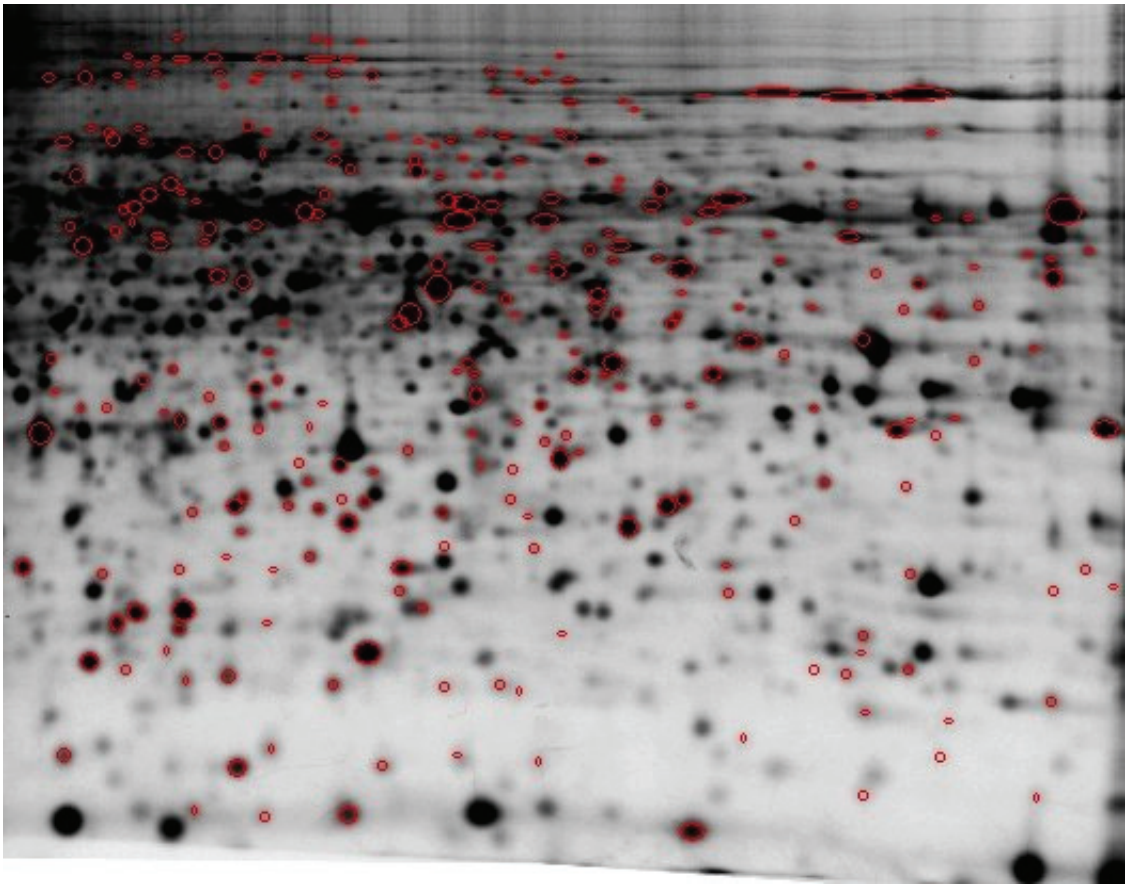

Figure 4.8 – Differential expression analysis. Image shows gel image used to create master gel from Fig. 4.7 of soluble fraction resolved using IPG strips pH 5.5-6.7. Red circles represent spots whose levels differ from control to BDNF stimulated condition (Table IV).

used in the autoradiography experiments. However, the amount of total protein used in the autoradiography experiments (250μg), which provided a good resolving power, was not enough for protein identification of most spots by MALDI-TOF MS. The increase in protein loading of IPG strips, up to 1mg, without compromising the gel resolution, was performed by using in-gel rehydration followed by cup loading. Thus, 500μg of total protein content were applied in each step, increasing the number of spots detected after staining with ruthenium followed by colloidal Coomassie (data not shown). The gels were then picked, digested and the proteins were identified by using MALDI-TOF or MALDI-TOF-TOF MS. The spectra obtained were subjected to peptide mass fingerprint database search, as a first approach. Whenever there was no positive ID, and if mass spectra returned peaks which quality met the requirement for TOF-TOF analysis, this method was used for further analysis using the 4

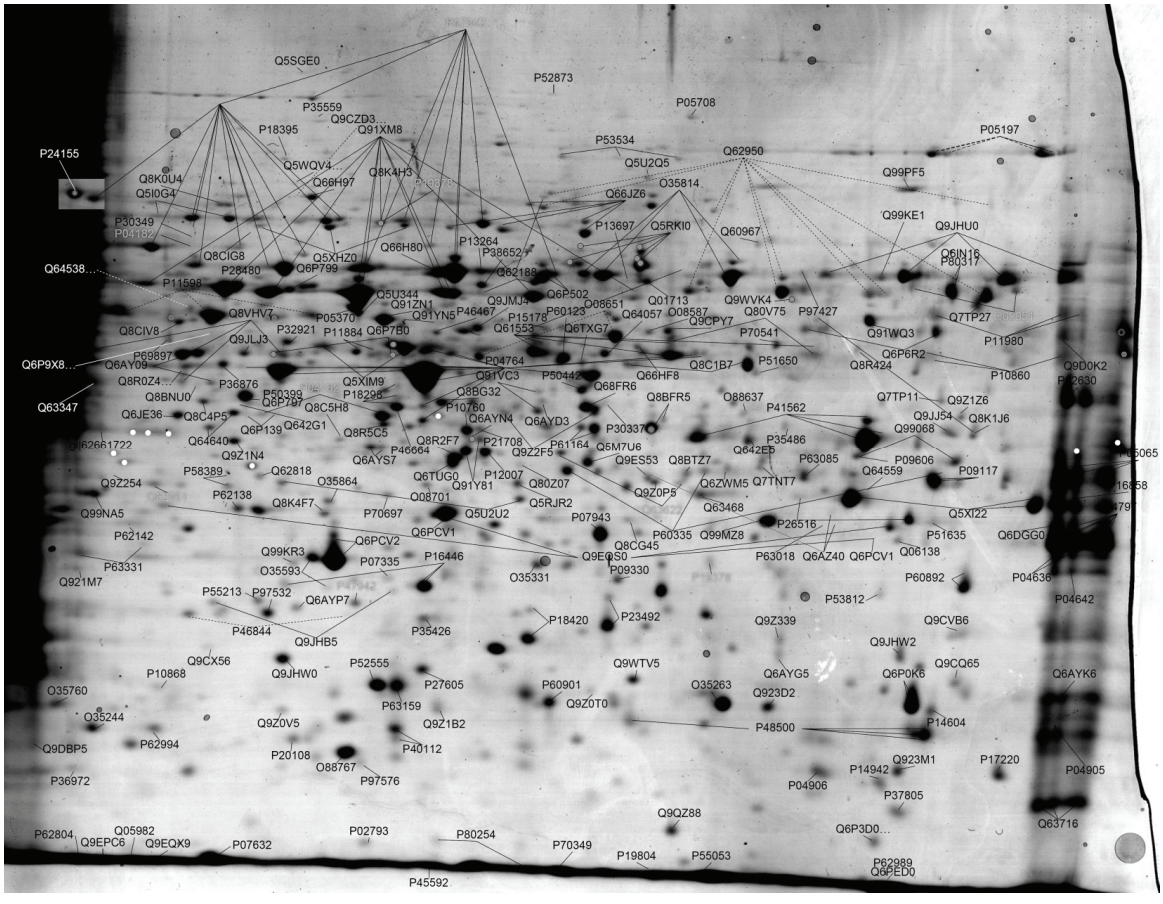

Figure 4.9 – Gel mapping. Proteins from the soluble fraction were treated and identified as stated in Fig. 3.5. The image shows a colloidal Coomassie stained gel of proteins focused in pH 5.5-6.7 IPG strips, and the accession numbers of identified spots.

peptides with best quality. Once the proteins were identified, their accession numbers were matched to their corresponding spots (Fig. 4.9).

The comparison of the autoradiograms obtained upon separation of radiolabelled proteins with the protein spot pattern detected after staining with colloidal Coomassie showed that although the general pattern was similar, not all spots matched (Fig. 4.8 and Fig. 4.9). Therefore, a gel prepared with radiolabelled proteins was silver stained and manual matching

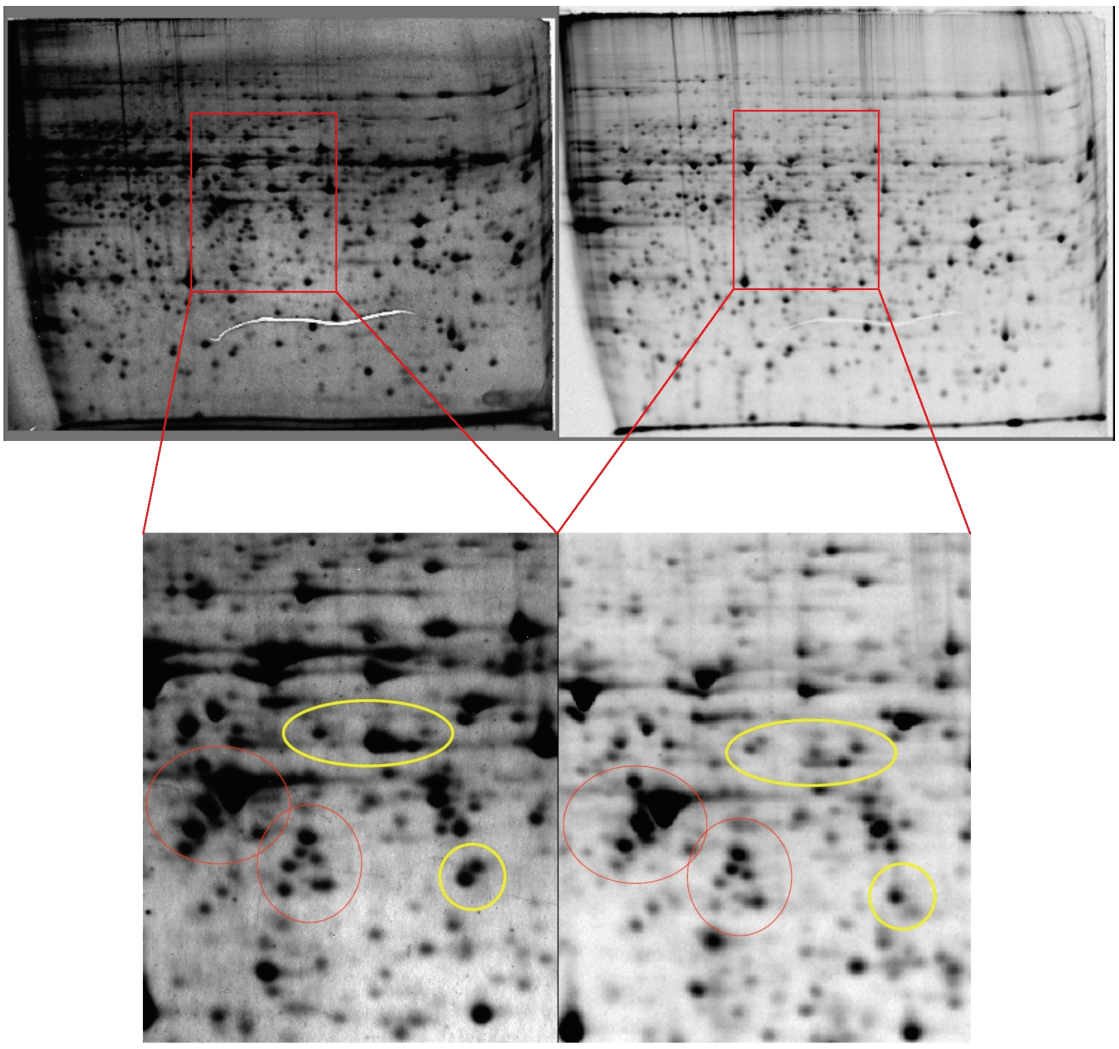

Figure 4.10 – Differences between the spot pattern in autoradiograms (radiolabelled proteins) and silver stained gels (total protein content). Radiolabelled proteins were treated as indicated in the caption of Fig. 4.6 (soluble fraction, pH 5.5-6.7) except that the gel was silver stained before being dried, and was then exposed to a phosphor screen. The same gel was scanned in an office scanner for silver staining (left), and in a laser scanner for radiolabelling (right). The zoomed images (bottom panel) show spot patterns in both images that are either conserved (red ellipses) or not (yellow ellipses).

was performed together with software analysis, showing that several spots were detected only in one of the two gel images, either silver stained or autoradiography. A double gel labelling allows a better analysis and matching between protein ID and differential expression analysis.

Given the differences between the spot pattern in the autoradiograms and the stained gels, the gel image containing differential expression analysis of autoradiograms shown in Fig. 4.8 was matched with the gel mapping image obtained from protein ID by MALDI-TOF MS shown in Fig. 4.9 (Fig 4.11).

The interpretation of the data obtained from the 2D-gels depends on its integration into a biologically meaningful structure (not fragmented). Therefore, the results were gathered in two formats: Excel spreadsheet (containing information regarding differential expression of all spots, protein ID, calculations, annotations, etc) and PowerPoint files (containing information gathered from different databases and presenting one by one relevant biological information) (Figs. 4.12 through 4.14). The information gathered in PowerPoint files comprised, in a first step, the visualization of matching between protein ID and differential expression in the presence of BDNF (Fig. 4.12). The protein accession number, protein name, gene name, and information regarding differential expression are presented in a simplified manner (supplementary information in CD). An algorithm was developed to automatically retrieve into Excel spreadsheets all gene names corresponding to the accession numbers obtained (not shown).

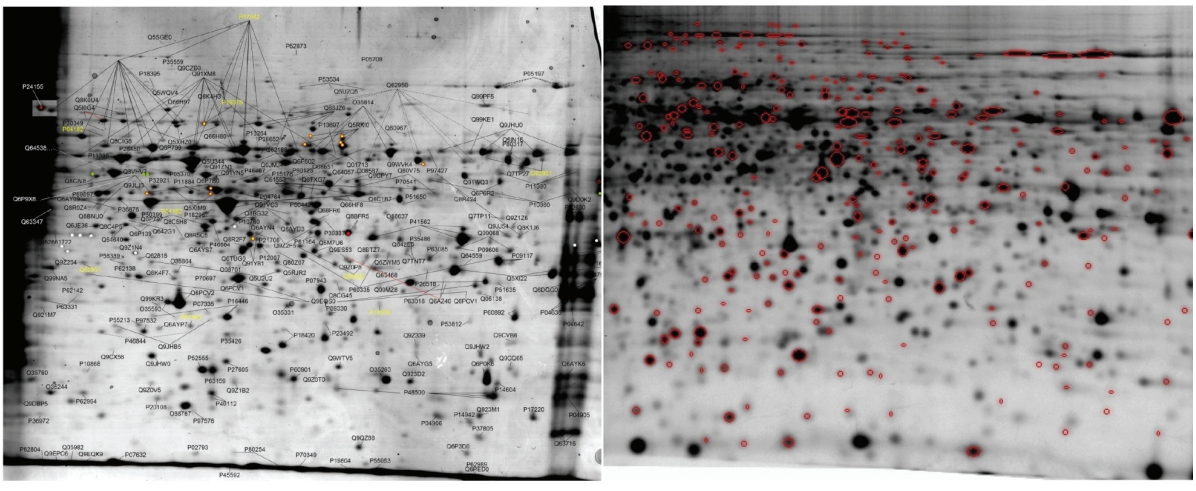

Figure 4.11 – Correlation between spot quantification and ID. Left image shows full mapping of soluble protein in the pH range 5.5-6.7 (Fig. 4.9). Right image highlights spots which expression changed in the soluble fraction from BDNF treated cells (Fig. 4.8). These images were used for manual correlation of spot ID and quantification.

Once the protein spots were identified, and the corresponding accession numbers obtained, additional information was retrieved from several different databases. This is made easier because the hyperlinks are identical, differing only in the accession number or gene name inside the hyperlink (e.g. gene name *ENO1* in the hyperlink http://discover.nci.nih.gov/textmining/cgi-bin/entry-preresults-post.cgi?datetype=2&relentrezdatefrom=2001/2&relentrezdateto=2006/4&text1=ENO1; or accession number P04764 in the hyperlink http://www.expasy.org/uniprot/p04764). In addition to the information obtained from databases such as UniProtKB/Swiss-Prot (Fig. 4.13A), another relevant source of information about the proteins of interest is the MedMiner database, which searches and organizes the PubMed literature on genes and drugs (Fig. 4.13B). This filter retrieves articles

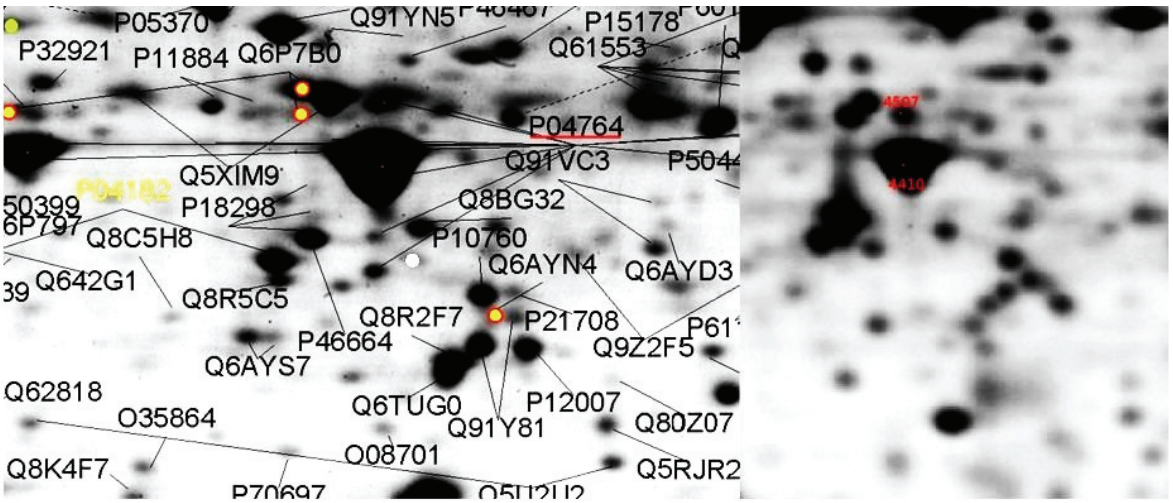

P04764 - Alpha enolase (EC 4.2.1.11) (2-phospho-D-glycerate hydro-lyase) (NNE) (Enolase 1)

Gene name: Eno1

Gene synonym:Eno-1

Spot	Ratio	Statistically different? (unpaired and paired)	
3406	0.88	No	No
3511	0.86	No	No
3512	0.94	No	No
4410	1.22	**Yes**	No
4507	1.11	No	**Yes**
5502	1.38	No	No
6402	1.02	No	No

Figure 4.12 – Manual correlation of spot quantification and ID. The image containing full mapping (left, Fig. 4.9) was manually correlated with the image containing quantification information (right, Fig. 4.8). The figure shows one example of protein ID and quantification matching. The protein P04764 (left) was identified in seven different spots which were quantified (right). Below gel images is some of the information retrieved about this protein: accession number, protein name, gene name and synonym, spot numbers, ratio (BDNF/Control) and information regarding statistical analysis using the Student's *t* test.

published in the last 5 years, extracting and organizing relevant sentences in the literature based on a gene, gene-gene or gene-drug query. The information obtained from these filters has to be manually validated because other abbreviations may be used with a complete different meaning for a given gene name (Fig. 4.13B).

Additional information about the protein of interest was retrieved from several different databases (Fig. 4.14). GeneCards contains information on signalling and/or metabolic pathways where a given gene is involved, in addition to the interaction with other proteins/genes, and the gene location in chromosome. The GeneCards is an integrated database of human genes that includes automatically-mined genomic, proteomic and transcriptomic information, as well as orthologies, disease relationships, SNPs, gene expression, gene function, and service links for ordering assays and antibodies. Information was also retrieved from GeneNote (Gene Normal Tissue Expression), a portrait of complete gene expression profiles in healthy human tissues using the Affymetrix GeneChip HG-U95 set (includes 62 839 probe-sets). The hybridization intensities of two replicates were


A

FUNCTION: Multifunctional enzyme that, as well as its role in glycolysis, plays a part in various processes such as growth control, hypoxia tolerance and allergic responses. May also function in the intravascular and pericellular fibrinolytic system due to its ability to serve as a receptor and activator of plasminogen on the cell surface of several cell-types such as leukocytes and neurons.
CATALYTIC ACTIVITY: 2-phospho-D-glycerate = phosphoenolpyruvate + H2O.
COFACTOR: Magnesium. Required for catalysis and for stabilizing the dimer.
PATHWAY: Carbohydrate degradation; glycolysis; pyruvate from D-glyceraldehyde 3-phosphate: step 4.
SUBUNIT: Mammalian enolase is composed of 3 isozyme subunits, alpha, beta and gamma, which can form homodimers or heterodimers which are cell-type and development-specific. ENO1 interacts with PLG in the neuronal plasma membrane and promotes its activation. The C-terminal lysine is required for this binding (By similarity).
SUBCELLULAR LOCATION: Cytoplasmic. Can translocate to the plasma membrane in either the homodimeric (alpha/alpha) or heterodimeric (alpha/gamma) form.
TISSUE SPECIFICITY: The alpha/alpha homodimer is expressed in embryo and in most adult tissues. The alpha/beta heterodimer and the beta/beta homodimer are found in striated muscle, and the alpha/gamma heterodimer and the gamma/gamma homodimer in neurons.
DEVELOPMENTAL STAGE: During ontogenesis, there is a transition from the alpha/alpha homodimer to the alpha/beta heterodimer in striated muscle cells, and to the alpha/gamma heterodimer in nerve cells. In brain, levels of ENO1 decrease around 10 dpc and then gradually increase to adult age. In embryonic heart, ENO1 levels decrease rapidly during cardiac development.
SIMILARITY: Belongs to the enolase family.

B

cancer

PMID 16359544 One alternative translated product of the ENO1 gene, known as MBP-1, acts as a negative regulator of the c-myc oncogene, making the ENO1 gene a candidate as a tumour suppressor gene.

PMID 16359544 These effects could also be shown in non-neuroblastoma cells (293-cells), indicating ENO1 to have general tumour suppressor activity.Expression of ENO1 is detectable in primary neuroblastomas of all different stages and no difference in the level of expression can be detected between 1p-deleted and 1p-intact tumour samples.

general effect

PMID 16466929 Nine proteins involved in glycolysis (triose-phosphate isomerase (TPI), phosphoglycerate kinase 1 (PGK1), and enolase 1 (ENO1)), lipid synthesis (fatty acid synthase (FASN)), stress-mediated chaperonage (heat shock protein 27 (Hsp27)), and antioxidant and detoxification pathways (haptoglobin, aldo-keto reductase (AKR), glyoxalase I (GLO), and prolyl-4-hydrolase beta-isoform (P4HB)) were found to be up-regulated in HER-2/neu-positive breast tumors.

molecular interaction

PMID 15784612 Furthermore, electrophoresis mobility shift assays demonstrated the presence of DNA-binding proteins in tachyzoite and bradyzoite nuclear lysates that bound to stress response elements (STRE), heat shock-like elements (HSE) and other cis-regulatory elements in the upstream regulatory regions of ENO1 and ENO2.

Figure 4.13 – Protein/Gene information gathered from databases (I). (A) Protein information collected from UniProtKB/Swiss-Prot database. (B) MedMiner database search result.

processed and analyzed to yield the complete transcriptome for twelve human tissues (Shmueli, O. et al., 2003).

Signalling and/or metabolic pathways obtained from the CGAP (Cancer Genome Anatomy Project) web site were retrieved directly from BioCarta (http://www.biocarta.com) and from KEGG (Kyoto Encyclopedia of Genes and Genomes - http://www.genome.ad.jp/kegg/).

Information regarding the interaction of the proteins of interest with other proteins/genes was retrieved from STRING, a database of known and predicted protein-protein interactions. These interactions may be direct (physical) or indirect (functional), and the information retrieved is derived from four sources: genomic context, high-throughput experiments, conserved coexpression, and previous knowledge (e.g. PubMed). Databases used for this purpose are dynamic sources of information and therefore the displayed information may vary depending on available information in databases by the time searches were performed.

The same approach was used for the other pH ranges analysed (4.5-5.5, 5.0-6.0 and 6.0-9.0) and also to the S126 fraction isolated from cultured hippocampal neurons (see Appendix - Supplementary data).

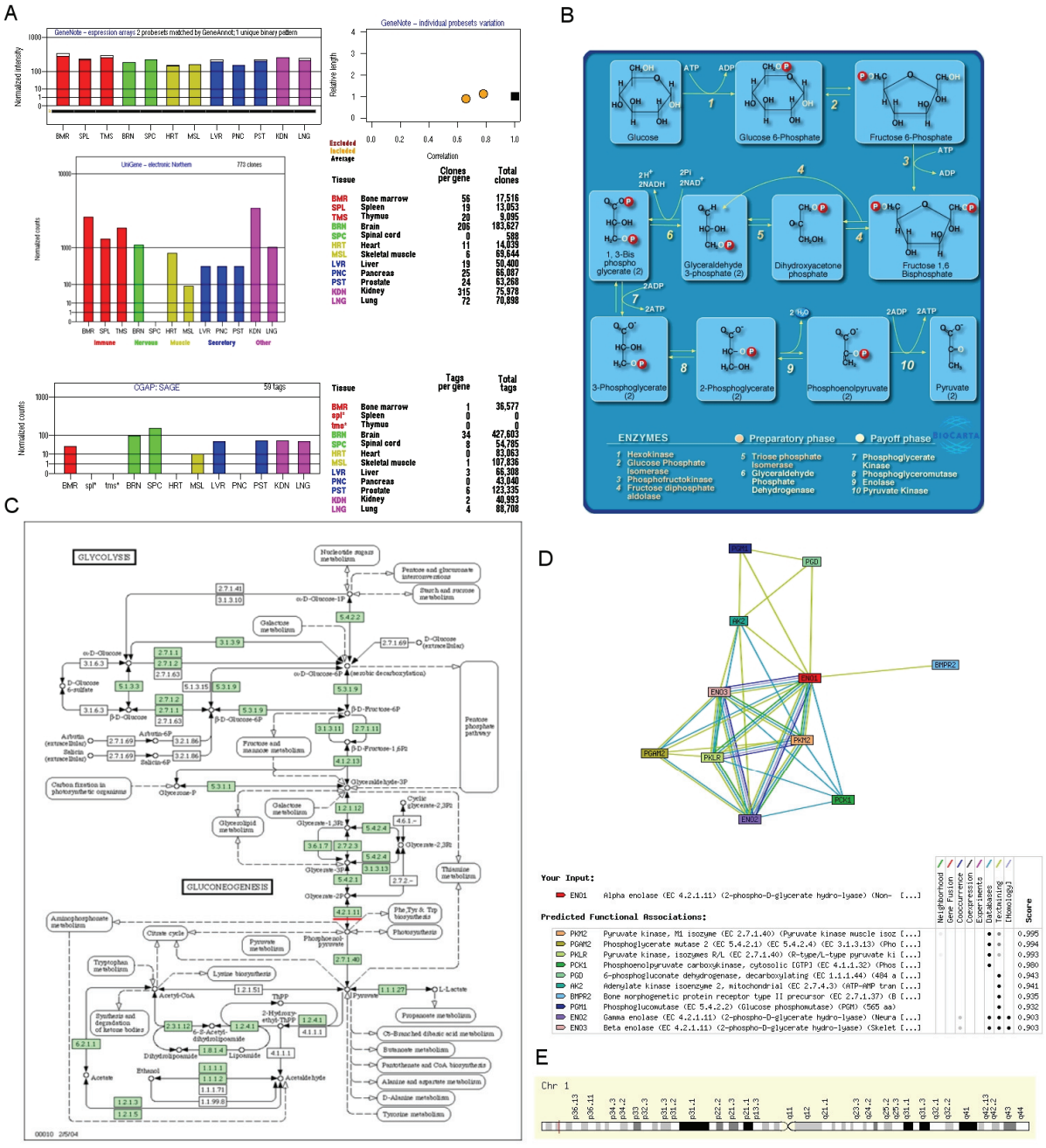

Figure 4.14 – Protein/Gene information gathered from databases (II). (**A**) Information from GeneCards (http://thr.cit.nih.gov/cards/index.shtml) for the ENO1 gene (http://thr.cit.nih.gov/cgi-bin/cards/carddisp.pl?gene=ENO1&search=ENO1&suff=txt). (**B, C**) Signalling and/or metabolic pathways containing the gene of interest (http://cgap.nci.nih.gov/Pathways/PathwayGenes?PATH_GENE=ENO1). (**D**) Interaction with other proteins/genes (*http://string.embl.de/*) using a search tool that gathers information from several databases (Harvester - http://rat.embl.de/rat/P047/P04764.htm). (E) Gene location in chromosome (highlighted in red) retrieved from GeneCards.

4.2.4 - Protein identification

Table V shows a compilation of the protein spots identified in the 2D-gels prepared from cultured hippocampal neurons of both fractions, soluble and S126, resolved in IPG strips pH 4.5-5.5, 5.0-6.0, 5.5-6.7 and 6.0-9.0.

Table V – Spots identified from protein extracts of culture hippocampal neurons. Spots from Figures 4.9, 4.17, 4.20, 4.23, 4.26, 4.29, 4.32, and 4.35 were identified by MALDI-TOF and MALDI-TOF-TOF mass spectrometry.

Accession number	Protein name	Gel(s)	Gene name:	Gene synonyms:
O08557	NG,NG-dimethylarginine dimethylaminohydrolase 1 (EC 3.5.3.18) (Dimethylargininase 1)	5.0-6.0 S	Ddah1	Ddah
O08587	Nucleoporin 50 kDa (Nuclear pore-associated protein 60 kDa-like)	5.5-6.7 S	Nup50	Npap60
O08651	D-3-phosphoglycerate dehydrogenase (EC 1.1.1.95) (3-PGDH)	5.5-6.7 S	Phgdh	
O08701	Arginase II, mitochondrial precursor (EC 3.5.3.1) (Non-hepatic arginase) (Kidney-type arginase)	5.5-6.7 S 5.5-6.7 M	Arg2	
O08749	Dihydrolipoyl dehydrogenase, mitochondrial precursor (EC 1.8.1.4) (Dihydrolipoamide dehydrogenase)	5.5-6.7 M	Dld	
O35244	Peroxiredoxin 6 (EC 1.11.1.15) (Antioxidant protein 2) (1-Cys peroxiredoxin) (1-Cys PRX)	4.5-5.5 S 5.5-6.7 M 5.5-6.7 S	Prdx6	Aipla2, Aop2, Tsa
O35263	Platelet-activating factor acetylhydrolase IB gamma subunit (EC 3.1.1.47) (PAF acetylhydrolase 29 kDa subunit) (PAF-AH 29 kDa subunit) (PAF-AH gamma subunit) (PAFAH gamma subunit)	5.5-6.7 S 5.5-6.7 M	Pafah1b3	Pafahg
O35331	Pyridoxal kinase (EC 2.7.1.35) (Pyridoxine kinase)	5.5-6.7 S	Pdxk	Pkh
O35593	26S proteasome non-ATPase regulatory subunit 14 (26S proteasome regulatory subunit rpn11) (MAD1)	5.5-6.7 S 5.5-6.7 M	Psmd14	Pad1
O35737	Heterogeneous nuclear ribonucleoprotein H (hnRNP H)	4.5-5.5 S 5.0-6.0 S 5.5-6.7 M	Hnrph1	Hnrph
O35760	Isopentenyl-diphosphate delta-isomerase 1 (EC 5.3.3.2) (IPP isomerase 1)	5.5-6.7 S 5.0-6.0 S	Idi1	
O35814	Stress-induced-phosphoprotein 1 (STI1) (Hsc70/Hsp90-organizing protein) (Hop)	5.5-6.7 S 5.5-6.7 M	Stip1	Hop
O35864	COP9 signalosome complex subunit 5 (EC 3.4.-.-) (Signalosome subunit 5) (SGN5) (Jun activation domain-binding protein 1) (Kip1 C-terminus interacting protein 2)	5.5-6.7 S	Cops5	Csn5, Jab1, Kic2
O35987	NSFL1 cofactor p47	4.5-5.5 S	Nsfl1c	
O54984	Arsenical pump-driving ATPase (EC 3.6.3.16) (Arsenite-translocating ATPase) (Arsenical resistance ATPase) (Arsenite-transporting ATPase) (ARSA)	4.5-5.5 S 4.5-5.5 M	Asna1	
O55096	Dipeptidyl-peptidase 3	4.5-5.5 S	Dpp3	
O55171	Acyl coenzyme A thioester hydrolase, mitochondrial precursor (EC 3.1.2.2) (Very-long-chain acyl-CoA thioesterase) (MTE-I) (ARTISt/p43)	5.5-6.7 M	Acot2	Mte1
O70351	3-hydroxyacyl-CoA dehydrogenase type II (EC 1.1.1.35) (Type II HADH)	6.0-9.0 M	Hadh2	Erab, Hsd17b10

O70593	Small glutamine-rich tetratricopeptide repeat-containing protein A	4.5-5.5 S	Sgta	Sgt, Stg
O88342	WD-repeat protein 1 (Actin interacting protein 1) (AIP1)	5.5-6.7 M	Wdr1	
O88569	Heterogeneous nuclear ribonucleoproteins A2/B1 (hnRNP A2 / hnRNP B1)	4.5-5.5 M	Hnrpa2b1	
O88637	Ethanolamine-phosphate cytidylyltransferase (EC 2.7.7.14) (Phosphorylethanolamine transferase) (CTP:phosphoethanolamine cytidylyltransferase)	5.5-6.7 S	Pcyt2	
O88767	DJ-1 protein (Contraception-associated protein 1) (CAP1 protein) (Fertility protein SP22)	5.5-6.7 S 5.0-6.0 S	Park7	Cap1
O89079	Coatomer epsilon subunit (Epsilon-coat protein) (Epsilon-COP)	4.5-5.5 M	Cope	Cope1
P00173	Cytochrome b5	4.5-5.5 M	Cyb5	
P00787	Cathepsin B [Precursor]	4.5-5.5 S	Ctsb	
P02544	Vimentin	4.5-5.5 S	VIM	
P02793	Ferritin light chain (Ferritin L subunit)	5.5-6.7 S	Ftl1	Ftl
P04182	Ornithine aminotransferase, mitochondrial precursor (EC 2.6.1.13) (Ornithine--oxo-acid aminotransferase)	5.5-6.7 S 5.5-6.7 M	Oat	
P04256	Heterogeneous nuclear ribonucleoprotein A1 (Helix-destabilizing protein)	4.5-5.5 M 6.0-9.0 M 5.0-6.0 M	Hnrpa1	
P04636	Malate dehydrogenase, mitochondrial precursor (EC 1.1.1.37)	5.5-6.7 S 6.0-9.0 M	Mdh2	Mor1
P04642	L-lactate dehydrogenase A chain (EC 1.1.1.27) (LDH-A) (LDH muscle subunit) (LDH-M)	5.5-6.7 S	Ldha	Ldh-1, Ldh1
P04691	Tubulin beta chain (T beta-15)	5.5-6.7 S 5.5-6.7 M		
P04757	Neuronal acetylcholine receptor protein, alpha-3 subunit precursor	5.0-6.0 S 5.0-6.0 S	Chrna3	Acra3
P04762	Catalase (EC 1.11.1.6)	5.5-6.7 M	Cat	Cas1
P04764	Alpha enolase (EC 4.2.1.11) (2-phospho-D-glycerate hydro-lyase) (Non-neural enolase) (NNE)	5.5-6.7 S 5.0-6.0 S 5.5-6.7 M	Eno1	Eno-1
P04785	Protein disulfide-isomerase precursor (EC 5.3.4.1) (PDI) (Prolyl 4-hydroxylase beta subunit) (Cellular thyroid hormone binding protein)	4.5-5.5 S 4.5-5.5 M	P4hb	Pdia1
P04797	Glyceraldehyde-3-phosphate dehydrogenase (EC 1.2.1.12) (GAPDH)	5.5-6.7 S 6.0-9.0 S	Gapdh	Gapd
P04905	Glutathione S-transferase Mu 1 (EC 2.5.1.18) (GSTM1-1) (Glutathione S-transferase Yb-1)	5.5-6.7 S 6.0-9.0 S	Gstm1	
P04906	Glutathione S-transferase P (EC 2.5.1.18) (GST 7-7) (Chain 7) (GST class-pi)	5.5-6.7 S 6.0-9.0 S 5.0-6.0 S	Gstp1	
P05065	Fructose-bisphosphate aldolase A (EC 4.1.2.13) (Muscle-type aldolase)	5.5-6.7 S 6.0-9.0 S	Aldoa	
P05197	Elongation factor 2 (EF-2)	5.5-6.7 S	Eef2	
P05370	Glucose-6-phosphate 1-dehydrogenase (EC 1.1.1.49) (G6PD)	5.5-6.7 S 5.0-6.0 S 5.5-6.7 M	G6pdx	G6pd
P05708	Hexokinase-1	5.5-6.7 S	Hk1	
P06761	78 kDa glucose-regulated protein precursor (GRP 78)	4.5-5.5 S	Hspa5	Grp78

		4.5-5.5 M		
P07323	Gamma enolase (EC 4.2.1.11) (2-phospho-D-glycerate hydro-lyase) (Neural enolase) (Neuron-specific enolase) (NSE) (Enolase 2)	4.5-5.5 S 4.5-5.5 M	Eno2	Eno-2
P07335	Creatine kinase B-type (EC 2.7.3.2) (Creatine kinase, B chain) (B-CK)	4.5-5.5 S 5.5-6.7 S 5.0-6.0 S 4.5-5.5 M	Ckb	Ckbb
P07632	Superoxide dismutase [Cu-Zn] (EC 1.15.1.1)	5.5-6.7 S	Sod1	
P07943	Aldose reductase (EC 1.1.1.21) (AR) (Aldehyde reductase)	5.5-6.7 S	Akr1b1	Akr1b4, Aldr1
P08113	Endoplasmin [Precursor]	4.5-5.5 S	Hsp90b1	Tra-1, Tra1
P09117	Fructose-bisphosphate aldolase C (EC 4.1.2.13) (Brain-type aldolase)	5.5-6.7 S 6.0-9.0 S 5.0-6.0 S	Aldoc	
P09330	Ribose-phosphate pyrophosphokinase II (EC 2.7.6.1) (Phosphoribosyl pyrophosphate synthetase II) (PRS-II)	5.5-6.7 S	Prps2	
P09456	cAMP-dependent protein kinase type I-alpha regulatory subunit	4.5-5.5 S	Prkar1a	
P09495	Tropomyosin alpha-4 chain	4.5-5.5 S	Tpm4	
P09606	Glutamine synthetase (EC 6.3.1.2) (Glutamate--ammonia ligase) (GS)	5.5-6.7 S 5.5-6.7 M	Glul	Glns
P10111	Peptidyl-prolyl cis-trans isomerase A (EC 5.2.1.8) (PPIase) (Rotamase) (Cyclophilin A)	5.0-6.0 S	Ppia	
P10719	ATP synthase beta chain, mitochondrial precursor (EC 3.6.3.14)	4.5-5.5 S 5.5-6.7 M 5.0-6.0 M 5.0-6.0 S 4.5-5.5 M	Atp5b	
P10760	Adenosylhomocysteinase (EC 3.3.1.1) (S-adenosyl-L-homocysteine hydrolase) (AdoHcyase)	5.5-6.7 S	Ahcy	
P10860	Glutamate dehydrogenase 1, mitochondrial precursor (EC 1.4.1.3) (GDH) (Memory-related protein 2)	5.5-6.7 S 5.5-6.7 M	Glud1	Glud
P10868	Guanidinoacetate N-methyltransferase (EC 2.1.1.2)	5.5-6.7 S	Gamt	
P11499	Heat shock protein HSP 90-beta	4.5-5.5 S	Hsp90ab1	Hsp84, Hsp84-1, Hspcb
P11598	Protein disulfide-isomerase A3 precursor (EC 5.3.4.1) (Disulfide isomerase ER-60) (ERp60)	5.5-6.7 S 5.0-6.0 S 5.5-6.7 M	Pdia3	Erp60, Grp58
P11884	Aldehyde dehydrogenase, mitochondrial precursor (EC 1.2.1.3) (ALDH class 2) (ALDH1) (ALDH-E2)	5.5-6.7 S 5.5-6.7 M	Aldh2	
P11960	2-oxoisovalerate dehydrogenase alpha subunit, mitochondrial precursor (EC 1.2.4.4) (Branched-chain alpha-keto acid dehydrogenase E1 component alpha chain) (BCKDH E1-alpha) (Fragment)	5.5-6.7 M	Bckdha	
P11980	Pyruvate kinase, isozymes M1/M2 (EC 2.7.1.40) (Pyruvate kinase muscle isozyme)	5.5-6.7 S 5.5-6.7 M	Pkm2	Pykm
P12007	Isovaleryl-CoA dehydrogenase, mitochondrial precursor (EC 1.3.99.10) (IVD)	5.5-6.7 S 5.5-6.7 M	Ivd	
P12369	cAMP-dependent protein kinase type II-beta regulatory subunit	4.5-5.5 S	Prkar2b	

P12815	Programmed cell death protein 6 (Probable calcium-binding protein ALG-2) (PMP41) (ALG-257)	4.5-5.5 M	Pdcd6	Alg2
P13084	Nucleophosmin (NPM) (Nucleolar phosphoprotein B23) (Numatrin) (Nucleolar protein NO38)	4.5-5.5 M	Npm1	
P13264	Glutaminase, kidney isoform, mitochondrial precursor (EC 3.5.1.2) (GLS) (L-glutamine amidohydrolase) (K-glutaminase)	5.5-6.7 S	Gls	
P13668	Stathmin (Phosphoprotein p19) (pp19) (Oncoprotein 18) (Op18) (Leukemia-associated phosphoprotein p18) (pp17) (Prosolin) (Metablastin) (Pr22 protein)	4.5-5.5 S	Stmn1	Lap18
P13697	NADP-dependent malic enzyme (EC 1.1.1.40) (NADP-ME) (Malic enzyme 1)	5.5-6.7 S	Me1	Mod-1, Mod1
P14152	Malate dehydrogenase, cytoplasmic (EC 1.1.1.37)	5.5-6.7 M	Mdh1	Mor2
P14604	Enoyl-CoA hydratase, mitochondrial precursor (EC 4.2.1.17) (Short chain enoyl-CoA hydratase) (SCEH) (Enoyl-CoA hydratase 1)	5.5-6.7 S 5.5-6.7 M	Echs1	
P14668	Annexin A5	4.5-5.5 S	Anxa5	Anx5
P14882	Propionyl-CoA carboxylase alpha chain, mitochondrial precursor (EC 6.4.1.3) (PCCase alpha subunit) (Propanoyl-CoA:carbon dioxide ligase alpha subunit) (Fragment)	5.5-6.7 M	Pcca	
P14942	Glutathione S-transferase 8 (EC 2.5.1.18) (GST 8-8) (Chain 8) (GST class-alpha)	5.5-6.7 S	Gsta4	
P15178	Aspartyl-tRNA synthetase (EC 6.1.1.12) (Aspartate--tRNA ligase) (AspRS)	5.5-6.7 S 5.5-6.7 M	Dars	Drs1
P15650	Acyl-CoA dehydrogenase, long-chain specific, mitochondrial precursor (EC 1.3.99.13) (LCAD)	5.5-6.7 M	Acadl	
P15999	ATP synthase alpha chain, mitochondrial precursor (EC 3.6.3.14)	4.5-5.5 M 5.0-6.0 S 6.0-9.0 M 5.0-6.0 M 5.5-6.7 M	Atp5a1	
P16446	Phosphatidylinositol transfer protein alpha isoform (PtdIns transfer protein alpha) (PtdInsTP)	5.5-6.7 S	Pitpna	Pitpn
P16612	Vascular endothelial growth factor A precursor (VEGF-A) (Vascular permeability factor)	5.0-6.0 M	Vegf	Vegfa
P16617	Phosphoglycerate kinase 1 (EC 2.7.2.3)	6.0-9.0 S	Pgk1	Pgk-1
P16858	Glyceraldehyde-3-phosphate dehydrogenase (EC 1.2.1.12) (GAPDH)	5.5-6.7 S	Gapdh	Gapd
P17220	Proteasome subunit alpha type 2 (EC 3.4.25.1) (Proteasome component C3)	5.5-6.7 S 6.0-9.0 M 5.5-6.7 M	Psma2	
P17425	Hydroxymethylglutaryl-CoA synthase, cytoplasmic (EC 2.3.3.10) (HMG-CoA synthase)	5.0-6.0 S	Hmgcs1	Hmgcs
P18298	S-adenosylmethionine synthetase gamma form (EC 2.5.1.6) (Methionine adenosyltransferase) (AdoMet synthetase) (MAT-II)	5.5-6.7 S	Mat2a	Ams2
P18395	UNR protein	5.5-6.7 S	Csde1	Unr
P18418	Calreticulin [Precursor]	4.5-5.5 S	Calr	
P18420	Proteasome subunit alpha type 1 (EC 3.4.25.1) (Proteasome component C2) (Macropain subunit C2) (Multicatalytic endopeptidase complex subunit C2) (Proteasome nu chain)	5.5-6.7 S 5.5-6.7 M	Psma1	
P18422	Proteasome subunit alpha type 3 (EC 3.4.25.1) (Proteasome component C8) (Macropain subunit C8) (Multicatalytic endopeptidase complex subunit C8) (Proteasome subunit K)	4.5-5.5 S 4.5-5.5 M	Psma3	

P18666	Myosin regulatory light chain 2-B, smooth muscle isoform	4.5-5.5 S	Rlc-b	
P18687	60 kDa heat shock protein, mitochondrial precursor (Hsp60) (60 kDa chaperonin) (CPN60)	5.0-6.0 S	HSPD1	HSP60
P18708	Vesicle-fusing ATPase (EC 3.6.4.6) (Vesicular-fusion protein NSF) (N-ethylmaleimide sensitive fusion protein) (NEM-sensitive fusion protein)	5.5-6.7 M	NSF	
P19234	NADH-ubiquinone oxidoreductase 24 kDa subunit, mitochondrial precursor (EC 1.6.5.3) (EC 1.6.99.3) (Fragment)	4.5-5.5 M	Ndufv2	
P19378	Heat shock cognate 71 kDa protein (Heat shock 70 kDa protein 8)	4.5-5.5 S 5.5-6.7 S	HSPA8	HSC70
P19527	Neurofilament triplet L protein (68 kDa neurofilament protein) (Neurofilament light polypeptide) (NF-L)	4.5-5.5 M	Nefl	Nf68, Nfl
P19804	Nucleoside diphosphate kinase B (EC 2.7.4.6) (NDK B) (NDP kinase B) (P18)	5.5-6.7 S 6.0-9.0 S 5.0-6.0 S	Nme2	
P19945	60S acidic ribosomal protein P0 (L10E)	5.5-6.7 M 5.0-6.0 M	Rplp0	
P20108	Thioredoxin-dependent peroxide reductase, mitochondrial [Precursor]	5.5-6.7 S	Prdx3	Aop1, Mer5
P20650	Protein phosphatase 2C isoform alpha	4.5-5.5 S	Ppm1a	Pp2c1, Pppm1a
P21107	Tropomyosin alpha-3 chain	4.5-5.5 S	Tpm3	Tpm-5, Tpm5
P21708	Mitogen-activated protein kinase 3 (EC 2.7.1.37) (Extracellular signal-regulated kinase 1) (ERK-1) (Insulin-stimulated MAP2 kinase) (MAP kinase 1) (MAPK 1) (p44-ERK1) (ERT2) (p44-MAPK) (Microtubule-associated protein-2 kinase) (MNK1)	5.5-6.7 S	Mapk3	Erk1, Prkm3
P23492	Purine nucleoside phosphorylase (EC 2.4.2.1) (Inosine phosphorylase) (PNP)	5.5-6.7 S	Np	Pnp
P23565	Alpha-internexin (Alpha-Inx)	4.5-5.5 S 5.0-6.0 S 4.5-5.5 M	Ina	Inexa
P24155	Thimet oligopeptidase (EC 3.4.24.15) (Endo-oligopeptidase A) (Endopeptidase 24.15) (PZ-peptidase) (Soluble metallo-endopeptidase)	5.5-6.7 S	Thop1	
P24268	Cathepsin D precursor (EC 3.4.23.5) [Contains: Cathepsin D 12 kDa light chain; Cathepsin D	5.0-6.0 S	Ctsd	
P26040	Ezrin (p81) (Cytovillin) (Villin 2)	5.5-6.7 M	Vil2	
P26443	Glutamate dehydrogenase 1, mitochondrial precursor (EC 1.4.1.3) (GDH)	5.5-6.7 M	Glud1	Glud
P26516	26S proteasome non-ATPase regulatory subunit 7 (26S proteasome regulatory subunit rpn8) (26S proteasome regulatory subunit S12) (Proteasome subunit p40) (Mov34 protein)	5.5-6.7 S 5.5-6.7 M	Psmd7	Mov-34, Mov34
P27605	Hypoxanthine-guanine phosphoribosyltransferase (EC 2.4.2.8) (HGPRT) (HGPRTase)	5.5-6.7 S	Hprt1	Hprt
P28073	Proteasome subunit beta type 6 precursor (EC 3.4.25.1) (Proteasome delta chain) (Macropain delta chain) (Multicatalytic endopeptidase complex delta chain) (Proteasome subunit Y) (Proteasome chain 5) (Fragment)	4.5-5.5 S 4.5-5.5 M	Psmb6	Psmb6l
P28480	T-complex protein 1, alpha subunit (TCP-1-alpha) (CCT-alpha)	5.5-6.7 S 5.5-6.7 M	Cct1	Ccta, Tcp1
P28663	Beta-soluble NSF attachment protein (SNAP-beta) (N-ethylmaleimide-sensitive factor attachment protein, beta) (Brain protein I47)	4.5-5.5 S 4.5-5.5 M	Napb	Snapb

P29391	Ferritin light chain 1 (Ferritin L subunit 1)	5.5-6.7 M	Ftl1	Ftl, Ftl-1
P30337	N-chimaerin (NC) (N-chimerin) (Alpha chimerin) (A-chimaerin) (Rho-GTPase-activating protein 2)	5.5-6.7 S	Chn1	Arhgap2, Chn
P30349	Leukotriene A-4 hydrolase (EC 3.3.2.6) (LTA-4 hydrolase) (Leukotriene A(4) hydrolase)	5.5-6.7 S	Lta4h	
P31000	Vimentin	4.5-5.5 S 5.0-6.0 M 4.5-5.5 M	Vim	
P31044	Phosphatidylethanolamine-binding protein (PEBP) (HCNPpp) (23 kDa morphine-binding protein)	4.5-5.5 S 5.0-6.0 S	Pebp1	Pbp, Pebp
P31399	ATP synthase D chain, mitochondrial (EC 3.6.3.14)	5.5-6.7 M	Atp5h	Atp5jd
P32921	Tryptophanyl-tRNA synthetase (EC 6.1.1.2) (Tryptophan--tRNA ligase) (TrpRS)	5.5-6.7 S	Wars	Wrs
P34022	Ran-specific GTPase-activating protein	4.5-5.5 S	Ranbp1	Htf9-a, Htf9a
P34058	Heat shock protein HSP 90-beta (HSP 84)	4.5-5.5 S 5.0-6.0 S	Hsp90ab1	Hsp84, Hspcb
P34064	Proteasome subunit alpha type 5 (EC 3.4.25.1) (Proteasome zeta chain) (Macropain zeta chain) (Multicatalytic endopeptidase complex zeta chain)	4.5-5.5 S 4.5-5.5 M	Psma5	
P35213	14-3-3 protein beta/alpha (Protein kinase C inhibitor protein-1) (KCIP-1) (Prepronerve growth factor RNH-1)	4.5-5.5 S 4.5-5.5 M	Ywhab	
P35426	Cell division protein kinase 4 (EC 2.7.1.37) (Cyclin-dependent kinase 4) (PSK-J3)	5.5-6.7 S	Cdk4	
P35486	Pyruvate dehydrogenase E1 component alpha subunit, somatic form, mitochondrial precursor (EC 1.2.4.1) (PDHE1-A type I)	5.5-6.7 S 5.5-6.7 M	Pdha1	Pdha-1
P35559	Insulin-degrading enzyme	5.5-6.7 S	Ide	
P35571	Glycerol-3-phosphate dehydrogenase, mitochondrial precursor (EC 1.1.99.5) (GPD-M) (GPDH-M)	5.5-6.7 M	Gpd2	
P35704	Peroxiredoxin 2 (EC 1.11.1.15) (Thioredoxin peroxidase 1)	4.5-5.5 S 5.0-6.0 S 4.5-5.5 M	Prdx2	Tdpx1
P36876	Serine/threonine protein phosphatase 2A, 55 kDa regulatory subunit B, alpha isoform (PP2A, subunit B, B-alpha isoform) (PP2A, subunit B, B55-alpha isoform) (PP2A, subunit B, PR55-alpha isoform) (PP2A, subunit B, R2-alpha isoform)	5.5-6.7 S	Ppp2r2a	
P36972	Adenine phosphoribosyltransferase (EC 2.4.2.7) (APRT)	5.5-6.7 S 5.0-6.0 S	Aprt	
P37397	Calponin-3 (Calponin, acidic isoform) (Calponin, non-muscle isoform)	5.0-6.0 S	Cnn3	
P37805	Transgelin-3 (Neuronal protein NP25)	5.5-6.7 S	Tagln3	Np25
P38650	Dynein heavy chain, cytosolic (DYHC) (Cytoplasmic dynein heavy chain) (MAP 1C)	5.0-6.0 S	Dync1h1	Dnch1, Dnchc1, Dnec1, Map1c
P38652	Phosphoglucomutase (EC 5.4.2.2) (Glucose phosphomutase) (PGM)	5.5-6.7 S	Pgm1	
P38983	40S ribosomal protein SA (p40) (34/67 kDa laminin receptor)	4.5-5.5 S 4.5-5.5 M	Rpsa	Lamr1
P39069	Adenylate kinase isoenzyme 1 (EC 2.7.4.3) (ATP-AMP transphosphorylase) (AK1) (Myokinase)	6.0-9.0 S	Ak1	
P40112	Proteasome subunit beta type 3 (EC 3.4.25.1) (Proteasome theta chain) (Proteasome chain 13) (Proteasome component C10-II)	5.5-6.7 S 5.5-6.7 M	Psmb3	

P40307	Proteasome subunit beta type 2 (EC 3.4.25.1) (Proteasome component C7-I) (Macropain subunit C7-I) (Multicatalytic endopeptidase complex subunit C7-I)	5.5-6.7 M	Psmb2	
P41498	Low molecular weight phosphotyrosine protein phosphatase (EC 3.1.3.48) (LMW-PTP)	5.0-6.0 S	Acp1	
P41562	Isocitrate dehydrogenase [NADP] cytoplasmic (EC 1.1.1.42) (Oxalosuccinate decarboxylase)	5.5-6.7 S 6.0-9.0 S 5.5-6.7 M	Idh1	
P42123	L-lactate dehydrogenase B chain (EC 1.1.1.27) (LDH-B) (LDH heart subunit) (LDH-H)	5.0-6.0 S	Ldhb	Ldh-2, Ldh2
P42669	Transcriptional activator protein PUR-alpha (Purine-rich single-stranded DNA-binding protein alpha)	5.5-6.7 M	Pura	
P45592	Cofilin-1 (Cofilin, non-muscle isoform)	5.5-6.7 S 5.0-6.0 S	Cfl1	
P46462	Transitional endoplasmic reticulum ATPase (TER ATPase) (15S Mg(2+)-ATPase p97 subunit)	4.5-5.5 S 5.0-6.0 S 4.5-5.5 M	Vcp	
P46467	SKD1 protein (Vacuolar sorting protein 4b)	5.5-6.7 S	Vps4b	Skd1
P46471	26S protease regulatory subunit 7 (MSS1 protein)	5.0-6.0 S	Psmc2	Mss1
P46664	Adenylosuccinate synthetase, non-muscle isozyme (EC 6.3.4.4) (IMP--aspartate ligase 2) (AdSS 2) (AMPSase 2)	5.5-6.7 S	Adss	Adss2
P46844	Biliverdin reductase A precursor (EC 1.3.1.24) (Biliverdin-IX alpha-reductase) (BVR A)	5.5-6.7 S	Blvra	Blvr
P47728	Calretinin	4.5-5.5 S	Calb2	
P47753	F-actin capping protein alpha-1 subunit (CapZ alpha-1)	4.5-5.5 S 5.0-6.0 S	Capza1	Cappa1
P47754	F-actin capping protein alpha-2 subunit (CapZ alpha-2)	5.0-6.0 S	Capza2	Cappa2
P47819	Glial fibrillary acidic protein, astrocyte (GFAP)	4.5-5.5 S 5.0-6.0 S 4.5-5.5 M	Gfap	
P47942	Dihydropyrimidinase-related protein 2 (DRP-2) (Turned on after division, 64 kDa protein)	4.5-5.5 S 5.5-6.7 M 5.0-6.0 S 5.5-6.7 S	Dpysl2	
P48500	Triosephosphate isomerase (EC 5.3.1.1) (TIM) (Triose-phosphate isomerase)	5.5-6.7 S	Tpi1	
P48670	Vimentin (Fragment)	4.5-5.5 S	VIM	
P48721	Stress-70 protein, mitochondrial precursor (75 kDa glucose regulated protein) (GRP 75)	4.5-5.5 M 5.0-6.0 M 5.0-6.0 S	Hspa9	Grp75
P49432	Pyruvate dehydrogenase E1 component beta subunit, mitochondrial precursor (EC 1.2.4.1) (PDHE1-B)	4.5-5.5 S 4.5-5.5 M	Pdhb	
P49722	Proteasome subunit alpha type 2 (EC 3.4.25.1) (Proteasome component C3) (Macropain subunit C3) (Multicatalytic endopeptidase complex subunit C3)	5.5-6.7 M	Psma2	Lmpc3
P50398	Rab GDP dissociation inhibitor alpha (Rab GDI alpha) (GDI-1)	4.5-5.5 S 5.0-6.0 S 4.5-5.5 M	Gdi1	Rabgdia
P50399	Rab GDP dissociation inhibitor beta-2 (Rab GDI beta-2) (GDI-3)	5.5-6.7 S 5.0-6.0 S	Gdi2	Gdi3

P50442	Glycine amidinotransferase, mitochondrial precursor (EC 2.1.4.1) (L-arginine:glycine amidinotransferase) (Transamidinase) (AT)	5.5-6.7 M	Gatm	Agat
P50443	Sulfate transporter	5.5-6.7 S	SLC26A2	DTD, DTDST
P50503	Hsc70-interacting protein	4.5-5.5 S	St13	Fam10a1, Hip
P50516	Vacuolar ATP synthase catalytic subunit A, ubiquitous isoform (EC 3.6.3.14)	4.5-5.5 S 5.0-6.0 S	Atp6v1a	Atp6a1, Atp6a2, Atp6v1a1
P50580	Proliferation-associated protein 2G4 (Proliferation-associated protein 1) (Protein p38-2G4)	5.5-6.7 M	Pa2g4	Ebp1, Plfap
P51146	Ras-related protein Rab-4B	5.0-6.0 S	Rab4b	
P51635	Alcohol dehydrogenase [NADP] (EC 1.1.1.2) (Aldehyde reductase) (Aldo-keto reductase family 1 member A1) (3-DG-reducing enzyme)	5.5-6.7 S	Akr1a1	Alr
P51650	Succinate semialdehyde dehydrogenase (EC 1.2.1.24) (NAD()-dependent succinic semialdehyde dehydrogenase)	5.5-6.7 S	Aldh5a1	Ssadh
P52555	Endoplasmic reticulum protein ERp29 precursor (ERp31)	5.5-6.7 S 5.5-6.7 M	Erp29	
P52873	Pyruvate carboxylase, mitochondrial precursor (EC 6.4.1.1) (Pyruvic carboxylase) (PCB)	5.5-6.7 S 5.5-6.7 M	Pc	
P53534	Glycogen phosphorylase, brain form (EC 2.4.1.1) (Fragment)	5.5-6.7 S	Pygb	
P53812	Phosphatidylinositol transfer protein beta isoform (PtdIns transfer protein beta) (PtdInsTP) (PI-TP-beta)	5.5-6.7 S	Pitpnb	
P54311	Guanine nucleotide-binding protein G(I)/G(S)/G(T) beta subunit 1 (Transducin beta chain 1)	4.5-5.5 M	Gnb1	
P54728	UV excision repair protein RAD23 homolog B	4.5-5.5 S	Rad23b	Mhr23b
P54921	Alpha-soluble NSF attachment protein (SNAP-alpha) (N-ethylmaleimide-sensitive factor attachment protein, alpha)	4.5-5.5 S 4.5-5.5 M	Napa	Snap, Snapa
P55051	Fatty acid-binding protein, brain (B-FABP) (Brain lipid-binding protein) (BLBP)	5.0-6.0 S	Fabp7	Blbp
P55053	Fatty acid-binding protein, epidermal (E-FABP) (Cutaneous fatty acid-binding protein) (C-FABP) (DA11)	5.5-6.7 S	Fabp5	
P55213	Caspase-3 precursor (EC 3.4.22.-) (CASP-3) (Apopain) (Cysteine protease CPP32) (Yama protein) (CPP-32) (SREBP cleavage activity 1) (SCA-1) (LICE) (IRP)	5.5-6.7 S	Casp3	Cpp32
P56399	Ubiquitin carboxyl-terminal hydrolase 5	4.5-5.5 S	Usp5	Isot
P58389	Protein phosphatase 2A, regulatory subunit B' (PP2A, subunit B', PR53 isoform) (Phosphotyrosyl phosphatase activator) (PTPA)	5.5-6.7 S	Ppp2r4	Ptpa
P59215	Guanine nucleotide-binding protein G(o), alpha subunit 1	4.5-5.5 M	Gnao1	Gna0, Gnao
P60123	RuvB-like 1 (EC 3.6.1.-) (49-kDa TATA box-binding protein-interacting protein) (49 kDa TBP-interacting protein) (TIP49a) (Pontin 52) (DNA helicase p50)	5.5-6.7 S	Ruvbl1	Tip49, Tip49a
P60335	Poly(rC)-binding protein 1 (Alpha-CP1) (hnRNP-E1)	5.5-6.7 S 5.5-6.7 M	Pcbp1	
P60711	Actin, cytoplasmic 1 (Beta-actin)	5.5-6.7 M	Actb	
P60892	Ribose-phosphate pyrophosphokinase I (EC 2.7.6.1) (Phosphoribosyl pyrophosphate synthetase I) (PRS-I)	5.5-6.7 S 5.5-6.7 M	Prps1	
P60901	Proteasome subunit alpha type 6 (EC 3.4.25.1) (Proteasome iota chain) (Macropain iota chain) (Multicatalytic endopeptidase complex iota chain)	5.5-6.7 S 5.5-6.7 M	Psma6	

P61023	Calcium-binding protein p22 (Calcium-binding protein CHP) (Calcineurin homologous protein)	4.5-5.5 M	Chp	
P61087	Ubiquitin-conjugating enzyme E2-25 kDa (EC 6.3.2.19) (Ubiquitin-protein ligase)	4.5-5.5 S	Hip2	
P61164	Alpha-centractin (Centractin) (Centrosome-associated actin homolog) (Actin-RPV) (ARP1)	5.5-6.7 S 5.5-6.7 M	Actr1a	Ctrn1
P61963	WD repeat protein 68	4.5-5.5 S	Wdr68	Han11
P61980	Heterogeneous nuclear ribonucleoprotein K (dC stretch-binding protein) (CSBP)	4.5-5.5 S 5.0-6.0 S 4.5-5.5 M	Hnrpk	Hnrnpk
P61983	14-3-3 protein gamma	4.5-5.5 S 4.5-5.5 M	Ywhag	
P62083	40S ribosomal protein S7 (S8)	4.5-5.5 M	Rps7	
P62138	Serine/threonine protein phosphatase PP1-alpha catalytic subunit (EC 3.1.3.16) (PP-1A)	5.5-6.7 S 5.0-6.0 S 5.5-6.7 M	Ppp1ca	Ppp1a
P62142	Serine/threonine protein phosphatase PP1-beta catalytic subunit (EC 3.1.3.16) (PP-1B)	5.5-6.7 S 5.0-6.0 S 5.5-6.7 M	Ppp1cb	
P62198	26S protease regulatory subunit 8 (Proteasome subunit p45) (p45/SUG)	6.0-9.0 M	Psmc5	Sug1
P62260	14-3-3 protein epsilon (14-3-3E) (Mitochondrial import stimulation factor L subunit) (MSF L)	4.5-5.5 S 4.5-5.5 M	Ywhae	
P62630	Elongation factor 1-alpha 1 (EF-1-alpha-1) (Elongation factor 1 A-1) (eEF1A-1) (Elongation factor Tu) (EF-Tu)	5.5-6.7 S	Eef1a1	Eef1a
P62703	40S ribosomal protein S4, X isoform	5.5-6.7 M	Rps4x	Rps4
P62716	Serine/threonine protein phosphatase 2A, catalytic subunit, beta isoform (EC 3.1.3.16) (PP2A-beta)	4.5-5.5 S 4.5-5.5 M	Ppp2cb	
P62804	Histone H4	5.5-6.7 S	Hist1h4b	Hist4, Hist1h4m, Hist4h4, H4ft
P62815	Vacuolar ATP synthase subunit B, brain isoform (EC 3.6.3.14) (V-ATPase B2 subunit)	5.0-6.0 S	Atp6v1b2	Atp6b2, Vat2
P62828	GTP-binding nuclear protein Ran (GTPase Ran) (Ras-like protein TC4)	6.0-9.0 S	Ran	
P62909	40S ribosomal protein S3	4.5-5.5 M	Rps3	
P62989	Ubiquitin	5.5-6.7 S 6.0-9.0 S	Rps27a	Uba80, Ubcep1, Uba52, Ubcep2, Ubb
P62993	Growth factor receptor-bound protein 2	5.5-6.7 M	GRB2	ASH
P62994	Growth factor receptor-bound protein 2 (GRB2 adapter protein) (SH2/SH3 adapter GRB2)	5.5-6.7 S 5.0-6.0 S	Grb2	Ash
P63018	Heat shock cognate 71 kDa protein (Heat shock 70 kDa protein 8)	4.5-5.5 S 5.5-6.7 S 5.0-6.0 S 5.5-6.7 M 4.5-5.5 M	Hspa8	Hsc70, Hsc73
P63029	Translationally controlled tumor protein (TCTP) (Lens epithelial protein)	4.5-5.5 S 4.5-5.5 M	Tpt1	Trt
P63039	60 kDa heat shock protein, mitochondrial precursor (Hsp60) (60 kDa	4.5-5.5 S	Hspd1	Hsp60

	chaperonin) (CPN60)	5.0-6.0 M 4.5-5.5 M		
P63085	Mitogen-activated protein kinase 1	5.5-6.7 S	Mapk1	Erk2, Mapk, Prkm1
P63086	Mitogen-activated protein kinase 1 (EC 2.7.1.37) (Extracellular signal-regulated kinase 2) (ERK-2) (Mitogen-activated protein kinase 2) (MAP kinase 2) (MAPK 2) (p42-MAPK) (ERT1)	5.5-6.7 M	Mapk1	Erk2, Mapk, Prkm1
P63102	14-3-3 protein zeta/delta (Protein kinase C inhibitor protein 1) (KCIP-1)	4.5-5.5 S	Ywhaz	Msfs1
P63159	High mobility group protein 1 (HMG-1) (Amphoterin) (Heparin-binding protein p30)	5.5-6.7 S	Hmgb1	Hmg-1, Hmg1
P63242	Eukaryotic translation initiation factor 5A-1	4.5-5.5 S	Eif5a	
P63259	Actin, cytoplasmic 2 (Gamma-actin)	5.5-6.7 S	Actg1	Actg
P63326	40S ribosomal protein S10	4.5-5.5 M	Rps10	
P63331	Serine/threonine protein phosphatase 2A, catalytic subunit, alpha isoform (EC 3.1.3.16)	4.5-5.5 S 5.0-6.0 S 5.5-6.7 S	Ppp2ca	
P67779	Prohibitin	4.5-5.5 M	Phb	
P68101	Eukaryotic translation initiation factor 2 subunit 1 (Eukaryotic translation initiation factor 2 alpha subunit) (eIF-2-alpha) (EIF-2alpha) (EIF-2A)	4.5-5.5 S 4.5-5.5 M	Eif2s1	Eif2a
P68255	14-3-3 protein theta	4.5-5.5 S	Ywhaq	
P68370	Tubulin alpha-1 chain (Alpha-tubulin 1)	5.5-6.7 M	Tuba1	
P68373	Tubulin alpha-6 chain (Alpha-tubulin 6) (Alpha-tubulin isotype M-alpha-6)	5.5-6.7 M	Tuba6	
P68511	14-3-3 protein eta	4.5-5.5 S 4.5-5.5 M	Ywhah	
P69897	Tubulin beta-5 chain	5.5-6.7 S 5.5-6.7 M	Tubb5	
P70297	Signal transducing adapter molecule 1	4.5-5.5 S	Stam	Stam1
P70333	Heterogeneous nuclear ribonucleoprotein H' (hnRNP H')	5.5-6.7 M 5.0-6.0 S	Hnrph2	
P70349	Histidine triad nucleotide-binding protein 1 (Adenosine 5'-monophosphoramidase) (Protein kinase C inhibitor 1) (Protein kinase C-interacting protein 1) (PKCI-1)	5.5-6.7 S	Hint1	Hint, Pkci, Pkci1, Prkcnh1
P70362	Ubiquitin fusion degradation protein 1 homolog (UB fusion protein 1)	5.5-6.7 M	Ufd1l	
P70541	Translation initiation factor eIF-2B gamma subunit (eIF-2B GDP-GTP exchange factor)	5.5-6.7 S	Eif2b3	Eif2bg
P70566	Tropomodulin-2 (Neuronal tropomodulin) (N-Tmod)	4.5-5.5 S 5.0-6.0 S	Tmod2	Ntmod
P70584	Acyl-CoA dehydrogenase, short/branched chain specific, mitochondrial precursor (EC 1.3.99.-) (SBCAD) (2-methyl branched chain acyl-CoA dehydrogenase) (2-MEBCAD) (2-methylbutyryl-coenzyme A dehydrogenase)	5.5-6.7 M	Acadsb	
P70615	Lamin B1	4.5-5.5 S 4.5-5.5 M	Lmnb1	
P70697	Uroporphyrinogen decarboxylase (EC 4.1.1.37) (URO-D) (UPD)	5.5-6.7 S	Urod	
P80254	D-dopachrome tautomerase (EC 5.3.3.-)	5.5-6.7 S	Ddt	

P80314	T-complex protein 1, beta subunit (TCP-1-beta) (CCT-beta)	5.5-6.7 M	Cct2	Cctb
P80316	T-complex protein 1, epsilon subunit (TCP-1-epsilon) (CCT-epsilon)	4.5-5.5 M	Cct5	Ccte
P80317	T-complex protein 1, zeta subunit (TCP-1-zeta) (CCT-zeta) (CCT-zeta-1)	5.5-6.7 S 5.5-6.7 M	Cct6a	Cct6, Cctz, Cctz1
P80318	T-complex protein 1, gamma subunit (TCP-1-gamma) (CCT-gamma) (Matricin)	5.5-6.7 M	Cct3	Cctg
P83888	Tubulin gamma-1 chain (Gamma-1 tubulin) (Gamma-tubulin complex component 1) (GCP-1)	5.5-6.7 M	Tubg1	Tubg
P83916	Chromobox protein homolog 1	4.5-5.5 S	CBX1	CBX
P97355	Spermine synthase	4.5-5.5 S	Sms	
P97379	Ras-GTPase-activating protein binding protein 2 (GAP SH3-domain binding protein 2) (G3BP-2)	5.5-6.7 M	G3bp2	
P97427	Dihydropyrimidinase related protein-1 (DRP-1) (Collapsin response mediator protein 1) (CRMP-1) (ULIP3 protein)	5.5-6.7 S 5.5-6.7 M	Crmp1	Dpysl1, Ulip3
P97532	3-mercaptopyruvate sulfurtransferase (EC 2.8.1.2) (MST)	5.5-6.7 S 5.0-6.0 S 5.5-6.7 M	Mpst	
P97576	GrpE protein homolog 1, mitochondrial precursor (Mt-GrpE#1)	5.5-6.7 S 5.5-6.7 M	Grpel1	Grepel1
P97697	Inositol monophosphatase	4.5-5.5 S	Impa1	Imp
P97726	Tropomyosin 5	4.5-5.5 S		
Q00715	Histone H2B	4.5-5.5 M		
Q00981	Ubiquitin carboxyl-terminal hydrolase isozyme L1 (EC 3.4.19.12)	4.5-5.5 S 5.0-6.0 S 6.0-9.0 S 4.5-5.5 M	Uchl1	
Q01713	Transcription factor BTEB1 (Basic transcription element binding protein 1) (BTE-binding protein 1) (GC box binding protein 1) (Krueppel-like factor 9)	5.5-6.7 S	Klf9	Bteb, Bteb1
Q02053	Ubiquitin-activating enzyme E1 1	4.5-5.5 S 5.0-6.0 S	Ube1x	Uba1, Ube1
Q05982	Nucleoside diphosphate kinase A (EC 2.7.4.6) (NDK A) (NDP kinase A)	5.5-6.7 S 5.0-6.0 S	Nme1	
Q06138	Calcium binding protein 39 (Mo25 protein)	5.5-6.7 S	Cab39	Mo25
Q06647	ATP synthase oligomycin sensitivity conferral protein, mitochondrial precursor (EC 3.6.3.14) (OSCP)	4.5-5.5 M	Atp5o	
Q08122	Transducin-like enhancer protein 3 (ESG) (Grg-3)	5.0-6.0 S	Tle3	Esg
Q32KG8	TPA: pol protein [Mus musculus]	5.0-6.0 M		
Q32PW9	Psmc6 protein [Fragment]	6.0-9.0 M	Psmc6	
Q3MHS9	Chaperonin subunit 6a (Zeta)	6.0-9.0 M	Cct6a	
Q3UY23	Adult male olfactory brain cDNA, RIKEN full-length enriched library, clone:6430547E06 product:hypothetical Ferredoxin-fold anticodon binding domain containing protein, full insert sequence	5.5-6.7 M	D630004A 14Rik	
Q5BK98	Peptidylprolyl isomerase A	6.0-9.0 S	Ppia	
Q5BM23	Histone H4 variant H4-v.1 (Germinal histone H4 gene)	5.0-6.0 M	Hist1h4b	Hist4, Hist1h4m, Hist4h4, H4ft

Q5FVM2	Proteaseome (Prosome, macropain) 28 subunit, 3 (Predicted)	5.0-6.0 S	Psme3	
Q5HZV9	Protein phosphatase 1 regulatory subunit 7	4.5-5.5 S	Ppp1r7	Sds22
Q5I0C3	Methylcrotonoyl-Coenzyme A carboxylase 1 (Alpha)	5.5-6.7 M	Mccc1	
Q5I0D5	Similar to phospholysine phosphohistidine inorganic pyrophosphate phosphata	4.5-5.5 S	MGC 95092	
Q5I0G4	Gars protein (Fragment)	5.5-6.7 S	Gars	
Q5M7U6	Actin-related protein 2	5.5-6.7 S	Actr2	Arp2
Q5M819	Phosphoserine phosphatase (EC 3.1.3.3) (PSP) (O-phosphoserine phosphohydrolase) (PSPase)	4.5-5.5 S 5.0-6.0 S	Psph	
Q5PPH0	E-1 enzyme	4.5-5.5 S	RGD 1309016	
Q5PPJ4	Deoxyhypusine hydroxylase	4.5-5.5 S	Dohh	
Q5PPN7	Coiled-coil domain containing 51	5.5-6.7 M	Ccdc51	
Q5PQN0	Neurocalcin delta	4.5-5.5 S	Ncald	
Q5RJK6	Inositol polyphosphate-1-phosphatase	4.5-5.5 S	Inpp1	
Q5RJR2	Similar to PTK9 protein tyrosine kinase 9	5.5-6.7 S	Ptk9	
Q5RKH2	Galactokinase 1	4.5-5.5 S	Galk1	
Q5RKI0	WD repeat protein 1	5.5-6.7 S	Wdr1	WDR1
Q5RKI1	Eukaryotic translation initiation factor 4A2	4.5-5.5 S	Eif4a2	
Q5SGE0	Leucine rich protein 157	5.5-6.7 S	Lrpprc	
Q5SXJ1	Novel zinc finger domain-containing protein	5.5-6.7 M	ORFNames: RP23-210M6.9-001	
Q5U1Y5	Heterogeneous nuclear ribonucleoprotein L	6.0-9.0 M	Hnrpl	
Q5U211	LOC684097 protein	6.0-9.0 S	LOC 684097	
Q5U2Q5	Ribonucleotide reductase M1	5.5-6.7 S	Rrm1_ mapped	
Q5U2U2	Similar to Crk-like protein	5.5-6.7 S	Crkl	
Q5U300	Similar to ubiquitin-protein ligase (EC 6.3.2.19) E1-mouse	4.5-5.5 S	LOC 314432	
Q5U344	Txnrd1 protein	5.5-6.7 S	Txnrd1	
Q5U347	G elongation factor	5.5-6.7 M	Gfm	
Q5U3Z7	Serine hydroxymethyl transferase 2 (Mitochondrial)	6.0-9.0 M	Shmt2	
Q5VLR5	BWK4	4.5-5.5 M		
Q5WQV4	Ezrin	5.5-6.7 S	Vil2	
Q5WQV5	Radixin	5.5-6.7 M		
Q5XHZ0	Tumor necrosis factor type 1 receptor associated protein	5.5-6.7 S 5.5-6.7 M	Trap1	
Q5XI22	Similar to acetyl CoA transferase-like	5.5-6.7 S 5.5-6.7 M	Acat2	
Q5XI32	F-actin capping protein beta subunit	5.0-6.0 S	Capzb	
Q5XI34	Alpha isoform of regulatory subunit A, protein phosphatase 2	4.5-5.5 S	Ppp2r1a	
Q5XI73	Rho GDP dissociation inhibitor (GDI) alpha	4.5-5.5 S 5.0-6.0 S 4.5-5.5 M	Arhgdia	
Q5XIM9	Chaperonin containing TCP1, subunit 2 (Beta)	5.5-6.7 S	Cct2	
Q60123	Carboxylesterase	5.5-6.7 M	estA	estA

Q60445	Coatomer subunit epsilon	4.5-5.5 S	COPE	
Q60597	2-oxoglutarate dehydrogenase E1 component, mitochondrial precursor (EC 1.2.4.2) (Alpha-ketoglutarate dehydrogenase)	5.5-6.7 M	Ogdh	
Q60930	Voltage-dependent anion-selective channel protein 2	5.5-6.7 M	Vdac2	Vdac6
Q60967	Bifunctional 3'-phosphoadenosine 5'-phosphosulfate synthetase 1	5.5-6.7 S	Papss1	Asapk, Atpsk1, Papss
Q60972	Chromatin assembly factor 1 subunit C (CAF-1 subunit C) (Chromatin assembly factor I p48 subunit) (CAF-I 48 kDa subunit) (CAF-Ip48) (Retinoblastoma binding protein p48) (Retinoblastoma-binding protein 4) (RBBP-4)	4.5-5.5 S 4.5-5.5 M	Rbbp4	Rbap48
Q60973	Histone-binding protein RBBP7	4.5-5.5 S	Rbbp7	Rbap46
Q61167	Microtubule-associated protein RP/EB family member 3	4.5-5.5 S	Mapre3	
Q61316	Heat shock 70 kDa protein 4	4.5-5.5 S	Hspa4	Hsp110
Q61553	Fascin (Singed-like protein)	5.5-6.7 S	Fscn1	Fan1, Snl
Q61699	Heat-shock protein 105 kDa	4.5-5.5 S	Hsph1	Hsp105, Hsp110, Kiaa0201
Q61MX7	Hypothetical protein CBG08292	4.5-5.5 S	CBG 08292	
Q62167	DEAD-box protein 3, X-chromosomal (DEAD-box RNA helicase DEAD3) (mDEAD3) (Embryonic RNA helicase) (D1PAS1 related sequence 2)	5.5-6.7 M	Ddx3x	D1Pas1-rs2, Ddx3, Dead3, Erh
Q62188	Dihydropyrimidinase-related protein 3 (DRP-3) (Unc-33-like phosphoprotein) (ULIP protein)	4.5-5.5 M 5.5-6.7 M	Dpysl3	Drp3, Ulip
Q62188	Dihydropyrimidinase-related protein 3 (DRP-3) (Unc-33-like phosphoprotein) (ULIP protein)	5.5-6.7 S	Dpysl3	Drp3, Ulip
Q62433	NDRG1 protein (N-myc downstream regulated gene 1 protein) (Protein Ndr1)	5.5-6.7 M	Ndrg1	Ndr1, Ndrl, Tdd5
Q62658	FK506-binding protein 1A (EC 5.2.1.8) (Peptidyl-prolyl cis-trans isomerase) (PPIase)	6.0-9.0 S	Fkbp1a	Fkbp1
Q62785	28 kDa heat- and acid-stable phosphoprotein (PDGF-associated protein)	5.0-6.0 S	Pdap1	Haspp28
Q62818	Translation initiation factor eIF-2B beta subunit (eIF-2B GDP-GTP exchange factor)	5.5-6.7 S	Eif2b2	Eif2bb
Q62848	ADP-ribosylation factor GTPase activating protein 1 (ADP-ribosylation factor 1 GTPase activating protein)	5.0-6.0 M	Arfgap1	Arf1gap
Q62871	Cytoplasmic dynein 1 intermediate chain 2	4.5-5.5 S	Dync1i2	Dnci2, Dncic2
Q62950	Dihydropyrimidinase related protein-1 (DRP-1) (Collapsin response mediator protein 1) (CRMP-1)	4.5-5.5 S 5.5-6.7 S	Crmp1	Dpysl1
Q62951	Dihydropyrimidinase related protein-4 (DRP-4) (Collapsin response mediator protein 3) (CRMP-3) (UNC33-like phosphoprotein 4) (ULIP4 protein) (Fragment)	4.5-5.5 S 5.5-6.7 S	Dpysl4	Crmp3, Ulip4
Q62952	Dihydropyrimidinase-related protein 3 (DRP-3) (Collapsin response mediator protein 4)	4.5-5.5 S 5.0-6.0 S	Dpysl3	Crmp4
Q63081	Protein disulfide-isomerase A6 precursor (EC 5.3.4.1) (Protein disulfide isomerase P5) (Calcium-binding protein 1) (CaBP1) (Fragment)	4.5-5.5 S 4.5-5.5 M	Pdia6	Cabp1, Txndc7
Q63083	Nucleobindin-1 [Precursor]	4.5-5.5 S	Nucb1	Nuc
Q63228	Glia maturation factor beta (GMF-beta)	4.5-5.5 S 5.0-6.0 S	Gmfb	
Q63347	26S protease regulatory subunit 7 (MSS1 protein)	5.5-6.7 S 5.5-6.7 M	Psmc2	Mss1

Q63468	Phosphoribosyl pyrophosphate synthetase-associated protein 1 (PRPP synthetase-associated protein 1) (39 kDa phosphoribosypyrophosphate synthetase-associated protein) (PAP39)	5.5-6.7 S	Prpsap1	
Q63525	Nuclear migration protein nudC (Nuclear distribution protein C homolog) (c15)	4.5-5.5 S 5.0-6.0 S	Nudc	
Q63569	26S protease regulatory subunit 6A (TAT-binding protein 1) (TBP-1) (Spermatogenic cell/sperm-associated TAT-binding protein homolog SATA)	4.5-5.5 S 4.5-5.5 M	Psmc3	Tbp1
Q63570	26S protease regulatory subunit 6B (TAT-binding protein-7) (TBP-7)	4.5-5.5 S 4.5-5.5 M	Psmc4	Tbp7
Q63600	Tropomyosin	4.5-5.5 S	Tpm3	TPM-gamma
Q63617	150 kDa oxygen-regulated protein [Precursor]	4.5-5.5 S	Hyou1	Orp150
Q63622	Channel associated protein of synapse-110 (Chapsyn-110) (Discs, large homolog 2) (Synaptic density protein PSD-93)	5.5-6.7 S	Dlg2	Dlgh2
Q63716	Peroxiredoxin 1 (EC 1.11.1.15) (Thioredoxin peroxidase 2)	5.5-6.7 S 6.0-9.0 S	Prdx1	Tdpx2
Q63768	Proto-oncogene C-crk (P38) (Adapter molecule crk)	4.5-5.5 S	Crk	Crko
Q63797	Proteasome activator complex subunit 1 (Proteasome activator 28-alpha subunit) (PA28alpha)	5.0-6.0 S	Psme1	
Q63798	Proteasome activator complex subunit 2 (Proteasome activator 28-beta subunit) (PA28beta) (	5.0-6.0 S	Psme2	
Q64057	Aldehyde dehydrogenase family 7 member A1 (EC 1.2.1.3) (Antiquitin 1) (Fragment)	5.5-6.7 S	Aldh7a1	Ald7a1
Q641Z6	EH-domain containing 1	5.5-6.7 M	Ehd1	
Q642E5	Mevalonate (Diphospho) decarboxylase	5.5-6.7 S	Mvd	
Q642G1	Adenosine kinase	5.5-6.7 S	Adk	
Q64361	Latexin (Endogenous carboxypeptidase inhibitor) (ECI) (Tissue carboxypeptidase inhibitor)	5.0-6.0 S	Lxn	
Q64538	Phosphoprotein phosphatase (Fragment)	5.5-6.7 S		
Q64559	Cytosolic acyl coenzyme A thioester hydrolase (EC 3.1.2.2) (Long chain acyl-CoA thioester hydrolase) (CTE-II) (CTE-IIa) (Brain acyl-CoA hydrolase) (ACT) (CTE-IIb) (LACH1) (MTE-II) (ACH1)	5.5-6.7 S	Acot7	Bach
Q64640	Adenosine kinase (EC 2.7.1.20) (AK) (Adenosine 5'-phosphotransferase)	5.5-6.7 S	Adk	
Q64674	Spermidine synthase (EC 2.5.1.16) (Putrescine aminopropyltransferase) (SPDSY)	4.5-5.5 S 5.0-6.0 S	Srm	
Q66H55	Heat shock 90kDa protein 1, beta	4.5-5.5 S	Hspcb	
Q66H80	Archain	5.5-6.7 S	Arcn1	Copd
Q66H97	Ezrin	5.5-6.7 S	Vil2	
Q66HA8	Heat-shock protein 105 kDa	4.5-5.5 S	Hsph1	Hsp105, Hsp110
Q66HF1	NADH dehydrogenase (Ubiquinone) Fe-S protein 1, 75kDa	4.5-5.5 S	Ndufs1	
Q66HF8	Aldehyde dehydrogenase 1 family, member B1	5.5-6.7 S 5.5-6.7 M	Aldh1b1	
Q66HR2	Microtubule-associated protein RP/EB family member 1 (APC-binding protein EB1)	4.5-5.5 S 5.0-6.0 S 4.5-5.5 M	Mapre1	
Q66JZ6	Gmps protein (Fragment)	5.5-6.7 S	Gmps	

		5.5-6.7 M		
Q68FR6	Elongation factor 1-gamma (EF-1-gamma) (eEF-1B gamma)	5.5-6.7 S 5.5-6.7 M	Eef1g	
Q68FR9	Eukaryotic translation elongation factor 1 delta	4.5-5.5 S 4.5-5.5 M	Eef1d	
Q68FY0	Ubiquinol-cytochrome c reductase core protein I	4.5-5.5 M	Uqcrc1	
Q68FZ8	Propionyl Coenzyme A carboxylase, beta polypeptide	5.5-6.7 M	Pccb	
Q68G33	Golgi reassembly stacking protein 2	4.5-5.5 S	Gorasp2	
Q68GV5	Heat shock protein 90	4.5-5.5 S	Hsp90	
Q6AXQ0	Ubiquitin-like 1 (Sentrin) activating enzyme E1A	4.5-5.5 S	Uble1a	
Q6AY09	Similar to Murine homolog of human ftp-3	5.5-6.7 S 5.5-6.7 M	LOC308650	
Q6AY53	Deoxyhypusine synthase	4.5-5.5 S	Dhps	
Q6AY84	Secernin 1	4.5-5.5 S	Scrn1	
Q6AYD3	Proliferation-associated 2G4, 38kDa	5.5-6.7 S	Pa2g4	
Q6AYG5	Enoyl Coenzyme A hydratase domain containing 1	5.5-6.7 S	Echdc1	
Q6AYK6	Similar to calcyclin binding protein	5.5-6.7 S	Cacybp	
Q6AYN4	Phytanoyl-CoA hydroxylase interacting protein-like	5.5-6.7 S	Phyhipl	
Q6AYP7	Similar to C330027I04Rik protein	5.5-6.7 S	Nt5c3l	
Q6AYS7	Acy1 protein	5.5-6.7 S	Acy1	
Q6AYU2	Pcbp2 protein	5.5-6.7 M	Pcbp2	
Q6AZ40	Prpsap2 protein	5.5-6.7 S	Prpsap2	
Q6DGG0	Peptidylprolyl isomerase D	5.5-6.7 S	Ppid	
Q6IFV6	Type I hair keratin KA30	4.5-5.5 S	Ka30	
Q6IFW6	Type I keratin KA10	4.5-5.5 S	Ka10	
Q6IN16	5-aminoimidazole-4-carboxamide ribonucleotide formyltransferase/IMP cyclohydrolase	5.5-6.7 S	Atic	
Q6JE36	N-myc downstream regulated 1	5.5-6.7 S	Ndr1	Ndrg1
Q6JHG6	Fusion protein [Fragment]	4.5-5.5 S		
Q6NXY2	2610208M17Rik protein (Fragment)	5.5-6.7 M	2610208M17 Rik	
Q6P0K6	Pgam1 protein	5.5-6.7 S 5.5-6.7 M	Pgam1	
Q6P139	Hypothetical protein (Fragment)	5.5-6.7 S		
Q6P3A8	Branched chain ketoacid dehydrogenase E1, beta polypeptide	4.5-5.5 S	Bckdhb	
Q6P3D0	2310041H06Rik protein	5.5-6.7 S	Nudt16	
Q6P3V8	Eukaryotic translation initiation factor 4A, isoform 1	4.5-5.5 S 5.0-6.0 S	Eif4a1	
Q6P4Z9	COP9 signalosome complex subunit 8 (Signalosome subunit 8) (SGN8) (JAB1-containing signalosome subunit 8) (COP9 homolog)	4.5-5.5 S 4.5-5.5 M	Cops8	Csn8
Q6P502	Chaperonin containing TCP1, subunit 3 (Gamma)	5.5-6.7 S	Cct3	
Q6P6R2	Dihydrolipoamide dehydrogenase (E3 component of pyruvate dehydrogenase complex, 2-oxo-glutarate complex, branched chain keto acid dehydrogenase complex)	5.5-6.7 S 5.5-6.7 M	Dld	
Q6P797	GDP dissociation inhibitor 2	5.5-6.7 S 5.5-6.7 M	Gdi2	
Q6P799	Seryl-aminoacyl-tRNA synthetase	5.5-6.7 S 5.5-6.7 M	Sars1	

Q6P7B0	Wars protein	5.5-6.7 S	Wars	
Q6P7Q4	Lactoylglutathione lyase	4.5-5.5 S	Glo1	
Q6P9U3	COMM domain containing protein 3	4.5-5.5 M	Commd3	
Q6P9V6	Proteasome (Prosome, macropain) subunit, alpha type 5	4.5-5.5 S	Psma5	
Q6P9V8	Ubiquitin carboxyl-terminal hydrolase isozyme L1	4.5-5.5 S	Uchl1	
Q6P9X8	Tubb5 protein	5.5-6.7 S		
Q6PCU2	ATPase, H+ transporting, V1 subunit E isoform 1	6.0-9.0 S	Atp6v1e1	
Q6PCV1	Transaldolase 1	5.5-6.7 S	Taldo1	
Q6PCV2	Malate dehydrogenase 1, NAD (Soluble)	5.5-6.7 S	Mdh1	Mdh
Q6PED0	Ribosomal protein S27a	5.5-6.7 S	Rps27a	
Q6QI16	LRRGT00192	5.5-6.7 M		
Q6TUG0	LRRGT00084	5.5-6.7 S	Dnajb11	
Q6TXG7	LRRGT00032	5.5-6.7 S		
Q6WVG3	BTB/POZ domain-containing protein KCTD12	4.5-5.5 S	Kctd12	Pfet1
Q6ZWM5	Mus musculus 2 days neonate thymus thymic cells cDNA, RIKEN full-length enriched library, clone:E430019K17 product:budding uninhibited by benzimidazoles 3 homolog (S. cerevisiae), full insert sequence	5.5-6.7 S	Bub3	
Q71RR7	Guanylate kinase (EC 2.7.4.8)	4.5-5.5 S 5.0-6.0 S		
Q76MZ3	Serine/threonine protein phosphatase 2A, 65 kDa regulatory subunit A, alpha isoform (PP2A, subunit A, PR65-alpha isoform) (PP2A, subunit A, R1-alpha isoform)	4.5-5.5 S 4.5-5.5 M	Ppp2r1a	
Q78NR3	eukaryotic initiation factor 5A isoform I variant CD [Mus musculus]	5.0-6.0 S	Eif5a	
Q794E4	Heterogeneous nuclear ribonucleoprotein F	4.5-5.5 S	Hnrpf	
Q7TMK9	Heterogeneous nuclear ribonucleoprotein Q (hnRNP Q) (hnRNP-Q) (Synaptotagmin binding, cytoplasmic RNA interacting protein) (Glycine-and tyrosine-rich RNA binding protein) (GRY-RBP) (NS1-associated protein 1) (pp68)	5.5-6.7 M	Syncrip	Hnrpq, Nsap1, Nsap1l
Q7TNT7	Sept3 protein	5.5-6.7 S 5.5-6.7 M	Sep-03	
Q7TP11	Cc2-27	5.5-6.7 S		
Q7TP27	Ba1-651	5.5-6.7 S		
Q7TQI3	Ubiquitin thioesterase protein OTUB1	4.5-5.5 S	Otub1	
Q80V75	Fscn1 protein (Fragment)	5.5-6.7 S	Fscn1	
Q80WE0	NADH dehydrogenase 1 alpha subcomplex 10-like protein	5.5-6.7 M	Ndufa10	
Q80Z07	ATP-binding cassette protein 5	5.5-6.7 S	Abca5	
Q8BFR5	Mus musculus adult male tongue cDNA, RIKEN full-length enriched library, clone:2300002G02 product:ELONGATION FACTOR TU, MITOCHONDRIAL (P43) homolog (Mus musculus 13 days embryo heart cDNA, RIKEN full-length enriched library, clone:D)	5.5-6.7 S 5.5-6.7 M	Tufm	
Q8BG32	26S proteasome non-ATPase regulatory subunit 11 (26S proteasome regulatory subunit S9) (26S proteasome regulatory subunit p44.5)	5.5-6.7 S 5.5-6.7 M	Psmd11	
Q8BK64	Activator of 90 kDa heat shock protein ATPase homolog 1 (AHA1)	4.5-5.5 S	Ahsa1	
Q8BL86	Mus musculus adult male corpora quadrigemina cDNA, RIKEN full-length enriched library, clone:B230336L16 product:hypothetical Metallo-beta-lactamase superfamily containing protein, full insert sequence	5.5-6.7 M	290002 4O10Rik	

Q8BNU0	Mus musculus 10 days neonate cortex cDNA, RIKEN full-length enriched library, clone:A830021H22 product:hypothetical Armadillo repeat/Armadillo/plakoglobin ARM repeat profile containing protein, full insert sequence (Armc6 protein)	5.5-6.7 S	Armc6	
Q8BP48	Methionine aminopeptidase 1 (EC 3.4.11.18) (MetAP 1) (MAP 1) (Peptidase M 1)	5.5-6.7 M	Metap1	
Q8BTZ7	Mus musculus 2 days neonate thymus thymic cells cDNA, RIKEN full-length enriched library, clone:E430010H19 product:GDP-MANNOSE PYROPHOSPHORYLASE B homolog (Gmppb-pending protein)	5.5-6.7 S	Gmppb	
Q8BWN3	NudC domain-containing protein 3	4.5-5.5 S	Nudcd3	Kiaa1068
Q8C1B7	Septin 11	5.5-6.7 S 5.5-6.7 M	Sep-11	D5Ertd606e
Q8C4F6	0 day neonate cerebellum cDNA, RIKEN full-length enriched library, clone:C230035J02 product:hypothetical protein, full insert sequence	4.5-5.5 S	4930506 M07Rik	
Q8C4P5	Mus musculus 16 days embryo head cDNA, RIKEN full-length enriched library, clone:C130039E20 product:hypothetical Armadillo repeat/Armadillo/plakoglobin ARM repeat profile containing protein, full insert sequence	5.5-6.7 S	Armc6	
Q8C5H8	Mus musculus adult male olfactory brain cDNA, RIKEN full-length enriched library, clone:6430595H05 product:hypothetical protein, full insert sequence. (Fragment)	5.5-6.7 S	1110020 G09Rik	
Q8C845	16 days embryo head cDNA, RIKEN full-length enriched library, clone:C130064C02 product:SWIPROSIN 1, full insert sequence	4.5-5.5 S	Efhd2	
Q8C8A1	Mus musculus 16 days embryo head cDNA, RIKEN full-length enriched library, clone:C130023E09 product:unclassifiable, full insert sequence	5.5-6.7 M	Idh3a	
Q8CAQ8	Mitochondrial inner membrane protein (Mitofilin)	4.5-5.5 M	Immt	
Q8CFE0	BC010843 protein (Fragment)	4.5-5.5 S	Tmprss13	Msp
Q8CG45	Aflatoxin B1 aldehyde reductase member 2	5.5-6.7 S	Akr7a2	Afar2, Aiar
Q8CG72	Ecto ADP-ribosylhydrolase [Precursor]	4.5-5.5 S	Adprhl2	arh3
Q8CI05	Cytosolic 5'-nucleotidase III	4.5-5.5 S	Nt5c3	
Q8CIG8	Protein arginine N-methyltransferase 5 (EC 2.1.1.-) (Shk1 kinase-binding protein 1 homolog) (SKB1 Homolog) (Jak-binding protein 1)	5.5-6.7 S	Prmt5	Jbp1, Skb1
Q8CIN7	Inositol monophosphatase 2 (EC 3.1.3.25) (IMPase 2) (IMP 2)	5.0-6.0 S	Impa2	
Q8CIV8	Tubulin-folding protein TBCE (Tubulin-specific chaperone e)	5.5-6.7 S	Tbce	
Q8K0U4	Heat shock 70 kDa protein 12A	5.5-6.7 S	Hspa12a	
Q8K1J6	tRNA-nucleotidyltransferase 1, mitochondrial precursor (EC 2.7.7.25) (mitochondrial tRNA nucleotidyl transferase, CCA-adding) (mt tRNA adenylyltransferase) (mt tRNA CCA-pyrophosphorylase) (mt tRNA CCA-diphosphorylase)	5.5-6.7 S 5.5-6.7 M	Trnt1	
Q8K2B3	Succinate dehydrogenase [ubiquinone] flavoprotein subunit, mitochondrial precursor (EC 1.3.5.1) (Fp) (Flavoprotein subunit of complex II)	5.5-6.7 M	Sdha	
Q8K310	Matrin 3	5.5-6.7 M	Matr3	
Q8K4F7	Histidine triad protein member 5	5.5-6.7 S	Dcps	Dcs1, Hint5

Q8K4H3	TUC-4b	5.5-6.7 S	Dpysl3	Crmp4
Q8R081	Heterogeneous nuclear ribonucleoprotein L (hnRNP L)	5.5-6.7 M	Hnrpl	
Q8R0Z4	Snx6 protein	5.5-6.7 S	Snx6	
Q8R2F7	CDCrel-1AI	5.5-6.7 S	Sep-05	Pnutl1
Q8R2W9	Pantothenate kinase 3 (EC 2.7.1.33) (Pantothenic acid kinase 3) (mPanK3)	5.0-6.0 S	Pank3	
Q8R317	Ubiquilin-1	4.5-5.5 S	Ubqln1	Plic1
Q8R424	AMSH (Associated molecule with the SH3 domain of STAM)	5.5-6.7 S	Stambp	Amsh
Q8R5C5	Beta-centractin (Actin-related protein 1B) (ARP1B)	5.5-6.7 S	Actr1b	
Q8VBV1	SH3 domain protein 2A	4.5-5.5 S	Sh3gl2	Sh3d2a
Q8VCW5	Ina protein	5.5-6.7 M	Ina	
Q8VD52	Pyridoxal phosphate phosphatase	4.5-5.5 S	Pdxp	Plp, Plpp, Rbp1
Q8VED9	RIKEN cDNA 1110067D22	4.5-5.5 S	1110067 D22Rik	RP23-455B19.1
Q8VHK3	EZRIN (Fragment)	5.5-6.7 M	Vil2	
Q8VHK7	Hepatoma-derived growth factor	4.5-5.5 S	Hdgf	
Q8VHV7	Ratsg1	5.5-6.7 S	Hnrnph1	
Q8VHX0	Voltage-dependent calcium channel gamma-3 subunit (Neuronal voltage-gated calcium channel gamma-3 subunit)	5.0-6.0 S	Cacng3	
Q8VIM9	FKSG27	4.5-5.5 S	Irgq	AF322649, FKSG27, Irgq1
Q91VC3	Probable ATP-dependent helicase DDX48 (DEAD-box protein 48)	5.5-6.7 S 5.5-6.7 M	Ddx48	
Q91VD9	NADH-ubiquinone oxidoreductase 75 kDa subunit, mitochondrial precursor (EC 1.6.5.3) (EC 1.6.99.3) (Complex I-75Kd) (CI-75Kd)	4.5-5.5 M	Ndufs1	
Q91WD5	NADH-ubiquinone oxidoreductase 49 kDa subunit, mitochondrial precursor (EC 1.6.5.3) (EC 1.6.99.3) (Complex I-49KD) (CI-49KD)	5.5-6.7 M	Ndufs2	
Q91WK2	Eukaryotic translation initiation factor 3 subunit 3 (eIF-3 gamma) (eIF3 p40 subunit) (eIF3h)	5.5-6.7 M	Eif3s3	
Q91WQ3	Tyrosyl-tRNA synthetase, cytoplasmic (EC 6.1.1.1) (Tyrosyl--tRNA ligase) (TyrRS)	5.5-6.7 S	Yars	
Q91XM8	Collapsin response mediator protein 4	5.5-6.7 S	Dpysl3	Crmp4
Q91XW0	Heat shock protein 86	4.5-5.5 S	hsp86	Hspca
Q91Y78	Ubiquitin carboxyl-terminal hydrolase isozyme L3	4.5-5.5 S	Uchl3	
Q91Y81	Vascular endothelial cell specific protein 11 (Septin 2)	5.5-6.7 S 5.5-6.7 M	Sep-02	VESP11
Q91YN5	UDP-N-acteylglucosamine pyrophosphorylase 1 homolog	5.5-6.7 S	Uap1	
Q91YR1	Twinfilin 1 (A6 protein) (Protein tyrosine kinase 9)	5.5-6.7 M	Ptk9	
Q91ZN1	CORO1A protein (Tryptophane aspartate-containing coat protein) (Coronin, actin binding protein 1A)	5.5-6.7 S	Coro1a	Taco
Q920J4	PREDICTED: similar to thioredoxin family Trp26 [Rattus norvegicus]	4.5-5.5 S 5.0-6.0 S	Txnl1	Trp
Q920L2	Succinate dehydrogenase [ubiquinone] flavoprotein subunit, mitochondrial precursor (EC 1.3.5.1) (Fp) (Flavoprotein subunit of complex II)	5.5-6.7 M	Sdha	
Q921F2	TAR DNA-binding protein-43 (TDP-43)	5.5-6.7 M	Tardbp	Tdp43
Q921M7	Protein FAM49B	5.5-6.7 S	Fam49b	

Q922Y1	UBA/UBX 33.3 kDa protein	5.0-6.0 S	D19Ertd721e	
Q923D2	Blvrb protein (Biliverdin reductase B) (Flavin reductase (NADPH))	5.5-6.7 S	Blvrb	
Q923M1	Peptide methionine sulfoxide reductase (EC 1.8.4.6) (Protein-methionine-S-oxide reductase) (PMSR) (Peptide Met(O) reductase)	5.5-6.7 S	Msra	
Q924S5	Lon	5.5-6.7 M	Prss15	Lon
Q925D6	Mitogen-activated protein kinase kinase 6	5.0-6.0 S	Map2k6	Mkk6
Q99068	Alpha-2-macroglobulin receptor-associated protein precursor (Alpha-2-MRAP) (Low density lipoprotein receptor-related protein-associated protein 1) (RAP) (GP330-binding 45 kDa protein) (Fragment)	5.5-6.7 S	Lrpap1	
Q99JB2	Stomatin-like protein 2 (SLP-2)	5.5-6.7 M	Stoml2	Slp2
Q99KE1	NAD-dependent malic enzyme, mitochondrial precursor (EC 1.1.1.38) (NAD-ME) (Malic enzyme 2)	5.5-6.7 S	Me2	
Q99KE2	Hnrpc protein	4.5-5.5 S 5.5-6.7 M 4.5-5.5 M	Hnrpc	Hnrnpc
Q99KJ8	Dynactin complex 50 kDa subunit (50 kDa dynein-associated polypeptide) (p50 dynamitin) (DCTN-50) (Dynactin 2) (Growth cone membrane protein 23-48K) (GMP23-48K)	4.5-5.5 S 4.5-5.5 M	Dctn2	
Q99KP6	PRP19/PSO4 homolog (Nuclear matrix protein 200) (Nuclear matrix protein SNEV)	5.5-6.7 M	Prpf19	Prp19, Snev
Q99KR3	Lactamase, beta 2 (Mus musculus 2 days neonate thymus thymic cells cDNA, RIKEN full-length enriched library, clone:E430032H21 product:similar to hypothetical protein CGI-83)	5.5-6.7 S	Lactb2	
Q99KV1	DnaJ homolog subfamily B member 11 precursor	5.5-6.7 M	Dnajb11	
Q99LC5	Electron transfer flavoprotein alpha-subunit, mitochondrial precursor (Alpha-ETF)	5.5-6.7 M	Etfa	
Q99MB4	COBW domain-containing protein 1	4.5-5.5 S	Cbwd1	
Q99MI5	Spermidine synthase	4.5-5.5 S	Srm	
Q99MZ8	LIM and SH3 domain protein 1 (LASP-1)	5.5-6.7 S	Lasp1	
Q99NA5	NAD+-specific isocitrate dehydrogenase a-subunit	5.5-6.7 S	Idh3a	
Q99PF5	Far upstream element binding protein 2 (FUSE binding protein 2) (KH type splicing regulatory protein) (KSRP) (MAP2 RNA trans-acting protein 1) (MARTA1)	5.5-6.7 S 5.5-6.7 M	Khsrp	Fubp2
Q9CPY7	Cytosol aminopeptidase (EC 3.4.11.1) (Leucine aminopeptidase) (LAP) (Leucyl aminopeptidase) (Proline aminopeptidase) (EC 3.4.11.5) (Prolyl aminopeptidase)	5.5-6.7 S 5.5-6.7 M	Lap3	Lapep
Q9CQ60	6-phosphogluconolactonase (EC 3.1.1.31) (6PGL)	4.5-5.5 S 5.0-6.0 S	Pgls	
Q9CQ65	S-methyl-5-thioadenosine phosphorylase (EC 2.4.2.28) (5'-methylthioadenosine phosphorylase) (MTA phosphorylase) (MTAPase)	5.5-6.7 S	Mtap	
Q9CQU0	Thioredoxin domain-containing protein 12 [Precursor]	4.5-5.5 S	Txndc12	Tlp19
Q9CRB9	Mus musculus 18-day embryo whole body cDNA, RIKEN full-length enriched library, clone:1110007B06 product:hypothetical protein, full insert sequence (Mus musculus adult male kidney cDNA, RIKEN full-length enriched library, clone:0610)	5.5-6.7 M	Chchd3	
Q9CS42	Ribose-phosphate pyrophosphokinase II (EC 2.7.6.1) (Phosphoribosyl pyrophosphate synthetase II) (PRS-II)	5.5-6.7 M	Prps2	

Q9CUB4	Mus musculus adult male testis cDNA, RIKEN full-length enriched library, clone:4933430B08 product:hypothetical protein, full insert sequence. (Fragment)	5.5-6.7 M	1110020 G09Rik	
Q9CVB6	Mus musculus adult male stomach cDNA, RIKEN full-length enriched library, clone:2210023N03 product:actin related protein 2/3 complex, subunit 2 (34 kDa), full insert sequence. (Fragment)	5.5-6.7 S 5.5-6.7 M	Arpc2	
Q9CX34	Suppressor of G2 allele of SKP1 homolog	4.5-5.5 S 4.5-5.5 M	Sugt1	
Q9CX56	26S proteasome non-ATPase regulatory subunit 8 (26S proteasome regulatory subunit S14)	5.5-6.7 S	Psmd8	
Q9CXW2	Mitochondrial 28S ribosomal protein S22 (S22mt) (MRP-S22)	5.5-6.7 M	Mrps22	Rpms22
Q9CYH1	Mus musculus 8 days embryo whole body cDNA, RIKEN full-length enriched library, clone:5730470C09 product:PARASPECKLE PROTEIN 1 ALPHA ISOFORM homolog	5.5-6.7 M	Pspc1	
Q9CZC8	Secernin 1	4.5-5.5 S 4.5-5.5 M	Scrn1	Kiaa0193
Q9CZD3	Glycyl-tRNA synthetase (EC 6.1.1.14) (Glycine--tRNA ligase) (GlyRS)	5.5-6.7 S 5.5-6.7 M	Gars	
Q9CZP1	WD repeat protein 61	4.5-5.5 S	Wdr61	
Q9D0K2	Succinyl-CoA:3-ketoacid-coenzyme A transferase 1, mitochondrial precursor (EC 2.8.3.5) (Somatic-type succinyl CoA:3-oxoacid CoA-transferase) (Scot-S)	5.5-6.7 S 5.5-6.7 M	Oxct1	Oxct, Scot
Q9D1E6	Tubulin-specific chaperone B	4.5-5.5 S	Ckap1	
Q9D1J3	Nuclear protein Hcc-1	5.5-6.7 M	Hcc1	
Q9D1L1	Mus musculus 18-day embryo whole body cDNA, RIKEN full-length enriched library, clone:1110003P10 product:unclassifiable, full insert sequence (Idh3a protein)	5.5-6.7 M	Idh3a	
Q9D1M0	SEC13-related protein	4.5-5.5 S	Sec13l1	
Q9D1Q6	Thioredoxin domain-containing protein 4 [Precursor]	4.5-5.5 S	Txndc4	Erp44, Kiaa0573
Q9D819	Inorganic pyrophosphatase	4.5-5.5 S	Ppa1	Pp, Pyp
Q9D880	Import inner membrane translocase subunit TIM50, mitochondrial [Precursor]	5.5-6.7 M	Timm50	Tim50
Q9D892	Inosine triphosphate pyrophosphatase	4.5-5.5 S	Itpa	
Q9D8Y0	EF-hand domain-containing protein 2	4.5-5.5 S	Efhd2	Sws1
Q9DAK9	14 kDa phosphohistidine phosphatase (EC 3.1.3.-) (Phosphohistidine phosphatase 1)	5.0-6.0 S	Phpt1	Php14
Q9DBP5	UMP-CMP kinase (EC 2.7.4.14) (Cytidylate kinase) (Deoxycytidylate kinase) (Cytidine monoph	5.5-6.7 S 5.0-6.0 S	Cmpk	Cmk, Uck, Umk, Umpk
Q9DCH4	Eukaryotic translation initiation factor 3 subunit 5 (eIF-3 epsilon) (eIF3 p47 subunit) (eIF3f)	4.5-5.5 S 4.5-5.5 M	Eif3s5	
Q9DCT2	NADH-ubiquinone oxidoreductase 30 kDa subunit, mitochondrial precursor (EC 1.6.5.3) (EC 1.6.99.3) (Complex I-30KD) (CI-30KD)	5.5-6.7 M	Ndufs3	
Q9EPC6	Profilin-2 (Profilin II)	5.5-6.7 S	Pfn2	
Q9EQS0	Transaldolase (EC 2.2.1.2)	5.5-6.7 S	Taldo1	
Q9EQX9	Bendless protein (Ubiquitin-conjugating enzyme E2N) (Homologous to yeast UBC13)	5.5-6.7 S 5.0-6.0 S	Ube2n	
Q9ER23	RP59 protein	6.0-9.0 M	Hemgn	Rp59

Q9ER34	Aconitate hydratase, mitochondrial precursor (EC 4.2.1.3) (Citrate hydro-lyase)	5.5-6.7 M	Aco2	
Q9ER34	Aconitate hydratase, mitochondrial precursor (EC 4.2.1.3) (Citrate hydro-lyase)	6.0-9.0 M	Aco2	
Q9ERS2	NADH-ubiquinone oxidoreductase B16.6 subunit (EC 1.6.5.3) (EC 1.6.99.3) (Complex I-B16.6)	5.0-6.0 S	Ndufa13	Grim19
Q9ES53	UFD1	5.5-6.7 S	Ufd1l	
Q9ES56	Trafficking protein particle complex subunit 4 (Synbindin) (TRS23 homolog)	5.5-6.7 M	Trappc4	Sbdn
Q9JHB5	Trax (Translin-associated factor X)	5.5-6.7 S	Tsnax	Trax
Q9JHL4	Drebrin-like protein	4.5-5.5 S	Dbnl	Sh3p7
Q9JHU0	Dihydropyrimidinase-related protein 5 (DRP-5) (ULIP6 protein)	5.5-6.7 S 6.0-9.0 S 6.0-9.0 M 6.0-9.0 S 5.5-6.7 M	Dpysl5	Ulip6
Q9JHU5	Arfaptin 1	5.5-6.7 M	Arfip1	
Q9JHW0	Proteasome subunit beta type 7 precursor (EC 3.4.25.1) (Proteasome subunit Z) (Macropain chain Z) (Multicatalytic endopeptidase complex chain Z)	5.5-6.7 S 5.5-6.7 M	Psmb7	
Q9JHW2	Nit protein 2 (Mus musculus 18-day embryo whole body cDNA, RIKEN full-length enriched library, clone:1190017B19 product:NIT PROTEIN 2 (CUA002) homolog)	5.5-6.7 S	Nit2	D16Ertd502e
Q9JHZ3	GRIP1-associated protein 1	4.5-5.5 S	Gripap1	Grasp1
Q9JIY5	Serine protease HTRA2, mitochondrial precursor (EC 3.4.21.-) (High temperature requirement protein A2) (HtrA2) (Omi stress-regulated endoprotease) (Serine proteinase OMI)	5.5-6.7 M	Htra2	Omi, Prss25
Q9JJ54	Heterogeneous nuclear ribonucleoprotein D0 (hnRNP D0) (AU-rich element RNA-binding protein 1)	5.5-6.7 S 5.5-6.7 M	Hnrpd	Auf1
Q9JKB3	RNA binding protein MSY4	5.5-6.7 M	Csda	Msy4, Ybx3
Q9JLJ3	4-trimethylaminobutyraldehyde dehydrogenase (EC 1.2.1.47) (TMABADH) (Aldehyde dehydrogenase 9A1) (EC 1.2.1.3)	5.5-6.7 S	Aldh9a1	
Q9JLP1	Sam68-like protein SLM-2	6.0-9.0 M	Khdrbs3	Slm2
Q9JLZ1	Thioredoxin-like 2 protein (PKC-interacting cousin of thioredoxin)	5.0-6.0 S	Txnl2	Picot
Q9JMA1	Ubiquitin carboxyl-terminal hydrolase 14	4.5-5.5 S	Usp14	
Q9JMB5	Adhesion-regulating molecule 1 [Precursor]	4.5-5.5 S	Adrm1	Gp110
Q9JMJ4	PRP19/PSO4 homolog (Neuronal differentiation-related gene protein)	5.5-6.7 S	Prpf19	Prp19
Q9QUL6	N-ethylmaleimide sensitive factor	5.5-6.7 M	Nsf	ERG1, NSF
Q9QUM9	Proteasome subunit alpha type 6 (EC 3.4.25.1) (Proteasome iota chain) (Macropain iota chain) (Multicatalytic endopeptidase complex iota chain)	5.5-6.7 M	Psma6	
Q9QXT0	MIR-interacting saposin-like protein [Precursor]	4.5-5.5 S	Tmem4	Msap, Zsig9
Q9QYB1	Chloride intracellular channel protein 4 (mc3s5/mtCLIC)	5.0-6.0 S	Clic4	
Q9QYF9	Protein NDRG3	4.5-5.5 S	Ndrg3	Ndr3
Q9QYU4	Mu-crystallin homolog (CDK108)	4.5-5.5 S 5.0-6.0 S 4.5-5.5 M	Crym	

Q9QZ06	Toll-interacting protein	4.5-5.5 S 4.5-5.5 M	Tollip	
Q9QZ88	Vacuolar protein sorting 29 (Vesicle protein sorting 29)	5.5-6.7 S 5.5-6.7 M	Vps29	
Q9QZD9	Eukaryotic translation initiation factor 3 subunit 2 (eIF-3 beta) (eIF3 p36) (eIF3i) (TGF-beta receptor interacting protein 1) (TRIP-1)	4.5-5.5 M	Eif3s2	Trip1
Q9R063	Peroxiredoxin 5, mitochondrial precursor (EC 1.11.1.15) (Prx-V) (Peroxisomal antioxidant enzyme)	6.0-9.0 S	Prdx5	
Q9R1T4	Septin 6	5.5-6.7 M	Sep-06	
Q9WTV5	26S proteasome non-ATPase regulatory subunit 9 (26S proteasome regulatory subunit p27) (Transactivating protein Bridge-1)	5.5-6.7 S	Psmd9	
Q9WVK4	EH-domain containing protein 1 (mPAST1)	5.5-6.7 S	Ehd1	Past1
Q9Z0P5	Twinfilin-2	5.5-6.7 S	Ptk9l	
Q9Z0T0	Thiopurine S-methyltransferase (EC 2.1.1.67) (Thiopurine methyltransferase)	5.5-6.7 S	Tpmt	
Q9Z0V5	PRx IV (Peroxiredoxin 4)	5.5-6.7 S 5.5-6.7 M	Prdx4	PRx IV
Q9Z0V6	PRx III	5.5-6.7 M	Prdx3	PRx III
Q9Z130	JKTBP (Heterogeneous nuclear ribonucleoprotein D-like)	5.5-6.7 M	Hnrpdl	
Q9Z1B2	Glutathione s-transferase M5 (EC 2.5.1.18)	5.5-6.7 S	Gstm5	
Q9Z1F9	Ubiquitin-like 1-activating enzyme E1B	4.5-5.5 S	Uble1b	Sae2, Uba2
Q9Z1N4	3'(2'),5'-bisphosphate nucleotidase 1 (EC 3.1.3.7) (Bisphosphate 3'-nucleotidase 1) (PAP-inositol-1,4-phosphatase) (PIP) (scHAL2 analogous 3)	5.5-6.7 S	Bpnt1	Sal3
Q9Z1Z2	Serine-threonine kinase receptor-associated protein (UNR-interacting protein)	4.5-5.5 M	Strap	Unrip
Q9Z1Z6	Protein phosphatase 2C	5.5-6.7 S	Ilkap	
Q9Z204	Heterogeneous nuclear ribonucleoproteins C1/C2 (hnRNP C1 / hnRNP C2)	4.5-5.5 M	Hnrpc	Hnrnpc
Q9Z254	RGS19-interacting protein 1 (GAIP C-terminus interacting protein GIPC) (RGS-GAIP interacting protein) (GLUT1 C-terminal binding protein) (GLUT1CBP)	5.5-6.7 S 5.5-6.7 M	Gipc1	Gipc, Rgs19ip1
Q9Z2F5	C-terminal binding protein 1 (EC 1.1.1.-) (CtBP1) (C-terminal binding protein 3) (CtBP3) (50 kDa BFA-dependent ADP-ribosylation substrate) (BARS-50)	5.5-6.7 S	Ctbp1	Bars, Ctbp3
Q9Z2I8	Succinyl-CoA ligase [GDP-forming] beta-chain, mitochondrial precursor (EC 6.2.1.4) (Succinyl-CoA synthetase, betaG chain) (SCS-betaG) (GTP-specific succinyl-CoA synthetase beta subunit) (Fragment)	5.5-6.7 M	Suclg2	
Q9Z2L0	Voltage-dependent anion-selective channel protein 1 (VDAC-1) (rVDAC1) (Outer mitochondrial membrane protein porin 1)	5.5-6.7 M 5.0-6.0 M 5.0-6.0 S	Vdac1	
Q9Z2Q6	Septin 5 (Peanut-like protein 1) (Cell division control related protein 1) (CDCREL-1) (Fragment)	5.5-6.7 M	Sep-05	Pnutl1
Q9Z2X1	Heterogeneous nuclear ribonucleoprotein F	4.5-5.5 S	Hnrpf	
Q9Z339	Glutathione transferase omega 1 (EC 2.5.1.18) (GSTO 1-1) (Glutathione-dependent dehydroascorbate reductase)	5.5-6.7 S	Gsto1	

Accession number, corresponding to Swiss-Prot/Uniprot database entry; **Protein name**, **Gene Name** and **Gene Synonym** were automatically retrieved from Swiss-Prot/Uniprot database; **Gel(s)** column indicates IPG strips used (4.5-5.5; 5.0-6.0; 5.5-6.7; or 6.0-9.0) and the protein fraction where the spot was found (**S**, soluble fraction from ultracentrifugation; **M**, pellet from ultracentrifugation – S126)

4.2.5 - Clustering analysis of proteomic changes induced by BDNF

Large scale protein identifications and differential expression data obtained from proteomic studies return large amounts of information with no functional interpretation. The excessive focusing on highly regulated genes may lead to the rejection of possibly relevant changes occuring in other proteins showing subtle abundance changes (Andersen, J. S. et al., 2005; Busold, C. H. et al., 2005). The functional clustering of the latter groups of proteins with other proteins showing higher expression changes contributes to functional interpretation of the results, highlighting groups of proteins, such as pathways, that represent challenging points for further analysis. Therefore, GOMiner "a tool for biological interpretation of 'omic' data" was used to cluster the genes of interest according to their ontologies.

After spot quantification and correlation with the data from spot identification, the results were organized in a format compatible with GOMiner. This software imports lists of genes and the information regarding their expression: downregulated (-1), up-regulated (1), or unchanged (0). This step required the manual analysis of each gene, mainly because some proteins were found in more than one spot, and the effect of BDNF was not always conserved in the various spots containing the same protein. Table VI shows data manually processed and imported into GOMiner, and contains **protein name**, **gene name** (automatically retrieved from Swiss/Prot using the **accession number**), spot number (**SSP**), and the pH range where the spot was detected. The fold change in the protein levels induced by BDNF when compared to the control condition, the statistical analysis of the results (using unpaired Student's *t* test; $p<0.05$) and whether the observed changes are statistically significant (Yes, No, or showing a "trend", as in Table IV) are also shown in Table VI. When a given protein was present in more than one spot and data were not consistent (with some spots showing an upregulation and other(s) showing a downregulation) the effect of BDNF on protein expression was decided considering the following importance order: statistically different (Yes) > trend (T) > not statistically different (NO). After importing this information into GOMiner, the software imports a database from the internet containing gene ontology and classifications, and clusters the genes according to their ontologies (Fig. 4.15 and Fig. 4.16).

Table VI – Data gathered from gel analysis (differential expression and protein ID) used for clustering analysis by GOMiner

Gene Name	Protein name	SSP	Ratio	Stat. dif?	Spot Up, down	Protein Up, down	pH range	Accession number
Actr1a	Alpha-centractin (ARP1)	5408	1.11	T	1	1	5.5-6.7	P61164
		6402	1.08	NO	1		5.5-6.7	
Actr2	Actin-related protein 2	6307	1.39	T	1	1	5.5-6.7	Q5M7U6
Aldh1b1	Aldehyde dehydrogenase 1 family, member B1	6507	1.41	YES	1	1	5.5-6.7	Q66HF8
Aldh2	Aldehyde dehydrogenase, mitochondrial precursor	4501	1.85	NO	1	1	5.5-6.7	P11884
		4503	1.21	NO	1		5.5-6.7	
Arcn1	Archain	4708	1.57	T	1	1	5.5-6.7	Q66H80
Arhgdia	Rho GDP dissociation inhibitor (GDI) alpha	4107	1.07	YES	1	0	4.5-5.5	Q5XI73
		4108	2.71	NO	1		4.5-5.5	
		3220	0.55	YES	-1		4.5-5.5	
Atp6v1a	Vacuolar ATP synthase catalytic subunit A, ubiquitous isoform	8701	0.85	T	-1	-1	4.5-5.5	P50516
Blvra	Biliverdin reductase A precursor	2103	0.76	YES	-1	-1	5.5-6.7	P46844
		4102	0.68	YES	-1		5.5-6.7	
Cab39	Calcium binding protein 39 (Mo25)	8203	1.89	NO	1	1	5.5-6.7	Q06138
Cct2	T-complex protein 1, beta subunit (TCP-1-beta)	4504	1.18	YES	1	1	5.5-6.7	P80314
		3504	1.40	NO	1		5.5-6.7	
Cct3	Chaperonin containing TCP1, subunit 3 (Gamma)	5709	1.44	YES	1	1	5.5-6.7	Q6P502
Cdk4	Cell division protein kinase 4 (Cyclin-dependent kinase 4)	4107	0.88	T	-1	-1	5.5-6.7	P35426
Crkl	Similar to Crk-like protein	3204	1.01	NO	0	-1	5.5-6.7	Q5U2U2
		5208	0.79	T	-1		5.5-6.7	
Crmp1	Dihydropyrimidinase related protein-1 (DRP-1)	6805	1.76	YES	1	1	5.5-6.7	Q62950
		7803	1.11	NO	1		5.5-6.7	
		7609	1.17	YES	1		5.5-6.7	
		7604	1.39	NO	1		5.5-6.7	
		8609	1.55	NO	1		5.5-6.7	
Crym	Mu-crystallin homolog	6310	0.87	YES	-1	-1	4.5-5.5	Q9QYU4
		5309	1.34	NO	1		4.5-5.5	
Ddt	D-dopachrome tautomerase	5008	0.62	T	-1	-1	5.5-6.7	P80254
Dlg2	Channel associated protein of synapse-110 (Chapsyn-110) (Synaptic density protein PSD-93)	6302	0.61	YES	-1	-1	5.5-6.7	Q63622
		7201	0.83	NO	-1		5.5-6.7	
Dnajb11	LRRGT00084	5302	1.52	YES	1	1	5.5-6.7	Q6TUG0
Dpysl2	Dihydropyrimidinase related protein-2 (DRP-2)	2713	0.98	NO	0	1	5.5-6.7	P47942
		2708	0.74	YES	-1		5.5-6.7	
		3703	1.35	NO	1		5.5-6.7	
		3707 ?	1.17	NO	1		5.5-6.7	
		3708 ?	0.93	NO	0		5.5-6.7	
		3710	1.36	NO	1		5.5-6.7	
		3713 ?	1.53	NO	1		5.5-6.7	
		3714	1.34	T	1		5.5-6.7	
		3716	1.39	NO	1		5.5-6.7	
		3906	1.73	YES	1		5.5-6.7	

		4702	0.95	NO	0		5.5-6.7	
		4705	1.39	YES	1		5.5-6.7	
		5602	1.38	T	1		5.5-6.7	
		5704	1.36	NO	1		5.5-6.7	
Dpysl3	Collapsin response mediator protein 4	2606	0.89	NO	-1	1	5.5-6.7	Q91XM8
		3602	0.96	NO	0		5.5-6.7	
		3605	1.02	NO	0		5.5-6.7	
		4601	0.88	NO	-1		5.5-6.7	
		5601	1.33	T	1		5.5-6.7	
		5606	1.62	T	1		5.5-6.7	
Dync1i2	Dynein intermediate chain 2	4709	2.2	T	1	1	4.5-5.5	Q62871
		5726	1	NO	0		4.5-5.5	
Eef1g	Elongation factor 1-gamma (EF-1-gamma)	6403	1.62	NO	1	1	5.5-6.7	Q68FR6
		6404	1.52	NO	1		5.5-6.7	
Eef2	Elongation factor 2 (EF-2)	8804	5.60	NO	1	1	5.5-6.7	P05197
Eif2b2	Translation initiation factor eIF-2B beta subunit (eIF-2B GDP-GTP exchange factor)	3305	0.86	T	-1	-1	5.5-6.7	Q62818
Eif3s5	Eukaryotic translation initiation factor 3 subunit 5 (eIF-3 epsilon)	5512	1.66	YES	1	1	4.5-5.5	Q9DCH4
Eno1	Alpha enolase (Enolase 1)	3406	0.88	NO	-1	1	5.5-6.7	P04764
		3511	0.86	NO	-1		5.5-6.7	
		3512	0.94	NO	-1		5.5-6.7	
		4410	1.22	YES	1		5.5-6.7	
		4507	1.11	T	1		5.5-6.7	
		5502	1.38	NO	1		5.5-6.7	
		6402	1.02	NO	1		5.5-6.7	
Eno2	Gamma enolase (Neural enolase)	4502	3.53	NO	1	1	4.5-5.5	P07323
		3514	1	NO	0		4.5-5.5	
		3505	2.01	NO	1		4.5-5.5	
Erp29	Endoplasmic reticulum protein ERp29 precursor (ERp31)	4106	0.88	T	-1	-1	5.5-6.7	P52555
Fscn1	Fascin (Singed-like protein)	5507	1.42	T	1	1	5.5-6.7	Q61553
		7501	1.99	YES	1		5.5-6.7	
Ftl1	Ferritin light chain (Ferritin L subunit)	4004	0.77	YES	-1	-1	5.5-6.7	P02793
Gamt	Guanidinoacetate N-methyltransferase	2102	0.66	T	-1	-1	5.5-6.7	P10868
Gars	Gars protein (Fragment)	2710	1.18	YES	1	1	5.5-6.7	Q5I0G4
		2715	1.54	T	1		5.5-6.7	
		3702	1.14	NO	1		5.5-6.7	
Gatm	Glycine amidinotransferase, mitochondrial precursor (Transamidinase)	6405	1.34	T	1	1	5.5-6.7	P50442
Glul	Glutamine synthetase	7312	0.88	T	-1	-1	5.5-6.7	P09606
Gmppb	GDP-Mannose pyrophosphorylase b homolog - RIKEN	7302	2.31	T	1	1	5.5-6.7	Q8BTZ7
Gmps	Gmps protein (Fragment)	5701	1.53	YES	1	1	5.5-6.7	Q66JZ6
		5708	1.23	T	1		5.5-6.7	
		6703	1.47	YES	1		5.5-6.7	
Gphn	Gephyrin	5811	2.99	T	1	1	4.5-5.5	Q03555
Grb2	Growth factor receptor-bound protein 2 (GRB2 adapter protein)	2005	0.84	YES	-1	-1	5.5-6.7	P62994

Gsta4	Glutathione S-transferase 8	8003	0.80	YES	-1	-1	5.5-6.7	P14942
Hnrpc	Hnrpc protein	2304	1.12	YES	1	1	4.5-5.5	Q99KE2
		3303	1.09	T	1		4.5-5.5	
Hnrpdl	JKTBP (Heterogeneous nuclear ribonucleoprotein D-like)	3207	2.33	YES	1	1	5.5-6.7	Q9Z130
		5201	1.10	T	1		5.5-6.7	
Hnrph1	Heterogeneous nuclear ribonucleoprotein H (hnRNP H)	2406	1.42	T	1	1	5.5-6.7	O35737
		2403	1.17	T	1		5.5-6.7	
Hnrph2	Heterogeneous nuclear ribonucleoprotein H2	2506	0.82	T	-1	1	5.5-6.7	Q6AY09
		2405	1.71	T	1		5.5-6.7	
		3401	1.00	NO	0		5.5-6.7	
Hnrpk	Heterogeneous nuclear ribonucleoprotein K	4701	2.4	YES	1	1	4.5-5.5	P61980
		5704	1.94	YES	1		4.5-5.5	
		5708	0.96	NO	-1		4.5-5.5	
		5710	1.04	NO	1		4.5-5.5	
		5725	0.99	NO	-1		4.5-5.5	
		7702	2.08	YES	1		4.5-5.5	
		7709	1.8	NO	1		4.5-5.5	
Hnrpl	Heterogeneous nuclear ribonucleoprotein L (hnRNP L)	8603	0.79	T	-1	-1	5.5-6.7	Q8R081
		8606	0.71	T	-1		5.5-6.7	
Hsp105	Heat shock protein 105	7802	1.51	NO	1	1	4.5-5.5	Q66HA8
Hspa4	Heat shock 70 kDa protein 4	5813	0.75	YES	-1	-1	4.5-5.5	Q61316
		5805	0.94	NO	-1		4.5-5.5	
Hspd1	60 kDa heat shock protein, mitochondrial precursor (Hsp60)	7605	1.1	YES	1	1	4.5-5.5	P63039
		7614	1.17	NO	1		4.5-5.5	
		7606	0.77	T	-1		4.5-5.5	
Ide	Insulin-degrading enzyme	3907	2.00	YES	1	1	5.5-6.7	P35559
Idh3a	Idh3a protein RIKEN	2201	1.15	YES	1	1	5.5-6.7	Q9D1L1
Itpa	Inosine triphosphate pyrophosphatase	7005	0.88	T	-1	-1	4.5-5.5	Q9D892
Khsrp	Far upstream element binding protein 2 (FUSE binding protein 2) (MARTA1)	8707	0.64	NO	-1	-1	5.5-6.7	Q99PF5
Lactb2	Lactamase, beta 2 - RIKEN	3209	2.02	NO	1	1	5.5-6.7	Q99KR3
Lrpap1	Alpha-2-macroglobulin receptor-associated protein precursor (Alpha-2-MRAP)	8308	0.69	YES	-1	-1	5.5-6.7	Q99068
Lrpprc	Leucine rich protein 157	3908	3.13	T	1	1	5.5-6.7	Q5SGE0
Mapre1	Microtubule-associated protein RP/EB family member 1	6212	0.74	T	-1	-1	4.5-5.5	Q66HR2
		6201	1.02	NO	0		4.5-5.5	
Mat2a	S-adenosylmethionine synthetase gamma form (MAT-II)	4407	1.42	YES	1	1	5.5-6.7	P18298
Mpst	3-mercaptopyruvate sulfurtransferase	3109	0.83	T	-1	-1	5.5-6.7	P97532
Napb	Beta-soluble NSF attachment protein (SNAP-beta)	6309	0.69	YES	-1	-1	4.5-5.5	P28663
Nme2	Nucleoside diphosphate kinase B	7003	0.74	YES	-1	-1	5.5-6.7	P19804
Np	Purine nucleoside phosphorylase	6111	0.82	NO	-1	1	5.5-6.7	P23492
		6106	1.33	YES	1		5.5-6.7	
Nt5c3l	5'-nucleotidase, cytosolic III-like	3107	0.80	T	-1	-1	5.5-6.7	Q6AYP7

Oat	Ornithine aminotransferase, mitochondrial precursor	3409 4406	0.35 1.18	T YES	-1 1	1	5.5-6.7 5.5-6.7	P04182
Oxct1	Succinyl-CoA:3-ketoacid-coenzyme A transferase 1, mitochondrial precursor	8508	0.77	T	-1	-1	5.5-6.7	Q9D0K2
Park7	DJ-1 protein (Contraception-associated protein 1)	4003	0.85	T	-1	-1	5.5-6.7	O88767
Pc	Pyruvate carboxylase, mitochondrial precursor	6901	1.54	T	1	1	5.5-6.7	P52873
Pcbp1	Poly(rC)-binding protein 1	6303 7302	0.88 2.31	YES T	-1 1	-1	5.5-6.7 5.5-6.7	P60335
Pcbp2	Pcbp2 protein	6302	2.00	NO	1	1	5.5-6.7	Q6AYU2
Pdia3	Protein disulfide-isomerase A3 precursor	2301	1.13	NO	1	1	5.5-6.7	P11598
Pdia6	Protein disulfide-isomerase A6 precursor (Calcium-binding protein 1) (CaBP1) (Fragment)	4505 4512	1.7 1.12	T NO	1 1	1	4.5-5.5 4.5-5.5	Q63081
Pdxk	Pyridoxal kinase	6102	1.18	T	1	1	5.5-6.7	O35331
Pdxp	Pyridoxal phosphate phosphatase	7210	0.66	YES	-1	-1	4.5-5.5	Q8VD52
Pgd	6-phosphogluconate dehydrogenase	8403	4.99	T	1	1	5.5-6.7	Q7TP11
Pgm1	Phosphoglucomutase	5703	1.23	T	1	1	5.5-6.7	P38652
Phgdh	D-3-phosphoglycerate dehydrogenase	5504 6505	1.18 1.89	NO T	1 1	1	5.5-6.7 5.5-6.7	O08651
Pitpna	Phosphatidylinositol transfer protein alpha isoform (PtdInsTP)	3105 4109	0.80 1.06	T NO	-1 0	-1	5.5-6.7 5.5-6.7	P16446
Ppm1a	Protein phosphatase 2C isoform alpha	5514	0.65	T	-1	-1	4.5-5.5	P20650
Ppp2r2a	Serine/threonine protein phosphatase 2A, 55 kDa regulatory subunit B, alpha isoform	3403	1.43	YES	1	1	5.5-6.7	P36876
Ppp2r4	Protein phosphatase 2A, regulatory subunit B'	3201	1.21	YES	1	1	5.5-6.7	P58389
Prdx2	Peroxiredoxin 2	5407	1.59	YES	1	1	4.5-5.5	P35704
Prdx6	Peroxiredoxin 6	7119 2002 2002	0.42 0.79 0.86	YES YES T	-1 -1 -1	-1	4.5-5.5 5.5-6.7 5.5-6.7	O35244
Psma2	Proteasome subunit alpha type 2	8003	2.08	NO	1	1	5.5-6.7	P49722
Psmb3	Proteasome subunit beta type 3	4112	0.83	T	-1	-1	5.5-6.7	P40112
Psmb7	Proteasome subunit beta type 7 precursor	3106	0.78	T	-1	-1	5.5-6.7	Q9JHW0
Psmc2	26S protease regulatory subunit 7 (MSS1 protein)	2401	1.17	T	1	1	5.5-6.7	Q63347
Psmc3	26S protease regulatory subunit 6A	5506	1.52	T	1	1	4.5-5.5	Q63569
Psmd14	26S proteasome non-ATPase regulatory subunit 14	3111	0.50	YES	-1	-1	5.5-6.7	O35593

Psmd7	26S proteasome non-ATPase regulatory subunit 7	7205	3.72	YES	1	1	5.5-6.7	P26516
		8217	2.15	YES	1		5.5-6.7	
Psmd8	26S proteasome non-ATPase regulatory subunit 8 (26S proteasome regulatory subunit S14)	2104	0.47	YES	-1	-1	5.5-6.7	Q9CX56
Pygb	Glycogen phosphorylase, brain form (Fragment)	6804	1.99	YES	1	1	5.5-6.7	P53534
		6811	1.45	YES	1		5.5-6.7	
		7801	1.64	NO	1		5.5-6.7	
Rplp0	60S acidic ribosomal protein P0 (L10E)	1209	1.36	T	1	1	5.5-6.7	P19945
Ruvbl1	RuvB-like 1 (DNA helicase p50)	4506	1.37	YES	1	1	5.5-6.7	P60123
		5508	1.09	NO	1		5.5-6.7	
Sars1	Seryl-aminoacyl-tRNA synthetase	3607	1.26	YES	1	1	5.5-6.7	Q6P799
Stip1	Stress-induced-phosphoprotein 1 (STI1)	6701	1.32	NO	1	1	5.5-6.7	O35814
		6704	1.02	NO	1		5.5-6.7	
		7704	1.33	T	1		5.5-6.7	
Tbce	Tubulin-folding protein TBCE	2504	1.61	NO	1	1	5.5-6.7	Q8CIV8
Thop1	Thimet oligopeptidase	1809	1.25	T	1	1	5.5-6.7	P24155
Tmod2	Tropomodulin-2	7403	0.73	YES	-1	-1	4.5-5.5	P70566
Trap1	Tumor necrosis factor type 1 receptor associated protein	4701	2.35	T	1	1	5.5-6.7	Q5XHZ0
		4706	3.43	T	1		5.5-6.7	
Trappc4	Trafficking protein particle complex subunit 4 (Synbindin)	3002	0.91	YES	-1	-1	5.5-6.7	Q9ES56
Tufm	Elongation factor Tu, Mitochondrial [percursor]	7401	1.56	T	1	1	5.5-6.7	Q8BFR5
		6409	1.58	YES	1		5.5-6.7	
Txndc12	Thioredoxin domain-containing protein 12 [Precursor].	7012	1.35	NO	1	1	4.5-5.5	Q9CQU0
Ube1x	Ubiquitin-activating enzyme E1 1	7801	1.73	NO	1	0	4.5-5.5	Q02053
		6824	0.76	NO	-1		4.5-5.5	
		6801	0.9	NO	-1		4.5-5.5	
Uchl1	Ubiquitin carboxyl-terminal hydrolase isozyme L1	4104	0.74	YES	-1	-1	4.5-5.5	Q00981
		5110	0.95	NO	-1		4.5-5.5	
		6112	0.82	NO	-1		4.5-5.5	
Usp14	Ubiquitin carboxyl-terminal hydrolase 14	5613	2.32	NO	1	1	4.5-5.5	Q9JMA1
Vcp	Transitional endoplasmic reticulum ATPase (Valosin-containing protein) (VCP)	5809	1.46	T	1	1	4.5-5.5	P46462
Vil2	Ezrin (Fragment)	2708	0.83	T	-1		5.5-6.7	Q8VHK3
	Ezrin	3811	1.50	T	1	1	5.5-6.7	Q66H97
		3808	1.43	YES	1		5.5-6.7	
Wdr1	WD repeat protein 1	6705	1.81	YES	1	1	5.5-6.7	Q5RKI0
	Phosphoprotein phosphatase (Fragment)*	2608	1.52	NO	1	1	5.5-6.7	Q64538

Gene Names were automatically retrieved from the Swiss-Prot/Expasy database, based on the **Accession Numbers** identified by mass spectrometry; **Protein name** retrieved from SwissProt; spot number from gel analysis (**SSP**); **Ratio** (BDNF/control); **statistical significance** (**Yes**, P<0.05; **No**, P>0.05, **T**, "Trend"); GOMiner imported value indicating **Protein up**regulation (1) **down**regulation (-1) or unchanged (0).
*unnamed gene, not imported into GOMiner

A

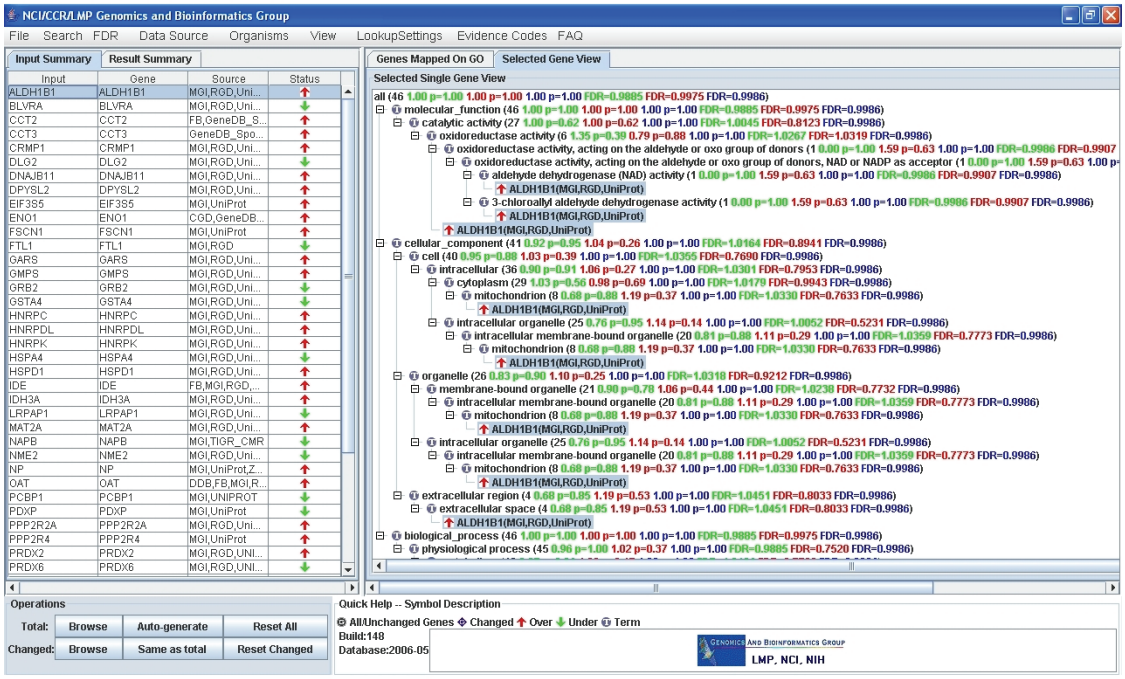

B

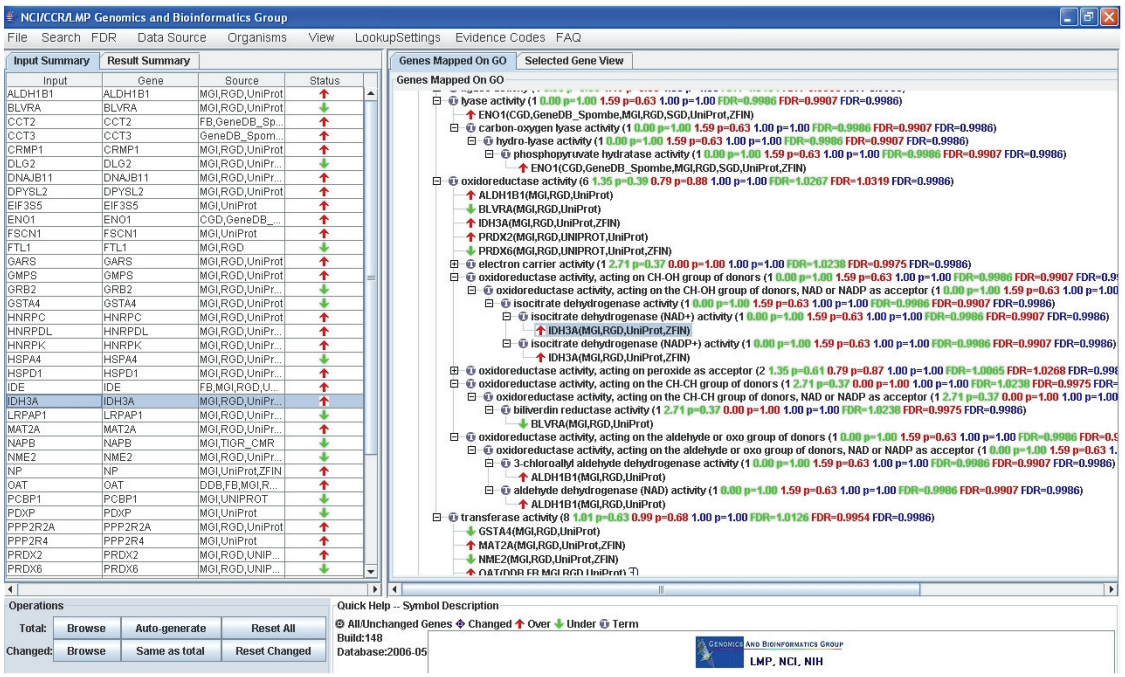

Figure 4.15 – Clustering software overview (I). (A) GOMiner overview showing on the left side the genes imported into the software, with information regarding the effect of BDNF on protein expression [upregulation (↑) or downregulation (↓)], and on the right side (selected gene view) the gene ontologies attributed to the specific gene. (B) On the right side, the software clusters genes according to their GO, and shows clusters for each ontology. For each ontology the software provides the following information: first, the number of genes comprised on that ontology, followed by the relative enrichement of underexpressed genes (green) and their Fisher's exact p-value; finally, it is shown the relative enrichement of overexpressed genes (red), their Fisher's exact p-value, and the false discovery rate (FDR) (Zeeberg, B. R. et al., 2003).

A

Input Summary | Result Summary

Change | Under | Over

Category Name	Tot	Chng	P-Chng	FDR-Chng	Category ID
synaptic vesicle	1	1	1.0000	0.9986	GO:00080...
protein transport	2	2	1.0000	0.9986	GO:00150...
organelle organization and biogene...	7	7	1.0000	0.9986	GO:00069...
alcohol biosynthesis	1	1	1.0000	0.9986	GO:00461...
alcohol catabolism	1	1	1.0000	0.9986	GO:00461...
response to unfolded protein	2	2	1.0000	0.9986	GO:00069...
response to oxidative stress	2	2	1.0000	0.9986	GO:00069...
pigment catabolism	1	1	1.0000	0.9986	GO:00461...
pigment biosynthesis	1	1	1.0000	0.9986	GO:00461...
immune response	1	1	1.0000	0.9986	GO:00069...
inflammatory response	1	1	1.0000	0.9986	GO:00069...
defense response	1	1	1.0000	0.9986	GO:00069...
response to stress	6	6	1.0000	0.9986	GO:00069...
nucleobase biosynthesis	1	1	1.0000	0.9986	GO:00461...
cell motility	1	1	1.0000	0.9986	GO:00069...
anti-apoptosis	1	1	1.0000	0.9986	GO:00069...
apoptosis	2	2	1.0000	0.9986	GO:00069...
ER to Golgi vesicle-mediated trans...	2	2	1.0000	0.9986	GO:00068...
intracellular protein transport	2	2	1.0000	0.9986	GO:00068...
UTP metabolism	1	1	1.0000	0.9986	GO:00460...
iron ion homeostasis	1	1	1.0000	0.9986	GO:00068...
metal ion homeostasis	1	1	1.0000	0.9986	GO:00068...
cell ion homeostasis	1	1	1.0000	0.9986	GO:00068...
GTP metabolism	1	1	1.0000	0.9986	GO:00460...
GMP metabolism	1	1	1.0000	0.9986	GO:00460...
CTP metabolism	1	1	1.0000	0.9986	GO:00460...
iron ion transport	1	1	1.0000	0.9986	GO:00068...
cation transport	1	1	1.0000	0.9986	GO:00068...
ion transport	1	1	1.0000	0.9986	GO:00068...
transport	9	9	1.0000	0.9986	GO:00068...
nitrogen compound metabolism	6	6	1.0000	0.9986	GO:00068...
oxygen and reactive oxygen specie...	2	2	1.0000	0.9986	GO:00068...
phosphate metabolism	3	3	1.0000	0.9986	GO:00067...

B

Input Summary | Result Summary

Change | Under | Over

Category Name	Tot	Undr	P-Undr	FDR-Undr	Category ID
3-chloroallyl aldehyde dehydrogena...	1	0	1.0000	0.9986	GO:00040...
ATP binding	9	2	0.9247	1.0186	GO:00055...
ATPase activity	2	0	1.0000	0.9877	GO:00168...
ATPase activity, coupled	1	0	1.0000	0.9986	GO:00426...
CTP biosynthesis	1	1	0.3696	0.9217	GO:00062...
CTP metabolism	1	1	0.3696	0.9217	GO:00460...
DNA binding	6	2	0.7338	0.9777	GO:00036...
DNA helicase activity	1	0	1.0000	0.9986	GO:00036...
DNA metabolism	2	0	1.0000	0.9877	GO:00062...
DNA modification	1	0	1.0000	0.9986	GO:00063...
DNA packaging	1	0	1.0000	0.9986	GO:00063...
DNA recombination	1	0	1.0000	0.9986	GO:00063...
ER to Golgi vesicle-mediated trans...	2	2	0.1314	1.1556	GO:00068...
F-actin capping protein complex	1	1	0.3696	0.9217	GO:00082...
G-protein coupled receptor activity	1	0	1.0000	0.9986	GO:00049...
G-protein coupled receptor protein ...	2	1	0.6077	0.9471	GO:00071...
GMP biosynthesis	1	0	1.0000	0.9986	GO:00061...
GMP metabolism	1	0	1.0000	0.9986	GO:00460...
GMP synthase (glutamine-hydrolyzi...	1	0	1.0000	0.9986	GO:00039...
GMP synthase activity	1	0	1.0000	0.9986	GO:00039...
GTP binding	1	0	1.0000	0.9986	GO:00055...
GTP biosynthesis	1	1	0.3696	0.9217	GO:00061...
GTP metabolism	1	1	0.3696	0.9217	GO:00460...
Golgi apparatus	2	2	0.1314	1.1556	GO:00057...
Golgi cis-face	1	1	0.3696	0.9217	GO:00058...
Golgi stack	1	1	0.3696	0.9217	GO:00057...
Golgi vesicle transport	2	2	0.1314	1.1556	GO:00481...
MAPKKK cascade	1	1	0.3696	0.9217	GO:00001...
Mo-molybdopterin cofactor biosynth...	1	0	1.0000	0.9986	GO:00067...
Mo-molybdopterin cofactor metabol...	1	0	1.0000	0.9986	GO:00197...
RNA binding	5	1	0.9134	1.0236	GO:00037...
RNA editing	1	0	1.0000	0.9986	GO:00165...
RNA metabolism	7	1	0.9708	1.0082	GO:00160...

C

Input Summary | Result Summary

Change | Under | Over

Category Name	Tot	Ovr	P-Ovr	FDR-Ovr	Category ID
3-chloroallyl aldehyde dehydrogena...	1	1	0.6304	1.0109	GO:00040...
ATP binding	9	7	0.2680	0.7810	GO:00055...
ATPase activity	2	2	0.3923	0.8164	GO:00168...
ATPase activity, coupled	1	1	0.6304	1.0109	GO:00426...
CTP biosynthesis	1	0	1.0000	0.9981	GO:00062...
CTP metabolism	1	0	1.0000	0.9981	GO:00460...
DNA binding	6	4	0.6111	0.9141	GO:00036...
DNA helicase activity	1	1	0.6304	1.0109	GO:00036...
DNA metabolism	2	2	0.3923	0.8164	GO:00062...
DNA modification	1	1	0.6304	1.0109	GO:00063...
DNA packaging	1	1	0.6304	1.0109	GO:00063...
DNA recombination	1	1	0.6304	1.0109	GO:00063...
ER to Golgi vesicle-mediated trans...	2	0	1.0000	0.9981	GO:00068...
F-actin capping protein complex	1	0	1.0000	0.9981	GO:00082...
G-protein coupled receptor activity	1	1	0.6304	1.0109	GO:00049...
G-protein coupled receptor protein ...	2	1	0.8686	1.0491	GO:00071...
GMP biosynthesis	1	1	0.6304	1.0109	GO:00061...
GMP metabolism	1	1	0.6304	1.0109	GO:00460...
GMP synthase (glutamine-hydrolyzi...	1	1	0.6304	1.0109	GO:00039...
GMP synthase activity	1	1	0.6304	1.0109	GO:00039...
GTP binding	1	1	0.6304	1.0109	GO:00055...
GTP biosynthesis	1	0	1.0000	0.9981	GO:00061...
GTP metabolism	1	0	1.0000	0.9981	GO:00460...
Golgi apparatus	2	0	1.0000	0.9981	GO:00057...
Golgi cis-face	1	0	1.0000	0.9981	GO:00058...
Golgi stack	1	0	1.0000	0.9981	GO:00057...
Golgi vesicle transport	2	0	1.0000	0.9981	GO:00481...
MAPKKK cascade	1	0	1.0000	0.9981	GO:00001...
Mo-molybdopterin cofactor biosynth...	1	1	0.6304	1.0109	GO:00067...
Mo-molybdopterin cofactor metabol...	1	1	0.6304	1.0109	GO:00197...
RNA binding	5	4	0.3812	0.7614	GO:00037...
RNA editing	1	1	0.6304	1.0109	GO:00165...
RNA metabolism	7	6	0.1800	0.5882	GO:00160...

Figure 4.16 - Clustering analysis overview (II). The image shows three screenshots for “results summary”: (A) Gene ontologies for the genes which expression was changed; (B) Gene ontologies for downregulated genes [Under], (C) Gene ontologies for upregulated genes [Over]. Each analysis indicates the total number of genes included in a given ontology, and the number of genes changed upon exposure of hippocampal neurons to BDNF (downregulated or upregulated genes and corresponding p-values and FDR) (Zeeberg, B. R. et al., 2003; Zeeberg, B. R. et al., 2005)

Once the data was imported into the GOMiner software, clustering analysis was performed for BDNF-induced changes in protein expression in cultured hippocampal neurons. The list of clusters formed shows that BDNF regulates the expression of proteins belonging to different functional groups, including “carbohydrate metabolism”, “cell proliferation”, “apoptosis”, “protein metabolism”, and “nucleobase, nucleoside, nucleotide and nucleic acid metabolism”. Figures 4.17 through 4.23 show these clusters, grouping proteins which expression was regulated by BDNF. The clusters show not only those proteins which expression changed in a statistically significant manner, but also those that showed less consistent variations, that did not reach statistical significance (refered as “NO” and “Trend” in Table VI).

Considering that the differential expression analysis of the effect of BDNF on the hippocampal proteome was performed by monitoring the incorporation of radiolabelled amino acids into newly sinthesized proteins, the effect of the neurotrophin on protein levels is likely to reflect induction or repression of gene expression. Furthermore, considering the regular turnover of the proteins analysed, a change in the abundance of a given protein spot may be due to the induction or repression of protein degradation. Post-translational modifications of the proteins may also contribute to the observed changes.

The results shown in Fig. 4.17 indicate that BDNF induced an overall increase in proteins involved in the “carbohydrate metabolism”, with ALDH1B1[a)] (Aldehyde dehydrogenase 1 family member B1), IDH3A (Idh3a protein), PYGB (Glycogen phosphorylase, brain form), and ENO1 (Alpha enolase - Enolase 1) being significantly upregulated in the presence of the neurotrophin (Fig. 4.17A). These proteins play key roles in glycolysis, citrate cycle, and in the carbohydrate, starch and sucrose metabolism. Other proteins that were also upregulated, although the results did not reach statistical significance, included ALDH2 (Aldehyde dehydrogenase, mitochondrial precursor), ENO2 (Gamma enolase - Neural enolase), PC (Pyruvate carboxylase, mitochondrial precursor), PGD (6-phosphogluconate dehydrogenase) and PGM1 (Phosphoglucomutase) (Fig. 4.17B). These are known to be expressed in the brain, according to GeneCards, and are involved in glycolysis, citrate cycle, pentose phosphate pathway, and in the galactose, starch and sucrose metabolism.

Several proteins belonging to the gene ontology “cell proliferation” were also regulated by BDNF in hippocampal neurons (Fig. 4.18). These include Fscn1 (Fscn1 protein - fragment) and NP (Purine nucleoside phosphorylase), which were upregulated, and LRPAP1 (Alpha-2-macroglobulin receptor-associated protein precursor), UCHL1 (Ubiquitin carboxyl-terminal

[a)] Gene names are underlined and preceded or followed by the protein name

hydrolase isozyme L1) and NME2 (Nucleoside diphosphate kinase B), which were significantly downregulated in the presence of BDNF (Fig. 4.18A). Other proteins of the same group were also downregulated by BDNF stimulation, including those translated from the genes CDK4 (Cell division protein kinase 4), MAPRE1 (Microtubule-associated protein RP/EB family member 1), and PARK7 (DJ-1 protein) (Fig. 4.18B), but these effects were not statistically significant.

Apoptosis related genes, such as HSPD1 (60 kDa heat shock protein, mitochondrial precursor) and PRDX2 (Peroxiredoxin 2) were significantly upregulated by BDNF (Fig. 4.19A). Other upregulated proteins belonging to this ontology included the products of VCP (Transitional endoplasmic reticulum ATPase), TRAP1 (Tumor necrosis factor type 1 receptor

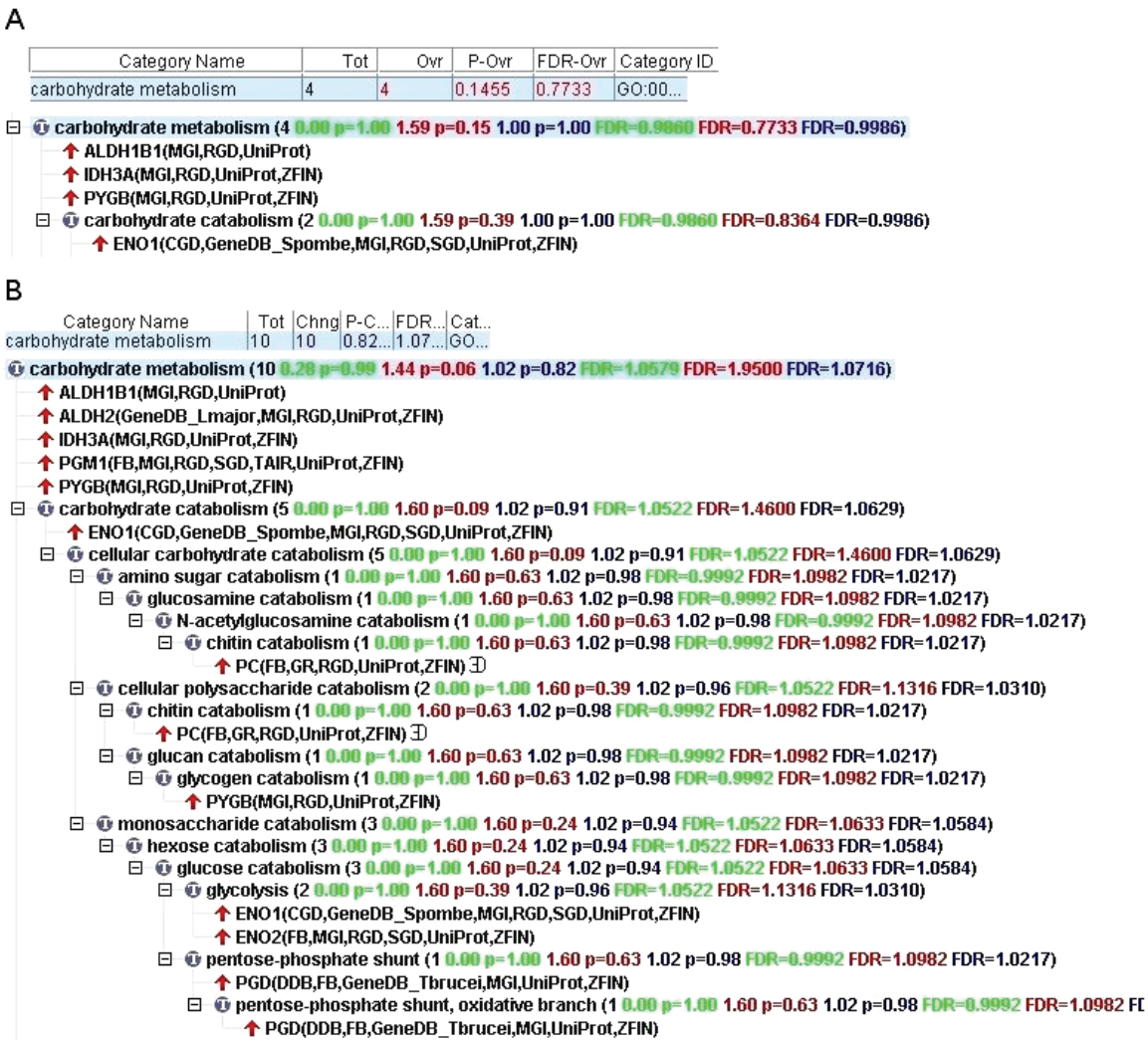

Fig. 4.17 – Cluster analysis of the BDNF-induced gene products involved in the carbohydrate metabolism. Genes which expression is significantly different in the presence of BDNF (A), and selected genes (B) based on the results shown in Table VI ("NO" and "Trend").

associated protein), PDIA3 (Protein disulfide-isomerase A3 precursor), and CCT3 (T-complex protein 1, gamma subunit) (Fig. 4.19B).

Another important set of proteins regulated by BDNF in cultured hippocampal neurons are those involved in "protein metabolism", including the ontologies "protein biosynthesis" and "translation" (Figures 4.20 and 4.21). These gene products include EIF3S5 (Eukaryotic translation initiation factor 3 subunit 5), GARS (Gars protein), SARS (Seryl-aminoacyl-tRNA synthetase), TUFM (Elongation factor Tu Mitochondrial), which were significantly upregulated by BDNF. In contrast TRAPPC4 (Trafficking protein particle complex subunit 4) was significantly downregulated by the neurotrophin (Figures 4.20). Other upregulated proteins belonging to this ontology included the products of the EEF1G (Elongation factor 1-gamma), EEF2 (Elongation factor 2) and RPLP0 (60S acidic ribosomal protein P0) genes, both upregulated by BDNF, and EIF2B2 (Translation initiation factor eIF-2B beta subunit) and KHSRP (Far upstream element binding protein 2), which were downregulated (Figures 4.21). These results show the upregulation of proteins involved in the protein synthesis mechanisms, including "translation" (arrow in Fig. 4.20, see section "4.3 – Discussion" for

Fig. 4.18 – Cluster analysis of gene products regulated by BDNF - cell proliferation ontology. Genes which expression is significantly changed in the presence of BDNF (A), and selected genes (B) based on the results shown in Table VI ("NO" and "Trend").

further details). In contrast, proteins participating in the "ubiquitin-dependent protein catabolism" were up- or downregulated, showing a complex pattern of regulation of this type of activity in the cell. The PSMD7 (26S proteasome non-ATPase regulatory subunit 7) gene product was upregulated, whereas the PSMD14 (26S proteasome non-ATPase regulatory subunit 14) and UCHL1 (Ubiquitin carboxyl-terminal hydrolase isozyme L1) gene products were downregulated (Fig. 4.20).

In addition to the control of protein levels through regulation of the biosynthesis mechanism, BDNF may also affect protein expression at the level of nucleic acids (Fig. 4.22 and 4.23), with several proteins involved in DNA, RNA, and tRNA metabolism being regulated in the presence of the neurotrophin. These include the gene products of HNRPDL (Heterogeneous nuclear ribonucleoprotein D-like), HNRPK (Heterogeneous nuclear ribonucleoprotein K),

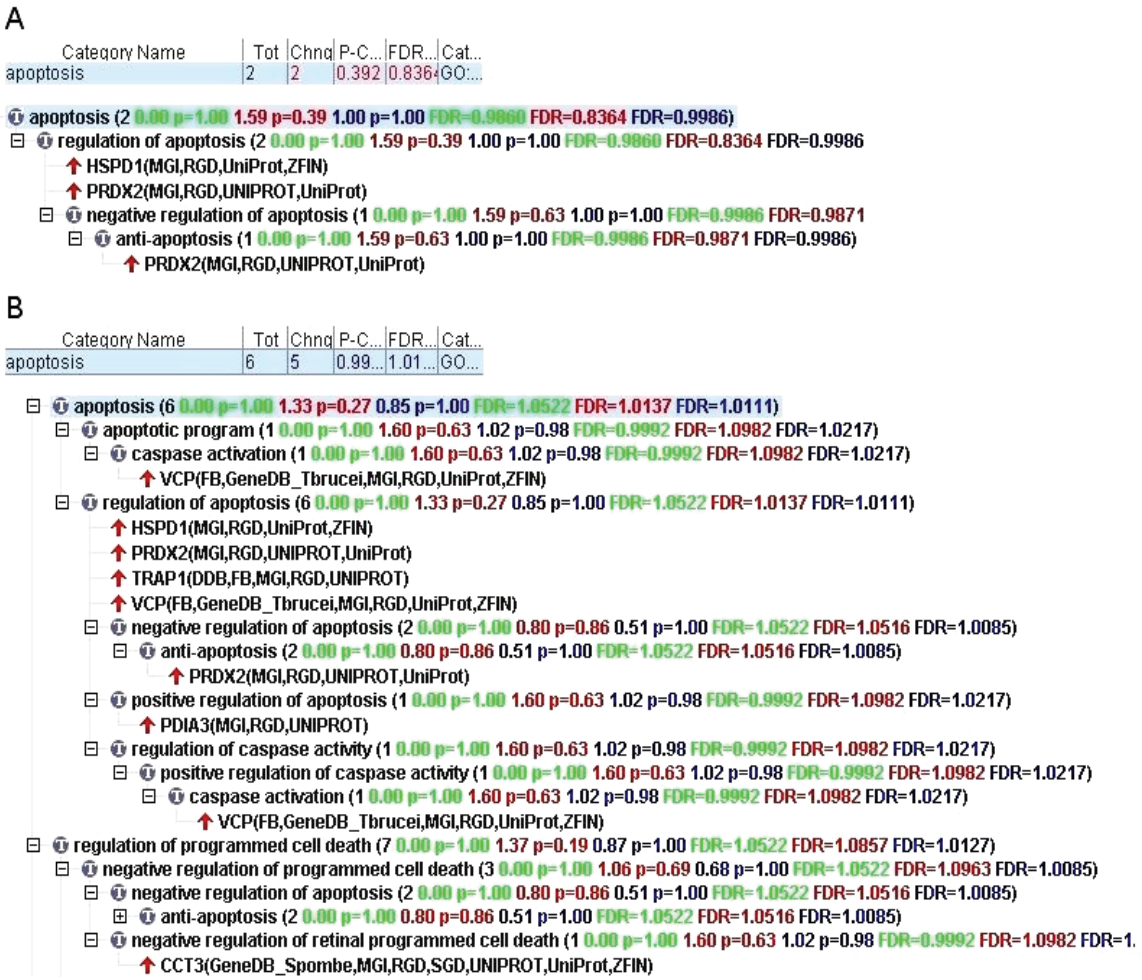

Fig. 4.19 – Cluster analysis of gene products regulated by BDNF - apoptosis ontology. Genes which expression is significantly different in the presence of BDNF (A) and seleted genes (B) based on the results shown in Table VI ("NO" and "Trend").

HNRPC (Heterogeneous nuclear ribonucleoprotein C) and SARS1 (Seryl-aminoacyl-tRNA synthetase), which were significantly upregulated by BDNF, and PCBP1 (Poly(rC)-binding protein 1), which was significantly downregulated by the neurotrophin (Fig. 4.22). Other proteins were also regulated by BDNF, although the results did not reached statistical significance, and included the HNRPH1 (Heterogeneous nuclear ribonucleoprotein H), PCBP2 (Pcbp2 protein) and EEF2 (Elongation factor 2) gene products, which were upregulated, in addition to the HNRPL (Heterogeneous nuclear ribonucleoprotein L) and KHSRP (Far upstream element binding protein 2), which were downregulated (see section "4.3 – Discussion" for further details).

Fig. 4.20 – Cluster analysis of gene products regulated by BDNF - protein metabolism ontology. Image shows gene products which expression was significantly different in the presence of BDNF, with those involved in translation indicated by the arrow. The analysis was performed based on the data shown in Table VI.

Fig. 4.21 – Cluster analysis of gene products regulated by BDNF - protein metabolism ontology. Image shows gene products which expression was significantly different in the presence of BDNF (as in the previous figure), as well as other selected genes based on the results shown in Table VI ("NO" and "Trend"). Gene products involved in translation are indicated by the arrow.

Fig. 4.22 – Cluster analysis of gene products regulated by BDNF - nucleobase, nucleoside, nucleotide and nucleic acid metabolism ontology. Image shows gene products which expression was significantly different in the presence of BDNF. The clustering was performed based on the results shown in Table VI.

Category Name	Tot	Ovr	P-Ovr	FDR-Ovr	Category ID
nucleobase, nucleoside, nucleotid...	27	21	0.0468	3.2000	GO:00061...

Fig. 4.23 – Cluster analysis of gene products regulated by BDNF - nucleobase, nucleoside, nucleotide and nucleic acid metabolism ontology. Image shows gene products which expression was significantly different (as in the previous figure), and also selected genes which expression changed in the presence of BDNF as indicated in Table VI ("NO" and "Trend").

4.2.6 - Proteomic changes induced by BDNF in the S126 fraction – Gel-based and gel-free approaches

Despite the achievements in reproducibility and sample solubilization accomplished in the gels analysed by autoradiography (Chapter 3.2.2), a higher amount of protein had to be applied to IPG strips for protein ID by MALDI-TOF MS (Fig. 4.9). The increase in protein loading of the strips causes inter-protein interactions, thereby decreasing their solubility. The S126 fraction contained membrane, membrane-associated proteins and other proteins insoluble in 50mM Tris/HCl that were also difficult to resolve in 2D-gels. Therefore, in order to further extend the analysis of the proteome of hippocampal neurons we used a different, high throughput, proteomics approach for protein ID and quantification of the S126 fraction, the 2D-LC-MS/MS. This technique overcomes most of the problems associated with protein solubility issues, because instead of proteins, peptides are being resolved, which are more stable, consistent and highly reproducible between different experiments.

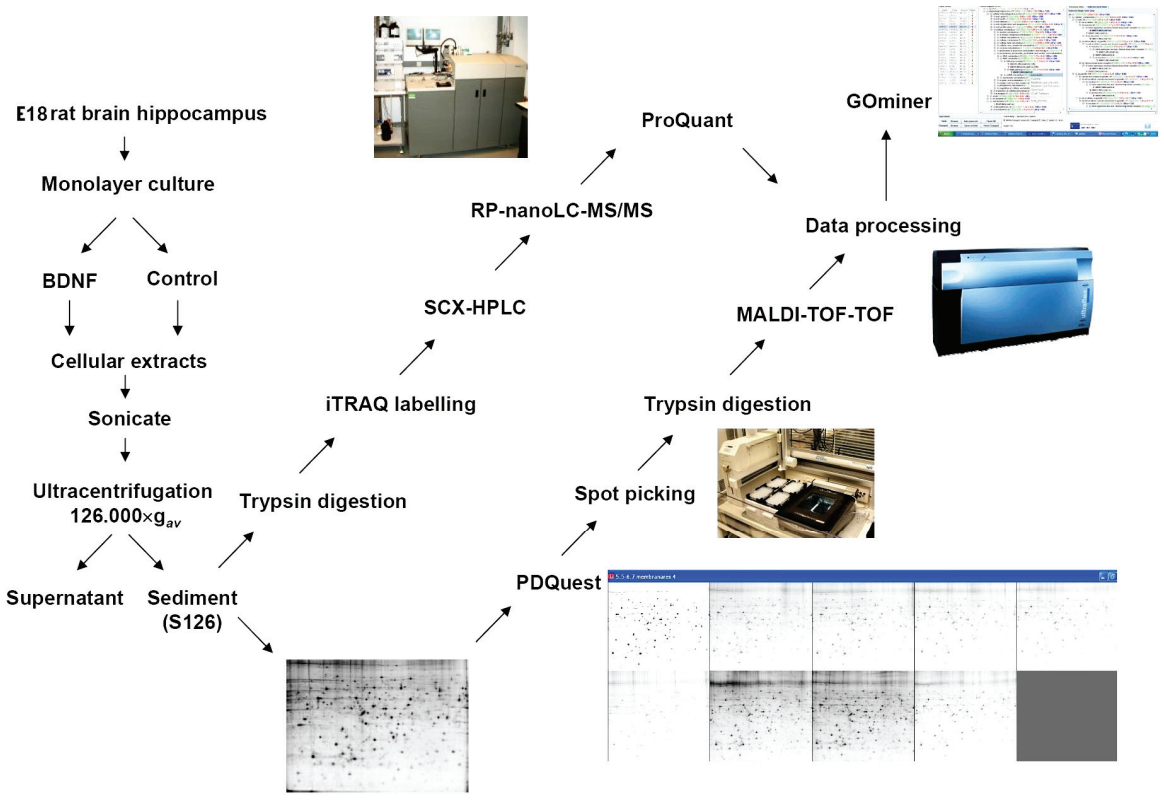

Figure 4.24 – Proteomics workflow for the analysis of the S126 fraction. Cultured hippocampal neurons were treated as indicated in the caption of Fig. 4.5. The S126 fraction was analysed either using 2D-SDS-PAGE, as in Fig. 4.5, followed by trypsin digestion and MALDI-TOF-TOF analysis, or by using 2D-LC-MS/MS of digested peptides (non-radiolabelled). Data was gathered in Microsoft Excel Spreadsheets, processed and analysed. Results were grouped using GOminer.

The signal intensity of the peptides retrieved from the MALDI-TOF analysis is not typically used to derive the quantity of the protein. Therefore, the intensity of the spot measured in the radiolabelled gels was correlated with the mass spectrometric protein ID, as a final step (see section 4.2.3.1 – General workflow). In the liquid based approach shown in this section, quantification and identification are performed in the same step. The results of protein quantification with the two approaches cannot be fully compared because in the gel-based approach only radiolabelled spots (newly synthesized proteins) were quantified, while in the liquid-based approach all proteins are quantified (as discussed ahead). Although the workflow for these two approaches is totally different (Fig. 4.24) – 2D-LC handles and resolves peptides whereas 2D-gels were used for intact proteins – data from both methods were collected, gathered and analysed by using GOminer. In the liquid based approach, the quantification was performed using the iTRAQ labelling reagents, and the ProQuant software package. Although a free version of iTRAQ quantification software is available (Shadforth, I. P. et al., 2005), data integration was faster using distinct packages of the same company. A stable isotope label was introduced into each of the four samples that were to be quantified relatively to each other. Samples were then mixed, analysed by 2D-LC-MS/MS, and proteins identified and quantified (ratio between peptides with each isotopic label) (Andersen, J. S. and Mann, M., 2000).

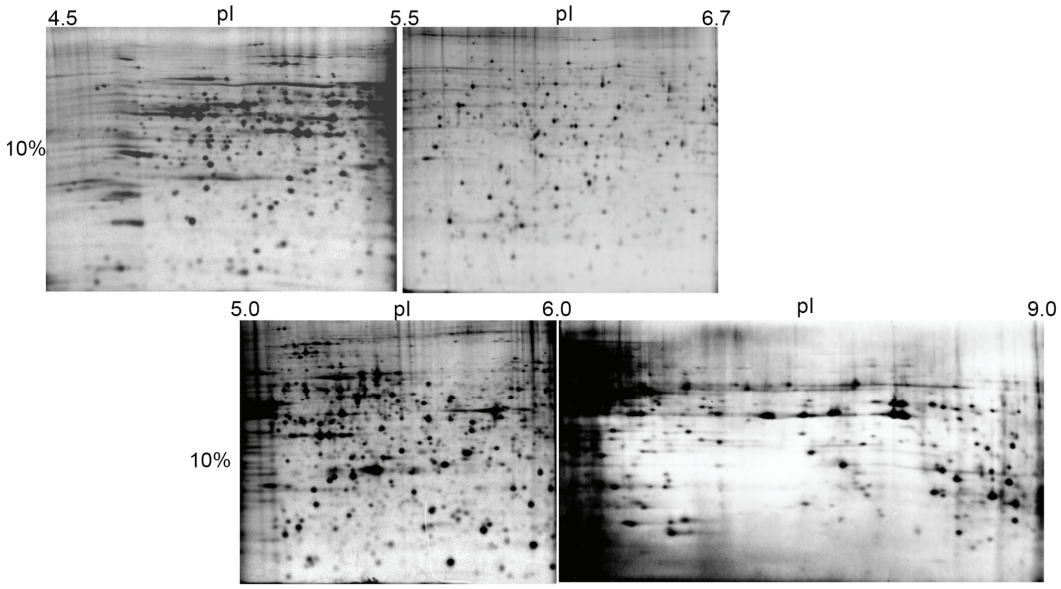

Figure 4.25 – Two-dimensional gel electrophoresis of the S126 fraction. Radiolabelled amino acids were incorporated into newly synthesized proteins for 12h, as indicated in Fig.4.5. Samples were then processed as in Fig. 3.5 (sonicated). Proteins were focused using IPG strips pH 4.5-5.5, 5.0-6.0, 5.5-6.7 and 6.0-9.0. After the second dimension, gels were dried and placed in contact with a phosphor screen. Images were acquired using a STORM laser scanner. Quantification was performed using PDQuest (Bio-Rad).

Using the 2D-gel approach, the proteins of the S126 fraction of cultured hippocampal neurons were resolved with IPG strips of pH 4.5-5.5, 5.0-6.0, 5.5-6.7 and 6.0-9.0 (Fig. 4.25, see also "Appendix – Supplementary data"). The workflow for the analysis of the S126 fraction using 2D-LC-MS/MS consisted briefly in the following: samples were digested with trypsin, labelled with iTRAQ labelling kit, fractionated with strong cation-exchange HPLC,

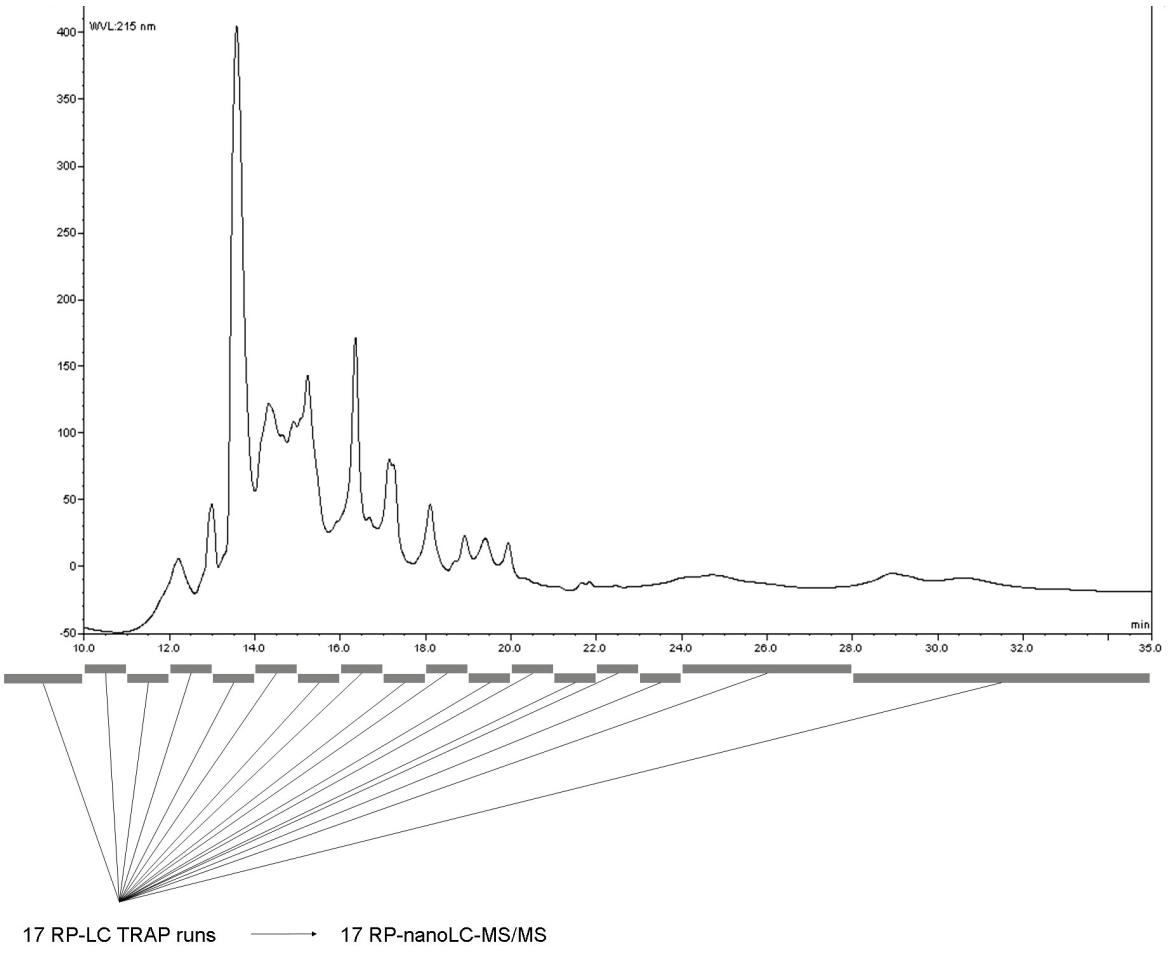

Figure 4.26 – Off-line 2D-LC-MS/MS of S126 fractions prepared from rat cultured hippocampal neurons. Figure shows strong cation exchange chromatogram (SCX) of the S126 fraction, after trypsin digestion and iTRAQ labelling, using a PolySULFOETHYL ATM column (200×4.6mm, 5µm, 1000Å). Mobile phase: 25% ACN, 10mM KH_2PO_4 pH 3. Gradient: linear increase to 75% of mobile phase B (25% ACN, 10mM KH_2PO_4 pH 3 and 1M KCl) from 5min to 35min at 1mL/min. Fractions containing 1mL were cleaned using RP ("trap") chromatography (mobile phase A: 2% ACN, 0.1% formic acid (FA) and mobile phase B: 98% ACN, 0.1% FA at 1mL/min). Peptides were eluted into the MS system with a binary gradient (300nL/min) from 100% mobile phase A (2% ACN, 0.5% FA) to 70% mobile phase B (98% ACN, 0.5% formic acid) over 110min, then 70 – 100% mobile phase B in 20min and held at mobile phase B for an additional 10min. The QSTAR XL was operated in an information-dependent acquisition (IDA) mode. Proteins were identified using Interrogator algorithm (Applied Biosystems) and Rat fasta UniProtKB/Swiss-Prot database.

resolved with reverse phase nano-HPLC and identified by tandem mass spectrometry (ESI-Qq-TOF). After peptide labelling, the samples from four different experiments (two controls and two BDNF stimulated extracts) were pulled and fractionated. Fig. 4.26 represents the chromatogram obtained from strong cation exchange HPLC. A total of 17 fractions were collected (boxes). The first fraction contained the first 10 minutes of elutes (sample that did not interact with the column). Then, 14 samples were individually collected, one for each minute (1mL), and a final fraction of 11mL was pulled together (comprising peptides with higher affinity for the column). Each fraction was subjected to a desalting step (to preserve the reverse phase column used before the MS), which consisted on using a trap column (C18 column, with low resolving capacity). Once bound to the column, peptides were desalted with mobile phase for 5min and eluted by switching from 0% mobile phase B to 100% mobile phase B (98% ACN, 0.5% formic acid) in a single step. The resulting elutions were dried under vacuum, and used in RP-LC-MS/MS. Proteins were identified using the UniProtKB/Swiss-Prot Rat FASTA file and Applied Biosystems software packages (Analyst, BioAnalyst, and Proquant). Table VII shows the gene products found in the S126 fraction isolated from hippocampal neurons, using 2D-LC-MS/MS or 2D-SDS-PAGE (Gene names are presented, instead of accession numbers, for direct use of the table with GOMiner, which accepts gene names as entry data).

In order to better visualize the complementary information retrieved from both methods, data from Table VII was imported into GOMiner (as described in chapter 4.2.5). Figure 4.27 shows two major clusters of proteins identified either by 2D-SDS-PAGE (green boxes) or by 2D-LC-MS/MS (red boxes), namely membrane and nuclear proteins. The results show that the liquid based approach increases the identification of membrane and membrane associated proteins, as well as nuclear proteins, although the gel based approach should not be ignored for this purpose, as some proteins were identified only by 2D-SDS-PAGE.

Table VII – Protein identification from the S126 fraction isolated from cultured hippocampal neurons. Combination of protein ID obtained from the gel based approach (2D-SDS-PAGE) using MALDI-TOF and MALDI-TOF-TOF mass spectrometry, and liquid based approach (2D-LC-MS/MS) using ESI-Qq-TOF mass spectrometry.

Gene name	Protein Name	Method
Acadl	Acyl-CoA dehydrogenase, long-chain specific, mitochondrial precursor (EC 1.3.99.13) (LCAD)	2D-SDS-PAGE
Acot2	Acyl coenzyme A thioester hydrolase, mitochondrial precursor (EC 3.1.2.2) (Very-long-chain acyl-CoA thioesterase) (MTE-I) (ARTISt/p43)	2D-SDS-PAGE
Acta1	Actin, alpha skeletal muscle	2D-LC-MS/MS
		2D-SDS-PAGE
Acta2	Actin, aortic smooth muscle	2D-LC-MS/MS
Actb	Actin, cytoplasmic 1 (Beta-actin)	2D-LC-MS/MS
		2D-SDS-PAGE
Actc	Actin, alpha cardiac	2D-LC-MS/MS
		2D-SDS-PAGE
Actg1	Actin, cytoplasmic 2 (Gamma-actin)	2D-LC-MS/MS
		2D-SDS-PAGE
Actg2	Actin, gamma-enteric smooth muscle	2D-LC-MS/MS
ACTR1A	Alpha-centractin (Centractin) (Centrosome-associated actin homolog) (Actin-RPV) (ARP1)	2D-SDS-PAGE
Agrn	Agrin [Precursor]	2D-LC-MS/MS
Akap6	A-kinase anchor protein 6	2D-LC-MS/MS
Aldh2	Aldehyde dehydrogenase, mitochondrial precursor (EC 1.2.1.3) (ALDH class 2) (ALDH1) (ALDH-E2)	2D-SDS-PAGE
Ap1b1	AP-1 complex subunit beta-1	2D-LC-MS/MS
Arg2	Arginase-2, mitochondrial precursor	2D-SDS-PAGE
Asna1	Arsenical pump-driving ATPase (EC 3.6.3.16) (Arsenite-translocating ATPase) (Arsenical resistance ATPase) (Arsenite-transporting ATPase) (ARSA)	2D-SDS-PAGE
Atp5a1	ATP synthase alpha chain, mitochondrial precursor (EC 3.6.3.14)	2D-LC-MS/MS
		2D-SDS-PAGE
Atp5b	ATP synthase beta chain, mitochondrial precursor (EC 3.6.3.14)	2D-LC-MS/MS
		2D-SDS-PAGE
Atp5h	ATP synthase D chain, mitochondrial (EC 3.6.3.14)	2D-SDS-PAGE
Bckdha	2-oxoisovalerate dehydrogenase alpha subunit, mitochondrial precursor (EC 1.2.4.4) (Branched-chain alpha-keto acid dehydrogenase E1 component alpha chain) (BCKDH E1-alpha) (Fragment)	2D-SDS-PAGE
BicD2	Bicaudal D protein	2D-LC-MS/MS
Brdt	Brdt protein	2D-LC-MS/MS
Cacna1d	Voltage-dependent L-type calcium channel alpha-1D subunit	2D-LC-MS/MS
Cat	Catalase (EC 1.11.1.6)	2D-SDS-PAGE

Cct1	T-complex protein 1, alpha subunit (TCP-1-alpha) (CCT-alpha)	2D-SDS-PAGE
Chad	Chondroadherin [Precursor]	2D-LC-MS/MS
Chp	Calcium-binding protein p22 (Calcium-binding protein CHP) (Calcineurin homologous protein)	2D-SDS-PAGE
Ckb	Creatine kinase B-type (EC 2.7.3.2) (Creatine kinase, B chain) (B-CK)	2D-SDS-PAGE
Cope	Coatomer epsilon subunit (Epsilon-coat protein) (Epsilon-COP)	2D-SDS-PAGE
Cops8	COP9 signalosome complex subunit 8 (Signalosome subunit 8) (SGN8) (JAB1-containing signalosome subunit 8) (COP9 homolog)	2D-LC-MS/MS
Cyb5	Cytochrome b5	2D-SDS-PAGE
Dars	Aspartyl-tRNA synthetase (EC 6.1.1.12) (Aspartate--tRNA ligase) (AspRS)	2D-SDS-PAGE
Dld	Dihydrolipoamide dehydrogenase (E3 component of pyruvate dehydrogenase complex, 2-oxo-glutarate complex, branched chain keto acid dehydrogenase complex)	2D-SDS-PAGE
Dpysl2	Dihydropyrimidinase-related protein 2 (DRP-2) (Turned on after division, 64 kDa protein)	2D-SDS-PAGE
Echs1	Enoyl-CoA hydratase, mitochondrial precursor (EC 4.2.1.17) (Short chain enoyl-CoA hydratase) (SCEH) (Enoyl-CoA hydratase 1)	2D-SDS-PAGE
Eif2s1	Eukaryotic translation initiation factor 2 subunit 1 (Eukaryotic translation initiation factor 2 alpha subunit) (eIF-2-alpha) (EIF-2alpha) (EIF-2A)	2D-SDS-PAGE
Eno1	Alpha enolase (EC 4.2.1.11) (2-phospho-D-glycerate hydro-lyase) (Non-neural enolase) (NNE)	2D-SDS-PAGE
Eno2	Gamma enolase (EC 4.2.1.11) (2-phospho-D-glycerate hydro-lyase) (Neural enolase) (Neuron-specific enolase) (NSE) (Enolase 2)	2D-SDS-PAGE
Enpep	Glutamyl aminopeptidase	2D-LC-MS/MS
Epha3	Ephrin type-A receptor 3 [Precursor]	2D-LC-MS/MS
Erp29	Endoplasmic reticulum protein ERp29 precursor (ERp31)	2D-SDS-PAGE
Fgf18	Fibroblast growth factor 18 [Precursor]	2D-LC-MS/MS
Fmo5	Dimethylaniline monooxygenase [N-oxide-forming] 5	2D-LC-MS/MS
Ftl1	Ferritin light chain 1 (Ferritin L subunit 1)	2D-SDS-PAGE
G6pdx	Glucose-6-phosphate 1-dehydrogenase (EC 1.1.1.49) (G6PD)	2D-SDS-PAGE
Gatm	Glycine amidinotransferase, mitochondrial precursor (EC 2.1.4.1) (L-arginine:glycine amidinotransferase) (Transamidinase) (AT)	2D-SDS-PAGE
Gdi1	Rab GDP dissociation inhibitor alpha (Rab GDI alpha) (GDI-1)	2D-SDS-PAGE
Gfap	Glial fibrillary acidic protein, astrocyte (GFAP)	2D-SDS-PAGE
Glud1	Glutamate dehydrogenase 1, mitochondrial precursor (EC 1.4.1.3) (GDH) (Memory-related protein 2)	2D-SDS-PAGE
Glul	Glutamine synthetase (EC 6.3.1.2) (Glutamate--ammonia ligase) (GS)	2D-SDS-PAGE
Gnal	Guanine nucleotide-binding protein G(olf), alpha subunit	2D-LC-MS/MS
Gnao1	Guanine nucleotide-binding protein G(o), alpha subunit 1	2D-SDS-PAGE
		2D-SDS-PAGE

Gnb1	Guanine nucleotide-binding protein G(I)/G(S)/G(T) beta subunit 1 (Transducin beta chain 1)	2D-SDS-PAGE
Gpd2	Glycerol-3-phosphate dehydrogenase, mitochondrial precursor (EC 1.1.99.5) (GPD-M) (GPDH-M)	2D-SDS-PAGE
Grb2	Growth factor receptor-bound protein 2	2D-SDS-PAGE
Grip1	Glutamate receptor-interacting protein 1	2D-LC-MS/MS
Hist1h1c	Histone H1.2	2D-LC-MS/MS
Hist1h1t	Histone H1t	2D-LC-MS/MS
HIST1H2AC	Histone H2A type 4	2D-LC-MS/MS
Hist1h2af	Histone H2A type 1-F	2D-LC-MS/MS
HIST1H2AG	Histone H2A type 1	2D-LC-MS/MS
Hist1h2ba	Histone H2B, testis	2D-LC-MS/MS
HIST1H2BC	Histone H2B	2D-LC-MS/MS
HIST1H2BD	Histone H2B type 1-D	2D-SDS-PAGE
Hist1h2bm	Histone H2B type 1-M	2D-SDS-PAGE
Hist1h4b	Histone H4	2D-LC-MS/MS
Hist3h2a	Histone H2a	2D-LC-MS/MS
Hnrpa1	Heterogeneous nuclear ribonucleoprotein A1	2D-SDS-PAGE
Hnrpa2b1	Heterogeneous nuclear ribonucleoprotein A2 B1	2D-SDS-PAGE
Hnrpc	Hnrpc protein	2D-LC-MS/MS
Hnrpdl	JKTBP (Heterogeneous nuclear ribonucleoprotein D-like)	2D-LC-MS/MS
Hnrph1	Hnrph1 heterogeneous nuclear ribonucleoprotein H1	2D-SDS-PAGE
Hnrpk	Heterogeneous nuclear ribonucleoprotein K (dC stretch-binding protein) (CSBP)	2D-SDS-PAGE
Hspa5	78 kDa glucose-regulated protein precursor	2D-SDS-PAGE
Hspa8	Heat shock cognate 71 kDa protein (Heat shock 70 kDa protein 8)	2D-LC-MS/MS
HSPA8	Heat shock cognate 71 kDa protein (Heat shock 70 kDa protein 8)	2D-SDS-PAGE
Hspa9	Stress-70 protein, mitochondrial precursor (75 kDa glucose regulated protein) (GRP 75)	2D-SDS-PAGE
Hspd1	60 kDa heat shock protein, mitochondrial precursor (Hsp60) (60 kDa chaperonin) (CPN60)	2D-SDS-PAGE
Idh1	Isocitrate dehydrogenase [NADP] cytoplasmic (EC 1.1.1.42) (Oxalosuccinate decarboxylase)	2D-SDS-PAGE
Idi1	Isopentenyl-diphosphate Delta-isomerase 1	2D-LC-MS/MS
Ina	Alpha-internexin (Alpha-Inx)	2D-SDS-PAGE
Ivd	Isovaleryl-CoA dehydrogenase, mitochondrial precursor (EC 1.3.99.10) (IVD)	2D-SDS-PAGE
Klhl10	Kelch-like protein 10	2D-LC-MS/MS
Llgl1	Lethal(2) giant larvae protein homolog 1	2D-LC-MS/MS
Mageb18	Hypothetical protein	2D-LC-MS/MS
Mamdc1	MAM domain-containing protein 1 [Precursor]	2D-LC-MS/MS
Mapk1	Mitogen-activated protein kinase 1	2D-SDS-PAGE
Mdh1	Malate dehydrogenase, cytoplasmic (EC 1.1.1.37)	2D-SDS-PAGE
Mecr	Trans-2-enoyl-CoA reductase, mitochondrial [Precursor]	2D-LC-MS/MS
MTERFD3	mTERF domain-containing protein 3, mitochondrial precursor	2D-LC-MS/MS

Napa	Alpha-soluble NSF attachment protein (SNAP-alpha) (N-ethylmaleimide-sensitive factor attachment protein, alpha)	2D-SDS-PAGE
Napb	Beta-soluble NSF attachment protein (SNAP-beta) (N-ethylmaleimide-sensitive factor attachment protein, beta) (Brain protein I47)	2D-SDS-PAGE
Ncam1	Neural cell adhesion molecule 1, 140 kDa isoform [Precursor]	2D-LC-MS/MS
Ndrg3	Protein NDRG3	2D-LC-MS/MS
Ndst1	Bifunctional heparan sulfate N-deacetylase/N-sulfotransferase 1	2D-LC-MS/MS
Ndufv2	NADH-ubiquinone oxidoreductase 24 kDa subunit, mitochondrial precursor (EC 1.6.5.3) (EC 1.6.99.3) (Fragment)	2D-SDS-PAGE
Nedd8	NEDD8 Ubiquitin-like protein NEDD8	2D-LC-MS/MS
Nefl	Neurofilament triplet L protein (68 kDa neurofilament protein) (Neurofilament light polypeptide) (NF-L)	2D-SDS-PAGE
Nfatc2ip	Nuclear factor of activated T-cells, cytoplasmic, calcineurin-dependent 2 interacting protein	2D-LC-MS/MS
Npm1	Nucleophosmin (NPM) (Nucleolar phosphoprotein B23) (Numatrin) (Nucleolar protein NO38)	2D-SDS-PAGE
Npr2	Atrial natriuretic peptide receptor B [Precursor]	2D-LC-MS/MS
Nrxn1	Neurexin-1-beta [Precursor]	2D-LC-MS/MS
Oat	Ornithine aminotransferase, mitochondrial precursor	2D-SDS-PAGE
P4hb	Protein disulfide-isomerase precursor	2D-SDS-PAGE
Pa2g4	Proliferation-associated protein 2G4 (Proliferation-associated protein 1) (Protein p38-2G4)	2D-SDS-PAGE
Pafah1b3	Platelet-activating factor acetylhydrolase IB alpha subunit	2D-SDS-PAGE
Pc	Pyruvate carboxylase, mitochondrial precursor (EC 6.4.1.1) (Pyruvic carboxylase) (PCB)	2D-SDS-PAGE
Pcbp1	Poly(rC)-binding protein 1 (Alpha-CP1) (hnRNP-E1)	2D-SDS-PAGE
Pcca	Propionyl-CoA carboxylase alpha chain, mitochondrial precursor (EC 6.4.1.3) (PCCase alpha subunit) (Propanoyl-CoA:carbon dioxide ligase alpha subunit) (Fragment)	2D-SDS-PAGE
Pdcd6	Programmed cell death 6-interacting protein	2D-SDS-PAGE
Pdha1	Pyruvate dehydrogenase E1 component alpha subunit, somatic form, mitochondrial precursor (EC 1.2.4.1) (PDHE1-A type I)	2D-SDS-PAGE
Pdia3	Protein disulfide-isomerase A3 precursor	2D-SDS-PAGE
Phb	Prohibitin	2D-SDS-PAGE
		2D-SDS-PAGE
Pkm2	Pkm2 protein	2D-SDS-PAGE
Plekhb1	Plekhb1 protein	2D-LC-MS/MS
PLEKHH3	Pleckstrin homology domain containing, family H (With MyTH4 domain) member 3	2D-LC-MS/MS
Pmm1	Phosphomannomutase 1	2D-LC-MS/MS
Ppfia4	Liprin-alpha-4 [Fragment]	2D-LC-MS/MS
Ppp1ca	Serine/threonine protein phosphatase PP1-alpha catalytic subunit (EC 3.1.3.16) (PP-1A)	2D-SDS-PAGE
Ppp2ca	Serine/threonine protein phosphatase 2A, catalytic subunit, alpha isoform (EC 3.1.3.16)	2D-SDS-PAGE

Ppp2r1b	Serine/threonine-protein phosphatase 2A 65 kDa regulatory subunit A beta isoform	2D-LC-MS/MS
Prdx2	Peroxiredoxin 2 (EC 1.11.1.15) (Thioredoxin peroxidase 1)	2D-SDS-PAGE
Prdx6	Peroxiredoxin 6	2D-SDS-PAGE
Prmt7	Protein arginine N-methyltransferase 7	2D-LC-MS/MS
Prps1	Ribose-phosphate pyrophosphokinase I (EC 2.7.6.1) (Phosphoribosyl pyrophosphate synthetase I) (PRS-I)	2D-SDS-PAGE
Psma1	Proteasome subunit alpha type 1 (EC 3.4.25.1) (Proteasome component C2) (Macropain subunit C2) (Multicatalytic endopeptidase complex subunit C2) (Proteasome nu chain)	2D-SDS-PAGE
Psma3	Proteasome subunit alpha type 3 (EC 3.4.25.1) (Proteasome component C8) (Macropain subunit C8) (Multicatalytic endopeptidase complex subunit C8) (Proteasome subunit K)	2D-SDS-PAGE
Psma5	Proteasome subunit alpha type 5 (EC 3.4.25.1) (Proteasome zeta chain) (Macropain zeta chain) (Multicatalytic endopeptidase complex zeta chain)	2D-SDS-PAGE
Psma6	Proteasome subunit alpha type 6 (EC 3.4.25.1) (Proteasome iota chain) (Macropain iota chain) (Multicatalytic endopeptidase complex iota chain)	2D-SDS-PAGE
Psmb2	Proteasome subunit beta type 2 (EC 3.4.25.1) (Proteasome component C7-I) (Macropain subunit C7-I) (Multicatalytic endopeptidase complex subunit C7-I)	2D-SDS-PAGE
Psmb3	Proteasome subunit beta type 3 (EC 3.4.25.1) (Proteasome theta chain) (Proteasome chain 13) (Proteasome component C10-II)	2D-SDS-PAGE
Psmb6	Proteasome subunit beta type 6 precursor (EC 3.4.25.1) (Proteasome delta chain) (Macropain delta chain) (Multicatalytic endopeptidase complex delta chain) (Proteasome subunit Y) (Proteasome chain 5) (Fragment)	2D-SDS-PAGE
Psmd14	26S proteasome non-ATPase regulatory subunit 14	2D-SDS-PAGE
Psmd7	26S proteasome non-ATPase regulatory subunit 7 (26S proteasome regulatory subunit rpn8) (26S proteasome regulatory subunit S12) (Proteasome subunit p40) (Mov34 protein)	2D-SDS-PAGE
Ptpru	Receptor type protein tyrosine phosphatase psi [Fragment]	2D-LC-MS/MS
Pura	Transcriptional activator protein PUR-alpha (Purine-rich single-stranded DNA-binding protein alpha)	2D-SDS-PAGE
Rad17	RAD17 homolog	2D-LC-MS/MS
Rom1	Rod outer segment membrane protein 1	2D-LC-MS/MS
Rpl6	60S ribosomal protein L6	2D-LC-MS/MS
Rpl8	60S ribosomal protein L8	2D-LC-MS/MS
Rplp0	60S acidic ribosomal protein P0 (L10E)	2D-SDS-PAGE
Rplp2	60S acidic ribosomal protein P2	2D-LC-MS/MS
Rps10	40S ribosomal protein S10	2D-SDS-PAGE
Rps3	40S ribosomal protein S3	2D-SDS-PAGE
Rps4x	40S ribosomal protein S4, X isoform	2D-SDS-PAGE
Rps7	40S ribosomal protein S7 (S8)	2D-SDS-PAGE
Rps9	40S ribosomal protein S9	2D-LC-MS/MS
Rpsa	40S ribosomal protein SA (p40) (34/67 kDa laminin receptor)	2D-SDS-PAGE

Rsn	CLIP-170	2D-LC-MS/MS
Ruvbl1	RuvB-like 1 (EC 3.6.1.-) (49-kDa TATA box-binding protein-interacting protein) (49 kDa TBP-interacting protein) (TIP49a) (Pontin 52) (DNA helicase p50)	2D-SDS-PAGE
Sfn	Vacuolar protein sorting-associated protein 26A	2D-LC-MS/MS
Slc4a7	Sodium bicarbonate cotransporter 3	2D-LC-MS/MS
Stip1	Stress-induced-phosphoprotein 1	2D-SDS-PAGE
Taar1	Trace amine-associated receptor 1	2D-LC-MS/MS
Tceb1	Transcription elongation factor B polypeptide 1	2D-LC-MS/MS
Tmem24	Transmembrane protein 24	2D-LC-MS/MS
Tpt1	Translationally controlled tumor protein (TCTP) (Lens epithelial protein)	2D-SDS-PAGE
Tuba3	Tubulin alpha-3 chain	2D-SDS-PAGE
Tuba7	Tubulin alpha-3/alpha-7 chain	2D-SDS-PAGE
TUBB1	Tubulin beta chain	2D-LC-MS/MS
Uxs1	UDP-glucuronic acid decarboxylase 1	2D-LC-MS/MS
Vcp	Transitional endoplasmic reticulum ATPase (TER ATPase) (15S Mg^{2+}-ATPase p97 subunit)	2D-SDS-PAGE
Vil2	Ezrin	2D-SDS-PAGE
Wfdc2	WAP four-disulfide core domain protein 2 [Precursor]	2D-LC-MS/MS
Ywhab	14-3-3 protein beta/alpha (Protein kinase C inhibitor protein-1) (KCIP-1) (Prepronerve growth factor RNH-1)	2D-LC-MS/MS 2D-SDS-PAGE
Ywhae	14-3-3 protein epsilon (14-3-3E) (Mitochondrial import stimulation factor L subunit) (MSF L)	2D-LC-MS/MS
YWHAE	14-3-3 protein epsilon (14-3-3E) (Mitochondrial import stimulation factor L subunit) (MSF L)	2D-SDS-PAGE
Ywhag	14-3-3 protein gamma	2D-LC-MS/MS 2D-SDS-PAGE
Ywhah	14-3-3 protein eta	2D-LC-MS/MS
Ywhaq	14-3-3 protein theta	2D-LC-MS/MS
Ywhaz	14-3-3 protein zeta/delta (Protein kinase C inhibitor protein 1) (KCIP-1)	2D-LC-MS/MS
Zfp111	Cys2/His2 zinc finger protein	2D-LC-MS/MS

Figure 4.27 – Complementary information about the proteome of the S126 fraction of cultured hippocampal neurons, obtained from 2D-SDS-PAGE and 2D-LC-MS/MS. Protein ID obtained from the 2D gels approach (Fig 4.25) and the 2D-LC approach (Fig. 4.26) was gathered in Excel, analyzed, and the gene names were retrieved from the Swiss-Prot web site. Genes were clustered and analyzed in GOminer. **Green** squares indicate genes identified by **2D-PAGE** and **red** squares represent genes identified by **2D-LC-MS/MS**. Results show complementary information from both techniques for membrane (**A**) and nuclear (**B**) proteins.

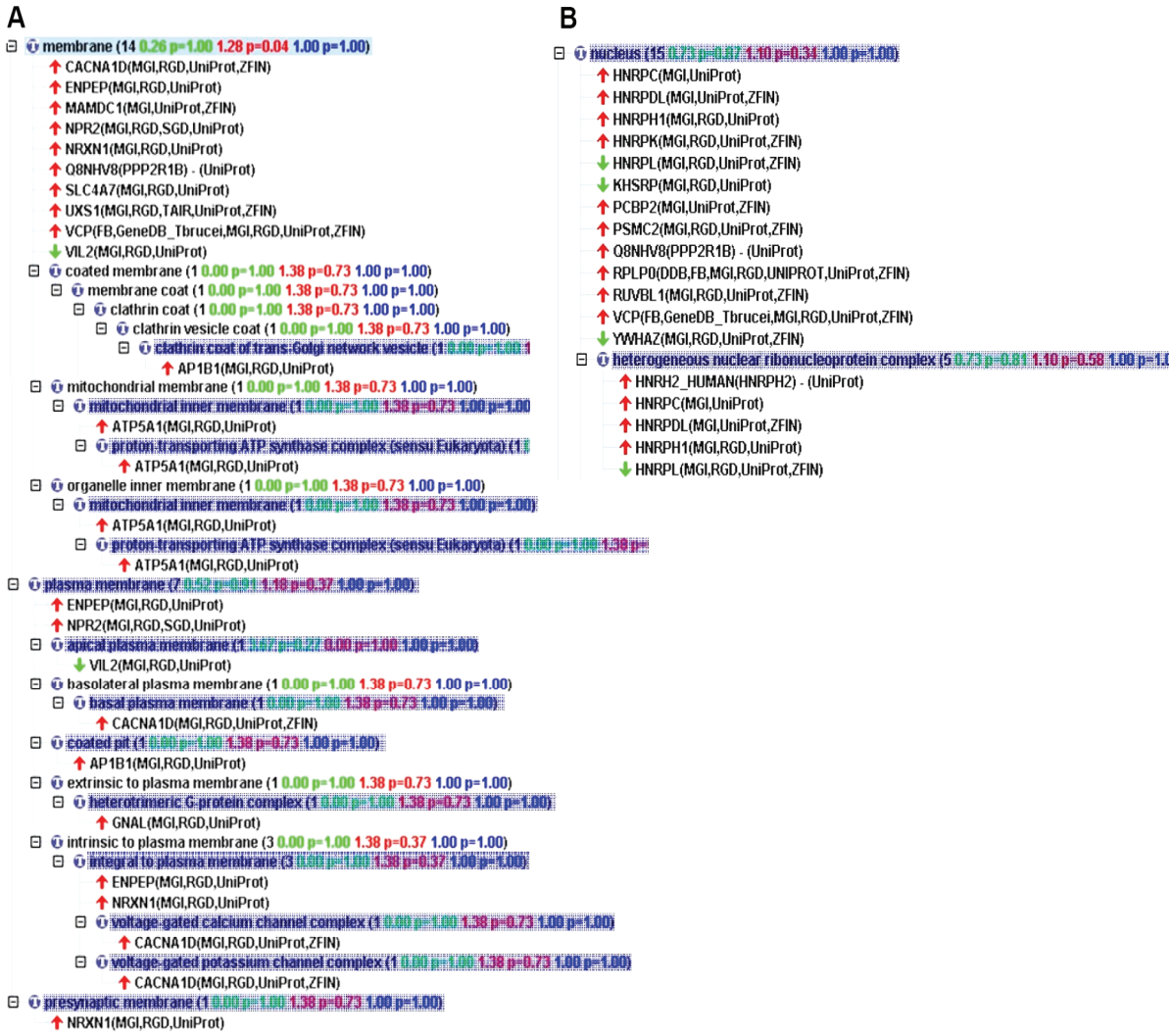

Figure 4.28 - Differential gene expression induced by BDNF in cultured hippocampal neurons. Protein ID from the previous figure was combined with differential expression levels observed from gels (PDQuest) and from LC-MS/MS (Proquant). Red arrows (↑) indicate gene products with increased expression upon BDNF stimulation; green arrows (↓) represent gene products with decreased protein expression. A and B show membrane and nuclear proteins, respectively. Hnrpdl is an example of a gene which expression was found to be upregulated by BDNF using both techniques.

4.3 - Discussion

The **hippocampus** is a brain region associated with memory formation and storage, ultimately contributing to what a human being is: what it reminds of. Therefore, there is a strong interest in the study of hippocampus, its development, functions and preservation. However, the number of publications on the rat hippocampal proteome is reduced, and allowed the identification of a reduced number of proteins. In one publication on the rat brain hippocampus proteome, using eight months old animals, 148 different gene products were identified, including enzymes, structural proteins and heat shock proteins (Fountoulakis, M. et al., 2005). Other authors have tried to map the proteome of the hippocampus of human subjects, and identified 165 proteins by applying 1mg of protein to pH 3-10 IPG strips (Yang, J. W. et al., 2004). Additional studies have evaluated the changes in the hippocampal proteome induced by various stimuli and drugs, such as chronic treatment with antidepressants, using 2D-PAGE. However, in these cases the analysis of the proteome was limited to the spots that showed variation between experimental conditions (Khawaja, X. et al., 2004). Given the main objective of this study, i.e. to characterize the BDNF-induced changes in the proteome of hippocampal neurons, a more extensive characterization of the protein content of the cells was performed. Furthermore, protein radiolabelling facilitated the analysis of the BDNF-induced de novo protein synthesis. For this purpose, radiolabelled amino acids were added to the culture media and once taken up by cultured hippocampal neurons (Fig. 4.1) were incorporated into newly synthesized proteins (Fig. 4.2). The 2D-PAGE approach used in this work shows that BDNF selectively affected the abundance of several protein spots, which were up- or downregulated. These results contrast with the lack of effect of the neurotrophin on the total protein labelling with [^{35}S]-methionine and [^{35}S]-cysteine for incubation periods with BDNF of 3-24h (Fig. 4.3). In cultured cerebrocortical neurons BDNF was shown to specifically enhance total protein synthesis for a stimulation period of 30min (Takei, N. et al., 2001). The differences between these results and our findings in cultured hippocampal neurons may be due to the pulse-chase labelling method used in the cerebrocortical study, which contrasts with the longer incubation periods with the radiolabelled amino acids and with the neurotrophin used in the present work. Another important difference concerns the cells used, and the results may suggest that BDNF modulates the expression of specific proteins in hippocampal neurons, and has a broader effect on protein synthesis in cerebrocortical neurons.

This extensive proteomics study was conducted aiming at identifying the BDNF-induced changes in the protein content of cultured hippocampal neurons. In order to obtain a good resolution of the effects of the neurotrophin, de novo protein synthesis was followed using radiolabelled amino acids, which allows subtracting the background protein content of the cells. The first approach used consisted in resolving total protein extracts from cultured hippocampal neurons in a 2D-gel using pH 3-10 IPG strips (Fig. 3.1). The results clearly indicated that this approach could only allow monitoring 1000-1300 spots, which is much lower then the expected total protein content of the cells. The number of spots resolved was increased by using “zoom” gels, resolving proteins in one pH unit IPG strips (Fig. 3.2), while maintaining the resolving power per gel (1000-1300 spots). The low reproducibility of gels obtained with samples prepared using standard methodologies lead us to a series of **improvements** consisting in the removal of contaminants (using TCA precipitation followed by acetone washing), increase in protein solubilization (using sonication in 2D buffer), and sample fractionation (using ultracentrifugation). Fractionation decreases gel complexity and results in the relative enrichment of low abundant proteins, bringing them into the detection levels of the techniques used (Righetti, P. G. et al., 2003). The results obtained showed an increase in the number of spots available for quantification, from 376 spots in the pH range of 5.5-6.7 using pH 3-10 IPG strip, to more then 2000 spots in the same range, using pH 5.5-6.7 IPG strips and sample fractionation (Figs. 3.2 through 3.6 and Tables I, II and III). An additional enrichment method was tested, consisting in nuclei isolation and separation of nuclear proteins (not shown), but the amount of raw material required did not allow proceeding with this approach. The interest in the study of the effect of BDNF on the nuclear proteome arises from the putative effects on the novo protein synthesis and also from the translocation of proteins into or away from the nuclear compartment [e.g. Manadas, B. J. et al., 2007 (in press)].

The **analysis** of the hippocampal proteome was initially focused on the soluble fraction of cultured hippocampal neurons, stimulated or not with BDNF, and incubated with radiolabelled amino acids, and the proteome was resolved in 2D-gels using IPG strips pH 5.5-6.7 (Fig. 4.6). This allowed spot detection by autoradiography, which is more sensitive than other staining methods, besides allowing the quantification of newly synthesized proteins (Manadas, B. J. et al., 2006). However, gels used for autoradiography are usually not processed for protein identification as radiolabelled spots are not visible in the gel. Also, there are some differences in the gel image obtained from an autoradiogram and from a

silver stained gel (Fig. 4.10). Furthermore, radiolabelled amino acids increase the isotopic mass of peptides which decreases protein identification. Therefore, the identification of the protein spots was performed using mass spectrometry of digested peptides obtained from non-radioactive gels, e.g stained with colloidal coomassie.

The quantification of the autoradiograms displaying the newly synthesized proteins, in control hippocampal neurons and in cells stimulated with BDNF, showed that some spots were significantly different (up- or downregulated) in the two experimental conditions. In addition to these protein spots, the analysis of the data also included spots showing consistent differences that did not achieve statistical significance, and other spots that showed variations lower than 1/1.5 or greater than 1×1.5. The list of selected spots based on these calculations was imported into PDQuest in order to highlight their location on gel images (Fig. 4.8). A crude analysis of the results showed that the same protein could be found in more than one spot, and these various spots were in some cases differentially affected by BDNF stimulation. Accordingly, the stress-induced-phosphoprotein 1 (Stip1) was identified in three neighbour spots, with slight differences in their quantification. These observations highlight the importance of **full mapping** of the gels with extensive identification of the spots and quantification of the changes in expression induced by each given stimuli, as performed in this study (Fig. 4.9 through 4.12). It should also be emphasized that some faint spots in the stained gels were identified while other strong spots were not, revealing that protein ID is not only dependent on the intensity of the spot but may also depend on the proteolytic cleavage, peptide recovery and ionization efficiency. Although spot identification was based on the gene product and not in the protein isoform, or in the protein form resulting from post-translational modifications, the quantification was performed based on newly synthesized proteins (autoradiograms). Therefore, a BDNF-induced change in spot location for a given protein may indicate that a distinct isoform is expressed and/or a different post-translational modification of the protein is induced.

A careful examination of the autoradiogram quantification and of the gel mapping data (Appendix) showed some similarities in the spot distribution in the soluble and S126 fractions, for each given pH range analysed. The analysis of the spots present in both fractions and possessing the same pI and MW range showed that they correspond to the same protein. In fact, several spots are present in both fractions, indicating that the S126 fraction is "**contaminated**" with proteins from the soluble fraction. However, the main purpose of the ultracentrifugation step used was to remove interfering substances (lipids, nucleic acids, and even membrane proteins) in order to apply clean and reproducible

samples to IPG strips, and this was clearly achieved in this work. When the same protein was found in gels prepared from the soluble and S126 fractions, a similar effect of BDNF was observed in both cases. For example, Peroxiredoxin 6 (Prdx6, accession number Q35244) was found in gels prepared from the soluble (Fig. 4.9, bottom left) and S126 (Fig. A.10, bottom left) fractions. In the former case, the spot showed a significant decrease to 0.79, whereas in the latter case the spot showed a decrease to 0.86 ($p>0.05$, Table VI). This indicates that although there is a contamination of the S126 fraction with proteins from the soluble fraction, this does not affect the results observed.

Although the overall spot distribution was similar in the autoradiogram gel images and after colloidal Coomassie gel staining for protein identification, some differences could be detected. Fig 4.10 clearly shows differences in gel images obtained for the same gel, silver stained and autoradiography (Fig. 4.10 left and right, respectively). Furthermore, the relative intensity of the spots also differed when the total protein content was compared with the protein labelling after 12h of incubation period with radiolabelled amino acids. This is caused by differences in the protein synthesis and turn-over rates, and may also be due to the relative content on methionine and cysteine residues (the radiolabelled amino acids added to cell culture) of each protein. This small divergence on spot pattern between the two approaches increased the time required for positive correlation of a given spot intensity and its identification.

Protein identification was performed by peptide mass fingerprint, using database search of obtained mass spectra from spots proteolitically digested with trypsin. In some cases, when PMF positive identification could not be obtained, peptide fragmentation was induced for MS/MS database search. The **database** used for these queries was the UniProtKB/Swiss-Prot database, a non-redundant database. This database was chosen taking into account the relation between obtained accession numbers and the access to other databases (Fig. 4.13 and Fig. 4.14). At this point, it was also important to gather as much relevant information as possible using different databases, which could allow further analysis based on the knowledge of involved signalling pathways, metabolic pathways, protein interaction (Fig. 4.14) and textmining on published papers (Fig. 4.13). The information obtained allows an easy, quick and off-line access to relevant information, mainly when combined with gene clustering.

After combining the results from spot identification and quantification, selected proteins were correlated with their expression levels, and gene names were automatically retrieved from

the UniProtKB/Swiss-Prot database (Table VI), using VBA programming and web queries in Microsoft Excel. In several cases, the same gene product was present in different spots with different expression levels, in control and BDNF stimulated cultured hippocampal neurons (e.g. Dpysl2, Table VI). When expression levels of the same gene were not consistent (one spot upregulated and other downregulated) upregulation or downregulation of a given gene product was decided considering spots with statistically different fold change.

In order to retrieve biologically meaningful information from the data obtained, we took advantage of several software packages used for data **clustering**, most of them designed for microarrays. The majority of the algorithms available lead to "heat clustering", where genes are grouped according to their fold changes between different experimental conditions. Other algorithms group genes according to their functions, but include relatively few categories. GOMiner uses all gene ontologies of selected and imported genes, and clusters genes according to their ontologies, leading to more detailed information on the grouping. For exemple, ENO1 belongs to the "carbohydrate catabolism", "glycolysis" and "carbohydrate metabolism" ontologies (Fig. 4.17A). Because "glycolysis" is a sub-category of the "carbohydrate metabolism" ontology, introducing ENO1 in "glycolysis" retrieves more information about the gene product then a higher level ontology as "carbohydrate metabolism", and groups ENO1 with ENO2 in a more specific and detailed ontology (Fig. 4.17B, "glycolysis").

As mentioned before BDNF plays an important role in the in vivo protection from transient brain ischemia, particularly in the hippocampus (Kokaia, Z. et al., 1996; Larsson, E. et al., 1999). Furthermore, BDNF was shown to protect hippocampal neurons from excitotoxic cell death, by a mechanism dependent on protein synthesis (Almeida, R. D. et al., 2005). The effect of BDNF on proteins of the carbohydrate metabolism (Fig. 4.17) may contribute to the development of more effective mechanisms of energy production, which is relevant during the period of recovery after the ischemia insult. The observed upregulation of Peroxiredoxin 2 (PRDX2, involved in redox regulation of the cell) and 60 kDa heat shock protein (HSPD1, implicated in mitochondrial protein import and macromolecular assembly, and may facilitate the correct folding of imported proteins) (Fig. 4.19) (Boeckmann, B. et al., 2005) may further contribute to neuroprotection by BDNF in the hippocampus.

BDNF also plays important roles in synaptogenesis and in synaptic plasticity (Ring, R. H. et al., 2006). The observed upregulation of Fascin (Fscn1) (Fig. 4.18) by BDNF may be relevant in this context, since Fascin organizes filamentous actin into bundles, and is probably

involved in the assembly of actin filament bundles present in microspikes, membrane ruffles and stress fibers (Boeckmann, B. et al., 2005). Fascin is highly expressed in the brain and according to the STRIGS database it interacts with protein kinase C. Although Fascin also belongs to the cell proliferation gene ontology (Fig. 4.18), other members of this ontology are downregulated, such as Cell division protein kinase 4 (CDK4), which promotes S phase and has been associated with melanomas, and Microtubule-associated protein RP/EB family member 1 (MAPRE1), which during mitosis is associated with the centrosomes and spindle microtubules, and is upregulated in children medulloblastoma (Boeckmann, B. et al., 2005). Taken together these results indicate that although BDNF can increase the activity of some proteins which are closely related to cancer mechanisms (such as Akt, PI3-K, and mutated Ras and Raf) (Bos, J. L., 1989; Chan, T. O. et al., 1999; Schreck, R. and Rapp, U. R., 2006), it also regulates cell proliferation by downregulating proteins involved in this process.

Other clusters of proteins regulated by BDNF include those involved in "protein metabolism" and "nucleobase, nucleoside, nucleotide and nucleic acid metabolism" (Figs. 4.20 through 4.23). These clusters include 20 and 14 gene products, respectively, which were significantly regulated by BDNF, and 23 and 13 other gene products were also regulated but the effects were not statistically significant.

The group of proteins involved in "**Protein biosynthesis**" contains gene products such as Eukaryotic translation initiation factor 3 subunit 5 (EIF3S5; possesses Translation initiation factor activity), Gars protein (GARS; catalizes the reaction ATP + glycine + tRNA[Gly] = AMP + diphosphate + glycyl-tRNA[Gly]), Seryl-aminoacyl-tRNA synthetase (SARS; catalizes the reaction ATP + L-serine + tRNA[Ser] = AMP + diphosphate + L-seryl-tRNA[Ser]), Mitochondrial Elongation factor Tu (TUFM; promotes the GTP-dependent binding of aminoacyl-tRNA to the A-site of ribosomes during protein biosynthesis) and Trafficking protein particle complex subunit 4 (TRAPPC4; may play a role in vesicular transport from endoplasmic reticulum to Golgi and in dendrite postsynaptic membrane trafficking). Other gene products clustered in this ontology, but showing effects that did not achieve statistical significance, include Elongation factor 1-gamma (EEF1G; may play a role in anchoring the complex to other cellular components), Elongation factor 2 (EEF2; promotes the GTP-dependent translocation of the nascent protein chain from the A-site to the P-site of the ribosome), Translation initiation factor eIF-2B beta subunit (EIF2B2; catalyzes the exchange of eukaryotic initiation factor 2-bound GDP for GTP), 60S acidic ribosomal protein P0 (RPLP0, which forms a pentameric complex by interaction with dimers of P1 and P2 in ribosomes), and Far upstream element binding protein 2 (KHSRP; leads to degradation of

inherently unstable mRNAs that contain AU-rich elements, among other functions) (Boeckmann, B. et al., 2005). All these gene products were upregulated in the presence of BDNF in cultured hippocampal neurons after an incubation period of 12h, except KHSRP, TRAPPC4 and EIF2B2, which were downregulated.

In the "**RNA processing**" ontology, the Heterogeneous nuclear ribonucleoprotein D-like (HNRPDL; involved in mRNA nucleocytoplasmic shuttling), Heterogeneous nuclear ribonucleoprotein K (HNRPK; one of the major pre-mRNA-binding proteins), Heterogeneous nuclear ribonucleoprotein C (HNRPC; binds pre-mRNA and nucleates the assembly of 40S hnRNP particles), and Seryl-aminoacyl-tRNA synthetase (SARS1; catalizes the reaction ATP + L-serine + tRNA[Ser] = AMP + diphosphate + L-seryl-tRNA[Ser]) were upregulated by BDNF, while the Poly(rC)-binding protein 1 (PCBP1; single-stranded nucleic acid binding protein that binds preferentially to oligo dC) was downregulated by BDNF. Other gene products upregulated by the neurotrophin include Heterogeneous nuclear ribonucleoprotein H (HNRPH1; component of the heterogenous nuclear ribonucleoprotein [hnRNP] complexes which provides the substrate for the processing events that pre-mRNAs undergo before becoming functional, translatable mRNAs in the cytoplasm), Pcbp2 protein (PCBP2; single-stranded nucleic acid binding protein that binds preferentially to oligo dC) and Elongation factor 2 (EEF2; promotes the GTP-dependent translocation of the nascent protein chain from the A-site to the P-site of the ribosome), but the effects did not achieve statistical significance. On the other hand, downregulated gene products belonging to this category include Heterogeneous nuclear ribonucleoprotein L (HNRPL; component of the heterogenous nuclear ribonucleoprotein [hnRNP] complexes that provide the substrate for the processing events that pre-mRNAs undergo before becoming functional and translatable mRNAs in the cytoplasm) and Far upstream element binding protein 2 (KHSRP; leads to degradation of inherently unstable mRNAs that contain AU-rich elements, among other functions) (Boeckmann, B. et al., 2005).

An increase of the hybridization signal intensity of heterogeneous nuclear ribonucleoprotein H (HNRPH1) was also observed after traumatic brain injury (Kobori, N. et al., 2002), which may be secondary to the upregulation of BDNF following the excitotoxic injury (Shetty, A. K. et al., 2004)

Taken together the results show that BDNF plays an important role in the control of the transcription and translation mechanisms. In addition to these effects, BDNF may induce rapid changes in the activity of transcription factors [Manadas, B. J. et al., 2007 (in press)] and in the protein synthesis machinery. The latter effect is mediated by phosphorylation of

eIF4E, which can be translocated to the synapse, increasing the total protein synthesis (Takei, N. et al., 2001). One of the proteins that can be produced at the dendrites is response to BDNF stimulation was Arc (Yin, Y. et al., 2002), but is was not found in the present study. eIF4E may serve to facilitate translation and capture of mRNA released from local storage granules as well as new mRNA coming into the dendrites (Bramham, C. R. and Messaoudi, E., 2005). The BDNF-induced upregulation of glycolysis proteins (Fig. 4.17) may lead to a rapid production of energy, facilitating the additional synthesis of proteins (Caraglia, M. et al., 2000).

The effects of BDNF on the proteome of the SY5Y-TrkB cell line (human neuroblastoma SY5Y cell line stably transfected with TrkB cDNA) was recently characterized, using different periods of stimulation with BDNF. In this study, samples from treated and non-treated cells were labelled with different DIGE (Diference Gel Electrophoresis) labels, pulled, the proteins were resolved using tube gels for IEF and protein ID was performed on selected spots by MALDI-TOF (Sitek, B. et al., 2005). In this study two Dynein intermediate chain proteins were identified, with one being upregulated and the other downregulated in the presence of BDNF. In cultured hippocampal neurons one spot corresponding to the dynein light chain 2 (Dync1i2) was found to be upregulated 2.2 times, although this effect was not statistically significant. Taken together, the two studies suggest that BDNF regulates dynein, a motor protein responsible for retrograde transport (Pfister, K. K. et al., 1996). Heterogeneous nuclear ribonucleoprotein K (HnRNPK or Hnrpk) was also identified in two spots in SY5Y-TrkB cells, with one having no differential expression and the other showing a rapid upregulation upon the stimulation with BDNF (0.5 to 1h after neurotrophin addition). In cultured hippocampal neurons, seven spots were identified as expressing this protein, with three showing a significant increase by 2.4, 1.94 and 2.08 in BDNF stimulated cultured hippocampal neurons when compared to the control (Table VI). hnRNPK and Hu specifically bind to CU-rich sequences in p21 mRNA 3'-UTR, thereby controlling in an opposite manner the timing of the switch from proliferation to neuronal differentiation (Yano, M. et al., 2005). This highlights the effect of the neurotrophin in the balance between neuronal proliferation and differentiation, as supported by other evidences [e.g. Davies, A. M., 1994; Dobrowsky, R. T. et al., 1995]

Another protein identified and quantified in our work and in SY5Y-TrkB cells was the Rho GDP dissociation inhibitor (GDI) alpha (Arhgdia - regulates the GDP/GTP exchange reaction of the Rho proteins by inhibiting the dissociation of GDP from them, and the subsequent

binding of GTP to them) (Boeckmann, B. et al., 2005). While in the cell line model the protein showed a delayed downregulation following exposure to BDNF (6 and 24 hours after neurotrophin stimulation), in hippocampal neurons three spots were identified and quantified, with one spot presenting a statistically significant increase to 1.07, the second showing a statistically significant decrease to 0.55 and the third spot had a 2.71 fold increase, although not statistically significant, in the presence of BDNF. Since some of the effects of neurotrophins are mediated by inhibition of Rho activity [e.g. neurotrophin-induced neurite outgrowth (Yamashita, T. and Tohyama, M., 2003)] the regulation of Rho GDI alpha protein protein levels by BDNF may provide a secondary mechanism to control long-term effects of BDNF.

The diversity of effects of BDNF on protein spots corresponds to the Rho GTP dissociation inhibitor (GDI) alpha shows the importance of covering as many spots as possible in the gels in order to have a better overview of possible heterogeneities in the response to a given stimulus. The diversity of effects that can be obtained for different spots corresponding to the same protein is also well illustrated by the results obtained concerning the effect of BDNF in Dihydropyrimidinase related protein-2 (Dpysl2) in cultured hippocampal neurons. In the present work this protein was identified in at least 11 spots, with two of them presenting a statistically significant increase of 1.39 and 1.73, and a third spot showing a statistically significant decrease of 0.74, in the presence of BDNF. Although Dihydropyrimidinase related protein-2 was shown to regulate axonal outgrowth (Carter, C. J., 2007), it remains to be determined its role in BDNF-induced axonal elongation.

Although the effects of BDNF in the proteome of SY5Y-TrB cells and hippocampal neurons were similar, to some extent, some of the gene products showed different results. It is noteworthy to mention that two major differences exist, the cells used and the quantification method applied. Cultured hippocampal neurons represent a physiological model of cells expressing their normal gene products and subjected to the exposure of BDNF, a neurotrophin usually expressed and released by these neurons (Farhadi, H. F. et al., 2000). On the other hand, SY5Y-cells do not express the TrkB receptor and possess a different basal proteome from hippocampal neurons, which can lead to different responses to the same stimuli. The other major difference between the two studies concerns the quantification methods used; while in the SY5Y-cell study the staining method used was DIGE, allowing the visualization and quantification of the overall protein content, in the cultured hippocampal study only newly synthesized proteins were monitored, using autoradiography.

In the present work we further analysed the proteome of the S126 fraction using a liquid-based approach (Table VI and Fig. 4.24), in order to overcome some of the difficulties in the study of membrane fractions using the gel based approaches. The comparison of the results obtained using the two approaches show that the combination of both methods leads to an increase of the proteome coverage and they provide complementary information (Fig. 4.29). Furthermore, the results indicate that each method alone is not sufficient for proteome coverage, with several proteins being identified by only one of the approaches (Fig. 4.29). The following proteins were identified by both methods: three actin isoforms, ATP synthase alpha and beta, Guanine nucleotide-binding protein G_o alpha subunit 1, Heat shock cognate 71 kDa protein, Prohibitin, 40S ribosomal protein S7, and three isoforms of the 14-3-3 protein. The low number of proteins identified using the liquid-based approach may be explained by two main reasons: (i) one is the collision energy applied at the CAD cell of the Qq-TOF mass spectrometer, which should have been higher in order to increase peptide fragmentation, as the iTRAQ labelling increases peptide stability; this technical limitation may have contributed to a decrease in protein identification and in the confidence in quantification, (ii) protein digestion may have also contributed to the low protein identification. Although proteins were denatured with SDS, trypsin digestion was performed after SDS removal. In the absence of detergents, highly hydrophobic domains of membrane proteins

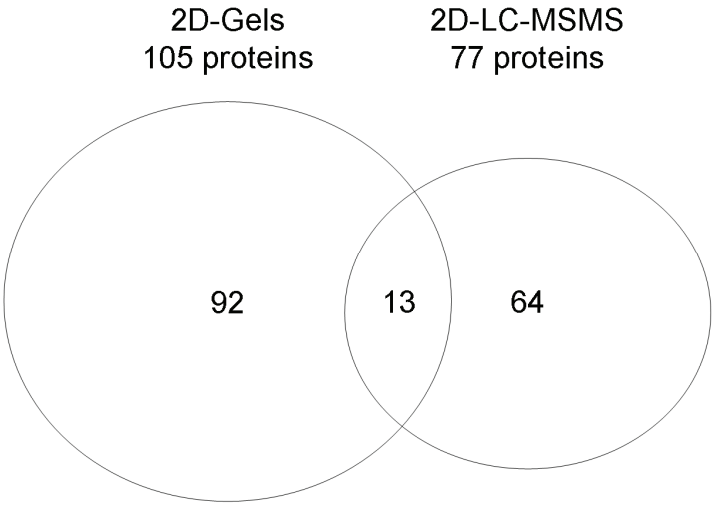

Figure 4.29 – Complementary proteome coverage from 2D-SDS-PAGE and 2D-LC-MS/MS. Both methods allowed the identifications of several proteins: 105 proteins identified by 2D-gels approach, 77 proteins identified by 2D-LC-MS/MS, and 13 of these were identified using both methods.

can interact and lead to the formation of complexes that reduce trypsin access to lysines and arginines. Therefore, a chemical cleavage approach, like cyanogen bromide (CNBr) or acidic cleavage, should be considered as an alternative or a complementary approach for the analysis of protein fractions enriched in hydrophobic domains (Quach, T. T. et al., 2003; Han, J. and Schey, K. L., 2004). Nonetheless, Fig. 4.27 clearly shows the complementary information and proteome coverage of membrane and membrane associated proteins, as well as nuclear proteins. The complementary information obtained from both approaches is also important at the quantification level, since in the gel-based approach only newly synthesized proteins were quantified, in contrast with the liquid-based approach where all peptides are labelled, resulting in total protein quantification.

Chapter 5

Conclusions

BDNF is one of the most studied neurotrophins, playing important roles in development, memory formation and storage, synaptic plasticity, neuroprotection, depression and in regeneration, among others. The main objective of this work was to perform a comprehensive proteome profiling of the effects of BDNF in primary cultures of hippocampal neurons, which will contribute to elucidate some of the physiological roles of the neurotrophin.

The methodologies available for the analysis of the proteome were improved to some extent, using cultured hippocampal neurons and rat brain tissue as a model, and allowed to increase the reproducibility of the results obtained using two-dimensional gel electrophoresis. Fractionation of the samples and the use of “zoom” gels increased the number of spots resolved. The protocol used also improved the reproducibility of protein solubilization and recovery after TCA precipitation, with an increase in the number of visualized spots. The optimization of sample preparation and focusing conditions resulted in an increase in reproducibility of gel images, allowing better and faster software analysis, with an increase in the ratio of automatic matching of gel spots across the gel image.

The present work focused on the proteome coverage of cultured hippocampal neurons and the changes in the proteome induced by BDNF. The use of sample fractionation and of “zoom” gels allowed to increase the proteome coverage when compared to previous studies. BDNF was found to change the abundance of proteins belonging to several distinct ontologies, including proteins involved in the “carbohydrate metabolism”, “protein metabolism” (with major focus on “protein biosynthesis”) and “nucleobase, nucleoside, nucleotide and nucleic acid metabolism” (with focus on “RNA processing”). The massive upregulation of proteins belonging to the last two ontologies account, at least in part, for the role of protein synthesis in many of the biological effects of BDNF, including its role in synaptic plasticity and in neuroprotection. The diversity of proteins which expression is affected by BDNF may also explain the multiplicity of effects of this neurotrophin in the nervous system.

The identification of the target genes and the grouping of differentially expressed proteins according to their ontologies represent important starting points for further analysis of the effects of BDNF in hippocampal neurons, and other neuronal systems, and might elucidate mechanisms, pathways, and physiological and phenotypic changes induced by the neurotrophin. In addition to the functional groups of proteins found to be regulated by BDNF, other proteins not belonging to a specific cluster were also regulated and may also contribute to elucidate the mechanisms of action o BDNF.

Appendix

Supplementary data

A.1 – Soluble fraction resolved using IPG strips pH 4.5-5.5

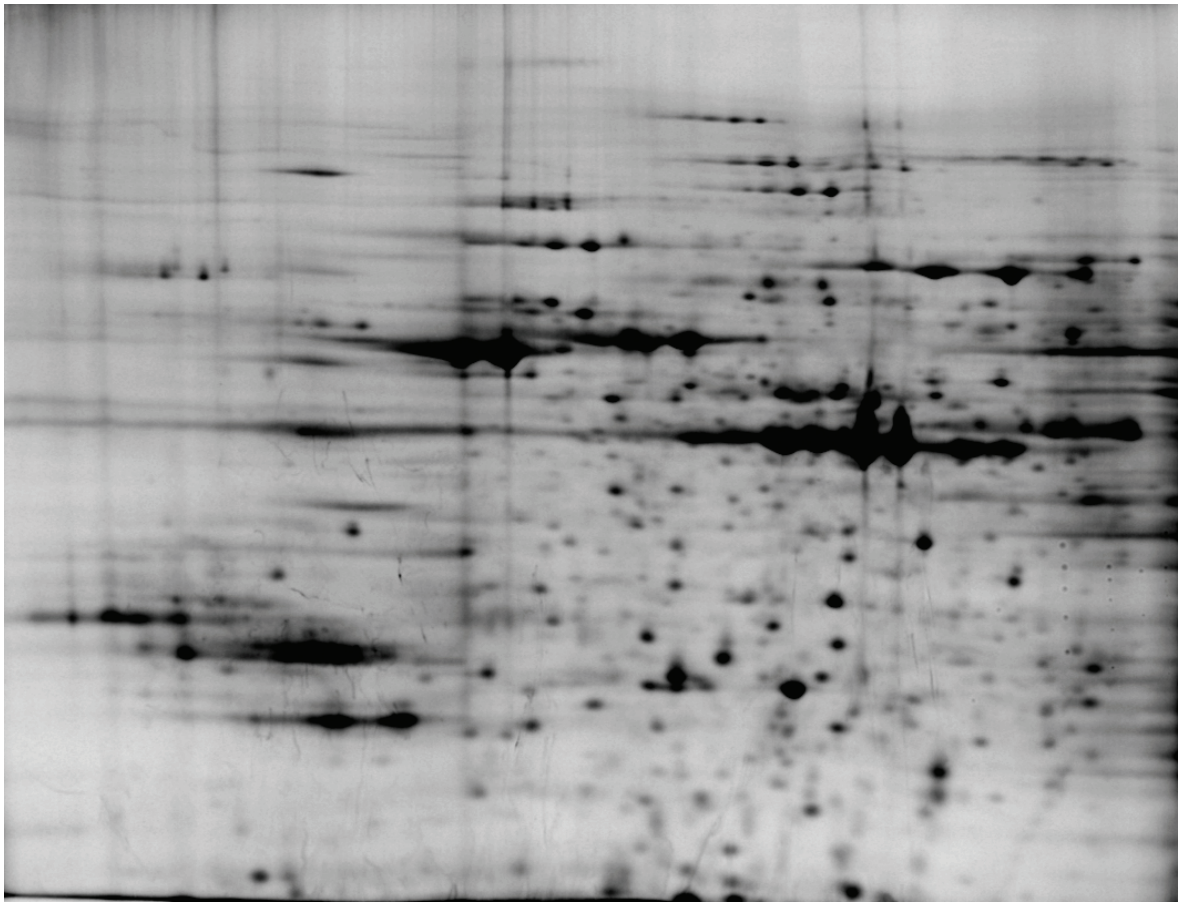

Figure A.1 – Two-dimensional gel electrophoresis of proteins from a soluble fraction isolated from cultured hippocampal neurons. Radiolabelled amino acids were incorporated into newly synthesized proteins for 12h and samples were processed as indicated in the caption of Fig. 4.4. Proteins were focused using IPG strips pH **4.5-5.5**. After the second dimension, gels were dried and placed in contact with a phosphor screen. Images were acquired using a STORM laser scanner.

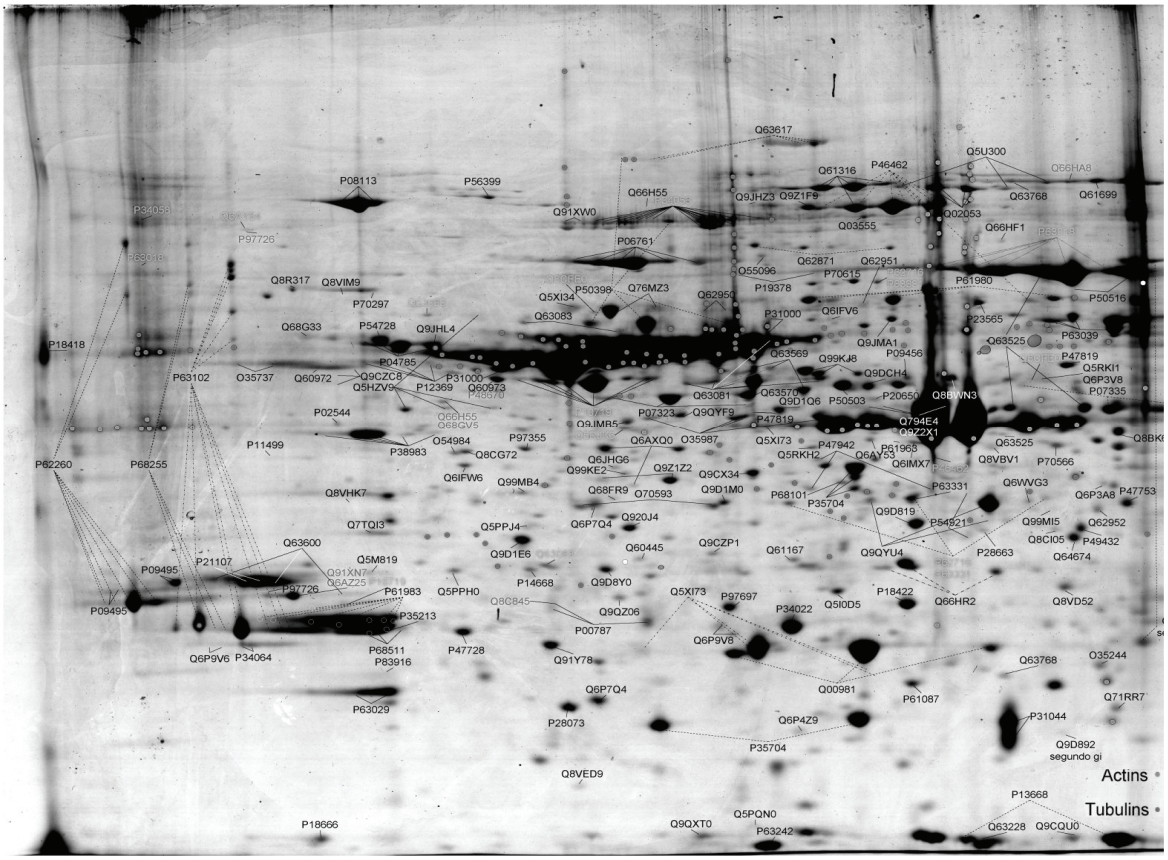

Figure A.2 - Gel mapping. Proteins from the soluble fraction were treated and identified as stated in Tab. III. Image shows a colloidal Coomassie stained gel of proteins focused in pH **4.5-5.5** IPG strips, and the accession numbers of identified spots.

A.2 – S126 fraction resolved using IPG strips pH 4.5-5.5

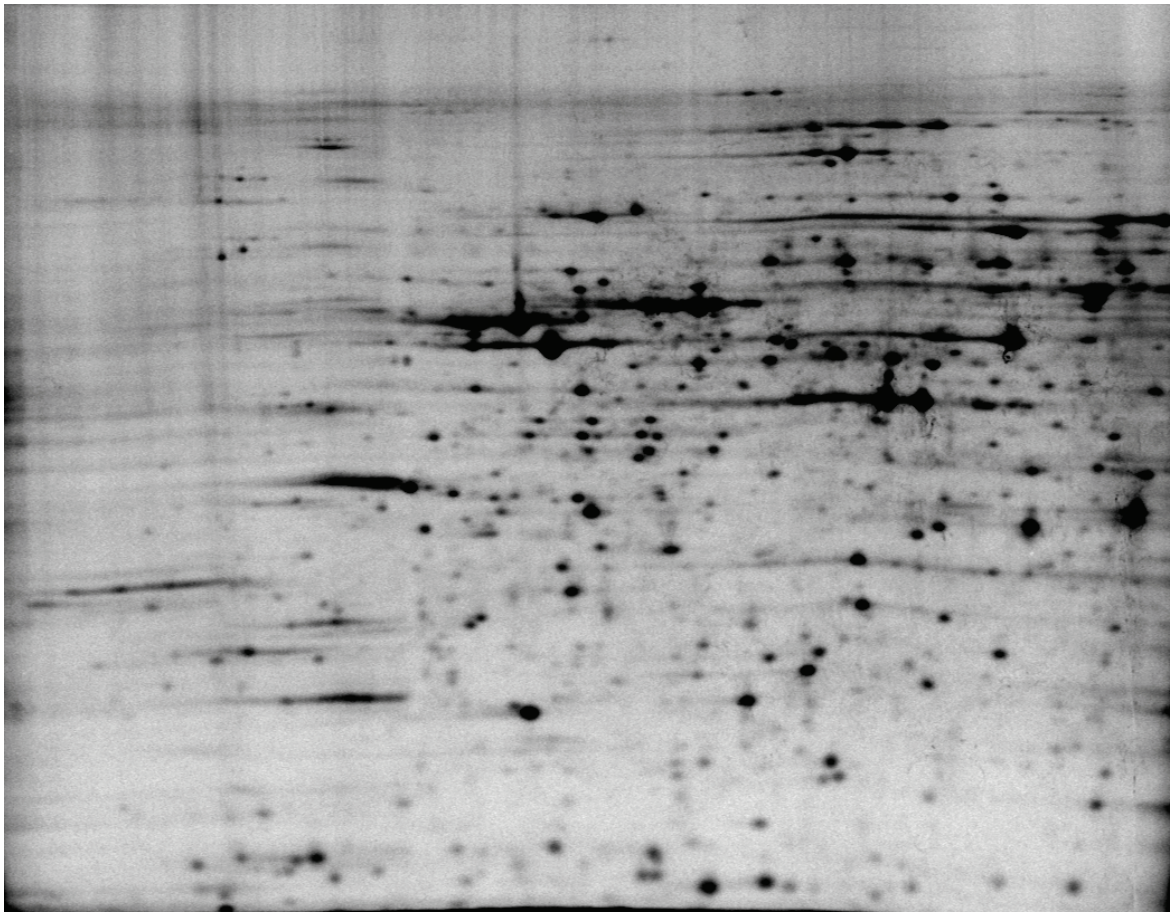

Figure A.3 – Two-dimensional gel electrophoresis of the S126 fraction. Radiolabelled amino acids were incorporated into newly synthesized proteins for 12h and samples were processed as indicated in the caption of Fig. 4.5. Proteins were focused using IPG strips pH **4.5-5.5**. After the second dimension, gels were dried and placed in contact with a phosphor screen. Images were acquired using a STORM laser scanner.

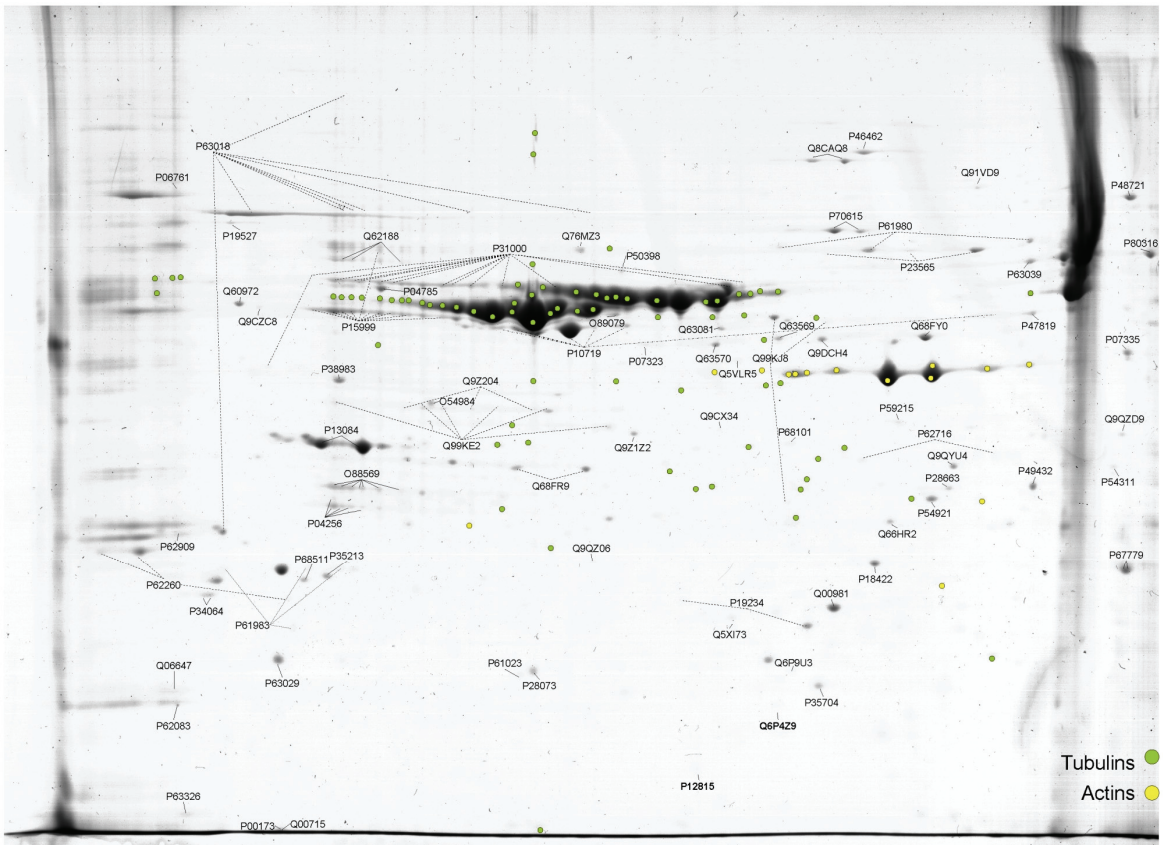

Figure A.4 - Gel mapping. Proteins of the S126 fraction were treated and identified as stated in Tab. III. Image shows a colloidal Coomassie stained gel of proteins focused in pH **4.5-5.5** IPG strips, and the accession number of identified spots.

A.2 – Soluble fraction resolved using IPG strips pH 5.0-6.0

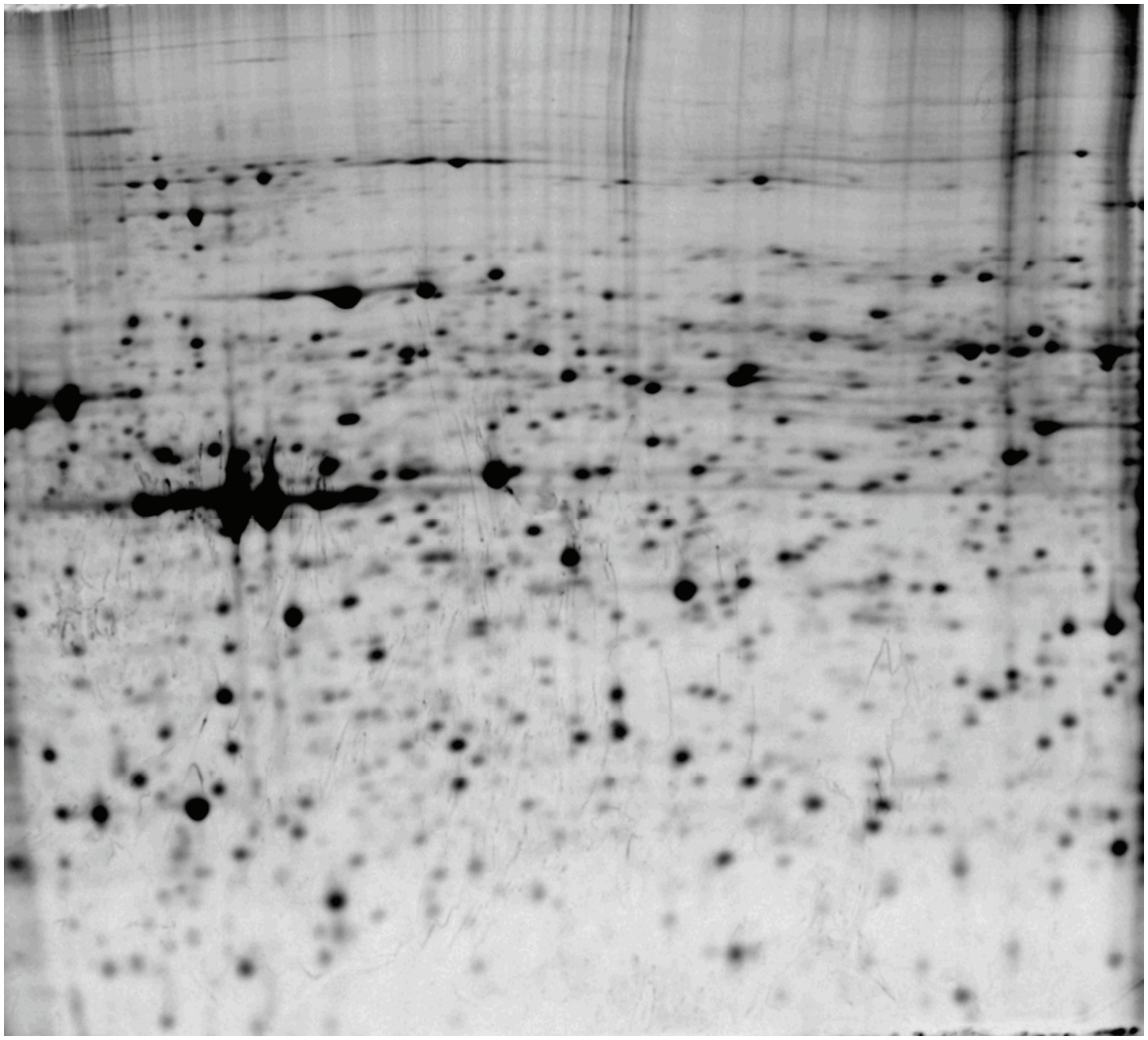

Figure A.5 – Two-dimensional gel electrophoresis of soluble proteins. Radiolabelled amino acids were incorporated into newly synthesized proteins for 12h and samples were processed as indicated in the caption of Fig. 4.4. Proteins were focused using IPG strips pH **5.0-6.0**. After second dimension, gels were dried and placed in contact with a phosphor screen. Images were acquired using a STORM laser scanner.

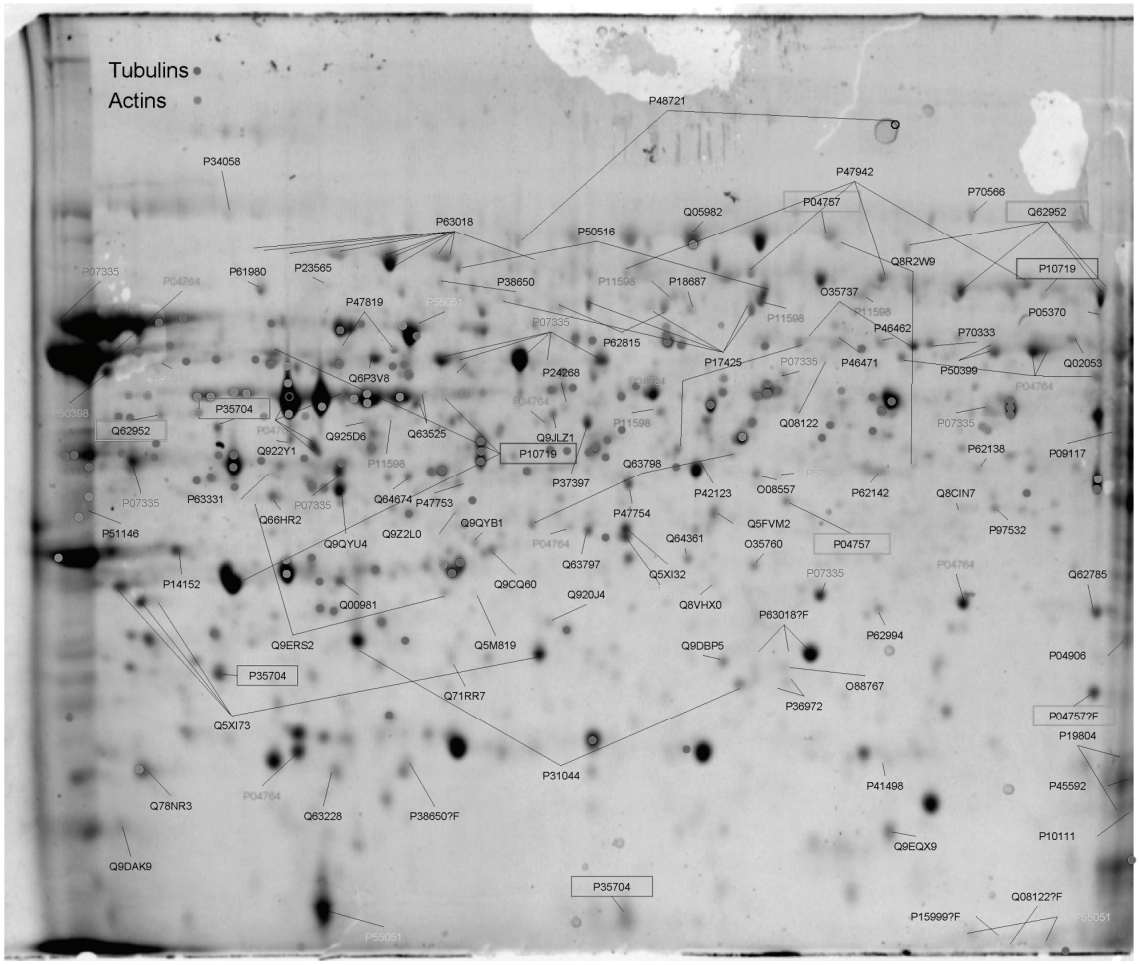

Figure A.6 - Gel mapping. Proteins of the soluble fraction were treated and identified as stated in Tab. III. Image shows colloidal Coomassie stained gel of proteins focused in pH **5.0-6.0** IPG strips with accession number of identified spots.

A.3 – S126 fraction resolved using IPG strips pH 5.0-6.0

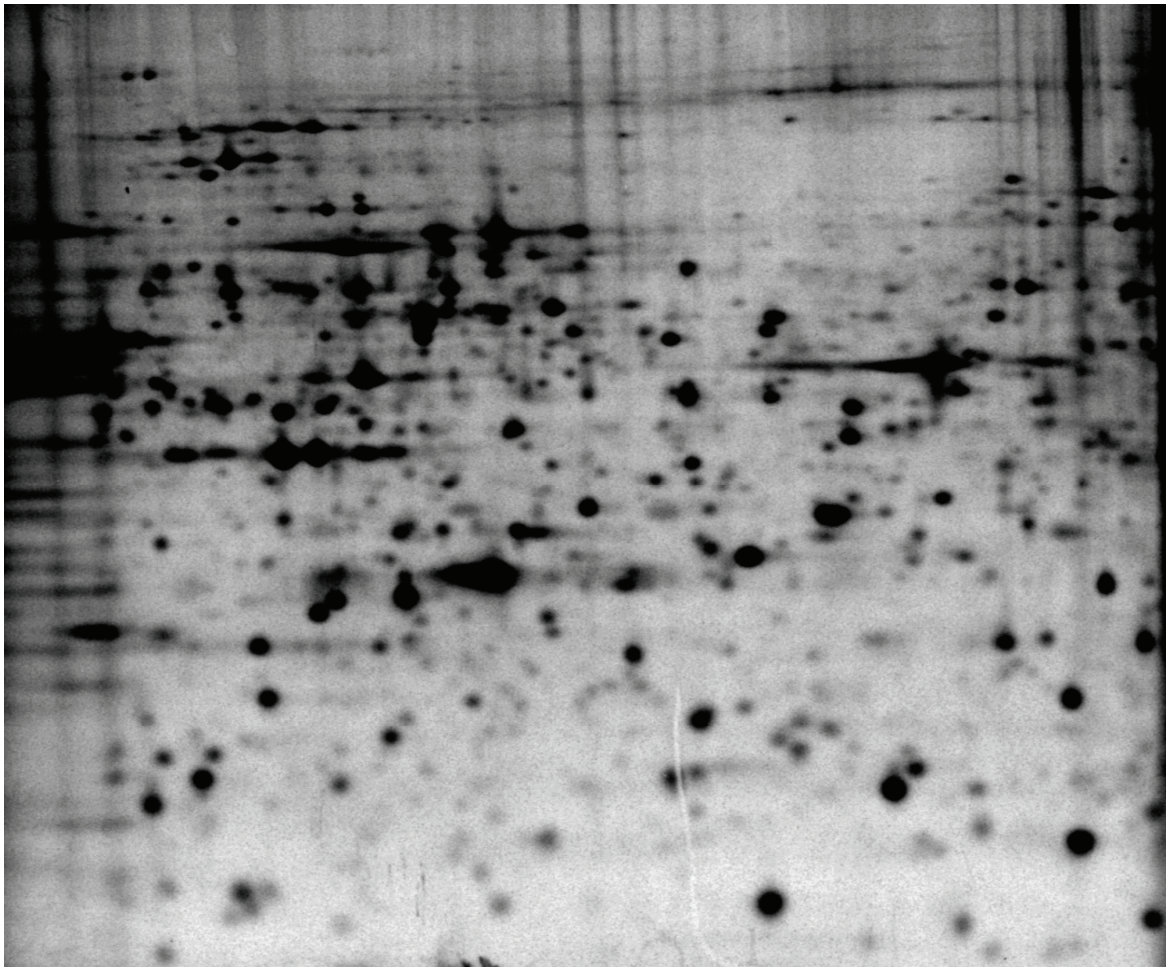

Figure A.7 – Two-dimensional gel electrophoresis of the S126 fraction. Radiolabelled amino acids were incorporated into newly synthesized proteins for 12h and samples were processed as indicated in the caption of Fig. 4.5. Proteins were focused using IPG strips pH **5.0-6.0**. After second dimension, gels were dried and placed in contact with a phosphor screen. Images were acquired using a STORM laser scanner.

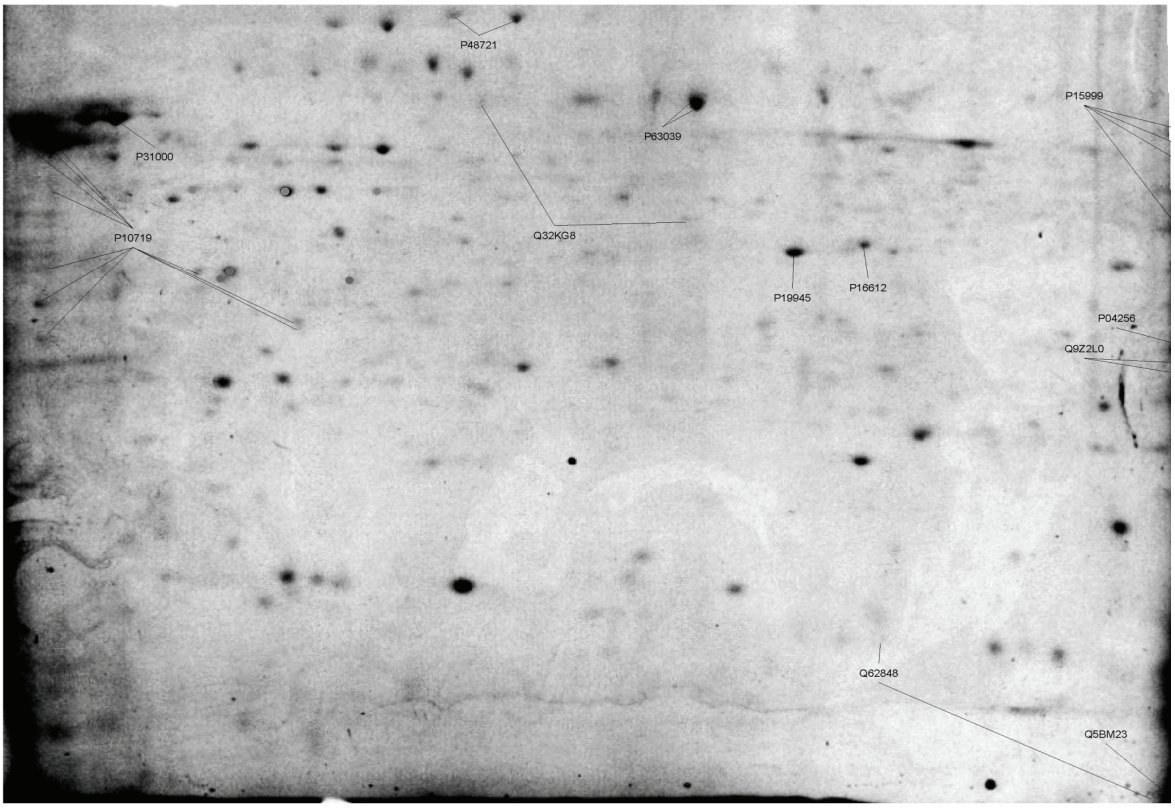

Figure A.8 - Gel mapping. Proteins of the S126 fraction were treated and identified as stated in Tab. III. Image shows colloidal Coomassie stained gel of proteins focused in pH **5.0-6.0** IPG strips with accession number of identified spots.

A.4 – S126 fraction resolved using IPG strips pH 5.5-6.7

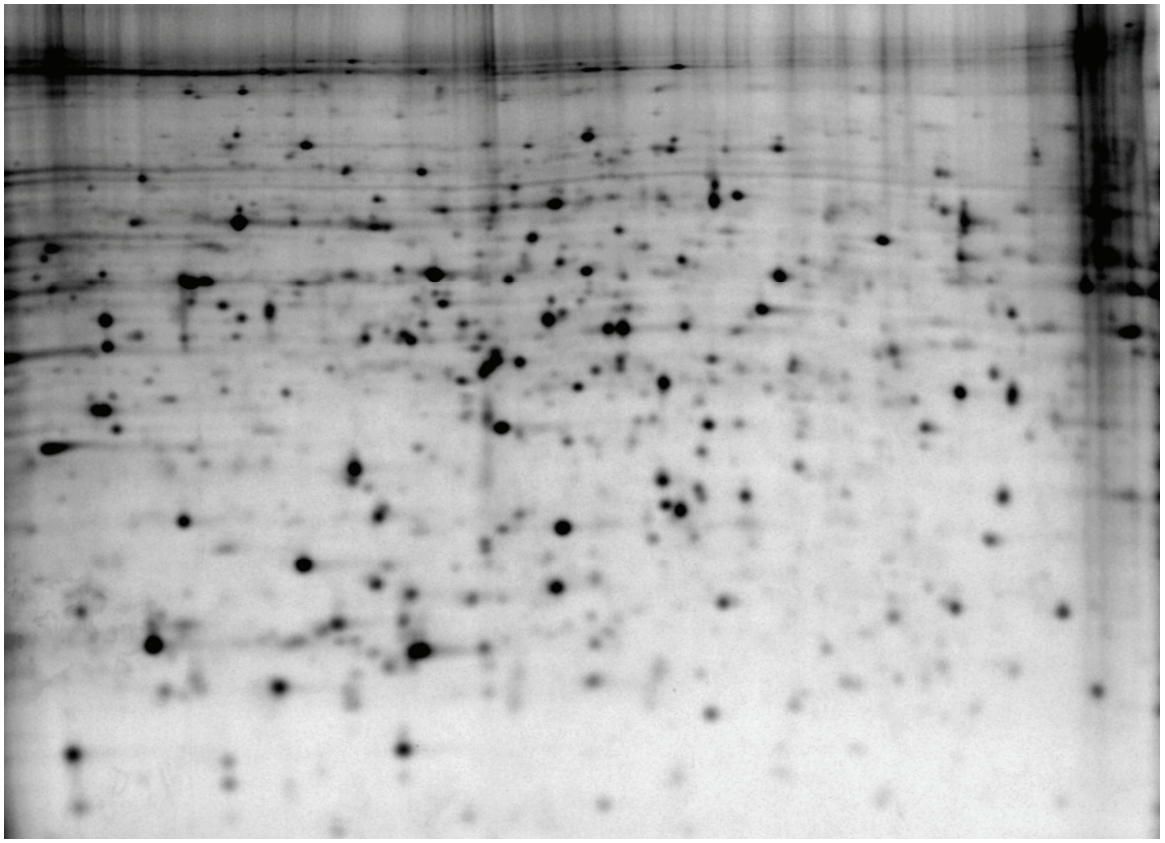

Figure A.9 – Two-dimensional gel electrophoresis of the S126 fraction. Radiolabelled amino acids were incorporated into newly synthesized proteins for 12h and samples were processed as indicated in the caption of Fig. 4.5. Proteins were focused using IPG strips pH **5.5-6.7**. After the second dimension, gels were dried and placed in contact with a phosphor screen. Images were acquired using a STORM laser scanner.

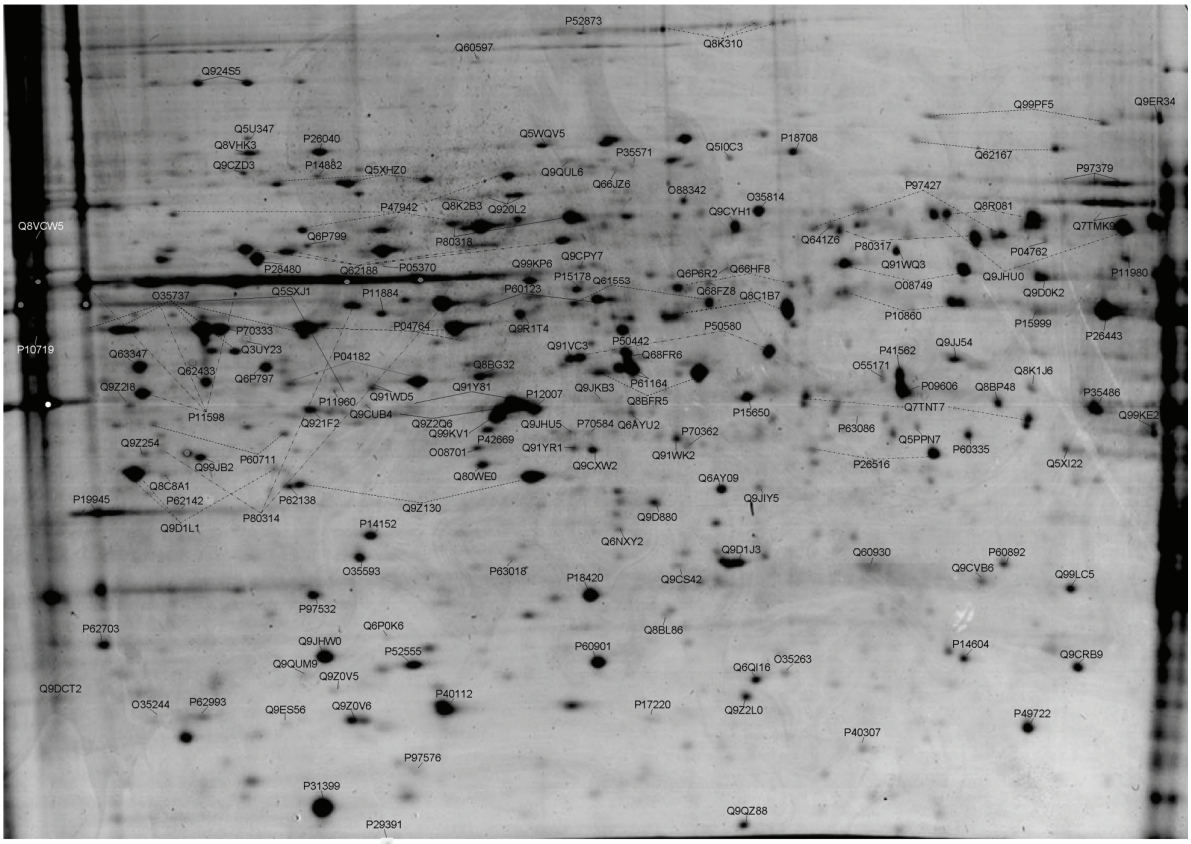

Figure A.10 - Gel mapping. Proteins of the S126 fraction were treated and identified as stated in Tab. III. Image shows colloidal Coomassie stained gel of proteins focused in pH **5.5-6.7** IPG strips with accession number of identified spots.

A.5 – Soluble fraction resolved using IPG strips pH 6.0-9.0

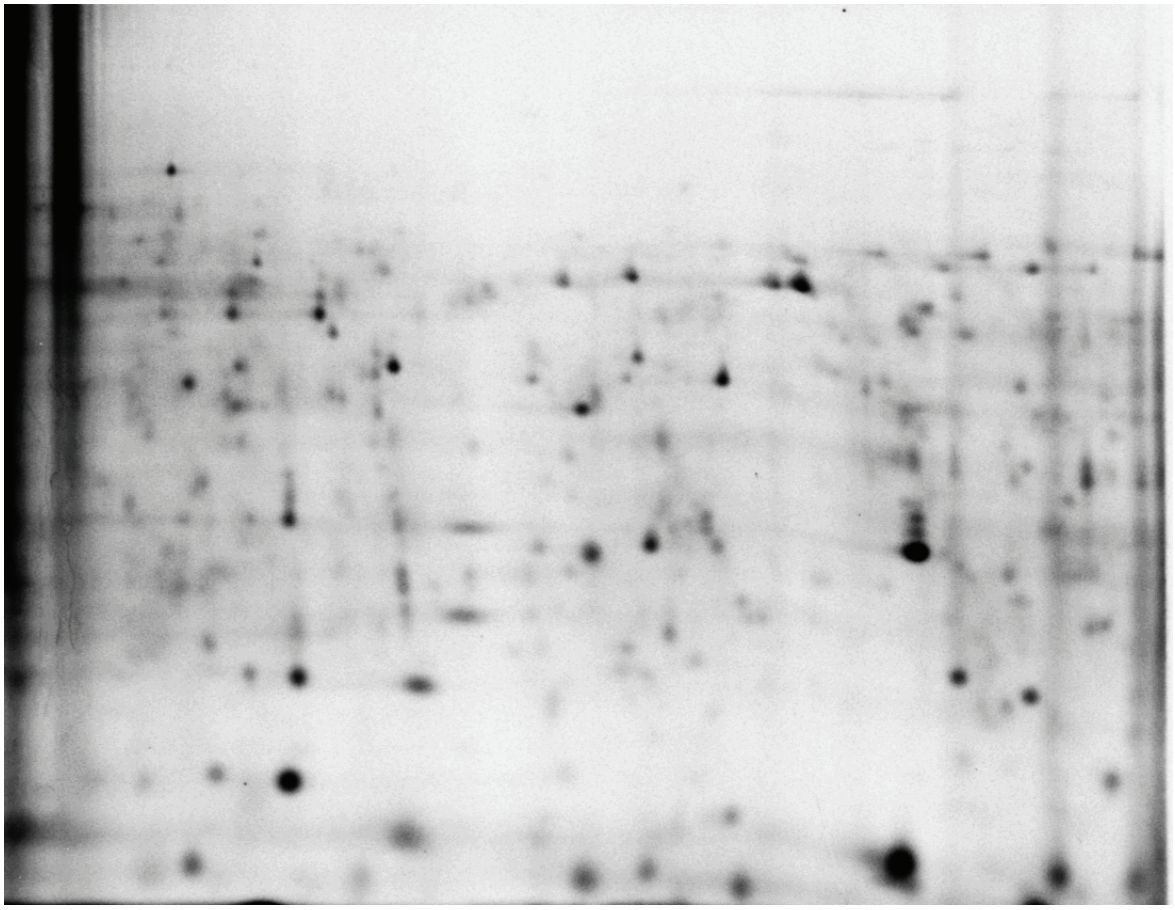

Figure A.11 – Two-dimensional gel electrophoresis of soluble proteins. Radiolabelled amino acids were incorporated into newly synthesized proteins for 12h and samples were processed as indicated in the caption of Fig. 4.4. Proteins were focused using IPG strips pH **6.0-9.0**. After second dimension, gels were dried and placed in contact with a phosphor screen. Images were acquired using a STORM laser scanner.

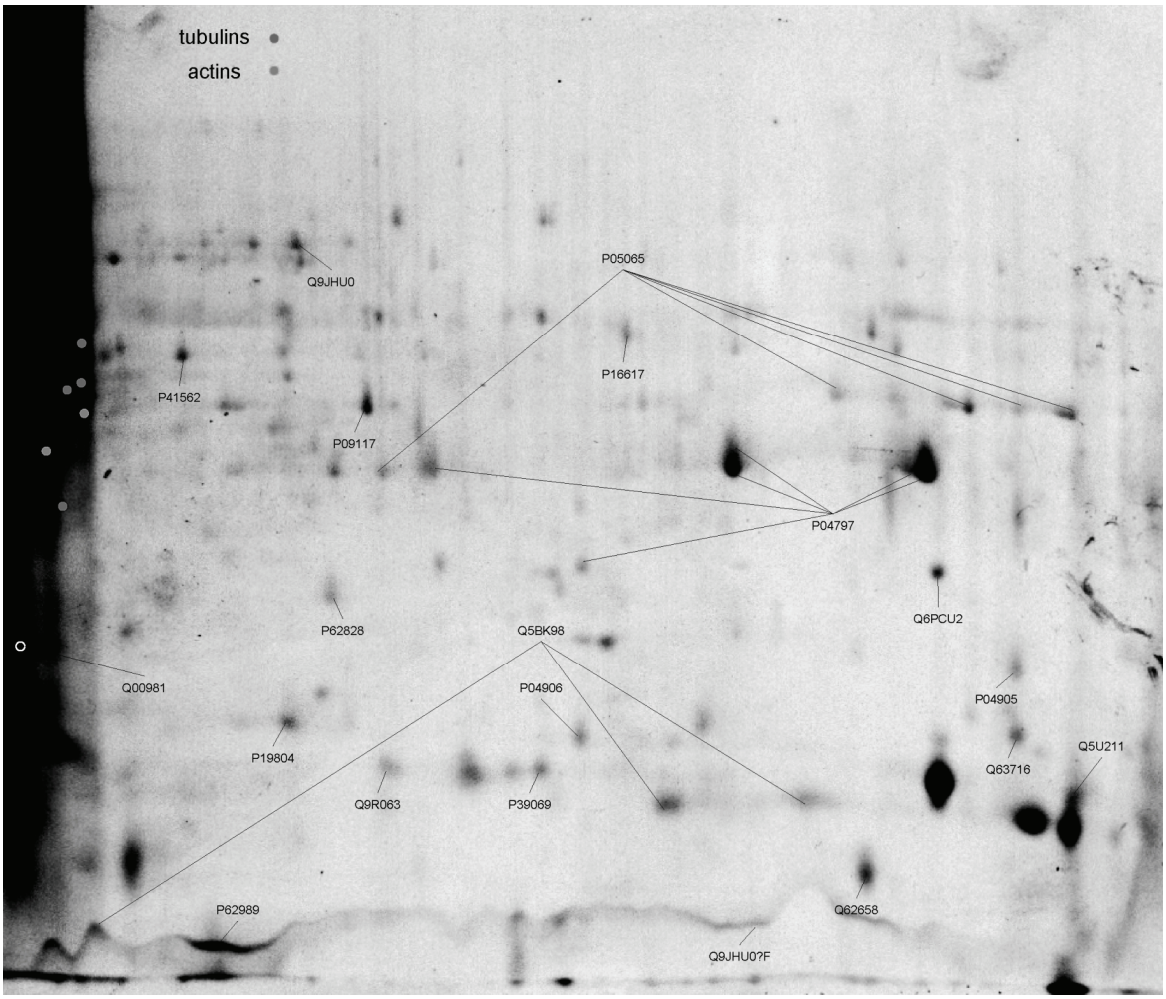

Figure A.12 - Gel mapping. Proteins of the soluble fraction were treated and identified as stated in Tab. III. Image shows colloidal Coomassie stained gel of proteins focused in pH **6.0-9.0** IPG strips with accession number of identified spots.

A.6 – S126 fraction resolved using IPG strips pH 6.0-9.0

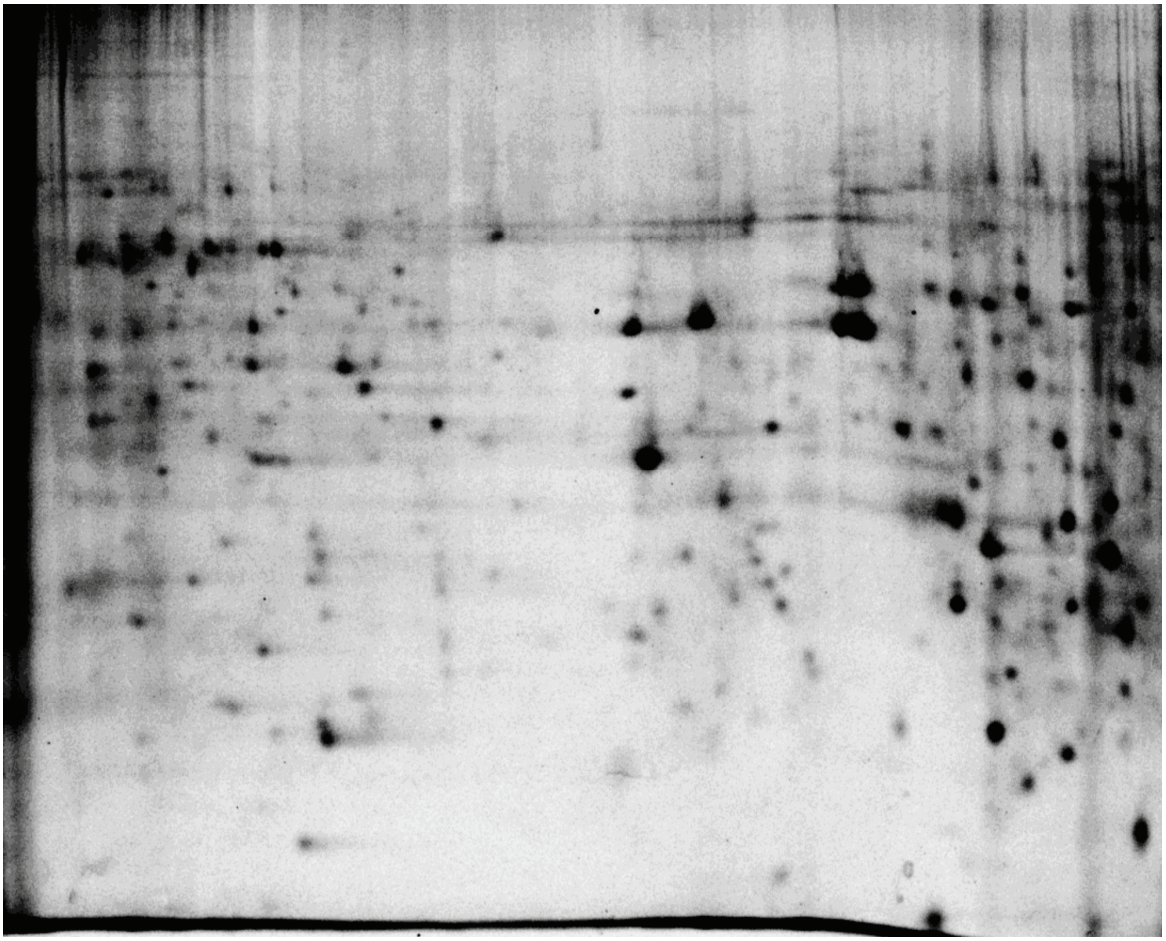

Figure A.13 – Two-dimensional gel electrophoresis of the S126 fraction. Radiolabelled amino acids were incorporated into newly synthesized proteins for 12h and samples were processed as indicated in the caption of Fig. 4.5. Proteins were focused using IPG strips pH **6.0-9.0**. After second dimension, gels were dried and placed in contact with a phosphor screen. Images were acquired using a STORM laser scanner.

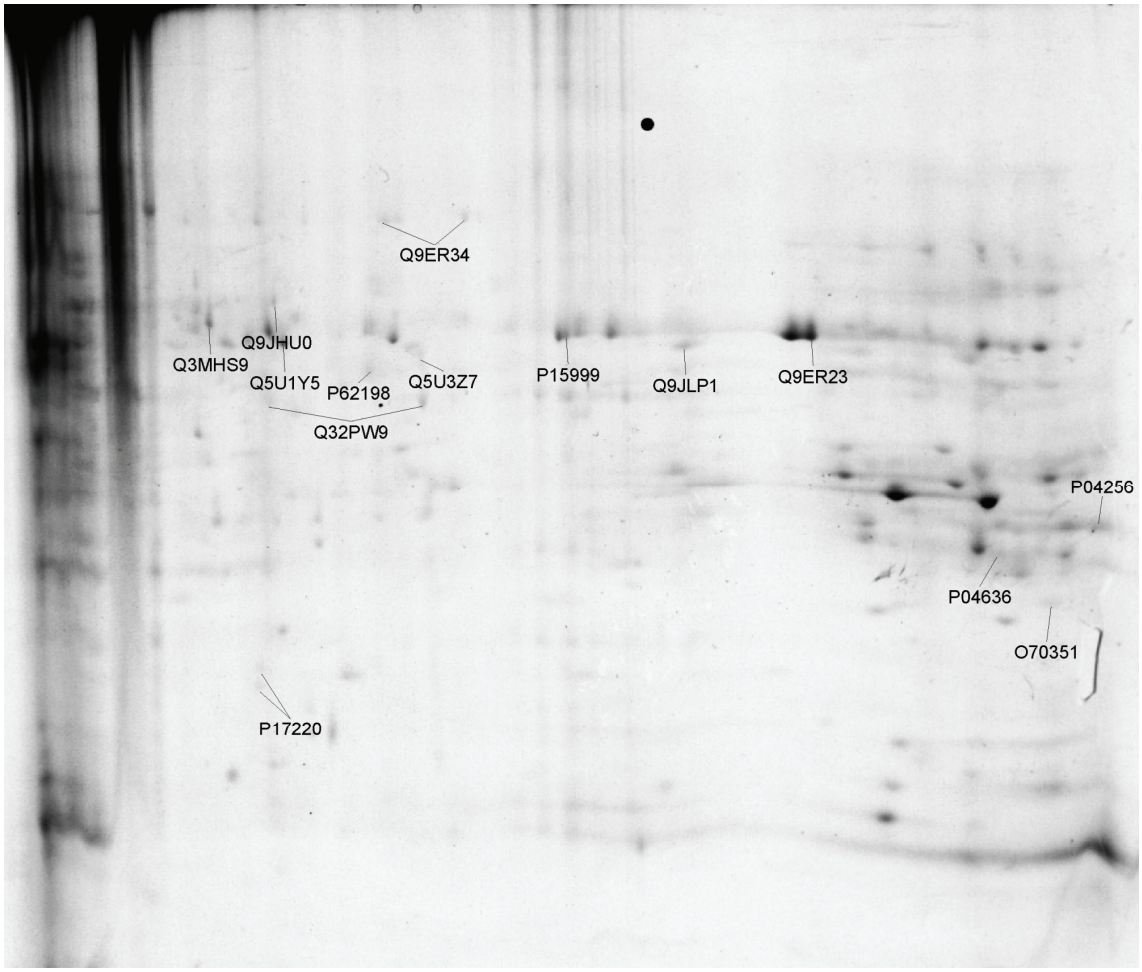

Figure A.14 - Gel mapping. Proteins of the S126 fraction were treated and identified as stated in Tab. III. Image shows colloidal Coomassie stained gel of proteins focused in pH **6.0-9.0** IPG strips with accession number of identified spots.

Chapter 6

References

Adachi, N., Kohara, K., and Tsumoto, T. 2005. Difference in trafficking of brain-derived neurotrophic factor between axons and dendrites of cortical neurons, revealed by live-cell imaging. *BMC Neurosci*. 6:42.

Aebersold, R., and Mann, M. 2003. Mass spectrometry-based proteomics. *Nature*. 422:198-207.

Alderson, R.F., Curtis, R., Alterman, A.L., Lindsay, R.M., and DiStefano, P.S. 2000. Truncated TrkB mediates the endocytosis and release of BDNF and neurotrophin-4/5 by rat astrocytes and schwann cells in vitro. *Brain Res*. 871:210-22.

Alfarano, C., Andrade, C.E., Anthony, K., Bahroos, N., Bajec, M., et al. 2005. The Biomolecular Interaction Network Database and related tools 2005 update. *Nucl. Acids Res.* 33:D418-424.

Almeida, R.D., Manadas, B.J., Melo, C.V., Gomes, J.R., Mendes, C.S., et al. 2005. Neuroprotection by BDNF against glutamate-induced apoptotic cell death is mediated by ERK and PI3-kinase pathways. *Cell Death Differ*. 12:1329-43. **Neuroprotection confered by BDNF against glutamate toxicity in primary hippocampal cultures**

Althaus, H.H., and Richter-Landsberg, C. 2000. Glial cells as targets and producers of neurotrophins. *Int Rev Cytol*. 197:203-77.

Althoff, R.R., Faraone, S.V., Rettew, D.C., Morley, C.P., and Hudziak, J.J. 2005. Family, twin, adoption, and molecular genetic studies of juvenile bipolar disorder. *Bipolar Disord*. 7:598-609. **Review on some aspects of juveline bipolar disorder**

Andersen, J.S., Lam, Y.W., Leung, A.K., Ong, S.E., Lyon, C.E., et al. 2005. Nucleolar proteome dynamics. *Nature*. 433:77-83.

Andersen, J.S., and Mann, M. 2000. Functional genomics by mass spectrometry. *FEBS Lett*. 480:25-31.

Anderson, D.H. 2006. Role of lipids in the MAPK signaling pathway. *Prog Lipid Res*. 45:102-19.

Bader, G.D., Betel, D., and Hogue, C.W.V. 2003. BIND: the Biomolecular Interaction Network Database. *Nucl. Acids Res.* 31:248-250.

Bai, F., Liu, S., and Witzmann, F.A. 2005. A "de-streaking" method for two-dimensional electrophoresis using the reducing agent tris(2-carboxyethyl)-phosphine hydrochloride and alkylating agent vinylpyridine. *Proteomics*. 5:2043-7.

Baker, M.A., Witherdin, R., Hetherington, L., Cunningham-Smith, K., and Aitken, R.J. 2005. Identification of post-translational modifications that occur during sperm maturation using difference in two-dimensional gel electrophoresis. *Proteomics*. 5:1003-12.

Barker, P.A. 2004. $p75^{NTR}$ is positively promiscuous: novel partners and new insights. *Neuron*. 42:529-33.

Barnidge, D.R., Tschumper, R.C., Jelinek, D.F., Muddiman, D.C., and Kay, N.E. 2005. Protein expression profiling of CLL B cells using replicate off-line strong cation exchange chromatography and LC-MS/MS. *J Chromatogr B Analyt Technol Biomed Life Sci*. 819:33-9.

Bartoletti, A., Cancedda, L., Reid, S.W., Tessarollo, L., Porciatti, V., et al. 2002. Heterozygous knock-out mice for brain-derived neurotrophic factor show a pathway-specific impairment of long-term potentiation but normal critical period for monocular deprivation. *J Neurosci*. 22:10072-7.

Bellacosa, A., Testa, J.R., Staal, S.P., and Tsichlis, P.N. 1991. A retroviral oncogene, akt, encoding a serine-threonine kinase containing an SH2-like region. *Science*. 254:274-7.

Biffo, S., Offenhauser, N., Carter, B.D., and Barde, Y.A. 1995. Selective binding and internalisation by truncated receptors restrict the availability of BDNF during development. *Development*. 121:2461-70.

Bilderback, T.R., Gazula, V.R., and Dobrowsky, R.T. 2001. Phosphoinositide 3-kinase regulates crosstalk between Trk A tyrosine kinase and $p75^{NTR}$-dependent sphingolipid signaling pathways. *J Neurochem*. 76:1540-51.

Binder, D.K., Croll, S.D., Gall, C.M., and Scharfman, H.E. 2001. BDNF and epilepsy: too much of a good thing? *Trends Neurosci*. 24:47-53. **Review on the role of BDNF in Epilepsy**

Binder, D.K., and Scharfman, H.E. 2004. Brain-derived neurotrophic factor. *Growth Factors*. 22:123-31.

Biosystems, A. 2004. QSTAR XL LC/MS/TOF system - Hardware Guide.

Blagoev, B., Kratchmarova, I., Ong, S.E., Nielsen, M., Foster, L.J., et al. 2003. A proteomics strategy to elucidate functional protein-protein interactions applied to EGF signaling. *Nat Biotechnol*. 21:315-8.

Bliss, T.V., and Collingridge, G.L. 1993. A synaptic model of memory: long-term potentiation in the hippocampus. *Nature*. 361:31-9.

Boeckmann, B., Blatter, M.C., Famiglietti, L., Hinz, U., Lane, L., et al. 2005. Protein variety and functional diversity: Swiss-Prot annotation in its biological context. *C R Biol*. 328:882-99.

Bonni, A., Brunet, A., West, A.E., Datta, S.R., Takasu, M.A., et al. 1999. Cell survival promoted by the Ras-MAPK signaling pathway by transcription-dependent and -independent mechanisms. *Science*. 286:1358-62.

Borrell-Pages, M., Zala, D., Humbert, S., and Saudou, F. 2006. Huntington's disease: from huntingtin function and dysfunction to therapeutic strategies. *Cell Mol Life Sci*. 63:2642-60.

Bos, J.L. 1989. ras oncogenes in human cancer: a review. *Cancer Res*. 49:4682-9.

Bramham, C.R., and Messaoudi, E. 2005. BDNF function in adult synaptic plasticity: the synaptic consolidation hypothesis. *Prog Neurobiol*. 76:99-125.

Brann, A.B., Tcherpakov, M., Williams, I.M., Futerman, A.H., and Fainzilber, M. 2002. Nerve growth factor-induced p75-mediated death of cultured hippocampal neurons is age-dependent and transduced through ceramide generated by neutral sphingomyelinase. *J Biol Chem*. 277:9812-8.

Brewer, G.J., Torricelli, J.R., Evege, E.K., and Price, P.J. 1993. Optimized survival of hippocampal neurons in B27-supplemented Neurobasal, a new serum-free medium combination. *J Neurosci Res*. 35:567-76. **Hippocampal cultures procedure with B27 supplement**

Brigadski, T., Hartmann, M., and Lessmann, V. 2005. Differential vesicular targeting and time course of synaptic secretion of the mammalian neurotrophins. *J Neurosci*. 25:7601-14.

Busold, C.H., Winter, S., Hauser, N., Bauer, A., Dippon, J., et al. 2005. Integration of GO annotations in Correspondence Analysis: facilitating the interpretation of microarray data. *Bioinformatics*.

21:2424-2429.

Caldwell, R.L., and Caprioli, R.M. 2005. Tissue profiling by mass spectrometry: a review of methodology and applications. *Mol Cell Proteomics*. 4:394-401.

Campostrini, N., Areces, L.B., Rappsilber, J., Pietrogrande, M.C., Dondi, F., et al. 2005. Spot overlapping in two-dimensional maps: a serious problem ignored for much too long. *Proteomics*. 5:2385-95.

Candiano, G., Bruschi, M., Musante, L., Santucci, L., Ghiggeri, G.M., et al. 2004. Blue silver: a very sensitive colloidal Coomassie G-250 staining for proteome analysis. *Electrophoresis*. 25:1327-33. **Protocol for home made colloidal Coomassie**

Caraglia, M., Budillon, A., Vitale, G., Lupoli, G., Tagliaferri, P., et al. 2000. Modulation of molecular mechanisms involved in protein synthesis machinery as a new tool for the control of cell proliferation. *Eur J Biochem*. 267:3919-36.

Carr, S., Aebersold, R., Baldwin, M., Burlingame, A., Clauser, K., et al. 2004. The need for guidelines in publication of peptide and protein identification data: Working Group on Publication Guidelines for Peptide and Protein Identification Data. *Mol Cell Proteomics*. 3:531-3.

Carter, C.J. 2007. Multiple genes and factors associated with bipolar disorder converge on growth factor and stress activated kinase pathways controlling translation initiation: Implications for oligodendrocyte viability. *Neurochem Int*. 50:461-90.

Cavanaugh, J.E., Ham, J., Hetman, M., Poser, S., Yan, C., et al. 2001. Differential regulation of mitogen-activated protein kinases ERK1/2 and ERK5 by neurotrophins, neuronal activity, and cAMP in neurons. *J Neurosci*. 21:434-43.

Celis, J.E., and Gromov, P. 1999. 2D protein electrophoresis: can it be perfected? *Curr Opin Biotechnol*. 10:16-21.

Challapalli, K.K., Zabel, C., Schuchhardt, J., Kaindl, A.M., Klose, J., et al. 2004. High reproducibility of large-gel two-dimensional electrophoresis. *Electrophoresis*. 25:3040-7.

Chan, J.R., Watkins, T.A., Cosgaya, J.M., Zhang, C., Chen, L., et al. 2004. NGF controls axonal receptivity to myelination by Schwann cells or oligodendrocytes. *Neuron*. 43:183-91.

Chan, L.L., Lo, S.C., and Hodgkiss, I.J. 2002. Proteomic study of a model causative agent of harmful red tide, Prorocentrum triestinum I: Optimization of sample preparation methodologies for analyzing with two-dimensional electrophoresis. *Proteomics*. 2:1169-86. **Cell disruption with sonication and use of TCA/Acetone precipitation**

Chan, T.O., Rittenhouse, S.E., and Tsichlis, P.N. 1999. AKT/PKB and other D3 phosphoinositide-regulated kinases: kinase activation by phosphoinositide-dependent phosphorylation. *Annu Rev Biochem*. 68:965-1014.

Chao, M.V. 2003. Neurotrophins and their receptors: a convergence point for many signalling pathways. *Nat Rev Neurosci*. 4:299-309.

Chemale, G., van Rossum, A.J., Jefferies, J.R., Barrett, J., Brophy, P.M., et al. 2003. Proteomic analysis of the larval stage of the parasite Echinococcus granulosus: causative agent of cystic hydatid disease. *Proteomics*. 3:1633-6. **Cell disruption with sonication and TCA and acetone cleaning of protein samples**

Chen, P., Li, X., Sun, Y., Liu, Z., Cao, R., et al. 2006. Proteomic analysis of rat hippocampal plasma membrane: characterization of potential neuronal-specific plasma membrane proteins. *J Neurochem*. 98:1126-40.

Chen, R., Kim, O., Yang, J., Sato, K., Eisenmann, K.M., et al. 2001. Regulation of Akt/PKB activation by tyrosine phosphorylation. *J Biol Chem*. 276:31858-62.

Chen, Z.Y., Ieraci, A., Teng, H., Dall, H., Meng, C.X., et al. 2005. Sortilin controls intracellular sorting of brain-derived neurotrophic factor to the regulated secretory pathway. *J Neurosci*. 25:6156-66.

Chen, Z.Y., Patel, P.D., Sant, G., Meng, C.X., Teng, K.K., et al. 2004. Variant brain-derived neurotrophic factor (BDNF) (Met_{66}) alters the intracellular trafficking and activity-dependent secretion of wild-type BDNF in neurosecretory cells and cortical neurons. *J Neurosci*. 24:4401-11.

Church, S. 2004. Advances in two-dimensional gel matching technology. *Biochem Soc Trans*. 32:511-6.

Churchward, M.A., Butt, R.H., Lang, J.C., Hsu, K.K., and Coorssen, J.R. 2005. Enhanced detergent extraction for analysis of membrane proteomes by two-dimensional gel electrophoresis. *Proteome Sci*. 3:5.

Condorelli, D.F., Dell'Albani, P., Mudo, G., Timmusk, T., and Belluardo, N. 1994. Expression of neurotrophins and their receptors in primary astroglial cultures: induction by cyclic AMP-elevating agents. *J Neurochem*. 63:509-16.

Copani, A., Bruno, V.M., Barresi, V., Battaglia, G., Condorelli, D.F., et al. 1995. Activation of metabotropic glutamate receptors prevents neuronal apoptosis in culture. *J Neurochem*. 64:101-8.

Cottrell, J.S. 1994. Protein identification by peptide mass fingerprinting. *Pept Res*. 7:115-24.

Craddock, N., O'Donovan, M.C., and Owen, M.J. 2005. The genetics of schizophrenia and bipolar disorder: dissecting psychosis. *J Med Genet*. 42:193-204.

Davies, A.M. 1994. The role of neurotrophins in the developing nervous system. *J Neurobiol*. 25:1334-48.

DeFreitas, M.F., McQuillen, P.S., and Shatz, C.J. 2001. A novel $p75^{NTR}$ signaling pathway promotes survival, not death, of immunopurified neocortical subplate neurons. *J Neurosci*. 21:5121-9.

del Toro, D., Canals, J.M., Gines, S., Kojima, M., Egea, G., et al. 2006. Mutant huntingtin impairs the post-Golgi trafficking of brain-derived neurotrophic factor but not its Val66Met polymorphism. *J Neurosci*. 26:12748-57.

Desmet, C.J., and Peeper, D.S. 2006. The neurotrophic receptor TrkB: a drug target in anti-cancer therapy? *Cell Mol Life Sci*. 63:755-9. **Short vision on the tumour formation and metastasis associated with TrkB**

Dobrowsky, R.T., Jenkins, G.M., and Hannun, Y.A. 1995. Neurotrophins induce sphingomyelin hydrolysis. Modulation by co-expression of $p75^{NTR}$ with Trk receptors. *J Biol Chem*. 270:22135-42.

Du, J., Feng, L., Yang, F., and Lu, B. 2000. Activity- and Ca^{2+}-dependent modulation of surface

expression of brain-derived neurotrophic factor receptors in hippocampal neurons. *J Cell Biol*. 150:1423-34.

Du, J., Feng, L., Zaitsev, E., Je, H.S., Liu, X.W., et al. 2003. Regulation of TrkB receptor tyrosine kinase and its internalization by neuronal activity and Ca^{2+} influx. *J Cell Biol*. 163:385-95.

Easton, J.B., Royer, A.R., and Middlemas, D.S. 2006. The protein tyrosine phosphatase, Shp2, is required for the complete activation of the RAS/MAPK pathway by brain-derived neurotrophic factor. *J Neurochem*. 97:834-45.

Farhadi, H.F., Mowla, S.J., Petrecca, K., Morris, S.J., Seidah, N.G., et al. 2000. Neurotrophin-3 sorts to the constitutive secretory pathway of hippocampal neurons and is diverted to the regulated secretory pathway by coexpression with brain-derived neurotrophic factor. *J Neurosci*. 20:4059-68.

Fawcett, J.P., Aloyz, R., McLean, J.H., Pareek, S., Miller, F.D., et al. 1997. Detection of brain-derived neurotrophic factor in a vesicular fraction of brain synaptosomes. *J Biol Chem*. 272:8837-40.

Fernandez-Espejo, E. 2004. Pathogenesis of Parkinson's disease: prospects of neuroprotective and restorative therapies. *Mol Neurobiol*. 29:15-30.

Fountoulakis, M. 2004. Application of proteomics technologies in the investigation of the brain. *Mass Spectrom Rev*. 23:231-58.

Fountoulakis, M., Tsangaris, G.T., Maris, A., and Lubec, G. 2005. The rat brain hippocampus proteome. *J Chromatogr B Analyt Technol Biomed Life Sci*. 819:115-29.

Friedman, W.J., and Greene, L.A. 1999. Neurotrophin signaling via Trks and p75. *Exp Cell Res*. 253:131-42. **Review on neurotrophins**

Fumagalli, F., Racagni, G., and Riva, M.A. 2006a. The expanding role of BDNF: a therapeutic target for Alzheimer's disease? *Pharmacogenomics J*. 6:8-15. **Review on the BDNF implication on Alzheimer's disease**

Fumagalli, F., Racagni, G., and Riva, M.A. 2006b. Shedding light into the role of BDNF in the pharmacotherapy of Parkinson's disease. *Pharmacogenomics J*. 6:95-104. **Review on the BDNF implication on Parkinson's disease**

Garavelli, J.S. 2004. The RESID Database of Protein Modifications as a resource and annotation tool. *Proteomics*. 4:1527-33.

Gardiol, A., Racca, C., and Triller, A. 1999. Dendritic and postsynaptic protein synthetic machinery. *J Neurosci*. 19:168-79.

Gasteiger, E., Gattiker, A., Hoogland, C., Ivanyi, I., Appel, R.D., et al. 2003. ExPASy: The proteomics server for in-depth protein knowledge and analysis. *Nucleic Acids Res*. 31:3784-8.

Gene Ontology Consortium. 2004. The Gene Ontology (GO) database and informatics resource. *Nucl. Acids Res.* 32:D258-261.

Gerstner, A., Csapo, Z., Sasvari-Szekely, M., and Guttman, A. 2000. Ultrathin-layer sodium dodecyl sulfate gel electrophoresis of proteins: effects of gel composition and temperature on the separation of sodium dodecyl sulfate-protein complexes. *Electrophoresis*. 21:834-40.

Gines, S., Bosch, M., Marco, S., Gavalda, N., Diaz-Hernandez, M., et al. 2006. Reduced expression of

the TrkB receptor in Huntington's disease mouse models and in human brain. *Eur J Neurosci*. 23:649-58.

Gorg, A., Obermaier, C., Boguth, G., Harder, A., Scheibe, B., et al. 2000. The current state of two-dimensional electrophoresis with immobilized pH gradients. *Electrophoresis*. 21:1037-53.

Haapasalo, A., Sipola, I., Larsson, K., Akerman, K.E., Stoilov, P., et al. 2002. Regulation of TrkB surface expression by brain-derived neurotrophic factor and truncated TrkB isoforms. *J Biol Chem*. 277:43160-7.

Hajszan, T., and MacLusky, N. 2006. Neurologic links between epilepsy and depression in women: is hippocampal neuroplasticity the key? *Neurology*. 66:S13. **Review on the link between BDNF and depression in women**

Hall, D., Dhilla, A., Charalambous, A., Gogos, J.A., and Karayiorgou, M. 2003. Sequence variants of the brain-derived neurotrophic factor (BDNF) gene are strongly associated with obsessive-compulsive disorder. *Am J Hum Genet*. 73:370-6.

Han, J., and Schey, K.L. 2004. Proteolysis and mass spectrometric analysis of an integral membrane: aquaporin 0. *J Proteome Res*. 3:807-12.

Hanash, S. 2003. Disease proteomics. *Nature*. 422:226-32.

Hanash, S.M., Strahler, J.R., Neel, J.V., Hailat, N., Melhem, R., et al. 1991. Highly resolving two-dimensional gels for protein sequencing. *Proc Natl Acad Sci U S A*. 88:5709-13.

Harrington, A.W., Leiner, B., Blechschmitt, C., Arevalo, J.C., Lee, R., et al. 2004. Secreted proNGF is a pathophysiological death-inducing ligand after adult CNS injury. *Proc Natl Acad Sci U S A*. 101:6226-30.

Hayden, E.P., and Nurnberger, J.I., Jr. 2006. Molecular genetics of bipolar disorder. *Genes Brain Behav*. 5:85-95. **Review on bipolar disorder**

Henningsen, R., Gale, B.L., Straub, K.M., and DeNagel, D.C. 2002. Application of zwitterionic detergents to the solubilization of integral membrane proteins for two-dimensional gel electrophoresis and mass spectrometry. *Proteomics*. 2:1479-88. **Zwitterionic detergents and membrane proteins**

Herbert, B. 1999. Advances in protein solubilisation for two-dimensional electrophoresis. *Electrophoresis*. 20:660-3.

Herbert, B., Galvani, M., Hamdan, M., Olivieri, E., MacCarthy, J., et al. 2001. Reduction and alkylation of proteins in preparation of two-dimensional map analysis: why, when, and how? *Electrophoresis*. 22:2046-57.

Hetman, M., Kanning, K., Cavanaugh, J.E., and Xia, Z. 1999. Neuroprotection by brain-derived neurotrophic factor is mediated by extracellular signal-regulated kinase and phosphatidylinositol 3-kinase. *J Biol Chem*. 274:22569-80.

Hilfiker, S., Pieribone, V.A., Czernik, A.J., Kao, H.T., Augustine, G.J., et al. 1999. Synapsins as regulators of neurotransmitter release. *Philos Trans R Soc Lond B Biol Sci*. 354:269-79.

Huang, E.J., and Reichardt, L.F. 2003. Trk receptors: roles in neuronal signal transduction. *Annu Rev Biochem*. 72:609-42. **Review on the Trk structure and signaling mechanisms**

Huber, L.A. 2003. Opinion: Is proteomics heading in the wrong direction? *Nat Rev Mol Cell Biol*. 4:74-80.

Huh, K.H., and Wenthold, R.J. 1999. Turnover analysis of glutamate receptors identifies a rapidly degraded pool of the N-methyl-D-aspartate receptor subunit, NR1, in cultured cerebellar granule cells. *J Biol Chem*. 274:151-7.

Husson, I., Rangon, C.M., Lelievre, V., Bemelmans, A.P., Sachs, P., et al. 2005. BDNF-induced white matter neuroprotection and stage-dependent neuronal survival following a neonatal excitotoxic challenge. *Cereb Cortex*. 15:250-61.

Iida, N., Namikawa, K., Kiyama, H., Ueno, H., Nakamura, S., et al. 2001. Requirement of Ras for the activation of mitogen-activated protein kinase by calcium influx, cAMP, and neurotrophin in hippocampal neurons. *J Neurosci*. 21:6459-66.

Inamura, N., Hoshino, S., Uchiumi, T., Nawa, H., and Takei, N. 2003. Cellular and subcellular distributions of translation initiation, elongation and release factors in rat hippocampus. *Brain Res Mol Brain Res*. 111:165-74.

Ito, H., Nakajima, A., Nomoto, H., and Furukawa, S. 2003. Neurotrophins facilitate neuronal differentiation of cultured neural stem cells via induction of mRNA expression of basic helix-loop-helix transcription factors Mash1 and Math1. *J Neurosci Res*. 71:648-58.

Ivanova, T., and Beyer, C. 2001. Pre- and postnatal expression of brain-derived neurotrophic factor mRNA/protein and tyrosine protein kinase receptor B mRNA in the mouse hippocampus. *Neurosci Lett*. 307:21-4.

Jiang, L., He, L., and Fountoulakis, M. 2004. Comparison of protein precipitation methods for sample preparation prior to proteomic analysis. *J Chromatogr A*. 1023:317-20.

Job, C., and Eberwine, J. 2001. Localization and translation of mRNA in dendrites and axons. *Nat Rev Neurosci*. 2:889-98.

Jovanovic, J.N., Czernik, A.J., Fienberg, A.A., Greengard, P., and Sihra, T.S. 2000. Synapsins as mediators of BDNF-enhanced neurotransmitter release. *Nat Neurosci*. 3:323-9.

Julka, S., and Regnier, F. 2004. Quantification in proteomics through stable isotope coding: a review. *J Proteome Res*. 3:350-63.

Kaczmarek, K., Walczak, B., de Jong, S., and Vandeginste, B.G. 2004. Preprocessing of two-dimensional gel electrophoresis images. *Proteomics*. 4:2377-89.

Katz, D.M. 2005. Regulation of respiratory neuron development by neurotrophic and transcriptional signaling mechanisms. *Respir Physiol Neurobiol*. 149:99-109. **Review on the neurotrophin action on respiratory neuron development**

Kesslak, J.P., So, V., Choi, J., Cotman, C.W., and Gomez-Pinilla, F. 1998. Learning upregulates brain-derived neurotrophic factor messenger ribonucleic acid: a mechanism to facilitate encoding and circuit maintenance? *Behav Neurosci*. 112:1012-9.

Khawaja, X., Xu, J., Liang, J.J., and Barrett, J.E. 2004. Proteomic analysis of protein changes developing in rat hippocampus after chronic antidepressant treatment: Implications for depressive disorders and future therapies. *J Neurosci Res*. 75:451-60.

Kingsbury, T.J., Murray, P.D., Bambrick, L.L., and Krueger, B.K. 2003. Ca^{2+}-dependent regulation of

TrkB expression in neurons. *J Biol Chem*. 278:40744-8.

Kobori, N., Clifton, G.L., and Dash, P. 2002. Altered expression of novel genes in the cerebral cortex following experimental brain injury. *Brain Res Mol Brain Res*. 104:148-58.

Kohara, K., Kitamura, A., Morishima, M., and Tsumoto, T. 2001. Activity-dependent transfer of brain-derived neurotrophic factor to postsynaptic neurons. *Science*. 291:2419-23.

Kokaia, Z., Nawa, H., Uchino, H., Elmer, E., Kokaia, M., et al. 1996. Regional brain-derived neurotrophic factor mRNA and protein levels following transient forebrain ischemia in the rat. *Brain Res Mol Brain Res*. 38:139-44.

Korsching, S. 1993. The neurotrophic factor concept: a reexamination. *J Neurosci*. 13:2739-48.

Korte, M., Carroll, P., Wolf, E., Brem, G., Thoenen, H., et al. 1995. Hippocampal long-term potentiation is impaired in mice lacking brain-derived neurotrophic factor. *Proc Natl Acad Sci U S A*. 92:8856-60.

Lamanda, A., Zahn, A., Roder, D., and Langen, H. 2004. Improved Ruthenium II tris (bathophenantroline disulfonate) staining and destaining protocol for a better signal-to-background ratio and improved baseline resolution. *Proteomics*. 4:599-608.

Larsson, E., Nanobashvili, A., Kokaia, Z., and Lindvall, O. 1999. Evidence for neuroprotective effects of endogenous brain-derived neurotrophic factor after global forebrain ischemia in rats. *J Cereb Blood Flow Metab*. 19:1220-8.

Lee, F.S., and Chao, M.V. 2001. Activation of Trk neurotrophin receptors in the absence of neurotrophins. *Proc Natl Acad Sci U S A*. 98:3555-60.

Lee, J., Duan, W., and Mattson, M.P. 2002. Evidence that brain-derived neurotrophic factor is required for basal neurogenesis and mediates, in part, the enhancement of neurogenesis by dietary restriction in the hippocampus of adult mice. *J Neurochem*. 82:1367-75.

Lee, R., Kermani, P., Teng, K.K., and Hempstead, B.L. 2001. Regulation of cell survival by secreted proneurotrophins. *Science*. 294:1945-8.

Levi-Montalcini, R. 1987. The nerve growth factor 35 years later. *Science*. 237:1154-62.

Levine, E.S., Dreyfus, C.F., Black, I.B., and Plummer, M.R. 1995. Brain-derived neurotrophic factor rapidly enhances synaptic transmission in hippocampal neurons via postsynaptic tyrosine kinase receptors. *Proc Natl Acad Sci U S A*. 92:8074-7.

Liebel, U., Kindler, B., and Pepperkok, R. 2005. Bioinformatic "Harvester": a search engine for genome-wide human, mouse, and rat protein resources. *Methods Enzymol*. 404:19-26.

Lou, H., Kim, S.K., Zaitsev, E., Snell, C.R., Lu, B., et al. 2005. Sorting and activity-dependent secretion of BDNF require interaction of a specific motif with the sorting receptor carboxypeptidase e. *Neuron*. 45:245-55.

Lu, B. 2003. BDNF and activity-dependent synaptic modulation. *Learn Mem*. 10:86-98.

Lu, B., Pang, P.T., and Woo, N.H. 2005. The yin and yang of neurotrophin action. *Nat Rev Neurosci*. 6:603-14. **Review on the neurotrophins action**

MacPhee, I.J., and Barker, P.A. 1997. Brain-derived neurotrophic factor binding to the p75

neurotrophin receptor reduces TrkA signaling while increasing serine phosphorylation in the TrkA intracellular domain. *J Biol Chem*. 272:23547-51.

Manadas, B.J., Vougas, K., Fountoulakis, M., and Duarte, C.B. 2006. Sample sonication after trichloroacetic acid precipitation increases protein recovery from cultured hippocampal neurons, and improves resolution and reproducibility in two-dimensional gel electrophoresis. *Electrophoresis*. 27:1825-31. **Increase in gel reproducibility after TCA precipitation**

McCarthy, J., Hopwood, F., Oxley, D., Laver, M., Castagna, A., et al. 2003. Carbamylation of proteins in 2-D electrophoresis--myth or reality? *J Proteome Res*. 2:239-42.

Mellstrom, B., Torres, B., Link, W.A., and Naranjo, J.R. 2004. The BDNF gene: exemplifying complexity in Ca^{2+}-dependent gene expression. *Crit Rev Neurobiol*. 16:43-9. **Review on the BDNF gene regulation mediated by calcium**

Merrick, B.A. 2003. The Human Proteome Organization (HUPO) and Environmental Health. *Environ Health Perspect*. 111:797-801.

Meyer-Franke, A., Wilkinson, G.A., Kruttgen, A., Hu, M., Munro, E., et al. 1998. Depolarization and cAMP elevation rapidly recruit TrkB to the plasma membrane of CNS neurons. *Neuron*. 21:681-93.

Meyer, H.E., Klose, J., and Hamacher, M. 2003. HBPP and the pursuit of standardisation. *Lancet Neurol*. 2:657-8.

Minichiello, L., Calella, A.M., Medina, D.L., Bonhoeffer, T., Klein, R., et al. 2002. Mechanism of TrkB-mediated hippocampal long-term potentiation. *Neuron*. 36:121-37.

Mizuno, M., Yamada, K., He, J., Nakajima, A., and Nabeshima, T. 2003. Involvement of BDNF receptor TrkB in spatial memory formation. *Learn Mem*. 10:108-15.

Molloy, M.P. 2000. Two-dimensional electrophoresis of membrane proteins using immobilized pH gradients. *Anal Biochem*. 280:1-10.

Morris, R.G. 2003. Long-term potentiation and memory. *Philos Trans R Soc Lond B Biol Sci*. 358:643-7.

Muller, G., Storz, P., Bourteele, S., Doppler, H., Pfizenmaier, K., et al. 1998. Regulation of Raf-1 kinase by TNF via its second messenger ceramide and cross-talk with mitogenic signalling. *Embo J*. 17:732-42.

Nagappan, G., and Lu, B. 2005. Activity-dependent modulation of the BDNF receptor TrkB: mechanisms and implications. *Trends Neurosci*. 28:464-71. **Review on the interplay between BDNF and activity**

Nakagawara, A., Azar, C.G., Scavarda, N.J., and Brodeur, G.M. 1994. Expression and function of Trk-B and BDNF in human neuroblastomas. *Mol Cell Biol*. 14:759-67.

Nakata, K., Ujike, H., Sakai, A., Uchida, N., Nomura, A., et al. 2003. Association study of the brain-derived neurotrophic factor (BDNF) gene with bipolar disorder. *Neurosci Lett*. 337:17-20.

Nandakumar, M.P., Shen, J., Raman, B., and Marten, M.R. 2003. Solubilization of trichloroacetic acid (TCA) precipitated microbial proteins via NaOH for two-dimensional electrophoresis. *J Proteome Res*. 2:89-93.

Nockher, W.A., and Renz, H. 2006. Neurotrophins in allergic diseases: from neuronal growth factors to intercellular signaling molecules. *J Allergy Clin Immunol*. 117:583-9. **Review on allergic diseases and neurotrophins expression levels**

Nosheny, R.L., Mocchetti, I., and Bachis, A. 2005. Brain-derived neurotrophic factor as a prototype neuroprotective factor against HIV-1-associated neuronal degeneration. *Neurotox Res*. 8:187-98.

Nykjaer, A., Willnow, T.E., and Petersen, C.M. 2005. $p75^{NTR}$--live or let die. *Curr Opin Neurobiol*. 15:49-57.

O'Connell, K.L., and Stults, J.T. 1997. Identification of mouse liver proteins on two-dimensional electrophoresis gels by matrix-assisted laser desorption/ionization mass spectrometry of in situ enzymatic digests. *Electrophoresis*. 18:349-59. **Optimized silver staining protocol**

O'Farrell, P.H. 1975. High resolution two-dimensional electrophoresis of proteins. *J Biol Chem*. 250:4007-21.

Oguri, T., Takahata, I., Katsuta, K., Nomura, E., Hidaka, M., et al. 2002. Proteome analysis of rat hippocampal neurons by multiple large gel two-dimensional electrophoresis. *Proteomics*. 2:666-72. **Large cybergel with 6677 spots**

Oppenheim, R.W. 1991. Cell death during development of the nervous system. *Annu Rev Neurosci*. 14:453-501.

Pang, P.T., Teng, H.K., Zaitsev, E., Woo, N.T., Sakata, K., et al. 2004. Cleavage of proBDNF by tPA/plasmin is essential for long-term hippocampal plasticity. *Science*. 306:487-91.

Pedersen, S.K., Harry, J.L., Sebastian, L., Baker, J., Traini, M.D., et al. 2003. Unseen proteome: mining below the tip of the iceberg to find low abundance and membrane proteins. *J Proteome Res*. 2:303-11.

Pennington, K., McGregor, E., Beasley, C.L., Everall, I., Cotter, D., et al. 2004. Optimization of the first dimension for separation by two-dimensional gel electrophoresis of basic proteins from human brain tissue. *Proteomics*. 4:27-30.

Petricoin, E.F., and Liotta, L.A. 2003. Clinical applications of proteomics. *J Nutr*. 133:2476S-2484S.

Pfister, K.K., Salata, M.W., Dillman, J.F., 3rd, Torre, E., and Lye, R.J. 1996. Identification and developmental regulation of a neuron-specific subunit of cytoplasmic dynein. *Mol Biol Cell*. 7:331-43.

Pollak, D.D., John, J., Hoeger, H., and Lubec, G. 2006. An integrated map of the murine hippocampal proteome based upon five mouse strains. *Electrophoresis*. 27:2787-98.

Poo, M.M. 2001. Neurotrophins as synaptic modulators. *Nat Rev Neurosci*. 2:24-32.

Popp, E., and Bottiger, B.W. 2006. Cerebral resuscitation: state of the art, experimental approaches and clinical perspectives. *Neurol Clin*. 24:73-87.

Prathikanti, S., and Weinberger, D.R. 2005. Psychiatric genetics--the new era: genetic research and some clinical implications. *Br Med Bull*. 73-74:107-22. **Review on some genetic aspects of neuropsychiatric illness**

Quach, T.T., Li, N., Richards, D.P., Zheng, J., Keller, B.O., et al. 2003. Development and applications

of in-gel CNBr/tryptic digestion combined with mass spectrometry for the analysis of membrane proteins. *J Proteome Res*. 2:543-52.

Rabilloud, T., Strub, J.M., Luche, S., van Dorsselaer, A., and Lunardi, J. 2001. A comparison between Sypro Ruby and ruthenium II tris (bathophenanthroline disulfonate) as fluorescent stains for protein detection in gels. *Proteomics*. 1:699-704. **Protocol for home made sypro ruby**

Rajagopal, R., Chen, Z.Y., Lee, F.S., and Chao, M.V. 2004. Transactivation of Trk neurotrophin receptors by G-protein-coupled receptor ligands occurs on intracellular membranes. *J Neurosci*. 24:6650-8.

Ravichandran, V., and Sriram, R.D. 2005. Toward data standards for proteomics. *Nat Biotechnol*. 23:373-6.

Reichardt, L.F. 2006. Neurotrophin-regulated signalling pathways. *Philos Trans R Soc Lond B Biol Sci*. 361:1545-64. **Review on neurotrophins**

Reiner, A., Albin, R.L., Anderson, K.D., D'Amato, C.J., Penney, J.B., et al. 1988. Differential loss of striatal projection neurons in Huntington disease. *Proc Natl Acad Sci U S A*. 85:5733-7.

Righetti, P.G., Castagna, A., Antonioli, P., and Boschetti, E. 2005. Prefractionation techniques in proteome analysis: the mining tools of the third millennium. *Electrophoresis*. 26:297-319. **Review on fractionation techniques**

Righetti, P.G., Castagna, A., Herbert, B., Reymond, F., and Rossier, J.S. 2003. Prefractionation techniques in proteome analysis. *Proteomics*. 3:1397-407.

Ring, R.H., Alder, J., Fennell, M., Kouranova, E., Black, I.B., et al. 2006. Transcriptional profiling of brain-derived-neurotrophic factor-induced neuronal plasticity: A novel role for nociceptin in hippocampal neurite outgrowth. *J Neurobiol*. 66:361-377.

Robinson, R.C., Radziejewski, C., Spraggon, G., Greenwald, J., Kostura, M.R., et al. 1999. The structures of the neurotrophin 4 homodimer and the brain-derived neurotrophic factor/neurotrophin 4 heterodimer reveal a common Trk-binding site. *Protein Sci*. 8:2589-97.

Rosenthal, A., Goeddel, D.V., Nguyen, T., Martin, E., Burton, L.E., et al. 1991. Primary structure and biological activity of human brain-derived neurotrophic factor. *Endocrinology*. 129:1289-94.

Roy, S., Plowman, S., Rotblat, B., Prior, I.A., Muncke, C., et al. 2005. Individual palmitoyl residues serve distinct roles in H-ras trafficking, microlocalization, and signaling. *Mol Cell Biol*. 25:6722-33.

Roymans, D., and Slegers, H. 2001. Phosphatidylinositol 3-kinases in tumor progression. *Eur J Biochem*. 268:487-98.

Ryu, J.K., Kim, J., Cho, S.J., Hatori, K., Nagai, A., et al. 2004. Proactive transplantation of human neural stem cells prevents degeneration of striatal neurons in a rat model of Huntington disease. *Neurobiol Dis*. 16:68-77.

Santi, S., Cappello, S., Riccio, M., Bergami, M., Aicardi, G., et al. 2006. Hippocampal neurons recycle BDNF for activity-dependent secretion and LTP maintenance. *Embo J*. 25:4372-80.

Santoni, V., Rabilloud, T., Doumas, P., Rouquie, D., Mansion, M., et al. 1999. Towards the recovery of hydrophobic proteins on two-dimensional electrophoresis gels. *Electrophoresis*. 20:705-11.

Savitski, M.M., Nielsen, M.L., and Zubarev, R.A. 2005. New Data Base-independent, Sequence Tag-based Scoring of Peptide MS/MS Data Validates Mowse Scores, Recovers Below Threshold Data, Singles Out Modified Peptides, and Assesses the Quality of MS/MS Techniques. *Mol Cell Proteomics*. 4:1180-8.

Schor, N.F. 2005. The p75 neurotrophin receptor in human development and disease. *Prog Neurobiol*. 77:201-14.

Schratt, G.M., Tuebing, F., Nigh, E.A., Kane, C.G., Sabatini, M.E., et al. 2006. A brain-specific microRNA regulates dendritic spine development. *Nature*. 439:283-9.

Schreck, R., and Rapp, U.R. 2006. Raf kinases: oncogenesis and drug discovery. *Int J Cancer*. 119:2261-71.

Seidah, N.G., Benjannet, S., Pareek, S., Chretien, M., and Murphy, R.A. 1996. Cellular processing of the neurotrophin precursors of NT3 and BDNF by the mammalian proprotein convertases. *FEBS Lett*. 379:247-50.

Shadforth, I.P., Dunkley, T.P., Lilley, K.S., and Bessant, C. 2005. i-Tracker: for quantitative proteomics using iTRAQ. *BMC Genomics*. 6:145.

Shetty, A.K., Rao, M.S., Hattiangady, B., Zaman, V., and Shetty, G.A. 2004. Hippocampal neurotrophin levels after injury: Relationship to the age of the hippocampus at the time of injury. *J Neurosci Res*. 78:520-32.

Shiina, N., Shinkura, K., and Tokunaga, M. 2005. A novel RNA-binding protein in neuronal RNA granules: regulatory machinery for local translation. *J Neurosci*. 25:4420-34.

Shmueli, O., Horn-Saban, S., Chalifa-Caspi, V., Shmoish, M., Ophir, R., et al. 2003. GeneNote: whole genome expression profiles in normal human tissues. *C R Biol*. 326:1067-72.

Sitek, B., Apostolov, O., Stuhler, K., Pfeiffer, K., Meyer, H.E., et al. 2005. Identification of dynamic proteome changes upon ligand-activation of Trk-receptors using two-dimensional fluorescence difference gel electrophoresis and mass spectrometry. *Mol Cell Proteomics*.

Skup, M., Dwornik, A., Macias, M., Sulejczak, D., Wiater, M., et al. 2002. Long-term locomotor training up-regulates $TrkB^{FL}$ receptor-like proteins, brain-derived neurotrophic factor, and neurotrophin 4 with different topographies of expression in oligodendroglia and neurons in the spinal cord. *Exp Neurol*. 176:289-307.

Snider, W.D. 1994. Functions of the neurotrophins during nervous system development: what the knockouts are teaching us. *Cell*. 77:627-38.

Sorkin, A., and Waters, C.M. 1993. Endocytosis of growth factor receptors. *Bioessays*. 15:375-82.

Stadelmann, C., Kerschensteiner, M., Misgeld, T., Bruck, W., Hohlfeld, R., et al. 2002. BDNF and gp145trkB in multiple sclerosis brain lesions: neuroprotective interactions between immune and neuronal cells? *Brain*. 125:75-85.

Stasyk, T., and Huber, L.A. 2004. Zooming in: fractionation strategies in proteomics. *Proteomics*. 4:3704-16. **Review on fractionation advantages**

Steen, H., Kuster, B., and Mann, M. 2001. Quadrupole time-of-flight versus triple-quadrupole mass spectrometry for the determination of phosphopeptides by precursor ion scanning. *J Mass Spectrom*. 36:782-90.

Steward, O., and Levy, W.B. 1982. Preferential localization of polyribosomes under the base of dendritic spines in granule cells of the dentate gyrus. *J Neurosci*. 2:284-91.

Steward, O., and Schuman, E.M. 2001. Protein synthesis at synaptic sites on dendrites. *Annu Rev Neurosci*. 24:299-325.

Sun, J., Yan, X., Xiao, H., Zhou, J., Chen, Y., et al. 2001. Restoration of Decreased N-Methyl-d-asparate Receptor Activity by Brain-Derived Neurotrophic Factor in the Cultured Hippocampal Neurons: Involvement of cAMP. *Arch Biochem Biophys*. 394:209-15.

Sun, Y.E., and Wu, H. 2006. The ups and downs of BDNF in Rett syndrome. *Neuron*. 49:321-3.

Syroid, D.E., Maycox, P.J., Soilu-Hanninen, M., Petratos, S., Bucci, T., et al. 2000. Induction of postnatal schwann cell death by the low-affinity neurotrophin receptor in vitro and after axotomy. *J Neurosci*. 20:5741-7.

Takei, N., Inamura, N., Kawamura, M., Namba, H., Hara, K., et al. 2004. Brain-derived neurotrophic factor induces mammalian target of rapamycin-dependent local activation of translation machinery and protein synthesis in neuronal dendrites. *J Neurosci*. 24:9760-9.

Takei, N., Kawamura, M., Hara, K., Yonezawa, K., and Nawa, H. 2001. Brain-derived neurotrophic factor enhances neuronal translation by activating multiple initiation processes: comparison with the effects of insulin. *J Biol Chem*. 276:42818-25.

Tardito, D., Perez, J., Tiraboschi, E., Musazzi, L., Racagni, G., et al. 2006. Signaling pathways regulating gene expression, neuroplasticity, and neurotrophic mechanisms in the action of antidepressants: a critical overview. *Pharmacol Rev*. 58:115-34. **Review on several drugs and antidepressant targets**

Tartaglia, N., Du, J., Tyler, W.J., Neale, E., Pozzo-Miller, L., et al. 2001. Protein synthesis-dependent and -independent regulation of hippocampal synapses by brain-derived neurotrophic factor. *J Biol Chem*. 276:37585-93.

Teng, K.K., and Hempstead, B.L. 2004. Neurotrophins and their receptors: signaling trios in complex biological systems. *Cell Mol Life Sci*. 61:35-48.

Timmusk, T., Lendahl, U., Funakoshi, H., Arenas, E., Persson, H., et al. 1995. Identification of brain-derived neurotrophic factor promoter regions mediating tissue-specific, axotomy-, and neuronal activity-induced expression in transgenic mice. *J Cell Biol*. 128:185-99.

Troy, C.M., Friedman, J.E., and Friedman, W.J. 2002. Mechanisms of p75-mediated death of hippocampal neurons. Role of caspases. *J Biol Chem*. 277:34295-302.

Unwin, R.D., Evans, C.A., and Whetton, A.D. 2006. Relative quantification in proteomics: new approaches for biochemistry. *Trends Biochem Sci*. 31:473-84.

Vaynman, S., and Gomez-Pinilla, F. 2005. License to run: exercise impacts functional plasticity in the intact and injured central nervous system by using neurotrophins. *Neurorehabil Neural Repair*. 19:283-95. **Review on the BDNF gene regulation mediated by exercise**

Vojtek, A.B., and Der, C.J. 1998. Increasing complexity of the Ras signaling pathway. *J Biol Chem*. 273:19925-8. **Minireview on RAS signaling**

Volosin, M., Song, W., Almeida, R.D., Kaplan, D.R., Hempstead, B.L., et al. 2006. Interaction of survival and death signaling in basal forebrain neurons: roles of neurotrophins and

proneurotrophins. *J Neurosci*. 26:7756-66.

Wang, H., and Hanash, S. 2005. Intact-protein based sample preparation strategies for proteome analysis in combination with mass spectrometry. *Mass Spectrom Rev*. 24:413-26.

Washburn, M.P., Wolters, D., and Yates, J.R., 3rd. 2001. Large-scale analysis of the yeast proteome by multidimensional protein identification technology. *Nat Biotechnol*. 19:242-7.

Westbrook, J.A., Yan, J.X., Wait, R., Welson, S.Y., and Dunn, M.J. 2001. Zooming-in on the proteome: very narrow-range immobilised pH gradients reveal more protein species and isoforms. *Electrophoresis*. 22:2865-71.

Whitlock, J.R., Heynen, A.J., Shuler, M.G., and Bear, M.F. 2006. Learning induces long-term potentiation in the hippocampus. *Science*. 313:1093-7.

Wooley, J.C. 2002. The grand challenge: facing up to proteomics. *Trends Biotechnol*. 20:316-7.

Wu, D. 2005. Neuroprotection in experimental stroke with targeted neurotrophins. *NeuroRx*. 2:120-8. **Short review on the usage of neurotrophins and modified neurotrophins as neuroprotective agents**

Yamashita, T., and Tohyama, M. 2003. The p75 receptor acts as a displacement factor that releases Rho from Rho-GDI. *Nat Neurosci*. 6:461-7.

Yamauchi, J., Chan, J.R., Miyamoto, Y., Tsujimoto, G., and Shooter, E.M. 2005. The neurotrophin-3 receptor TrkC directly phosphorylates and activates the nucleotide exchange factor Dbs to enhance Schwann cell migration. *Proc Natl Acad Sci U S A*. 102:5198-203.

Yang, J.W., Czech, T., and Lubec, G. 2004. Proteomic profiling of human hippocampus. *Electrophoresis*. 25:1169-74.

Yano, M., Okano, H.J., and Okano, H. 2005. Involvement of Hu and heterogeneous nuclear ribonucleoprotein K in neuronal differentiation through p21 mRNA post-transcriptional regulation. *J Biol Chem*. 280:12690-9.

Yin, Y., Edelman, G.M., and Vanderklish, P.W. 2002. The brain-derived neurotrophic factor enhances synthesis of Arc in synaptoneurosomes. *Proc Natl Acad Sci U S A*. 99:2368-73.

Ying, S.W., Futter, M., Rosenblum, K., Webber, M.J., Hunt, S.P., et al. 2002. Brain-derived neurotrophic factor induces long-term potentiation in intact adult hippocampus: requirement for ERK activation coupled to CREB and upregulation of Arc synthesis. *J Neurosci*. 22:1532-40.

Yuen, E.C., and Mobley, W.C. 1999. Early BDNF, NT-3, and NT-4 signaling events. *Exp Neurol*. 159:297-308.

Zeeberg, B.R., Feng, W., Wang, G., Wang, M.D., Fojo, A.T., et al. 2003. GoMiner: a resource for biological interpretation of genomic and proteomic data. *Genome Biol*. 4:R28.

Zeeberg, B.R., Qin, H., Narasimhan, S., Sunshine, M., Cao, H., et al. 2005. High-Throughput GoMiner, an 'industrial-strength' integrative gene ontology tool for interpretation of multiple-microarray experiments, with application to studies of Common Variable Immune Deficiency (CVID). *BMC Bioinformatics*. 6:168.

Zheng, W.H., Kar, S., and Quirion, R. 2002. FKHRL1 and its homologs are new targets of nerve growth factor Trk receptor signaling. *J Neurochem*. 80:1049-61.

Zhou, H., Summers, S.A., Birnbaum, M.J., and Pittman, R.N. 1998. Inhibition of Akt kinase by cell-permeable ceramide and its implications for ceramide-induced apoptosis. *J Biol Chem*. 273:16568-75.

Zhou, S., Bailey, M.J., Dunn, M.J., Preedy, V.R., and Emery, P.W. 2005. A quantitative investigation into the losses of proteins at different stages of a two-dimensional gel electrophoresis procedure. *Proteomics*. 5:2739-47. **Study on protein losses in 2D steps**

Zhu, D., Lipsky, R.H., and Marini, A.M. 2002. Co-activation of the phosphatidylinositol-3-kinase/Akt signaling pathway by N-methyl-D-aspartate and TrkB receptors in cerebellar granule cell neurons. *Amino Acids*. 23:11-7.

Zuccato, C., Liber, D., Ramos, C., Tarditi, A., Rigamonti, D., et al. 2005. Progressive loss of BDNF in a mouse model of Huntington's disease and rescue by BDNF delivery. *Pharmacol Res*. 52:133-9.